Mechanical and Hydromechanical Stimulation of Chondrocytes for Articular Cartilage Tissue Engineering

by

Homeyra Pourmohammadali

A thesis

presented to the University of Waterloo

in fulfillment of the

thesis requirement for the degree of

Doctor of Philosophy

in

Mechanical Engineering

Waterloo, Ontario, Canada, 2014

Author's Declaration

I hereby declare that I am the sole author of this thesis. This is a true copy of the thesis, including any required final revisions, as accepted by my examiners.

I understand that my thesis may be made electronically available to the public.

Abstract

Tissue engineering approaches have attempted to address some of the problems associated with articular cartilage defect repair, but grafts with sufficient functional properties have yet to reach clinical practice. Mechanical loads are properly controlled in the body to maintain the functional properties of articular cartilage. This inspires the inclusion of mechanical stimulation in any *in vitro* production of tissue engineered constructs for defect repair. This mechanical stimulation must improve the functional properties (both biochemical and structural) of engineered articular cartilage tissue. Only a few studies have applied more than two loading types to mimic the complex *in vivo* load/flow conditions. The general hypothesis of the present thesis proposes that the generation of functional articular cartilage substitute tissue *in vitro* benefits from load and fluid flow conditions similar to those occurring *in vivo*. It is specifically hypothesized that application of compression, shear and perfusion on chondrocyte-seeded constructs will improve their properties. It is also hypothesized that protein production of the cell-seeded constructs can be improved in a depth-dependent manner with some loading combinations.

Thus, a hydromechanical stimulator system was developed that was capable of simultaneously applying compression, shear and perfusion. Functionality of system was tested by series of short-term pilot studies to optimize some of the system parameters. In these studies, agarose-chondrocytes constructs were stimulated for 2 weeks. Then, longer-term (21- 31 days) studies were performed to examine the effects of both mechanical (compression and dynamic shear) and hydromechanical (compression, dynamic shear and fluid flow) stimulation on glycosaminoglycan and collagen production. The effects of these loading conditions were also investigated for three layers of construct to find out if protein could be localized differently depth-wise.

In one of the longer-term studies, the chosen mechanical and hydromechanical stimulation conditions increased total collagen production, with higher amount of collagen for hydromechanical compared with mechanical loading condition. However, their effectiveness in increasing total glycosaminoglycan production was inconclusive with the current loading regimes. The hydromechanically stimulated construct could localize higher collagen production to the top layer compared with middle and bottom layers. Some effectiveness of hydromechanical stimulation was demonstrated in this thesis. Future studies will be directed towards further optimization of parameters such as stimulation frequency and duration as well as fluid perfusion rate to produce constructs with more glycosaminoglycan and collagen.

Acknowledgements

I would like to sincerely thank my advisors, Professor Naveen Chandrashekar and Professor John Medley, for providing me with the opportunity to join their research group and mentoring me throughout this scientific journey. Your guidance and support in many aspects allowed me to appreciate my research area, explore new venues and accomplish my interests.

I am thankful to my committee members, Professors Stephen Waldman, Maud Gorbet, Carolyn Ren and Hyock Ju Kwon, who provided me with constructive suggestions to refine this research with their intellectual visions.

I specially thank Dr. James Kaupp, who greatly helped me to learn about cell culturing techniques. He was patiently answering my questions and generously shared his experience with mechanical stimulation. I truly appreciate your time for insightful scientific and technical discussions.

I wish I could have enough words to thank all my friends in general and have enough thanks for their emotional support throughout these years and for their motivating and encouraging words. Thank you all, who made this journey more enjoyable and meaningful.

I especially thank my parents for their endless love and support through every step, leading up to this. I have always been delighted with positive energy and winning spirit of my father and have overjoyed never-ending kindness of my mother. I am indebted for all your dedications and commitments in life for creating such a happy and cooperative family, and very thankful for all your great efforts and support towards my education. I am grateful that you always believed in me and built enough confidence and strength in me. I am really proud of having you as my parents. I love you forever.

I am grateful for all encouraging words of my dear sisters and brothers, who have practically and attentively supported me in every step and have kindly shared with me their great long-life experiences. As the youngest member of our family, I have been the most privileged to never miss any joy of your meaningful presence throughout all years of my life. I have always felt happy to be surrounded by your love, care and cooperation.

I really thank my son, Ali, who has been the best joy of my all times. Ali, I appreciate your patience and understanding throughout these years. I am very grateful for presence of you in my life and your love in my heart.

Last not the least, I would like to exclusively thank my husband, Professor Ehsan Toyserkani, for all his love, friendship and care throughout these years. Ehsan, I truly appreciate your understanding, motivation and encouragement, for patiently standing beside me, for being an insightful and responsible companion throughout this journey.

Table of Contents

List of Figures

List of Tables

Chapter 1

Introduction

Articular cartilage is a functional tissue in synovial joints, which acts in distribution of normal loads and helps in the reduction of related frictional forces. A thin layer of articular cartilage covers the articulating surfaces of bones, such as hip, knee and ankle to protect them and to provide them with resilient and compliant bearing surfaces. Synovial joint surfaces are not perfectly conforming and so the compliant nature of cartilage helps increase the contact area and thus reduces the average contact stress. Free movement of the joint is facilitated by presence of low friction between these bearing surfaces. The low friction and low contact stress allows the tissue to withstand the high loads that act during the motions needed to perform daily activities. Despite its important functional role in facilitating joint movement, articular cartilage has limited ability to regenerate and repair, due to its avascular nature and the lack of access to a pool of reparative cells. It lacks a supply of blood or lymphatic fluid which normally nourishes other parts of the body [2,3]. Thus, relatively small amounts of damage to articular cartilage tissue may lead to a major progressive damage due to its non-regenerative nature. This problem has raised a great demand for functional substitutes that should be biologically, biochemically and biomechanically compatible with natural articular cartilage tissue.

There are several surgical treatments available for the repair of damaged articular cartilage depending on the extent of the damage. Osteochondral grafting, chondroplasty (reparative surgery of cartilage), and prosthetic joint replacement are among the most common conventional strategies for articular cartilage repair. These treatments involve shifting parts of a joint surface or replacing it

with synthetic materials [4], [5]. Their use can be limited by problems such as risk of infection, inadequate availability of donor tissue, donor site morbidity, abrasion of articular cartilage surface, loosening of implants, and limited durability of prosthetics. To eliminate these problems, provide better options to patients, and offer higher levels of treatment, researchers have focused on the regeneration of tissues by the principles of the tissue engineering [6-16].

Tissue engineering integrates a variety of science and engineering disciplines to create tissues for transplantation, restoration or improvement of the function of articular cartilage tissues. In a basic tissue engineering procedure, patient's cells (articular chondrocytes) are isolated, expanded in a cell culture, seeded into a proper carrier and grafted back to the defect site of the same patient [17]. This procedure does not always work well and needs to be optimized by considering the biomechanical as well as the biological and biochemical functions of engineered tissues [18]. Significant role of mechanical loading has been well established in regulating chondrocyte metabolism and maintaining healthy normal activities of natural articular cartilage in the body [8], [11], [19-40]. The loading of synovial joints causes the cartilage to experience a complex combination of compressive, tensile and shear deformations (and stresses), pressurization of the fluid within and surrounding the cartilage along with a flow of both the fluid and the ions within the fluid. This motion of the ion containing fluid causes a shift in electric potentials that feedback to influence both flow and stresses. The contribution of loads to the cellular activity should be identified in order to optimize loading conditions on a cartilage tissue implant, while it is being prepared. Despite significant recent progress in the field of functional tissue engineering, mechanobiology and mechanotransduction, the loading conditions for *in vitro* experiments has yet to be optimized.

Many of the previous research studies have investigated the relationship between mechanical loadings and cell responses to improve procedures for articular cartilage repair or regeneration. Each of them applies specific types of loads, assumes different environmental conditions for their experiments and/or uses specific specimen cultures (e.g., single cell layer, actual tissue or 3D scaffold). The effects of application of different types of mechanical loadings individually have been extensively explored by *in vitro* studies. These loading types included static/dynamic compression (confined or unconfined), intermittent/cyclic compression, dynamic shear (sometimes fluid-induced), or constant/intermittent hydrostatic pressure. However, very few *in vitro* studies have reported combined loading regimes [41-52] to better simulate the complex physiological loading of the *in vivo* environment of articular cartilage.

The present research aims to apply such combined loading regimes by implementing a new stimulation technique for *in vitro* conditioning of articular cartilage tissue grafts. It includes a variety of mechanical loads that are related to those occurring *in vivo*. The hypothesis in the present thesis relies mainly on the following findings from previous research studies:

- Dynamic mechanical loading, by means of compression [53-62] or shear [61], [63-68] improved functional mechanical and structural properties of natural and engineered articular cartilage tissue [69].
- Combined compression and shear forces were found to be more beneficial because they were closer to the *in vivo* conditions than just compression or shear forces alone [44], [70], [71].
- Frictional shear stress was also beneficial as it modified the superficial layer of the cartilage [41-43], [45], [72].

- Hydrostatic pressure, either static or cyclic, in the physiological range enhanced structural characteristics of articular cartilage [73-85].
- Fluid convection of fresh/recirculated nutrient through and around cartilage tissues helped the growth by increasing the overall mass transport and provided mechanical stimulus as modulators of chondrocyte metabolism [69], [86-92].

1.1 Hypotheses

The above studies all addressed aspects of the overall hypothesis that the generation of functional articular cartilage substitute tissue *in vitro* required controlled mechanical environments to create a matrix that is biochemically and biomechanically similar to natural tissue. The present thesis hypothesizes that the combination of compression loading, frictional shear, shear due to fluid perfusion, and hydrostatic pressure, applied within physiological ranges will provide a better mechanical stimulation for *in vitro* cartilage constructs (Figure 1.1).

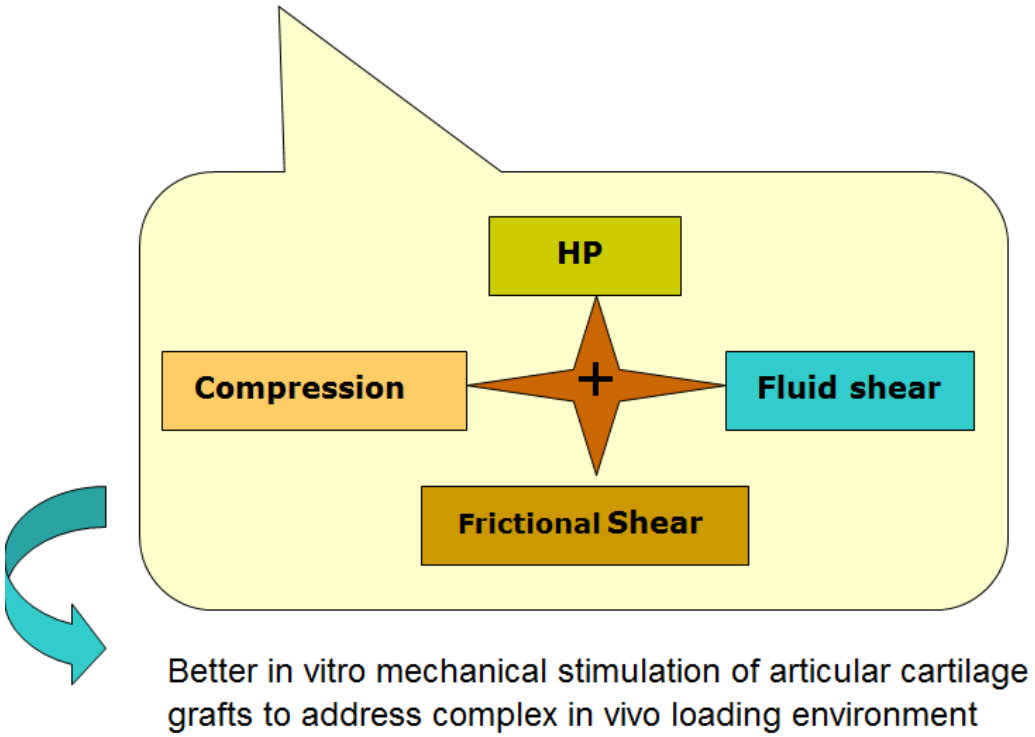

Figure 1.1 The main hypothesis of the present thesis. HP: hydrostatic pressure.

1.2 Research Objectives

The objective of the present research was to implement a new technique and procedure for the *in vitro* mechanical stimulation of chondrocyte-seeded constructs by means of simultaneous cyclic application of compression, shear, friction, frictional fluid shear and hydrostatic pressure causing fluid flow into the construct surface.

The present study examined the effects of combined mechanical loadings on chondrocyte-seeded agarose constructs *in vitro*. The effects of various combinations of mechanical stimulation were assessed by examining biochemical properties of the stimulated constructs.

1.3 Scope of Research

1) Design and develop a functional "hydromechanical" stimulator to apply *in vitro* combined mechanical loads within physiological range on multiple chondrocyte-seeded constructs.
2) Optimize parameters of the studies to some extent, so the system can accommodate constructs for long-term culture under various loading conditions.
3) Produce and culture unloaded cell-seeded constructs as well as loaded ones under the various loading conditions and loading durations.
4) Determine the biochemical properties of loaded cell-seeded constructs (mainly the amounts of proteoglycan and collagen) relative to unstimulated constructs.

1.4 Research Contributions

This thesis made the following general contributions to the area of cartilage tissue engineering:

The novel application of compression, perfusion and shear through a hydrostatic bearing indenter provided a mechanical stimulation for chondrocytes in a three dimensional environments. The stimulator could operate in a mixed film regime and apply cyclic time-varying frictional shear stress by direct contact and through a fluid film. The current research investigated the effects of this type of stimulation on the bioactivity of chondrocytes in producing proteoglycans and collagen.

1.5 Thesis Organization

The present thesis has the following organization. **Chapter 2** provides a review of relevant literature related to articular cartilage structure, function, disorders and methods for its

repair/regeneration. In addition, information from the literature is presented on the topic of articular cartilage tissue engineering, including its challenges and hopes along with the various stimulation techniques. In addition, the effects of these stimulations are examined regarding the activities of the chondrocytes and health of either natural cartilage tissue or chondrocyte-seeded biomaterials. The rationales for using the agarose hydrogel in mechanically or hydro-dynamically loaded constructs in previous studies are reviewed. **Chapter 3** presents the "hydromechanical" stimulator and gives details of its design and commissioning. **Chapter 4** describes the experimental methods, including the production of cell-seeded constructs, culture and loading conditions and loading durations in each study. **Chapter 5** presents the results and gives brief discussion of the findings of each study. **Chapter 6** provides the detailed discussions about all of the studies and compares them with similar studies. Finally, **Chapter 7** gives the conclusions of the research and recommendations for future research.

Chapter 2

Background and Literature Review

2.1 Cartilage

Cartilage is a connective tissue in many areas in the body, including the ear, nose, larynx, rib cage, and intervertebral discs. It also forms the bearing surfaces in synovial sometimes called diarthrodial) joints such as the hip, knee, ankle, shoulder, elbow and spinal facets. Cartilage is made by a single cell type, called a chondrocyte, which is capable of producing extracellular matrix (ECM). This ECM is composed of collagen fibers, ground substance rich in proteoglycan (PG), elastin fibers and water (both bound and unbound). There are different relative amounts of the main components and some dissimilarity in the structure, elasticity and strength of the cartilage found at various locations in the body. Thus cartilage is categorized into three main groups: 1) articular or hyaline cartilage (found on synovial joint surfaces), 2) fibrocartilage (such as in the vertebral disks), 3) elastic cartilage (such as external ear or larynx).

Articular or hyaline cartilage is the most abundant in the human body. The main focus of studies present in this thesis is on articular cartilage and chondrocytes.

2.2 Synovial Joints and Articular Cartilage Functions

Synovial joints are mechanisms to move the skeletal segments of the body and facilitate large ranges of motions required for performing daily activities. While doing this, they transmit high loads (often several times body weight). Knee, hip and elbow are some examples of the synovial joints. Typically, these joints are surrounded by a fibrous capsule (supported by ligaments) that is lined by the synovium or synovial membrane, containing the synovial fluid that acts as a lubricant for the joints [34]. The ends of articulating bones are covered with thin layer of hyaline cartilage (~ 2 mm in humans) and often a rough fibrous meniscus acts to carry load and improves the conformity of the joints (Figure 2.1).

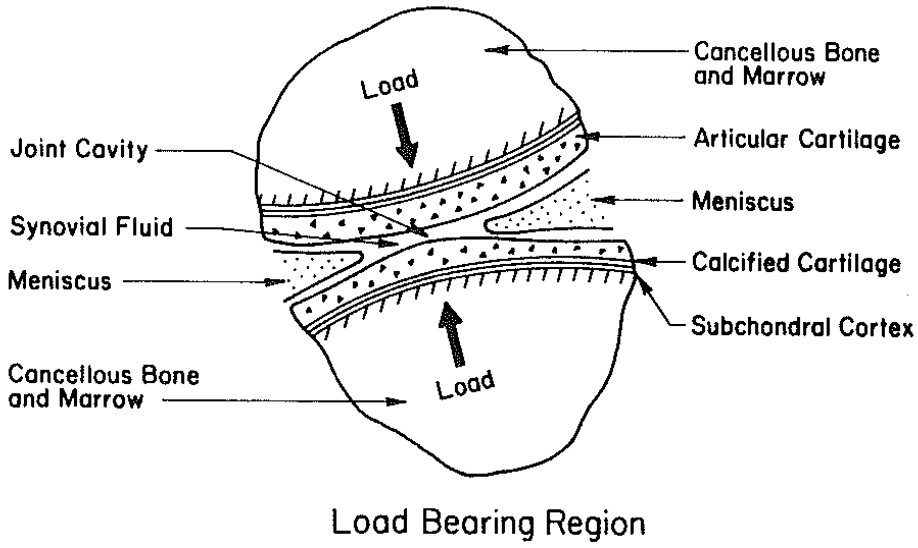

Figure.2.1 Load bearing regions of cartilage adopted from [34].

The general function of articular cartilage is to reduce the contact stress while providing a low friction gliding surface to facilitate motion of synovial joints. The low contact stress allows load to

be transmitted through the joint to the underlying subchondral bone [34] without damaging either the cartilage or the bone [2]. Articular cartilage is relatively compliant viscoelastic material, which can recover its shape quickly when the deforming stress is removed. It is the key component of synovial joints and helps maintain their excellent tribological characteristics such as low levels of friction and wear and efficient mode of lubrication [93]. All these features of synovial joints allow them to survive the repetitive or excessive loads that they must transmit [94].

The joint cavity is surrounded by a fibrous capsule, the inner lining of which is called the synovial membrane (or synovium). The capsule essentially acts as a seal to keep the synovial fluid in the joint cavity and keep it available for lubrication. However, the capsule does allow a very slow fluid transport into and out of the joint cavity. The behaviour of the synovial fluid within the joint space is governed by the chemical attachment of some of its molecules to the cartilage surfaces and fluid entrainment caused by the motion of the surfaces.

The synovial membrane synthesizes synovial fluid and permits fluid to pass in and out of the joint space. The synovial fluid, composed of about 75% water, is supplemented with hyaluronic acid, proteins, and polysaccharide; they carry nutrient to the chondrocytes and capture the waste products from cellular components within the joints [2], [95]. Substantial amount of the loads is carried by pressurized fluid inside the articular cartilage tissue and synovial fluid films between the cartilage surfaces [96].

2.3 Articular Cartilage Composition

2.3.1 Extracellular Matrix

Articular cartilage is a non-homogeneous connective tissue that consists of two main phases: a liquid phase which includes water and electrolytes (dissolved inorganic salts such as sodium, calcium, chloride and potassium) and a solid phase which contains chondrocytes, collagen, proteoglycans and other glycoproteins [97]. The interaction of these two phases defines the tissue's mechanical properties of stiffness and resilience [98]. The extracellular matrix of articular cartilage tissue is shown in Figure.2.2.

2.3.2 Collagen

The majority of the content of solid phase of the articular cartilage tissue is collagen which is 50-80% of the dry weight or about 10-20% of the wet weight [99]. The main molecular component of this collagen is type II collagen (~ 95%) with traces of other collagen types including type XI (~ 3%) and types III, VI, IX , X, , XII and XIV (~ each ~ 0-1%) [100-102]. The collagen forms a dense network of fibrils embedded in a high concentration of proteoglycans [103] thus forming a composite structure that can resist both swelling pressure and compression while the collagen fibres themselves remain in tension (Figure.2.2).

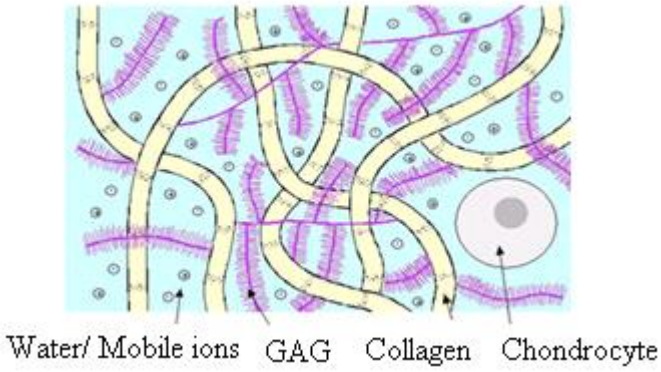

Figure.2.2 Schematic representation of articular cartilage extracellular matrix components [104].

2.3.3 Proteoglycan

Proteoglycan (PG) is the second largest portion of the articular cartilage solid phase, accounting for 5-10% of the wet weight. Various proteoglycans within the cartilage contribute in its functions. Aggrecan, decorin, biglycan, fibromodulin and lumican are types of cartilage proteoglycans [105], in which their functions are defined by their core protein and their glycosaminoglycan (GAG) chains (polysaccharide chains made of repeating disaccharides containing amino sugar). Hyaluronic acid, chondroitin sulfate, keratan sulfate and dermatan sulfate are glycosaminoglycans found in articular cartilage, which their concentrations vary depending on the sites, age and health of tissue [98]. The negatively charged carboxylate or sulfate group in disaccharide unit causes to repel other strings or molecules with negative charges and to attract positively charged ones [98].

Under physiological conditions, proteoglycans are negatively charged and have hydrophilic properties (attract water strongly). These hydrophilic properties can cause articular cartilage to swell. Thus, proteoglycan contributes to compressive and shear stiffness of articular cartilage tissue as well as regulation of tissue hydration and Donnan osmotic pressure (created due to

charged particles in solution that fail to distributed evenly on two sides of a semi-permeable membrane because there is a fixed charge substance on one side) [99]. A schematic representation of collagen and proteoglycan is shown in Figure.2.3.

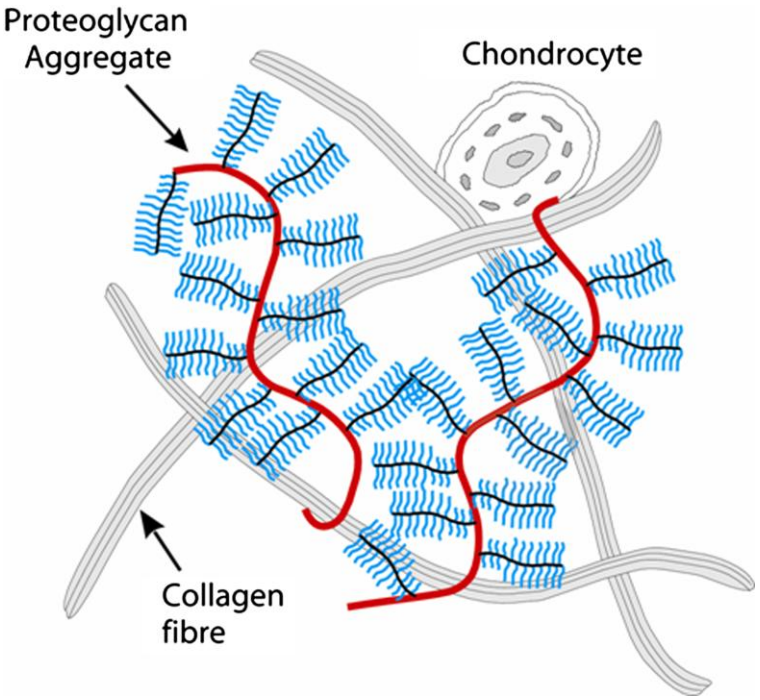

Figure.2.3 Proteoglycan structure [106].

2.3.4 Chondrocyte

Chondrocytes, as the only cell type of articular cartilage, play a central role in producing and replacing the matrix molecules and maintaining the tissue. They make about 1% of volume of adult human articular cartilage [107], [98] and up to 10% of the wet weight of tissue [2]. They can survive under very low oxygen tension; they synthesize, assemble and organize extracellular matrix [108] around themselves and do not have cell-to-cell contact. The chondrocytes can be distinguished from other cells by their spheroidal shape, synthesis of type II collagen, large

aggregating proteoglycans (PG) and some noncollagenous proteins [98]. Type II collagen is known as marker of chondrocyte differentiation [109].

Healthy chondrocytes are able to maintain and restore the articular cartilage tissue. Any factor changing the cellular functions (such as aging), alters their proliferative capacity and limits their proteoglycan synthesis, which leads to progression of tissue degeneration [98]. The balance between the extracellular degradation and matrix turnover and their metabolism is affected by biochemical and biomechanical signals. The healthy chondrocytes are able to detect the alterations in matrix molecular composition and organization. The degraded molecules are sensed and an appropriate types and amount of new molecules are synthesized by the cells. The mechanical, electrical and physicochemical signals received by chondrocytes of loaded articular cartilage tissue, help the cells to direct their synthetic and degradative activities [110].

2.3.5 Water and Dissolved Electrolytes

Water and dissolved electrolytes which make up to 80% of articular cartilage tissue's wet weight [98], have great influence on mechanical properties of the tissue. Some of this fluid is in intracellular space, about 30% in the interfibrillar space within the collagen fibers, and the rest in proteoglycan molecules [99]. The amount of water depends on the proteoglycan concentration and their swelling pressure, organization of collagens, strength and stiffness of their network surrounding the proteoglycans [99]. High amount of cations (positive ions) in the fluid can balance the negatively charged proteoglycans. Large aggregating proteoglycans keep the fluid within the matrix and maintain the electrolyte concentration of the fluid [98]. The water and ions flow through the porous permeable matrix of solid phase due to the applied pressure on articular cartilage tissue. The interstitial fluid flow causes a large frictional drag force which is the main mechanism for load

bearing ability of synovial joints [2], controls their compressive behaviour and facilitates some energy dissipation [99].

2.4 Zonal Organization of Articular Cartilage Structure

The distribution and arrangement of components of articular cartilage tissue is not uniform, but it is organized into four distinct structural zones: a) superficial (tangential), b) middle (transitional), c) deep, and d) calcified cartilage (Figure.2.4.). The content and structure of the collagen and proteoglycan is depth dependent.

The superficial zone covers about 10-20% of the total thickness of cartilage. In this zone, the shapes of chondrocytes are flatter and more elongated under a sheet of collagen fibres which is oriented parallel to the surface [98]. There are relatively low quantities of proteoglycan (~15% dry weight), but high amount of collagen (~ 86% dry weight, highest compared with other zones) and water (~ 84% wet weight).

The superficial zone provides a smooth surface that encourages a gel layer of molecules from the synovial fluid to form and thus permit easy sliding motion without incurring damage to itself [111], [112], resists shear, and deforms approximately 25 times more than the middle zone [113]. Superficial zone proteins (SZP) on or below the surface are involved in the gel layer and help protect the surface during sliding motion. SZP are sometimes used as a marker to distinguish this zone from the others [72], [113-115].

In the middle zone (~ 40-60% of the total thickness), chondrocytes have a more spherical shape; compared to other zones, the amount of proteoglycan is highest (~ 25% of dry weight), the water

and collagen concentration is lower, and the collagen fibres (with larger diameters) are distributed more randomly

The deep zone (~ 30% of the total thickness) is characterized by collagen fibres that are perpendicular to the underlying bone, and columns of chondrocytes arrayed along the axis of fibre orientation [99]. The cell density reduces in the middle and deep zones. The calcified zone is partly mineralized with minimum amount of collagen and water, comparing with the other zones, and it acts as the transition between cartilage and the underlying subchondral bone.

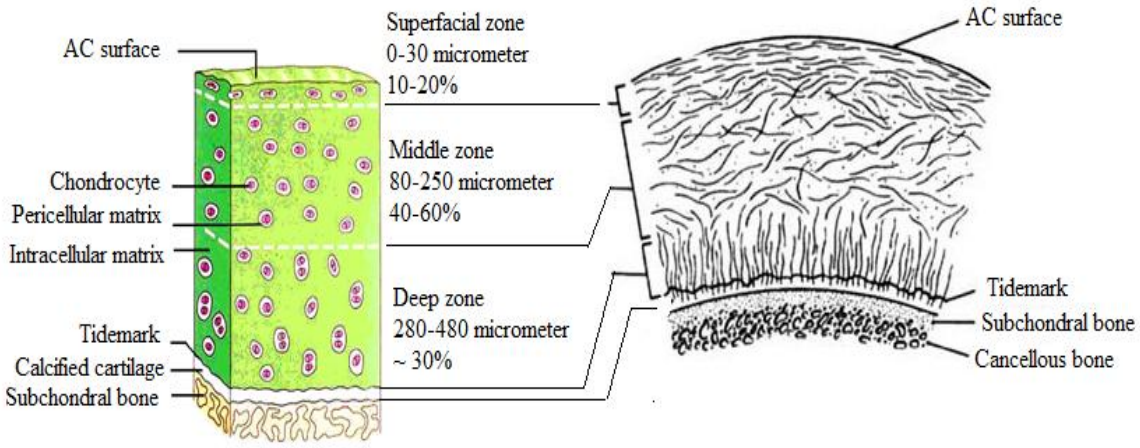

Figure.2.4 Different zones of articular cartilage: left: the chondrocytes shapes and distribution and right: the collagen fibres alignments [116].

2.5 Biomechanical Properties of Articular Cartilage Material

The role of biomechanics in development and regeneration for a tissue that experience various static and dynamic mechanical loads has been examined in many research studies. Due to its unique composition and structure, the articular cartilage can tolerate various physiological loads

such as compression, tension and shear [98]. The behavior of articular cartilage material under each of these loading conditions and tests is discussed separately in the following sections.

2.5.1 Compression

Articular cartilage is primarily loaded under compression. The compressed tissue experiences alteration in its volume and internal pressure [117]. Due to biphasic nature of articular cartilage (solid- and liquid-phase interacting material), the internal pressure change causes an interstitial fluid to flow through the pores of the solid extracellular matrix. The fluid flow makes frictional resistance within the tissue, which is major part of its viscoelastic behavior [2]. So, the stress within the solid phase, the stress within the fluid phase, and the frictional drag of fluid through the solid phase interact with each other to help the tissue to perform viscoelastically under the compression [2].

The compressive behavior of the tissue is quantified by either the confined compression tests [117-122] or indentation tests [123- 129]. The confined compression experiments are either done as a creep or a stress-relaxation test.

In confined compression creep tests, a constant load or stress is applied by a rigid-porous platen (which allows free fluid exudation) to the surface of a specimen that is confined in cylindrical ring (which allows uniaxial flow and motion). The deformation over time is measured. The stress is proportional to the deformation; and when it balances the applied load, the fluid flow and the deformation stop [2]. In confined compression stress-relaxation tests, displacement is imposed at a constant rate and then the displacement is held constant and the load is measured as it varies over time. In indentation tests the load is applied to the surface of specimen by a cylindrical porous-permeable indenter [2].

Cartilage load deformation behaviour at an instant in time depends on the existing cartilage strain amplitude, the loading amplitude and the loading rate. For example, during stair climbing, the cartilage in the hip or knee joints could be subjected to the dynamic compressive stress as high as 15-20 MPa which could cause 1-3% compressive strain. However, the strain could rise to 35-45% when much lower stress of about 3.5 MPa is statically applied to the knee joint for 5-30 minutes [98]. For small strains under 20%, both human and bovine articular cartilage have shown a linear stress-strain relationship [99], [117], [130].

For human articular cartilage, the equilibrium aggregate modulus (obtained from a confined compression creep test and defined as the constant stress divided by the equilibrium strain) is inversely proportional to the water content [131], but directly to the proteoglycan content per wet weight with no correlation between equilibrium compressive stiffness and collagen content (shows the important role of PG in compressive stiffness). This explains why the loss of proteoglycan due to degeneration, substantially changes the joint function.

2.5.2 Shear

The loads applied to the tissue surface create shear stress within the matrix of tissue [2]. The application of loads parallel to the surface is particularly effective in imposing shear on the cartilage tissue matrix (Figure 2.6).

The stiffness of the collagen fibres in tension and their containment of proteoglycan make the composite solid matrix of cartilage resist shear. Thus, although the proteoglycans have low shear modulus, they indirectly affect shear stress by holding the collagen network [2], [132], [133].

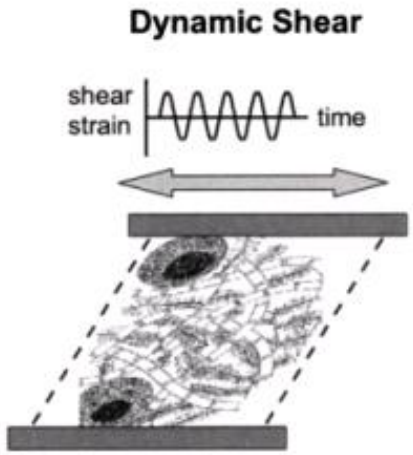

Figure.2.5 Dynamic shear test and changes within extracellular matrix [134], [61].

2.5.3 Tension

Despite the fact that the articular cartilage is a tissue under compressive loads, but its tensile property is important because a significant tensile stress is produced within its matrix when it is compressed. Tensile action helps to holds the content of tissue as it experiences large compression [2]. The main component that is contributing to the tensile properties of cartilage is collagen fibers and their orientation [2]. Orientation-dependent tensile behavior (anisotropy) explains why the specimens that are harvested parallel to are stiffer than the ones perpendicular to the split-line. The relative movement of the collagen network and the proteoglycans influences the viscoelastic behavior of the tissue [135], [136]. Tensile modulus measurement for articular cartilage may vary depending on the source of tissue, age of tissue [137], sub-location in the joint, depth or zone and also tissue degeneration status; and it is found to be in the range of 1-10 MPa [137], [99].

The proteoglycan content has shown to have no effect on the tensile modulus range [138] indicating that the collagen and proteoglycan bonding is not covalent [99]. The tensile modulus of

superficial zone cartilage is higher than the middle zone, which is consistent with more collagen concentration in that zone [99]. Tensile modulus decreases as the cartilage is degraded from its normal condition due to osteoarthritis.

2.5.4 Fluid Flow and Permeability

Fluid flow through the porous and permeable articular cartilage creates a frictional drag that highly contributes to the load bearing ability of the tissue in the moving joint. Permeability is inversely proportional to the frictional drag of the fluid, to compressive strain and to hydraulic pressure, but may show nonlinear behaviour at high pressure and strain [2]. The permeability of normal cartilage is in the range of $1\text{-}10^{-15}$ [m^4 /N.s] and for the degenerated cartilage about 10^{-14} [m^4 /N.s] [99].

2.5.5 Osmotic Pressure and Swelling

The swelling of the articular cartilage tissue is accompanied by an increase in its water content. This increase affects the permeability and fluid flow within the matrix and the compressive stiffness of the tissue [93], [139-142]. The proteoglycans have negatively charged groups (SO_3^-, COO^-) attached to their chains and thus have a fixed charged density (FCD). When the ion concentration of the external bathing solution is higher than inside of the tissue, it causes an inequality in the ion charges. The imbalance creates interstitial fluid pressure (higher than ambient pressure) because the mobile ions try to distribute themselves evenly through the tissue. However, the fixed negative charges cannot move and so the motion of the mobile ions in the interstitial fluid cause fluid move into the matrix causing swelling and a higher fluid pressure. This higher pressure

is called Donnan osmotic pressure [99], [143] which causes the fluid move within the tissue and the tissue to swell to maintain the osmotic equilibrium [2].

In addition to the Donnan osmotic pressure, another cause of articular cartilage swelling is a repulsive force between the closely located charged groups in GAG chains of the solid matrix [99]. This effect is called chemical-expansion stress (or electrostatic repulsion) [2]. The positive ions in solution floating around the proteoglycans tend to neutralize the fixed negatively charged groups [2]. However, upon compression these positive ions are carried out by the fluid flow and thus the fixed negative charges repulse each other and create the chemical expansion stress. So, the total swelling pressure is the sum of both Donnan osmotic pressure and the chemical expansion stress and this influences cartilage stiffness [2]. In the small region of cartilage that sustain tensile deformation, the chemical expansion stress and the Donnan osmotic pressure again act together but this time they act with and not against the deformation.

2.5.6 Viscoelasticity

Articular cartilage is viscoelastic material due to the fluid flow within its solid matrix and to a lesser extent the viscoelasticity of the matrix itself [117], [93], [144]. The deformation behaviour of the loaded tissue is influenced by both flow-dependent and flow-independent mechanisms [145]. The pattern of the fluid flow depends on the kinematics of loading, strain amplitude, moduli and permeability of solid matrix. The magnitude of the fluid drag force and stiffness of the matrix act to give a viscoelasticity to the tissue [146]. Cartilage deforms rapidly at first after loading and then continues to deform slowly over time; in equilibrium, the load is balanced with no more deformation [2].

2.6 Biotribology of Articular Cartilage

Most of the organs with surfaces in relative motion face tribological challenges which essentially involve friction, wear and lubrication. Biotribology is the science and engineering of interacting surfaces in relative motion that involves biological surfaces and/or lubricants [147], [148], [34], [149], [150]. Biotribology is important in understanding, maintenance and regenerating functions of many living tissues such as articular cartilage, heart, blood vessels, ligaments, tendons and skin [147]. The levels of friction and wear have functional role in the living organisms to accomplish their required daily activities. For instance, there is a need for high friction for feet to walk, low friction for blood cells to pass through veins; high wear to clean the teeth and low friction for joints to easily articulate and eyes to blink. Lubrication influences friction and wear. Furthermore, through surface interaction, cells often sense and communicate with each other [147].

In human body, the major focus of biotribology is on the load-bearing synovial joints in the lower limbs such as hip, knee and ankle, and the minor one is on the low load-bearing joints in the upper limbs such as fingers, wrist, elbow and shoulder [149] or other body parts such as the facet joints in the spine. During daily activities, the joints transmit dynamic loads. The human knee joints tolerate forces in the range of 1.9 to 7.2 times the body weight in doing different activities [151] and the loads of the human hip joints can reach to about 2.5 to 5.8 times the body weight [147] which result in apparent hip contact stresses as high as 18 MPa [152], [153]. The loads in the lower limb joints are transient during common activities such as walking. For example, the cycle time of knee joint (with similar pattern in the hip) during typical walking, when the heel strikes the ground and the toe is pushing off, is about 1.2 s with 1500 N maximum force [154]. The loading occurs in short period of about 0.01-0.15 s for high loads, and longer period of about 0.5 s for lower loads.

The highest loads correspond to positions of low surface velocities and lowest ones to maximum velocities [154].

Synovial joints are considered as bearings with novel extra features compared with conventional bearings in machines [155]. The contact regions accept loads of varying magnitude and directions. The bearing material is articular cartilage with 1-5 mm thickness which is attached to subchondral bone. Synovial fluid, within the synovial membrane lining a fibrous capsule, lubricates the bearing surfaces [155]. Low loads and high entrainment velocities help form thicker fluid film [154].

2.6.1 Friction and Wear

The friction force is the resistance of movement of a body against another body in the opposite direction of motion. The friction develops in tiny microscopic and isolated contact points called asperity contacts. This direct contact between surfaces can involve chemical and/or physical phenomena. The friction in this case can be produced by weak or strong chemical adhesion. It can also be produced by elastic (reversible) or plastic (non-reversible) deformation of asperities [156].

A wide range of friction values and thus coefficients of friction (friction force divided by normal force) have been measured for contacts involving articular cartilage surfaces. For example, the coefficient of friction of contacts involving cartilage during several hours under the dynamic load has been measured in the very low range of 0.002-0.02 [157], and in a higher range of 0.2-0.4 under static loads [157-159].

Wear of the articular cartilage tissue happens when its asperities deform or sub-surface damage causes delamination of the surface. In both cases, tissue is removed from the surfaces in contact [160]. Wear of cartilage, which may happen due to sub-surface fatigue, adhesion, abrasion, impact,

erosion or corrosion (mainly caused by osteoarthritis), is one of the reasons of loss of tissue and thus plays a role in degenerative joint disease such as osteoarthritis [147].

Both friction and wear of articular cartilage vary due to contact stress [157], [161], [162] or area [163], [164] sliding distance or speed [165] and loading time [159], [166], [157]. Articular cartilage experiences both static and dynamic loads due to sliding and rolling of the moving joint surfaces and subjected to millions of cycles in a life time, but the biochemical and mechanical properties of cartilage tissue enable it to withstand these loading regimes by minimizing the wear. The reduction of frictional forces by some sort of lubrication action (fluid film and/ or boundary) is likely to have reduced forces on the cartilage tissue and wear [160].

The frictional behavior of articular cartilage has been explained in previous studies by various lubrication mechanisms [166] such as fluid film lubrication [167], [111], boundary lubrication [96], [168], [164], [169] and mixed lubrication [166], [170].

In classical fluid film lubrication, the thickness of the lubricant film must be greater than the surface roughness to prevent the direct contact [147]. When separation of surfaces is produced by a fluid film that is created by external pressurization (e.g., pump), lubrication is called hydrostatic lubrication [147], [160]. However, if the fluid film is produced by entrainment due to the kinematics of the surfaces it is called hydrodynamic lubrication. The sliding speed, load, fluid viscosity, surface macrogeometry and surface roughness influence the thickness of hydrodynamic fluid film [147], [160]. When the pressure of hydrodynamic fluid film is high enough to cause elastic deformation, the lubrication is called elastohydrodynamic [147], [93]. It is likely that synovial joints experience some aspects of classical fluid film lubrication but there are other complex biological phenomena that also act.

Mucins, a family of glycosylated proteins, coat many surfaces in the human body and seem to act as boundary lubricants [147], [171]. Superficial zone proteins (SZP), more commonly referred to as Proteoglycan 4 [172], [147], is a glycoprotein with mucin-like domains [173], [172], [147]. They may function as boundary lubricants [174], [175], [168], [176], [96], [169] or perhaps contribute to a surface gel layer that helps promote fluid film lubrication [177], [112], [178], [111]. SZP is sometimes called "lubricin" [174], [147] and is encoded by the PRG4 gene [172], [147]. Apparently, in synovial joints, it is mostly released into the synovial fluid rather than remaining in the cartilage matrix [173], [147]. The other proposed boundary lubricants of articular joints are hyaluronan, SZP/lubricin/PRG4, surface active phospholipid (SALP), or their combinations [147], [96], [174], [179], [180], [181].

Articular cartilage and synovial fluid are very complex and are subject to various loading types and conditions in synovial joints. Thus, synovial joints may have more than one lubrication mode [34], [111]. The regions of articular cartilage under conditions of both elastohydrodynamic and boundary lubrication, can be said to experience mixed lubrication [147]. For synovial joints, this mixed lubrication may also involve interstitial fluid and some sort of surface amorphous layer [111], [112], [177], [178], [182], [183].

2.6.2 Effects of Some Specific Cartilage Components

The effects of cartilage components such as collagen, glycosaminoglycan/proteoglycan and surface amorphous layer will be reviewed in the following subsections.

2.6.2.1 Collagen

The role of collagen fibers in the biomechanical properties of articular cartilage has been discussed in previous sections. However, the integrity of the collagen network seems to be as important as the

collagen itself, particularly in the superficial zone near and at the surface [148]. Contacts involving articular cartilage with disrupted collagen networks showed higher friction level comparing with those involving normal articular cartilage [184], [185].

2.6.2.2 Glycosaminoglycan/Proteoglycan

Tribological behaviour of articular cartilage is affected by its interstitial fluid flow when loaded [148]. The fine collagen fiber network and the negatively charged glycosaminoglycan chains of the proteoglycans as explained in previous sections, provide resistance to interstitial fluid flow, and this results in the low value for permeability ($\sim 10^{-15}\ m^4/N.s$) [148]. GAG depleted articular cartilage deforms more and results in higher friction forces in a bovine articular cartilage against cast cobalt alloy contact in the presence of Ringer's solution [186]. The reduction of fluid load support [187], [188] and/or presence of chondroitin sulphate at articular cartilage surface [183], [189] are considered the main reasons for this behaviour.

2.6.2.3 Surface Amorphous Layer

Surface amorphous layer found on top of superficial tangential zone of articular cartilage contains sulphated sugars, glycoproteins and lipids and contributes to the tribological properties of contacts involving articular cartilage by protecting the underlying bulk cartilage from the full effect of dynamic loads [112], [177], [178], [183], [189], helping in the load-bearing properties of tissue and shielding the surface to prevent its micro-damages [148]. The surface amorphous layer may also play a role in fluid film lubrication but, as yet, this has not been explored.

2.6.3 Effects of Some Specific Synovial Fluid Components

2.6.3.1 Hyaluronic Acid

Hyaluronic acid is part of synovial fluid and it seems that it can penetrate the surface of articular cartilage and accumulate around lacunae of chondrocyte. Also, it elevates the viscosity of synovial fluid above that of water due to its high molecular weight and concentration [93], [174], [160]. Apparently, hyaluronic acid affects the fluid film lubrication and its presence resulted in lower startup coefficient of friction under conditions that encouraged boundary lubrication [190], even for osteoarthritic joints. The studies on the role of hyaluronic acid in both healthy and damaged tissues showed its effectiveness as boundary lubricant under static condition but with less effectiveness under dynamic conditions [184].

2.6.3.2 Lubricin

Lubricin, another component of the synovial fluid, is made by synoviocytes of the joint capsules and the chondrocytes of superficial zone of articular cartilage [173]. It is sometimes called superficial zone protein; it is identified or encoded by PRG4 gene [191]. It reduced friction for both *in vivo* and *in vitro* studies by decreasing the adhesion between the opposing surfaces [192]. There is some suggestion that it does this by combining with glycosaminoglycan hyaluronate [192].

2.6.3.3 Surface Active Phospholipids

Phospholipids have highly hydrophobic fatty acids that facilitated the lubrication process. The surface active phospholipid caused the reduction of coefficient of friction of articular cartilage when it was articulated against the glass with low contact stress [193], [194], [148].The removal of lipids from the surface of cartilage when it was articulated against cobalt-chrome plate with low

contact stress slightly increased the coefficient of friction at shorter loading times and had no effect at longer times [186]. So, it would seem that these phospholipids only act at low contact stresses.

2.7 Articular Cartilage Injuries/Disorders

Trauma, disease or aging causes major progressive damage in articular cartilage. Matrix disruption, partial or full thickness defect can occur in articular cartilage due to injuries or aging. The injuries can lead to pain, joint dysfunction and degeneration [110], [98]. Aging can significantly change the articular cartilage structure, by fibrillation of the tissue surface, decreasing in the size and aggregation of aggrecans (large proteoglycans that form a major structural component of articular cartilage), and increasing the collagen cross-linking [195], [196]. Aging also resulted in a decrease in tensile strength length and abundance of GAG side-chains [197], [196]. The extracellular matrix protein synthesis as well as responsiveness to growth factors decreased due to aged chondrocytes [197], [195], [196].

High impact non-physiological loads (much greater than those occurring during daily activities such as walking, running or jumping) were found to be a main cause of cartilage matrix disruption [198]. These impact loads could cause structural damage to cartilage and cause it to gradually show osteoarthritic-type symptoms such as tissue swelling, collagen denaturation and cell death [199]. The death rate of cells was found to be very high, and the cells that could survive the impact load, secreted degradative factors [200], [198]. The histological views of the level of damage are shown in Figure.2.6.

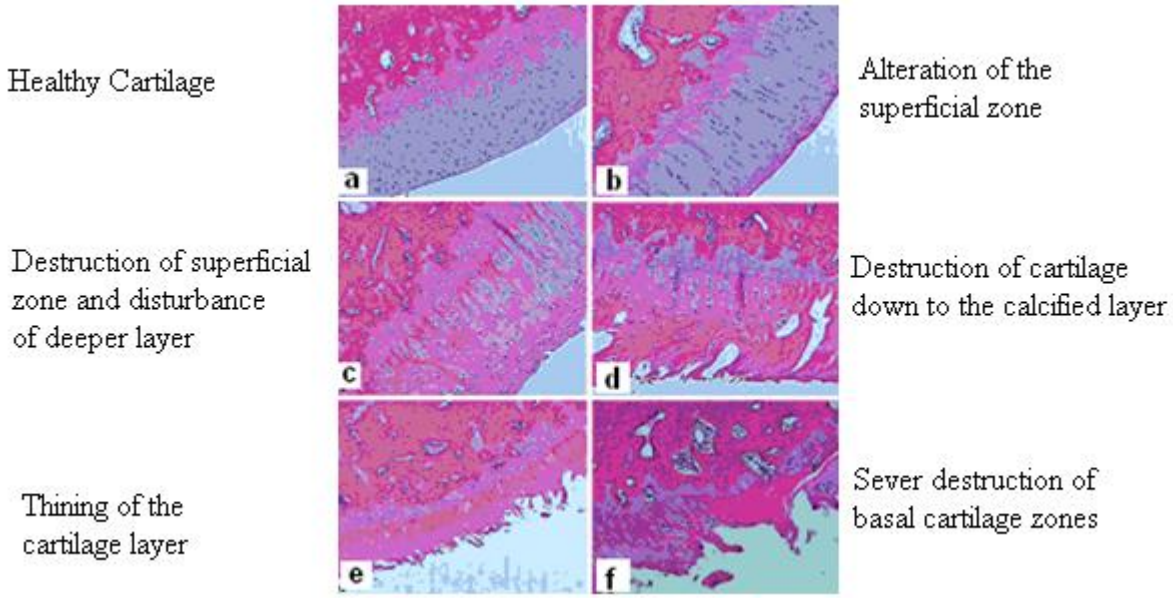

Figure.2.6 The sequence of changes in histology of articular cartilage from (a) healthy articular cartilage to (f) severely destructed articular cartilage [201].

If only the cartilage surface was damaged without extending to the subchondral bone, the chondral defect was not likely to be filled completely by the repair process. This was due to insufficient migration of cells and inadequate proliferation of chondrocytes that were trapped in the extracellular matrix [94]. However, in a full thickness defect that included damage to both the cartilage surface and the subchondral bone, the osteochondral defect had access to the pool of cells from the bone marrow [110], [94], [202] which facilitated repair process. However, the repaired tissue had different characteristics from the native one with less stiffness and more permeability [203], [204]. The generated tissue in the defect site had biomechanical properties that were similar to those of fibrocartilage, with less structural organization and a higher amount of collagen type I than found in healthy articular cartilage [94]. Thus, the produced tissue was mechanically inferior

and with time and loading, it was broken down, fragmented or disintegrated [202], [110], [205], [94].

Despite the load bearing ability of articular cartilage, it could be gradually damaged due to repetitive wear and tear, which might advances further into osteoarthritis (OA) [206]. Due to the limited ability of articular cartilage for repair, any untreated injuries, might advance further into osteoarthritis. Osteoarthritis has been described as the most common form of joint disorder and characterized as imbalance between the synthesis and degradation of the articular cartilage [207], [206] .

The weight-bearing joints, such as hip and knee are the main targets of this disease. Osteoarthritic joints experience some structural changes such as a) narrowing of the joint space because of cartilage loss, b) formation of osteophytes (bone spurs) at the joint margins, and c) bony sclerosis (more density and thickness of subchondral bone) [196] .There is a sequence of changes in the joint due to osteoarthritis (Figure.2.7, Figure.2.8). The structural component and mechanical quality of osteoarthritic articular cartilage changes and this is reviewed by Knecht et al. [208].

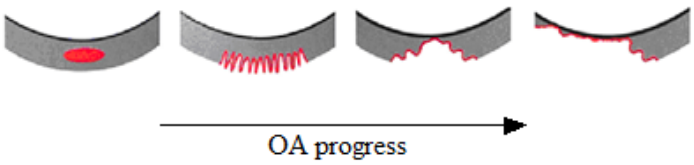

Figure.2.7 The depth-wise damage to articular cartilage due to osteoarthritis [206].

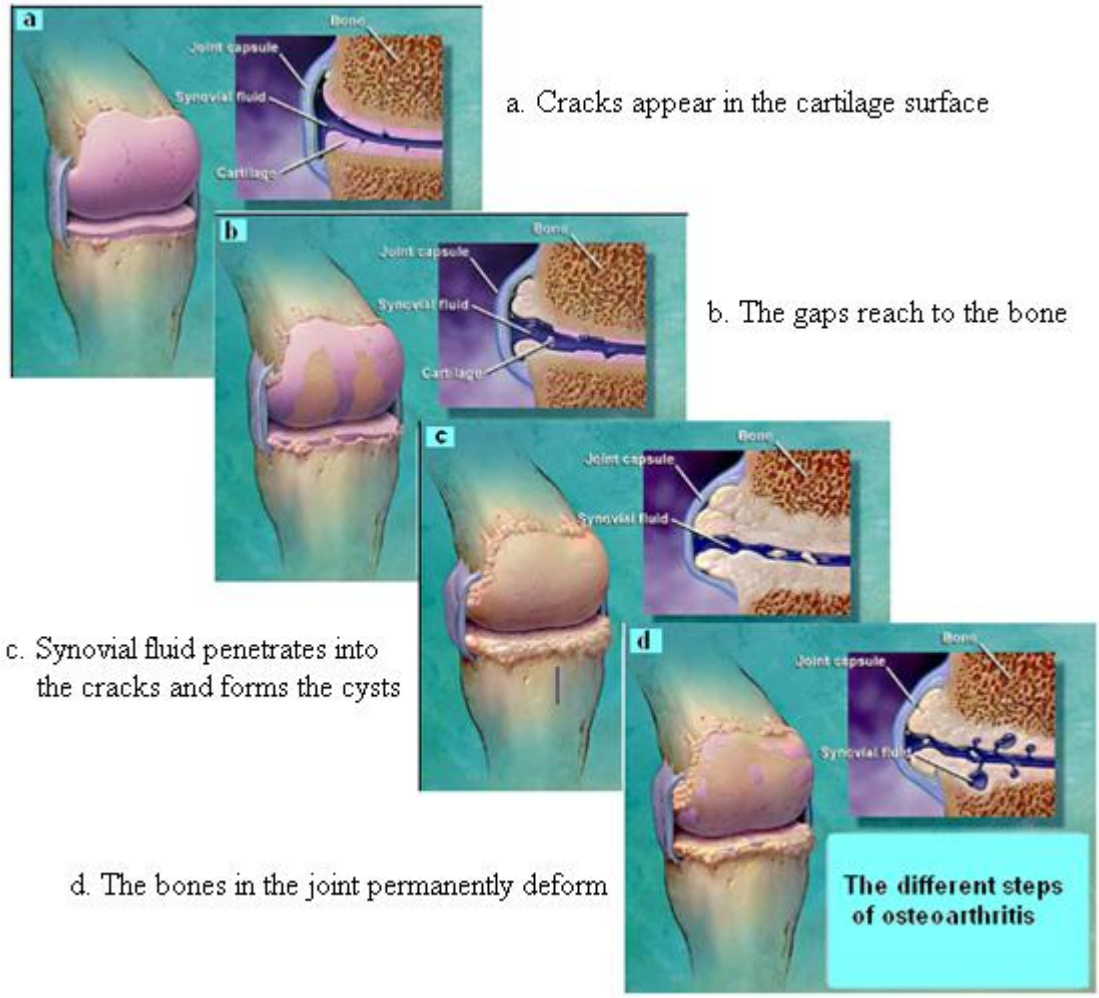

Figure.2.8 The sequence of changes (from (a) to (d)) in the appearance of the knee joint in the progress of osteoarthritis [209].

Persons with articular cartilage disorders need to be treated to relieve their pain and improve their joint function in order to accomplish their daily activities and maintain their activity levels. The surgical options for treatment of articular cartilage lesions and restoration of the function are discussed in the next section.

2.8 Traditional Methods for Articular Cartilage Repair

As mentioned previously, cartilage has a very limited ability to regenerate or to repair due to its avascular nature which prevents its access to adequate numbers of reparative cells. Generally the surgical repair methods or options are grouped in three categories: palliative (arthroscopic debridement), reparative and restorative [210]. The applied techniques are patient-specific and depend on the size and location of the defect, the patients' physical demands and treatment goal and history [210].

For small and shallow defects, usually marrow stimulation (reparative group) using a microfracture technique is recommended. In this technique, the defect is drilled out with penetration to the subchondral bone. This promotes bleeding and migration of stem cells and other factors to form reparative fibrocartilage tissue [210]. The joints that undergo such treatments often suffer from abrasion of the opposing surfaces after surgery since the developed tissue in the defect site is not functionally comparable with the articular cartilage.

Other surgical options (restorative group) for the repair of cartilage defects include transplantation of the osteochondral graft from the same patient (autograft) [211-214] or from a donor (allograft) [214-219], [205]. Autografts are usually harvested from the non-weight bearing locations and are best fitted and integrated in defect areas less than 2 cm^2 [220]. Allograft transplantation can treat larger lesions of more than 2.5 cm^2 and those with significant bone loss [210]. Complications of the osteochondral grafting techniques has been inadequate availability of donor tissue [210], donor site morbidity [220], [221], risk of infection, unsatisfactory filling of cartilage defects and fibrocartilage hypertrophy of the donor site [221-223].

Articular cartilage tissue can be regenerated in the defect area using autologous chondrocyte implantation (ACI). First, chondrocytes are harvested from a biopsy of cartilage in the non-load

bearing regions of the joint to be expanded *in vitro* for 3-4 weeks or until the volume increased to 30-fold for implantation in the defect site [210], [221]. Then, a bed for cellular adhesion, is provided by debridement process (removed damaged tissue to reveal the healthy cells beneath), then a periosteal patch (usually 2 mm larger than defect size) is harvested and sewn to the cartilage. A small opening is left for injection of chondrocyte under the periosteal flap that is then sealed by fibrin glue [221], [224-228]. Despite good clinical results at short-to-medium follow-up , graft hypertrophy and arthrofibrosis had been the most common complications after autologous chondrocyte implantation [229], [230], [231]. The schematic representation of the autologous chondrocyte implantation procedure is shown in Figure.2.9.

Orthopaedic implants are used to replace the entire joint (total joint arthroplasty) for patients with joint diseases like osteoarthritis and for defects that are larger and deeper than the size that can be handled by grafting techniques. These implants are anchored to the bone surrounding the joint. Complications for total joint arthroplasty (surgical repair of joint) include infection, post-operative dislocation, leg length discrepancy, wear and loosening of the implant [232-234]. However, for badly damaged joints, either by disease or trauma, there is no current clinically viable alternative.

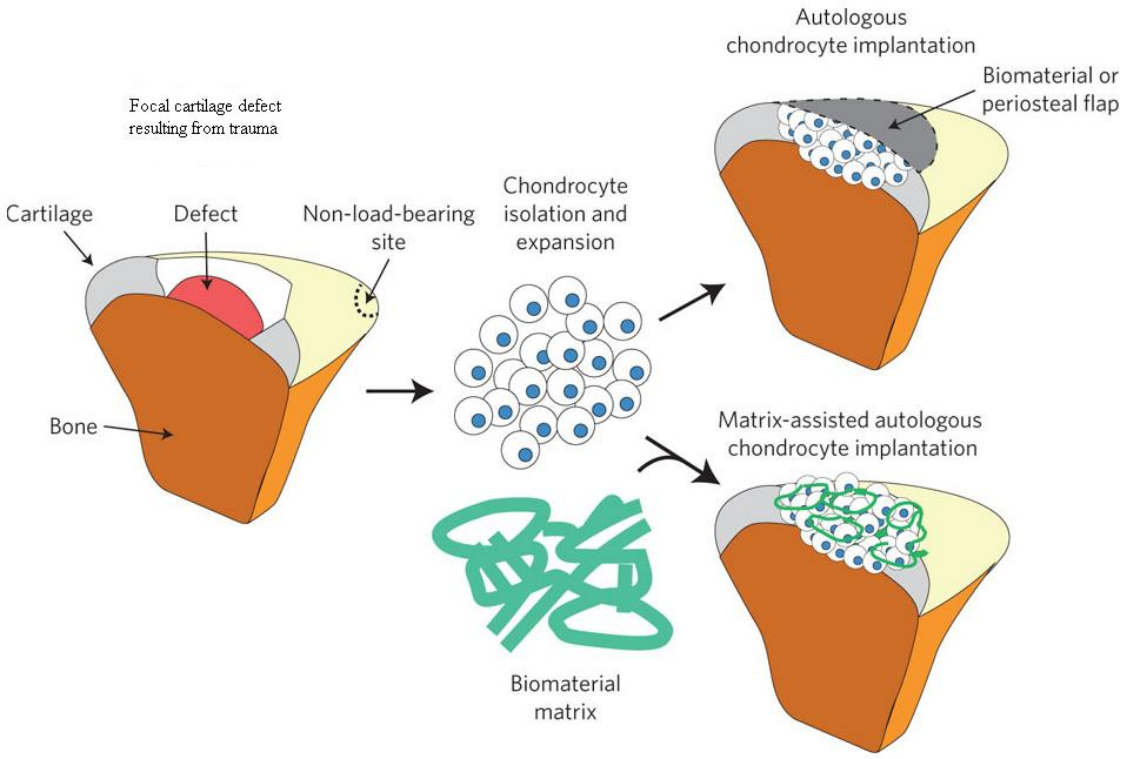

Figure.2.9. Autologous chondrocyte implantation (ACI) [235].

The surgical strategies for articular cartilage repair, has shown hopeful short-term clinical results for small damaged regions, but have not yet been able to achieve a breakthrough in its long-term outcomes [236]. However, new approaches based on tissue engineering are being developed in attempts to address the limitations associated with the above-mentioned clinical techniques, as described in the following section.

2.9 Articular Cartilage Tissue Engineering

Tissue engineering techniques have emerged as potential regenerative therapies for treatment of articular cartilage injuries. These techniques involve developing biological substitutes that could

restore, preserve and improve the functions of damaged tissues [237], [238]. It integrates a variety of science and engineering disciplines to create functional constructs with the potential of providing a permanent solution to articular cartilage damage or loss [16] or reducing the problems associated with the current cartilage treatments. It combines the knowledge developed in cell and molecular biology, material science, engineering and chemistry and also medical science to produce hybrid substitutes [239]. The biodegradable matrices, cells, signalling molecules (e.g. growth factors) made hybrid substitutes that used natural signalling pathways and components of organisms to restore tissue functions [240], [241], [242], [243], [240], [239].

Ideally, the regenerated articular cartilage tissue should have similar structure, zonal organization, biochemical composition and mechanical properties as natural articular cartilage [15]. The regeneration process could be fully or partially done *in vitro* and completed *in vivo*. The *in vitro* regeneration of articular cartilage was considered to be relatively simple due to absence of vascularity and innervation of the tissue and its limited cell diversity [244]. However, it was found to be very challenging to mimic structurally organized zones of this tissue that were needed when placing regenerated cartilage in the very demanding *in vivo* environment [244]. Articular cartilage exhibits many levels of complexity; the extracellular matrix, interstitial fluid, and ions serves as a signal transducer in articular cartilage, converts joint or explants loading to various extracellular signals (e.g. deformation, pressure and electrokinetic phenomena) that influences chondrocytes biosynthetic or catabolic activities [39].

Tissue engineering of articular cartilage has been either scaffold-based [17], [245-252] scaffold-free [74], [253-261].

2.9.1 Scaffold-Based Method of Tissue Engineering

Scaffold-based methods involve taking cells from a patient, increasing the numbers of cells in an *in vitro* culture, placing cells on a three-dimensional scaffold, generating a graft or tissue engineered construct and placing it back into the body [15] (Figure.2.10). The scaffolds can provide the initial structural support where the cells can adhere to for certain amount of time and gradually grow their own matrix. They can also help transport target cells into cartilage defect sites and mechanically support it from the physiological load [262]. They can guide the shape of the tissue; fulfill various functions of the native tissue temporarily and enhance tissue restoration by their material composition and porous microstructure [13].

The success of scaffold-based method was found to depend on the properties of scaffolds material such as its biocompatibility (chemical and mechanical) and biodegradability. The structure of scaffold itself was also important such as the porosity, size, density, distribution and interconnectivity of the pores. Various natural or synthetic biomaterials (polymers, hydrogels and composite materials), with different fabrication techniques have been made and used to address the requirement for functional scaffolds with material, mechanical and structural properties that provide the right chemistry for good cell distribution and attachment [263]. In case of using the biodegradable scaffolds, the structure of scaffold are supposed to degrade when the cells made their own matrix [264] either during or after healing of the cartilage injury [13].

Specially, for load-bearing structures, such as for cartilage, the scaffold was found to need mechanical properties to provide adequate initial stability at the defect site and it was supposed to gradually transfer the physiological mechanical stimuli under functional loading to newly formed tissue [39]. As an implant for articular cartilage, the scaffolds were required to be non-toxic and non-antigenic along with being capable of fixation in the defect site, able to facilitate cell

attachment, able to regulate cell expansion and possess high cell/tissue biocompatibility to prevent any adverse cellular/tissue reactions [13]. Good integration of newly developed tissue with the host tissue was also highly desired. The scaffolds could be a matrix of collagen, a structural protein, or synthetic biodegradable polymers; laced with chemicals to stimulate the growth and multiplication of cells.

One problem that sometimes happened in the experimental research using scaffolds for engineering of articular cartilage was the rapid formation of tissue on the outer edge of the scaffold at the expense of tissue in the centre, which becomes necrotic due to limitations of cell penetration and nutrient and waste exchange [265].

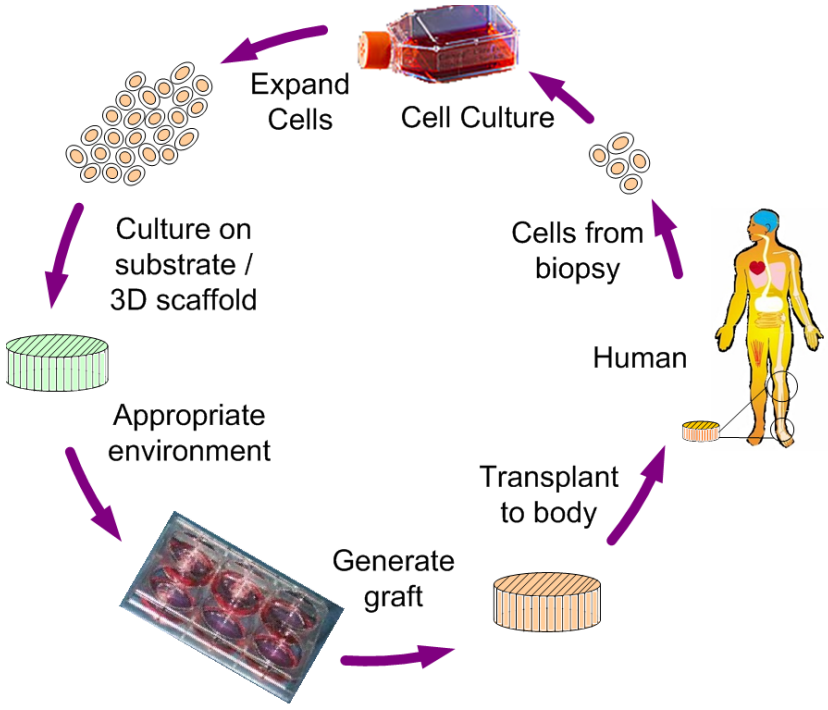

Figure.2.10 Basic and common steps of scaffold-based tissue engineering.

2.9.2 Scaffold-Free Method of Tissue Engineering

The scaffold-free method may eliminate some difficulties associated with the use of scaffolds such as their degradability characteristics and biocompatibility of their materials [256]. Some scaffold-free methods for tissue engineering used alginate gel, agarose gel, rotational-wall vessel, and a suspension culture of aggregating chondrocytes. Nagai et al. [257], [258] and Furukawa et al. [266] believed that these approaches as with a conventional culture, induced differentiation of chondrocytes from dedifferentiated chondrocytes, but with difficulty in the regulation of arbitrary (non-geometrical) shapes. Scaffold-free constructs could be created in a few weeks by seeding cells at a high density (~2-20 million/cm^2) [88, 89]. A method for generating a scaffold-free cartilage construct using porous calcium polyphosphate substrate was introduced in some studies [63, 64], [267-269]. Another method called the alginate- recovered-chondrocyte (ARC) method used mature bovine and human articular chondrocytes to also make 3D scaffold-free cartilaginous tissue constructs [261].

The scaffold-free approach for building three-dimensional constructs was often used for scientific studies rather than developing tissue grafts. In these studies, chondrocyte behaviour and cartilage development in three-dimensional environment were examined, considering the effects of different growth factors, antagonists and medium supplements [9], [270], [262]. Pellet culture was another scaffold-free model made by centrifugation of small number of cells. The insufficient pellet size was the limiting factor in its use for cartilaginous tissue, despite the high quality of tissue and its easy production [271]. Suspension culture, as another model, could be made from higher number of cells to form a highly packed cell aggregation in suspension culture [272], [262]. Differentiated chondrocytes were encapsulated in alginates for redifferentiation of the cells, and these cells were then isolated and cultured in multilayer to produce a cartilage tissue [271].

2.9.3 Cell Source

An ideal cell source for tissue engineering should potentially be capable of proliferation and then differentiation *in vitro*, in a way that can be reproducibly controlled [273]. Many types of cell sources have been used in tissue engineering of articular cartilage, depending on the strategy of the regeneration process [108]. The cells could be from donors in various age ranges: embryonic, neonatal, adult or immature. They could be used in various differentiation stages, such as precursor cells or phenotypically mature cells. The method of their preparation could also differ (selection, expansion, gene transfer) [13]. The source could be bovine, rabbit, equine, human chondrocytes or embryonic chick limb bud cells, or mesenchaymal stem cells from bone marrow [273].

The choice of cell type influenced *in vivo* function of engineered cartilage constructs such as potential for integration and *in vitro* culture requirements such as structure and degradation rate of scaffold, or medium supplement [273]. Adult chondrocytes were not easily harvested but cells from younger donors better responded to environmental stimuli [273]. The appropriate number of cells and their potential to differentiate, shape and preserve the correct phenotype to do specific functions was found to be very important in the general success of tissue engineering [274]. The production of extracellular matrix with the correct organization, secretion of signalling molecules, and interaction with other surrounding cells and tissues were found necessary function of cells [274]. The presence of biosynthetically active could regulate the ability of the tissue engineered graft for continued development and integration after implantation *in vivo* [13].

Primary cells are mature cells obtained from the enzymatic digestion of articular cartilage tissue from biopsies of the patients, followed by their isolation and then expansion *in vitro* [239]. Primary cells have desirable immunological compatibility, but low proliferation potential [274]. Their expansion often generated few cells with low growth rate. This gave a limited number of cells

available for seeding onto the scaffolds [239]. The longer the expansion of chondrocytes took, the more there was dedifferentiation of cells with a degradation of their functionality and loss of their phenotype or their original properties such as shape and protein expression [239]. The dedifferentiation of chondrocyte caused the production of fibrocartilage instead of hyaline cartilage. Alternative cell sources such as stem cells had the potential to reduce some of the challenges associated with using primary cells [275]. Stem cells are undifferentiated cells that could differentiate into one or two types of cells [274], [264], [276]. They could be isolated from embryos, fetuses or from adult tissue. Adult stem cells are found in various tissue niches such as bone marrow, brain, liver, and skin. They could be removed from a patient, incorporated into a tissue construct and placed back into the same person. However, problems with accessibility, problems with restricted differentiation problem, and poor growth limited their application in general tissue engineering [274].

2.10 Chondrocytes Seeding and Culturing Conditions

As it was explained before, in scaffold-based method of articular cartilage tissue engineering, chondrocytes during their *in vitro* culture time need a three-dimensional biomaterial scaffolds to maintain their phenotype and dynamic yet controlled environment to produce functional tissue. For effective regeneration, similar environment as *in vivo* have been provided *in vitro* by considering cell-cell and cell-matrix interactions and their critical role in biological signals [277], [278].

Bioreactors have been developed in attempts to provide an *in vitro* environment for systematic development of functional tissue structures by isolated cells on three-dimensional scaffolds [13]. They were designed to regulate conditions in culture medium such as temperature, pH, osmolality,

nutrients, metabolites or regulatory molecules; to help in mass transfer between the cells and the culture environment; to provide mechanical signals such as interstitial fluid flow, shear, compression or hydrostatic pressure; and sometimes to make spatially uniform concentrations of cells in scaffolds [13].

Besides cell population [268], [279], [280] and cell density [281-284], cell seeding conditions (static or dynamic) have played a crucial role in enhancing the process of cartilage regeneration. Previous studies reported that seeding of scaffolds under dynamic conditions (such as in spinner flasks or bioreactors), compared to static ones, facilitated high seeding densities and more even distributions of cells [285-288]. Convective mixing enhanced the kinetic rate, efficiency, and spatial uniformity of cell seeding on three-dimensional scaffolds and improved tissue structure and composition. Hydrodynamic factors modified function of cells and development of tissue. They affected mass transport between the developing tissue and culture medium; and on physical stimulation of the cells (e.g., shear, pressure) [273]. In dynamic cell seeding conditions, perfusion of medium and the provision of nutrient permitted better growth and maintenance of the tissue throughout the three-dimensional scaffold and made it more effective compared to static condition [289]. In mixed flasks, mechanical stirring of fluid enhanced mass transport in bulk medium, but created turbulent shear which could be detrimental to the cells and tissue development [290]. However, in rotating vessels, dynamic fluctuation happened in the laminar fluid flow which could improve mass transport without adverse hydrodynamic effects [13], [290]. Direct perfusion through cultured constructs could also stimulate chondrogenesis (how chondrocytes make cartilage) due to combined effects of enhanced mass transport and fluid shear in the cell microenvironment (at physiological interstitial flow velocities) [273].

In static conditions, there are no stirring, shaking, or perfusion during the cultivation [290]. The mass transfer between the culture medium and tissue construct in static condition is slow due to absence of hydrodynamic shear at the surfaces of the construct [290].

The cell culture conditions are more important for seeding large scaffolds to make implants for potential clinical use. High yield will be required to maximize the utilization of donor cells; high kinetic rate was needed to minimize the time in suspension for anchorage-dependent and shear-sensitive cells; and high and spatially uniform distribution of attached cells was needed for rapid and uniform tissue regeneration [286].

2.11 Mechanical Loading of Engineered Articular Cartilage

Biomechanical interactions of chondrocytes with biomaterials scaffolds or matrices affect cell attachment, cell viability and the overall function [33]. Mechanical loading of cartilage and chondrocytes caused intracellular cell signaling that produced various molecules involved in viability of chondrocytes and maintenance of cartilage [291]. For articular cartilage, the physiological mechanical loads influence and control the growth and hemostasis of tissue [292], [33], the chondrocyte metabolism and synthesis of matrix proteins [58], [293-298].

Engineered cartilage tissues that were dynamically loaded had better properties compared to unloaded tissues (e.g. better distribution of GAG or collagen, and stiffer outer edges of constructs) [299]. The stem cells in three-dimensional culture environments that received proper mechanical stimulation and the effect of loading on chondrogenesis have been studied extensively [29], [46], [84], [300-314].

To study the dynamics of tissue and cells and also relevant tissue engineering processes, articular cartilage has been loaded by many types of forces such as compression, tension, shear, hydrostatic pressure or electric forces via different mechanical stimulators [106]. Several bioreactors and mechanical stimulators for tissue engineering of articular cartilage have been developed to apply mechanical loading to natural cartilage (explants), tissue-engineered cartilage, or cell-seeded constructs during *in vitro* culture. Several techniques were implemented to include such loads in a system for mechanical stimulation.

2.12 *In-vitro* Loading Experiments

To improve the strategies for engineering of articular cartilage, and to overcome the problem of inferiority of mechanical properties for regenerated tissues or cell-seeded constructs, recent studies focused on the application of mechanical loads on chondrocytes and mesenchaymal stem cells [236]. One of the central challenges in advancing the field of tissue engineering and regenerative medicine was stated as the design and operation of bioreactors that could connect the applied loads to the forces sensed by cells, and could relate nutrient delivery to cells using mechanotransduction pathways [33]. Understanding how a chondrocyte integrated the stimuli into response of interest and controlling how these stimuli were applied to chondrocytes in growing cartilage were important in success of tissue development *in vitro* [33].

Simplified loading regimes enabled the development of models and helped in gaining knowledge about mechanobiological processes. The design of bioreactors which could provide nutrient delivery and/or mechanical stimulation progressed to include and to integrate various loadings and motion with the opposing surfaces that received compression, shear and sliding [315].

Functional tissue engineering involves the *in vitro* application of mechanical stimulation to the tissue constructs within the physiological loading range to make a similar environment that could meet the *in vivo* functional (mechanical) demands [283], [296], [316]. Cell functions in three-dimensional engineered tissue were controlled to promote appropriate tissue development *in vitro* by application of biochemical and mechanical stimulation. Several approaches were examined to improve *in vitro* production of articular cartilage tissue. Some techniques such as gene therapy, stimulation by growth factors and mechanical conditioning have shown some benefits for improving the engineered articular cartilage ECM [317].

Articular cartilage experiences various mechanical loads in physiological conditions, such as compression, frictional shear, fluid induced shear, and hydrostatic pressure. The physiological loading was found to affect the behavior of chondrocyte during articular cartilage development [278] and could regulate the function of cartilage growth and maturation *in vivo*. Different regimes of joint loading have led to great differences in articular cartilage structure (e.g. thickness), composition (e.g. proteoglycan content) and mechanical properties (e.g. indentation stiffness) [3].

To study the mechanism behind translation of the mechanical load into a biochemical signal, *in vitro* systems were developed that applied simplified versions of the complex *in vivo* loading situation. The effects of mechanical stimuli, such as static, dynamic compression, hydrostatic pressure and fluid shear on the metabolic activities of cartilage explants and cells, were examined by *in vitro* experiments using these systems. Although, the simplified loading conditions did not fully represent the complexities of joint loading and articulation, they could be applied in a controlled manner with full knowledge of the loading history. These *in vitro* systems provided a preconditioning environment for engineered tissue or cell-seeded constructs (before implantation) to help them reach to certain level of maturity that could enhance their *in vivo* performance [236].

The results of all previous studies [18], [20], [318], [319], agreed on the positive effects of the mechanical forces on the rates of matrix.synthesis.

2.12.1 Mechanical Stimulation by Static and Dynamic Compression

Mechanical compression has been applied either to chondrocytes in matrix in various ranges of amplitude and frequency. It is generally believed that the application of non-physiological load range could be either ineffective or injurious to articular cartilage tissue. High impact loads have been shown to cause matrix injury [198] and chondrocyte apoptosis [320], [199]. High impact loads are not applied in the present study and therefore the subsequent discussion is on loads in the normal physiological range.

The effects of different modes of compression were extensively studied on explants especially in older studies [53], [56, 57], [59], [297], [321- 339]. These effects were further studied on the *in vitro* regenerated articular cartilage [44], [47], [63, 64], [340, 341] or the chondrocyte-seeded constructs [50], [298], [342-358].

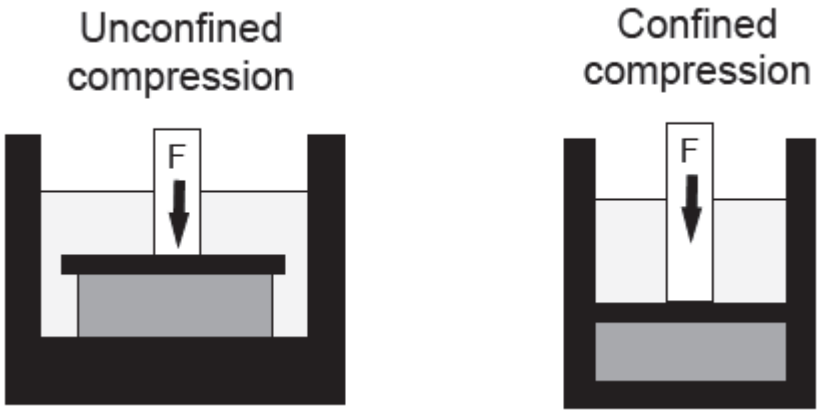

Figure 2.11 Two examples of compression loading methods [1].

The unconfined compression (Figure 2.11) was considered to be the most common form of loading for *in vitro* testing protocols [359]. In this kind of compression, the cartilage explant specimens or cell constructs were compressed vertically while radial expansion was not restricted. The effect of compression was related to biophysical changes such as cell and matrix deformation, intratissue (or interstitial) fluid flow (with its associated pressure gradient), changes in pH and charge density [70], [360] and was correlated to some physiochemical changes such as altered matrix content, fixed charge density, mobile ion concentration and osmotic pressure. Any of these signals (mechanical, chemical or electrical) could alter matrix metabolism [134].

Static compression of cartilage had negative effects by decreasing synthesis of proteoglycan and collagens through metabolic modifications at the cellular level [361]. Static compression at 50% amplitude on tissue engineered cartilage constructs made by seeding the primary chondrocytes onto fibrous non-woven poly-glycolic acid (PGA) scaffolds, suppressed the synthesis of both sulfated GAG and protein by 35% and 57%, respectively [297].

In another study [362] the cell death were tracked in different zones of live articular cartilage explants which were statically compressed by approximately 65% of their original thickness in either the axial direction (giving a depth-dependent strain profile) or the transverse direction (giving a uniform strain gradient). The results after 12 h of static loading showed more cell death in statically loaded samples with respect to the unloaded controls. More importantly, they found that the depth profiles for chondrocyte death did not correlate with compressive strain profile. However, they did find that more superficial zone chondrocytes died and thus they hypothesized that superficial zone chondrocytes were simply less tolerant of static loading (but not strain) than

chondrocytes in the middle and deep zone. They speculated that the superficial zone chondrocyte were different in some way than the middle and deep zone chondrocytes.

In contrast, the dynamic compression studies have reported the stimulation of the production of matrix proteoglycans and proteins by the chondrocytes. Application of cyclic compression in an attempt to simulate the walking cycle showed to have stimulatory effects on the transport of nutrient and soluble factors in articular cartilage.

The amplitude of mechanical stimulation was found to have an effect in the synthesis of the extracellular matrix macromolecules [336], [363]. High strain amplitude (up to 15%) of compressive forces was beneficial for proteoglycan synthesis whereas low amplitude (~ 3%) was good for the synthesis of collagen [363]. Frequency of mechanical stimulation was another influential factor in matrix synthesis. The frequencies between 0.01 and 1 Hz could stimulate matrix synthesis whereas frequencies less than 0.01 Hz suppressed matrix synthesis [321], [359], [64]. Duration and length of experiment changed the final results of matrix synthesis.

The long-term effects of intermittent mechanical stimulation in both long periods of stimulation (3 hr/day) [58], and short periods of stimulation (6 min/day) [64] for 4 weeks, resulted in increased matrix accumulation as well as improved the mechanical performance of the developed tissue compared to unstimulated tissue. The stimulated tissues in long-term experiment contained approximately 40% more collagen and 30% more proteoglycans as well as two to three fold increase in compressive mechanical properties [64].

2.12.2 Mechanical Stimulation by Shear Loading

Rather than just transmitting compressive joint loads to the underlying subchondral bone, native articular cartilage also provides a low friction interface between contacting cartilage surfaces of the

joints. Mimicking this loading condition has been attempted in some *in vitro* studies to investigate the effects of shear with different methods (e.g. one apparatus for shear loading is shown in Figure 2.12). The rationale behind shear loading studies was the hypothesis that cell matrix deformation due to shear would stimulate chondrocyte biosynthesis even without significant interstitial fluid flow and pressure gradients [328], [364], [365]. It was noted that shear deformation of a homogeneous isotropic poroelastic tissue caused minimal volumetric changes and therefore made minimal intra-tissue (interstitial) fluid flow or its associated pressure gradient [365]. Shear loading was applied at frequencies of 0.01–1.0 Hz and in the 1–3% range of shear strain, which was within the range of physiological tissue loading [365]. The results reflected the stimulatory potential of macroscopic matrix shear (without fluid flow) and it showed that tissue shear could regulate matrix biosynthesis.

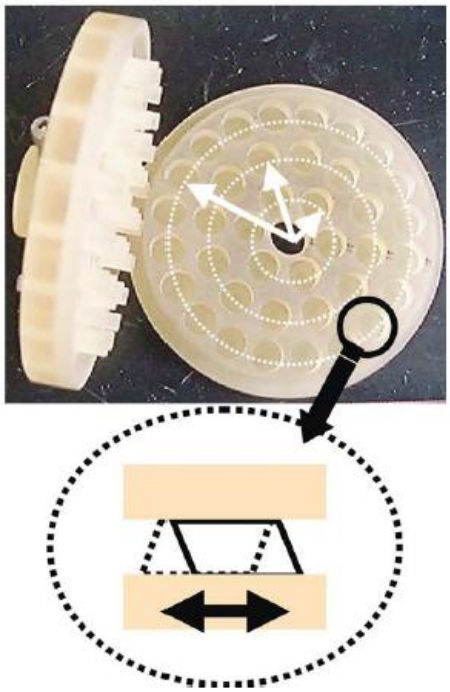

Figure 2.12 Shear loading chamber, including three groups of wells located in various radii from the center, to be able to apply three different magnitudes of shear strain [70].

The increase in proteoglycan synthesis has also been observed by the application of fluid – induced shear forces to chondrocyte monolayer cultures in rotating culture vessels. Long-term culture under this condition increased matrix accumulation and improved mechanical properties of the tissue *in vitro*, but also unfavorably increased synthesis of inflammatory cytokines and matrix metalloproteinases. According to Waldman et al [364] the long-term (4 week) application of intermittent cyclic shear forces during tissue formation resulted in 40% more collagen, 35% more proteoglycans, threefold increase in compressive load-bearing capacity and six fold increase in stiffness compared to the static control. They also found that low amplitude (1-3%) of shear strain stimulation favored collagen and proteoglycan synthesis, whereas high amplitude (~10%)

suppressed synthesis of these macromolecules. The frequencies between 0.01-1 Hz stimulated matrix synthesis, but frequencies lower than 0.01 Hz prohibited matrix synthesis. The application of frictional shear stress was also useful as it modified the superficial layer of the cartilage [41-43], [45], [72]. This is discussed in subsequent sections.

2.12.3 Mechanical Stimulation by Hydrostatic Pressure

Different techniques were used for hydrostatic pressure application on articular cartilage tissue or cell-seeded constructs. They either compressed a gas phase that transmitted load through the medium to the cells (Figure.2.13), or compressed only the fluid phase using a hydraulic press that was directly attached to a piston connected to fluid-filled chamber [82]. The first method allowed controlled changes of partial pressures within the medium with possible risk of alteration in gas concentration within the culture medium.

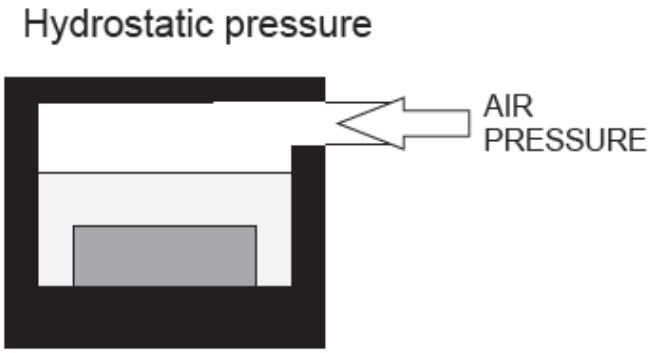

Figure.2.13 Schematic representation of one of the methods of hydrostatic pressure application [1].

During the periods of loading *in vivo,* chondrocytes of articular cartilage can sense hydrostatic pressure due to interstitial fluid flow within the matrix. The assumption that hydrostatic pressure might increase matrix synthesis of *in vitro* engineered cartilage, change the extracellular matrix

production, or mechanical properties of loaded tissue or construct, has motivated many studies. Either static or cyclic hydrostatic pressure, was applied on the articular cartilage tissues or cell-seeded constructs in various experiments [74-81], [83, 84], [366] as an agent for increasing the metabolic activity of chondrocytes in tissue engineering studies. These experiments investigated the effects of either static or dynamic hydrostatic pressure with various magnitude, frequency and duration on chondrocyte differentiation/metabolism, on matrix accumulation in tissue such as collagen and GAG production, on collagen and GAG synthesis, and on mechanical properties of the tissue or constructs such as compressive and tensile stiffness. These studies and their effects were collected and discussed in review article by Elder et al. [82].

The application of physiological hydrostatic pressure (5-10 MPa) showed beneficial effects on articular cartilage properties. When 3D cultures received static hydrostatic pressure their functional properties were enhanced. The application of dynamic hydrostatic pressure showed more benefits than static hydrostatic pressure and controls [82], [367]. The effect of frequency and magnitude of hydrostatic pressure were more pronounced in collagen production rather than GAG [368].

2.12.4 Mechanical Stimulation by Fluid Convection/ Perfusion

Creating hydrostatic pressure difference between two sides of the construct (Figure.2.14) was one of the methods that forced the fluid to flow through the construct [1]. The flow of the fluid parallel to the top surface of the construct (Figure.2.15) also created a fluid induced shear and could affect the biochemical and mechanical properties of the superficial layer.

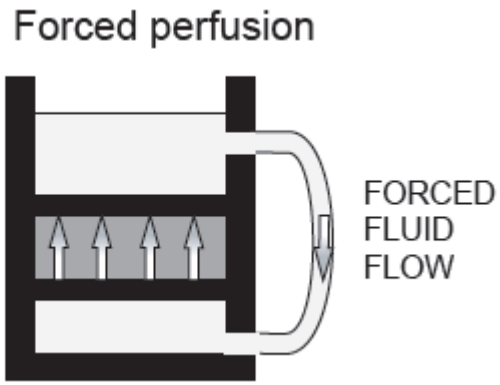

Figure.2.14 Schematic representation of forced fluid perfusion through the construct [1].

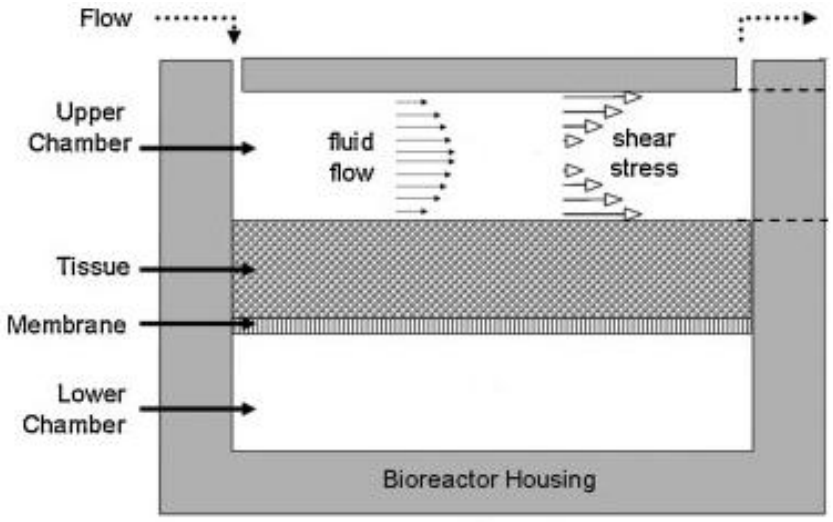

Figure.2.15 Application of fluid-induced shear on tissue by recirculating nutrient media through the upper chamber and creating laminar flow parallel to the top surface [69].

Fluid convection (fresh/recirculated nutrient) through and around cartilage tissues helped to develop tissue by increasing the overall mass transport and provided mechanical stimulus as modulators of chondrocyte metabolism [86-92]. Active perfusion ensured supply of nutrient and

removal of waste products and created fluid-induced shear stress which could stimulate the expression of cartilage specific matrix markers [369]. Agarose chondrocyte constructs which were exposed to perfusion (0.5 ml/min, hourly intermittent perfusion, 10 min + 50 min rest, every day for 21 days) had a 1.9 times higher sGAG/DNA content than statically cultured constructs [369].

2.12.5 Mechanical Stimulation by Combined Loading

2.12.5.1 Compression and Shear Incorporation

Combined compression and shear concurrently were more beneficial because they profoundly mimicked the real physiological conditions of the articular cartilage comparing to sole compression or shear force [44], [46], [48], [49], [328].

In Frank et al [328] constructs were compressed and received cyclic (0.01- 1 Hz) shear deformation with 0.4-1.6% strain range. These constructs were compared with control constructs held at the same compression but without shear using a custom designed loading apparatus as shown in Figure.2.16. The disks that were exposed to 0.1 Hz and 1% shear stain, had higher 35 S-sulfate and 3H-proline incorporation (measures of proteoglycan and protein synthesis [363]) by 25% and 41% respectively.

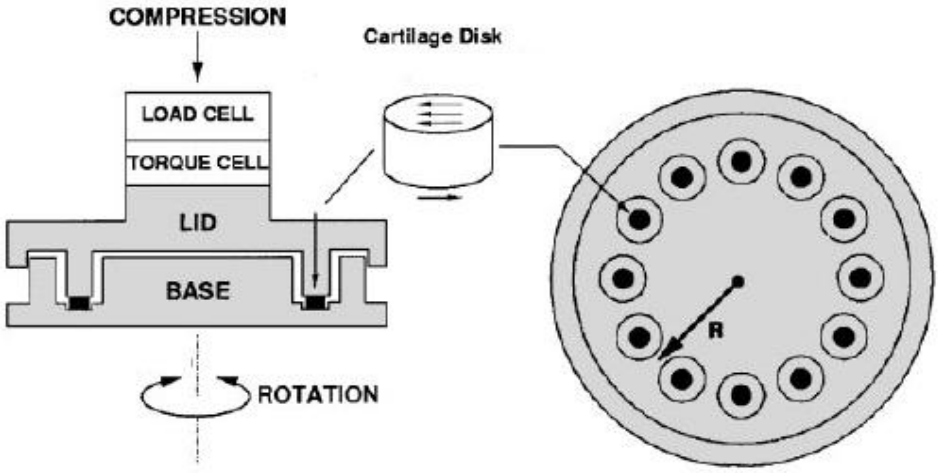

Figure.2.16 Apparatus for application of compression and shear for cartilage explants. The explants were placed in wells in the base of chamber; the platen were roughened (no adhesive) to conduct the shear loading experiments [328].

In Waldman et al [44], 5% compression combined with 5% shear strain also increased the synthesis of both collagen and proteoglycan over the static controls. This mechanical conditioning of *in vitro* grown articular cartilage from bovine chondrocytes in the period of 4 weeks resulted in more extracellular matrix accumulation and better mechanical properties comparing to untreated tissues. The mechanically conditioned tissues had 54% more collagen and 46% more proteoglycan but lower DNA content compared to unstimulated controls. The average 3-fold increase in compressive modulus and 1.75 –fold increase in shear modulus was also found for mechanically stimulated samples.

The role of shear on the fate of stem cell differentiation and the effect of surface shear superimposed on cyclic axial compression on chondrogenic differentiation of human bone-marrow derived stem cells were investigated [46]. The samples were exposed to unconfined dynamic compression at 1 Hz with 0.4 mm sinusoidal strain superimposed on a 0.4 mm static offset strain

which made strain amplitude of 10-20% of the scaffold height at the construct's centre. They received shear through oscillating ball on the construct's surface (~ ± 25 º at 1 Hz). The effects of each individual loading as well as combined loading were investigated. The combined loading treatment of the samples influenced chondrogenic gene expression. The amount of GAG per DNA of combined loading group was higher over controls, but for the individually loaded groups, the shear only load could influence the GAG per DNA, and not the compression only [46].

Pingguan- Murphy and Nawi [48], applied 10% direct compression and 1% shear on bovine chondrocytes seeded in three-dimensional agarose hydrogel during 12 h (followed by 12 h rest) and showed significant increase in GAG synthesis compared to uniaxial or unloaded samples.

An *in vitro* loading system for the combined application of cyclic compression and shear on 3D chondrocyte-agarose constructs was also introduced by Di Federico et al [370]. The loading system could provide strain via a vertical actuator and its functionality was validated only by application of loading regimes at 1 Hz for up to 48 h and tracking the cell viability. Their stimulation had a non-destructive effect on viability of chondrocytes within a short period of time. But long-term effects of their loading are unknown and the benefit of this technique for enhancement of the cartilage-like properties is yet out of reach.

2.12.5.2 Compression and Fluid Perfusion Incorporation

Tran et al [47] applied cyclic unconfined compression with fluid perfusion simultaneously to three dimensional cell cultures (chondrocytes isolated from femoral condyles and femoral heads of neonatal pigs, seeded in 2% agarose) using CartiGen C9-x bioreactor from Tissue Growth Technologies. The medium was recirculated through the samples at constant flow rate of 0.5 ml/min. Then, they were subjected to 1 Hz sinusoidal unconfined compression for 4h/day, 5

days/week, beginning with 0.5 N and increasing to 10 and 20 N the second and third weeks respectively. After 1 week of static culture and 4 weeks of stimulation, the samples both perfused and loaded groups had significantly higher equilibrium and dynamic modulus compared to static groups (with higher value for perfused group compared with the loaded ones). The GAG measurement (retained GAG only) revealed higher content in perfused and loaded group compared to both static group and native cartilage (with almost similar content in perfused and loaded groups). However, the collagen contents of all static, perfused and loaded groups were similar and significantly lower than native porcine cartilage.

Complex loading regimes were also attempted by Spitters et al [51] using a dual flow bioreactor for articular cartilage explants. The bioreactor combined mechanical stimulation (confined cyclic compression) with a system that nutrient was supplied only by diffusion from opposite sides of the construct. The dual compartment bioreactor facilitated the formation of gradients of nutrients and growth factors. However, the cartilage explants under 0.25 MPa compressive load (~ 0.25% strain) for 24 h including cycles of 1 h compression and 7 h rest showed considerable cell death at its top and bottom. This response was in contrast to negligible cell death in static or dynamic culture of explants.

2.12.5.3 Sliding Contact Inclusion in Combined Loading

A study by Shahin and Doran [49], investigated the effects of combined loading on cell seeded constructs made from polyglycolic acid (PGA) mesh or PGA-alginate scaffolds during the longer exposure time, using a mechanobioreactor (shown in Figure.2.17). The constructs were precultured in shaking T-flasks for 2.5 or 4 weeks before mechanical stimulation. This mechanobioreactor, applied frictional shear and compression at frequency of 0.05 Hz with peak-to peak strain amplitude of 2.2 % superimposed on static axial strain of 6.5% for compression up to 2.5 weeks

(10 min per day). Shear direction changed after 5 min, and the samples were completely unloaded after 10 minutes of stimulation. Such a stimulation regime enhanced (on per cell basis) the synthesis of both GAG and collagen type II by up to 5.3- and 10-fold respectively. The amount of collagen type II as percentage of total collagen also increased due to mechanical stimulation about 3.4-fold in each construct.

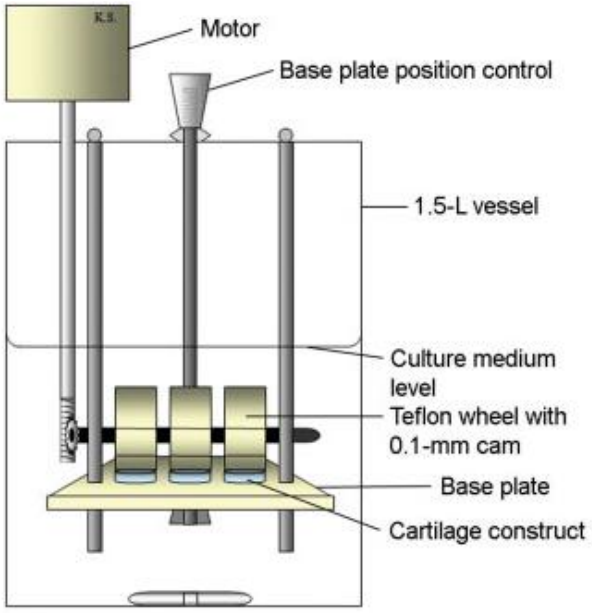

Figure.2.17 Schematic diagram of mechanobioreactor components capable of application of both compression and shear to the constructs. It contains three wheels above a movable base plate holding three tissue constructs [49].

Grad et al [42], [43] , [72] and Wimmer et al [41], adopted the technique of combined loading by adding the articulation and oscillation of a ceramic ball to static or dynamic compression on the constructs made from polyurethane seeded with bovine chondrocytes (shown in Figure 2.2.18).

The articular motion of ceramic ball applied frictional shear to the surface of constructs that stimulated the production of superficial layer proteins (SZP). Dynamic compression 0.1 Hz, 5, 10 or 20% strain + equal static offset strain) and ball oscillation (0.6 Hz with ±60º amplitude) applied on the constructs (for 1 h/ time, 2 times/day, 3 days) with free swelling in between the loading intervals, resulted in significant increase of mRNA expression and release of superficial zone protein with respect to controls (held at same level of static or dynamic compression).

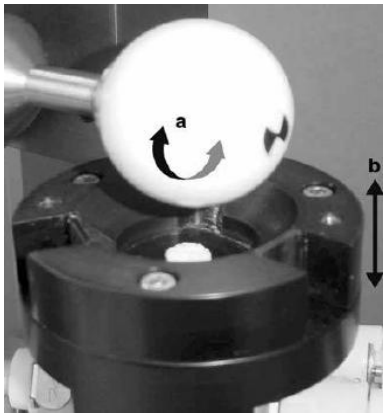

Figure 2.2.18 Reciprocating motion by oscillation of the ceramic ball and compression the vertical direction [72].

Kaupp et al [50] applied combined loading regime on chondrocyte-agarose hydrogels with the intention of generating superficial like layer on top of the construct surface using commercially available two-axis Mach-1micromechanical testing system V500C (Biomomentum Inc., Laval, QC). A "moving point of contact" type stimulation (MPS) [371] was applied at frequencies of 0.5, 1 and 2 Hz under a constant compressive load of 10 mN for durations between 5 and 60 minutes for 3 consecutive days. Through these studies, it was found that gene expression of superficial markers was dependent on the frequency of stimulation, where 1 Hz frequency could result in maximum expression of PRG4 and collagen type II.

Huang and co-researchers [372], designed a bioreactor which used impermeable spherical indenter (Ø25 mm) to apply sliding contact (SLC) to the 2% agarose hydrogel strips (41.5 mm × 7.5 mm × 1.5 mm) seeded with mesenchymal stem cells (MSC) with cell density of 20 million cells/ml after 21 days of culture before stimulation. The indenter moved with velocity of ± 2.5 mm/s (0.1 Hz) over sliding range of ±12.5 mm centered along the construct's length and applied 20% of axial strain for 3 h/day, 5 days/week for long period of times. The sliding contact stimulation improved tensile properties of MSC-seeded constructs after 42 days (including 21 days preculture time). Their biochemical analyses included measurement of GAG, collagen and DNA that was accumulated only within the constructs. DNA content decreased, both GAG and collagen contents increased due to sliding contact compared with controls, but collagen couldn't gain more than ¼ of GAG content.

Kock et al [373] also developed an sliding indentation loading regime that applied dynamic tension as well as depth varying strain field to the cell-seeded constructs. In this study 0.5% chondrocyte-agarose was sandwiched between two cell-free 3% agarose layers, and received sliding indentation at 10% depth and 1Hz for 4 h/day for 28 days. This type of stimulation resulted in a depth-dependent response at gene-expression levels, with the highest response in the highest strains regions. It also increased the collagen content, but did not influence the GAG retained within or released from the constructs.

Recently, the design of a magneto-mechano stimulation bioreactor that could simultaneously apply electrokinetic and mechanical stimuli was introduced by Brady et al [52]. The design adopted the contactless magnetic actuation with integrated sensing system to measure the applied forces and construct thickness directly and mechanical properties of construct indirectly. The beneficial effect of magneto-mechano stimulation using this bioreactor on protein accumulation on chondrocyte-

seeded constructs has not been reported yet. The functionality of the bioreactor has only been validated by measurement of thickness and applied force on the constructs over 1h dynamic loading repeatable for 3 weeks.

2.13 Concluding Remarks about Mechanical Stimulation

Static loading is a destructive pathway, whereas the dynamic loading in normal physiological range, in certain amplitude and frequency can be beneficial for the formation of articular cartilage and its matrix biosynthesis. Intermittent hydrostatic pressure has been shown to have positive results on the matrix synthesis, but the static hydrostatic pressure had some detrimental effects on collagen II mRNA production. However, the responses of the chondrocytes and articular cartilage matrix to the combination of these loads are not clear. Since each of the dynamic loading, intermittent cyclic loading (compression, shear or hydrostatic pressure) in certain amplitude, frequency and environmental condition had positive effects on the matrix production and biosynthesis; it can only be assumed that applying combination of some of these loading regimens may be in favor for regeneration of articular cartilage *in vitro* or represent better results for its matrix biosynthesis. This assumption seems to be supported with finding of the previous studies.

The controlled combination of these loadings may better mimic the complex environment of articular cartilage and chondrocytes. However, as seen in some studies, control of these loadings to favour matrix production and articular cartilage biosynthesis may be difficult. As indicated by Kock et al [8] and Teuschl et al [236] long-term clinical success has not been achieved. The aim of the present thesis is to investigate the optimal combination of loads that would lead to production of a better articular cartilage constructs to be used for defect repair.

2.14 Agarose Hydrogel in Articular Cartilage Tissue Engineering

2.14.1 Agarose and Rationales for its Use

Beside a few metallic and ceramic materials, numerous polymeric materials have been explored for their use in articular cartilage tissue engineering [273]. Many scaffolds have been developed with various material chemistry, geometry, structure, mechanical properties or rate of degradation. The sponge-like materials with interconnected porosity have been mostly used either alone or with cells seeded in their matrix. Despite the spatial arrangement of chondrocytes in three dimensional forms within these structures, the cells tendency is towards attaching to two dimensional surfaces, which alters their natural phenotype. The initial phenotype of cells and the maintenance of this phenotype throughout the process of regeneration greatly influence on the proper healing of defects in articular cartilage. Therefore, it is better to transfer cells to an environment that is more similar to natural extracellular matrix (ECM) rather than sponge-like surrounding [273].

Structures, like hydrogels with comparable morphology to ECM, are good candidates for cell encapsulation [374]. Unlike when the cells are expanded in monolayer culture, encapsulation in hydrogels allows the cells to maintain phenotypes more like natural ones. Hydrogel scaffolds were used to make a three dimensional environment for chondrocytes so they could initiate good cellular functions and generate functional tissues by preserving the cell phenotype. They formed a regulated extracellular environment that provided the opportunity for the *in vitro* studies to investigate three dimensional interactions of either cells with other cells or cells with their surrounding extracellular matrix. Gaining such information about the cellular interactions and their environment has been helpful in design of engineered tissue with certain properties or functions [374].

As noted by Buschmann et al [375] and Mauck et al [58], agarose is a hydrogel that has been extensively used in articular cartilage tissue engineering and mechanical stimulation studies for different applications (Figure.2.19). Agarose is a three dimensional network of hydrophilic [376] carbohydrate-based polymer [377] with almost up to 10% dry matter and about 90 % water. The water molecules are loosely attached to the dry matter and easily exchanged with water molecules of surrounding extracellular matrix [376]. When dry agarose and water mixture are heated to 60°-90°C, depending on the type of agarose used, it forms a solution that becomes a gel when the temperature is lowered to room temperature [374].

Proteoglycan and type II collagen are two structural macromolecules that have been used to define the chondrocyte-specific differentiated phenotype [378]. Previous research studies on synthesis of type II collagen and aggrecan (cartilage-specific proteoglycan core protein) showed that chondrocytes which were isolated from bovine [280], rabbit [378], avian [379], and human [380] cartilage tissue, and then cultured in agarose gel, were able to maintain their phenotype. However when the chondrocytes were grown on plastic Petri dishes or culture plates (2D surfaces), rabbit and human chondrocytes flattened after attachment, dedifferentiated and had fibroblastic phenotype [375].

The high water content of the agarose facilitated the nutrient exchange and solute transport [381]; and its swelling nature helped the encapsulated cells to be in an aqueous environment similar to soft tissues [281]. Because of agarose transparency, it was sometimes possible to image the transitions in cell shapes due to gel deformation and to track the size of cells or their colony formation during the culture period [375].

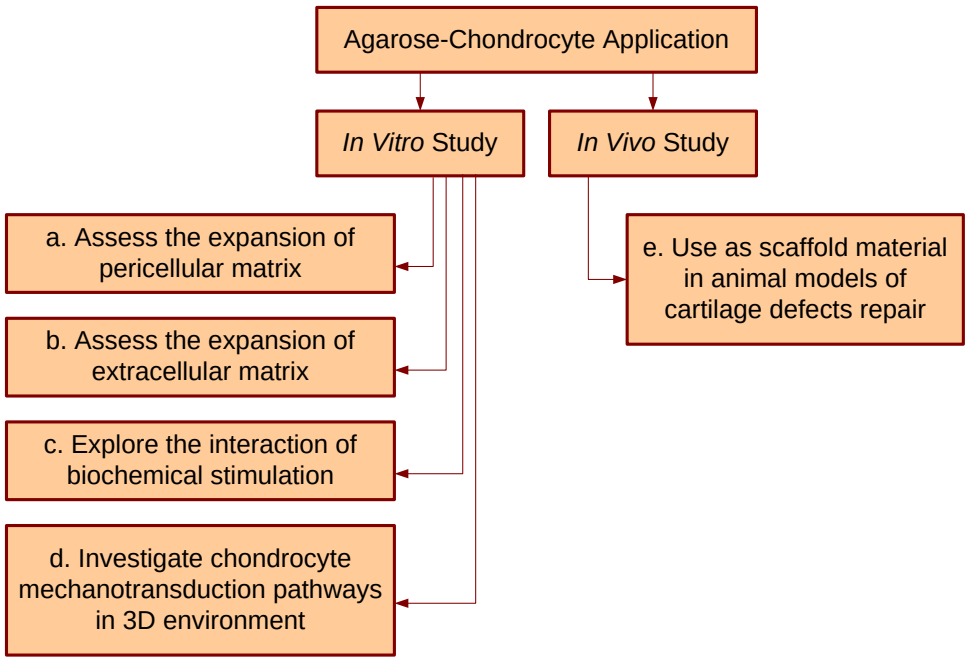

Figure.2.19 The application of agarose-chondrocyte constructs for different applications for articular cartilage tissue engineering. References: a [382], b [383], c [384], [385], [386], d [281], e [387], [388].

The chondrocytes seeded in agarose could produce homogenous extracellular matrix that could fully surround the cells and allow proper transmission of mechanical forces to the cells. This permitted the examination of mechanical stimuli on chondrogenic activities [281] and thus made it a convenient *in vitro* model system. This model was used for investigation of the intracellular variability in the displacements and strains within individual cells. It was particularly effective, because the gross compression could generate uniform homogenous cell deformation in agarose (in the absence of significant extracellular matrix) [389].

Despite the fact that agarose has been extensively used in molecular biology, the non-degradable nature of this hydrogel has been stated [374] as a possible limiting factor for accumulation of new tissue over time and thus its application in tissue engineering. However it is

still a common model for the study of the effect of loading on articular chondrocytes.

Some of the common types of agarose, concentrations of agarose, cell sources, cell densities, and construct sizes in previous studies, which involved applying loads to agarose-chondrocyte constructs, are summarized in Table A.1 to Table. A.7 in Appendix A.

2.15 Chapter Outlook

Reviewing the previous studies provided a pathway for understanding the complexity of the articular cartilage tissue and challenges associated with its *in vitro* engineering and maintaining its biochemical and mechanical properties comparable with the natural tissue. This review revealed the main requirements for *in vitro* engineering of articular cartilage and main considerations for its mechanical stimulation. It provided the knowledge about different available and helpful techniques for mechanical stimulation of either the natural/*in vitro* engineered articular cartilage or cell-seeded constructs. It shed light on main restrictions and current limitations, as well as benefits of various types of loading techniques in an attempt to mimic the *in vivo* loading. The studies that involved loading the agarose-chondrocyte was reviewed with the aim of better understating the behavior of this specific hydrogel under various loadings and finding out the common type and concentration of agarose, the cell density, and loading range and the effects of stimulation. The inclusion of review about agarose-chondrocyte was considered, because many of the experiments in our studies were conducted using this construct to develop the present hydromechanical stimulator (despite the potential use of variety of cell-seeded biomaterials with the current stimulator). Next chapter will exclusively explain the concept of our hydromechanical stimulation technique, features of

designing an apparatus that can apply such technique, and the system development of such stimulator before describing the experimental methods.

Chapter 3

Mechanical/Hydromechanical Stimulation System

This chapter, first, introduces the concept of our stimulation technique. Then, it explains the features of the designed and developed system that applies a variety of loading conditions per group either as mechanical or hydromechanical stimulation simultaneously on multiple cell-seeded constructs. The characteristics of components that fulfill the system requirements are explained in details. Finally the assembly of all of these components are presented.

3.1 Stimulation Technique

In order to investigate the hypothesis of the present thesis, a method for hydromechanical stimulation was developed that applied the combination of different loading regimes on cell-seeded constructs. An indenter was used to apply this stimulation technique. First, the indenter itself and, in some cases, additional externally attached weights applied a dead load to the cell-seeded constructs. Second, when the construct moves under the indenter the frictional shear is produced in between the opposing surfaces in relative motion. Third, the creation of fluid induced shear was possible by cannulating the indenter to let the nutrient fluid pass through it and come out of small tube (or pore) at the tip of indenter. Fourth, since the constructs were moving under the indenter and the contact zone was small compared with the total construct surface area, all normal and shear loads were applied dynamically to the construct and the chondrocytes within it (Figure 3.1).

Therefore, in this hydromechanical stimulator, the application of combination of different loading regimes was possible (Figure .**3.2**). However, it was not known for certain whether the fluid film completely separated the surfaces (although this was likely as discussed subsequently).

The fluid was nutrient media used for culturing the cells seeded within the three dimensional construct. A pocket was made at the tip of indenter to allow the forces to be applied more uniformly through a thin fluid film that was created by pumping fluid between the contacting surfaces. The created fluid film might have protected the surface to some extent from damage that could occur from the frictional forces acting directly on the surface.

The technique developed in this study represented a bioreactor-like environment by creating a dynamic environment for cells within the constructs to be cultured and receive the appropriate mechanical signals. Both fluid injection on top of the surface and also recirculation of fluid within the chamber could indicate the dynamic fluid flow environment that could encourage the cells for matrix production by continuous perfusion.

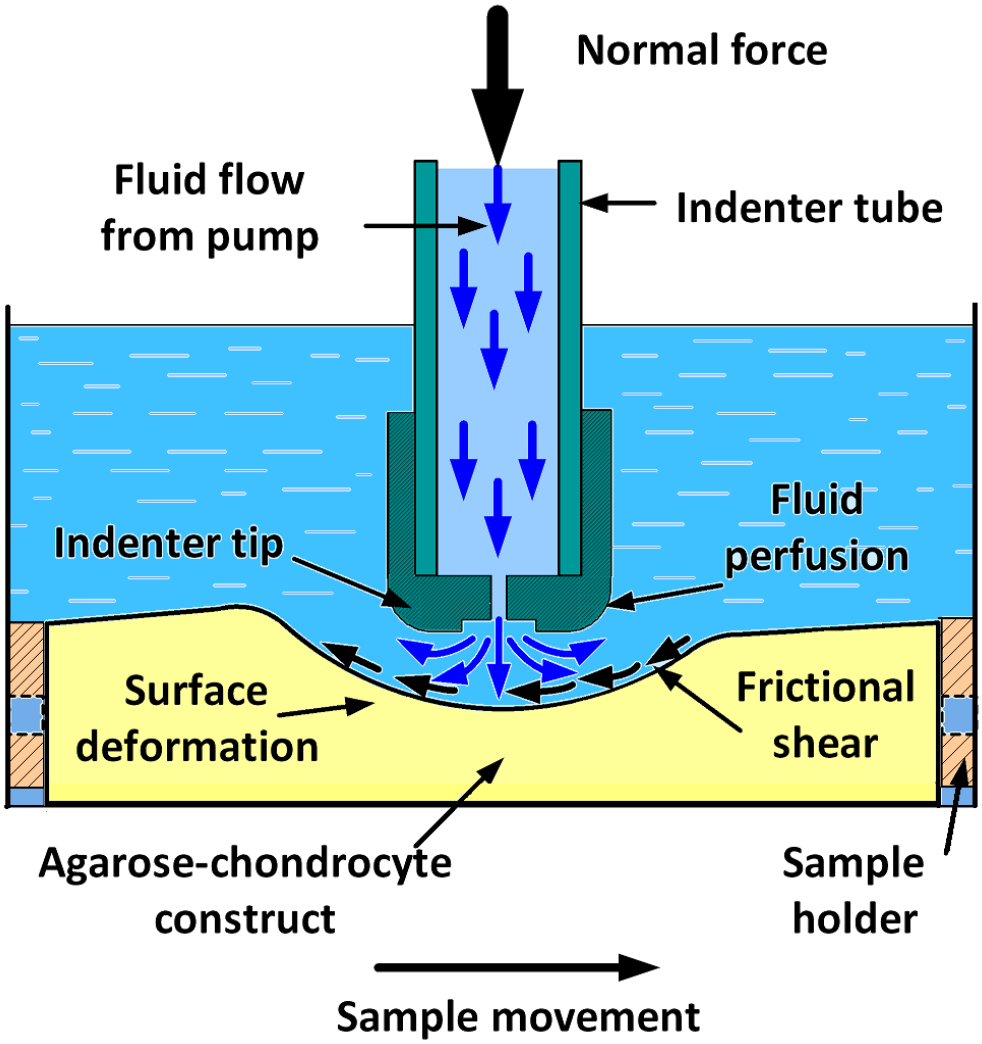

Figure 3.1 Schematic representation of hydromechanical stimulation technique. The deformation of construct surface due to loading was exaggerated to show the action of indenter when the underlying sample was moving in a specific direction.

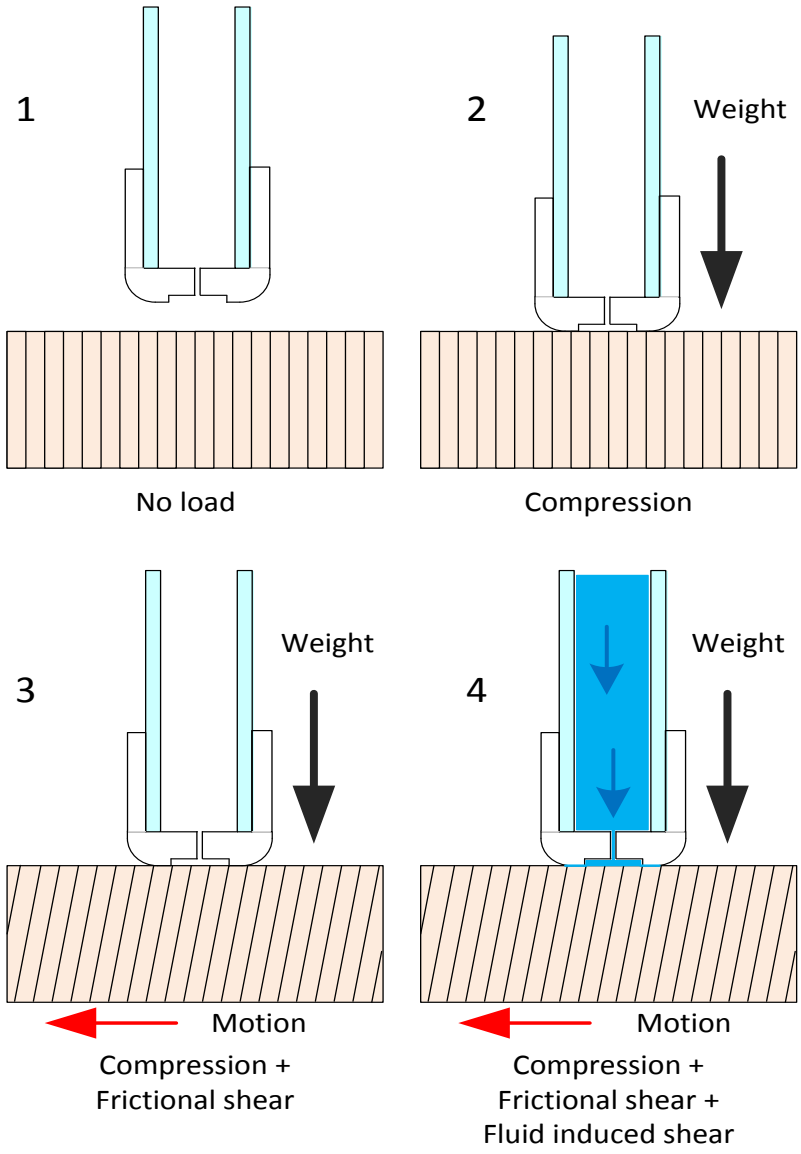

Figure .3.2 Four different loading conditions of hydromechanical stimulation: 1) The stationary construct receives no load; there is no contact between the indenter and construct; 2) A region of the stationary construct receives only static compression due to weighted indenter, 3) A region of the moving construct under the weighted indenter receives both compression and frictional shear, 4) A region of the moving construct under the weighted indenter which injects the fluid, receives combination of compression, frictional shear and fluid induced shear.

3.1.1 Equations for a Hydrostatic Bearing

Schematic representation of hydrostatic bearing with a rigid construct is shown in Figure 3.3.

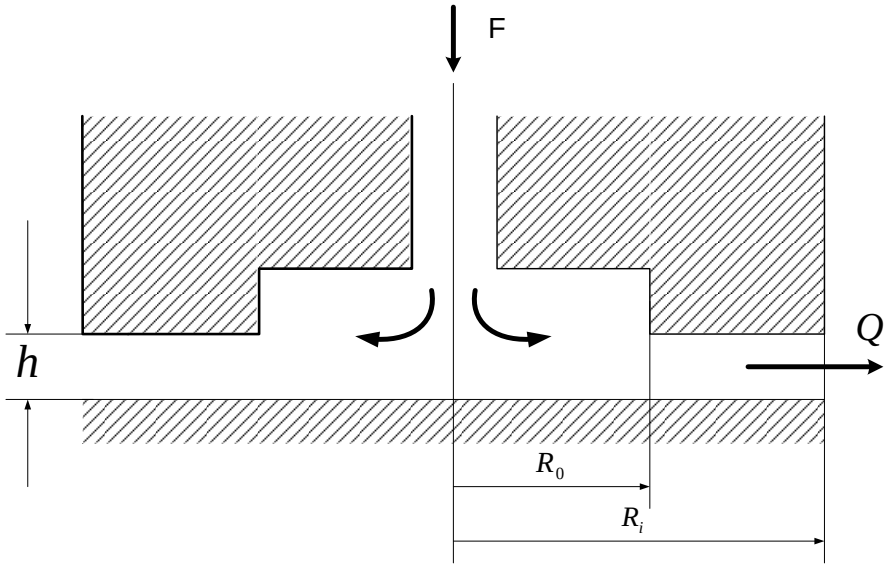

Figure 3.3 Schematic representation of hydrostatic bearing with a rigid construct.

By applying the basic governing formula for hydrostatic bearing [390]and rearranging them with parameters of the presented hydrostatic bearing model, the fluid film can be found as function of both fluid flow rate and applied normal load. Given η (viscosity), R_i (radius of bearing), R_0 (radius of pocket), Q (flow rate of lubricant/fluid) and F (applied load on bearing), the expression for h (fluid film thickness) is desired.

Reynolds equation in cylindrical coordinates: $\frac{\partial}{\partial r}\left(r \frac{\partial p}{\partial r} \right) = 0$

Boundary conditions: ($p = 0$ at $r = R_0$) and ($p = p_s$ at $r = R_i$)

Where p_s = supply pressure in pocket.

Integrating twice and finding constants, by applying the boundary condition, the pressure is:

$$p = p_s \frac{\ln\left(\frac{r}{R_0}\right)}{\ln\left(\frac{R_i}{R_0}\right)} \quad \text{or} \quad p = p_s \frac{\ln\left(\frac{R_0}{r}\right)}{\ln\left(\frac{R_0}{R_i}\right)}$$

The load is: $F = p_s.(\pi.R_i^{\,2}) + \int_{R_1}^{R_0} p.(2\pi.dr)$

Substituting in the expression for pressure:

$$\Rightarrow F = \pi.R_0^{\,2} p_s.\left[\frac{1-\left(\frac{R_i}{R_0}\right)^2}{2\ln\left(\frac{R_0}{R_i}\right)}\right]$$

Poiseuille flow equation in cylindrical coordinates is:

$$\frac{Q}{2\pi r} = \frac{h^3}{12\eta}\left(\frac{-\partial p}{\partial r}\right) \quad \text{where } \frac{Q}{2\pi r} \text{ is the volume flow rate per width}$$

Since h and Q are constant: $-\frac{\pi h^3}{6\eta}.dp = Q\frac{dr}{r}$

$$\Rightarrow \frac{\pi h^3 p}{6\eta}. = -Q\ln r + C_1$$

At $p = p_s$ at $r = R_i$: $p_s = \frac{6\eta Q}{\pi h^3}.\ln\left(\frac{R_0}{R_i}\right)$

Substituting into the expression for F:

$$\Rightarrow F = \frac{3\eta . {R_0}^2 Q}{h^3}\left(1 - \left(\frac{R_i}{R_0}\right)^2\right)$$

$$\Rightarrow h = \left[\frac{3\eta . {R_0}^2 Q}{F}\left(1 - \left(\frac{R_i}{R_0}\right)^2\right)\right]^{\frac{1}{3}}$$

3.2 Design Features

The design features of this hydromechanical stimulator include the types of loading and their combination, their dynamic or static application, the ease of assembly and maintenance of components and programmability of the constructs motions with respect to the indenters. Features such as capability of simultaneous loading of multiple constructs for instance, definitely saves times when there are large numbers of constructs to be tested.

Features of the Hydromechanical Stimulator

1) Each cell-seeded construct can receive compression on its top surface as well as fluid induced shear and/or reciprocating frictional shear due to relative motion between construct and the indenter.

2) The fluid induced shear can be applied to the construct via the same indenter that applies the frictional shear.

3) The indenter contains a large central tube for conveying the nutrient fluid with a smaller tube at the tip that conveys the fluid to a central pocket. The pocket applies fluid pressure and shear to the construct through a fluid film (see previous section 3.1.1 between two opposing surfaces that are in relative motion.

4) Multiple constructs can be stimulated simultaneously within the same culture plate while each constructs can receive their own individual compression depending on the weight of the indenter plus any added external weight that is added.

5) One multichannel pump (eight channel capacity) can recirculate the nutrient fluid to all six chambers both simultaneously and individually.

6) The construct can be moved in both lateral (X and Y) directions with a contact pattern that can be specified by programming the controllers of stepper motors. A single central computer hosts the driver programming software for both motors.

7) Feeding and loading stimulation of the cell-seeded constructs can be done within the wells of standard available culture plates, without the need of having special chambers.

8) The assembled non-electrical components are compact enough to fit inside an incubator (0.56 × 0.56 × 0.56 m, with shelves that can be placed at various levels).

9) The electrical wires can be securely and safely transferred through the incubator opening. Sealing is done to avoid any changes to the inner environment condition of the incubator that could occur if outside air had access.

10) The components of the stimulator system do not melt, degrade, or corrode while exposed to temperature and humidity condition of the incubator (37º C, high humidity up to 95%) during short or long term culture periods.

11) The material of the mechanical components in direct contact with cell-seeded construct and cell culture media are biocompatible and non-toxic, with no adverse effect on the culturing.

12) The construct can be submerged in nutrient culture media and remains in this condition during the mechanical stimulation period and free swelling.

13) The nutrient media almost fills each well and thus acts as a reservoir for the pump so the fluid can recirculate throughout the stimulation period.

14) The constructs and culture plates can be easily removed from the tray to be replaced with another culture plate (for stimulating other groups of samples).

15) The indenter holder plate maintains each of the indenters and suction tubes in a vertical orientation.

16) The indenter holder plate has only a small gap of less than 1 mm between it and the top of culture plate.

17) The indenter holder plate is made from transparent poly (methyl methacrylate) (PMMA) so that inside the well is visible from the top for better initial adjustment of indenter tip position with respect to the construct.

18) Each well of the culture plate has individual loading stimulation of the constructs and provides a reservoir for the pump in its recirculation of nutrient media.

19) In order to move the construct in a pattern that involved both X and Y directions, a hub and its programming software are used for synchronization.

Challenges

1) Direct exposure of many components of the system to the cell culture media increases the chance of bacterial contamination.

2) The maintenance of high viability of cells within the loaded construct which are in direct contact with the tip of indenter throughout the stimulation period requires the need for frequent sterilization of inside and outside of each cannulated indenter and the inside of the pump tubing. This must be done right after each stimulation period. After stimulation of all constructs, the indenter tubing and the indenter holder plate must be detached and sterilized, while the whole system is inside the incubator.

3.3 System Components

The components of system can be categorized in three different groups: mechanical, electrical and fluid flow components (Figure.3.4). The interaction of system components and method of their connection are shown in Figure.3.5.

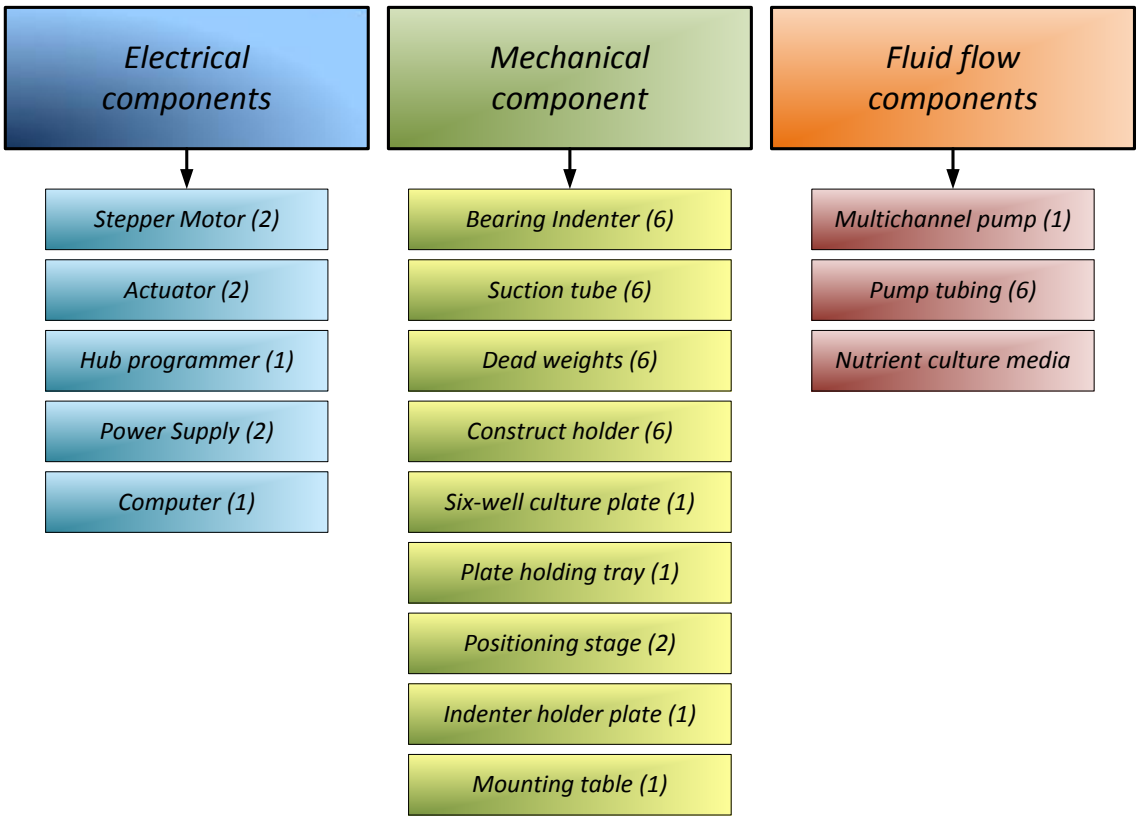

Figure.3.4 Three categories of system component, and their detailed components with current or maximum available number of individual component in the current system.

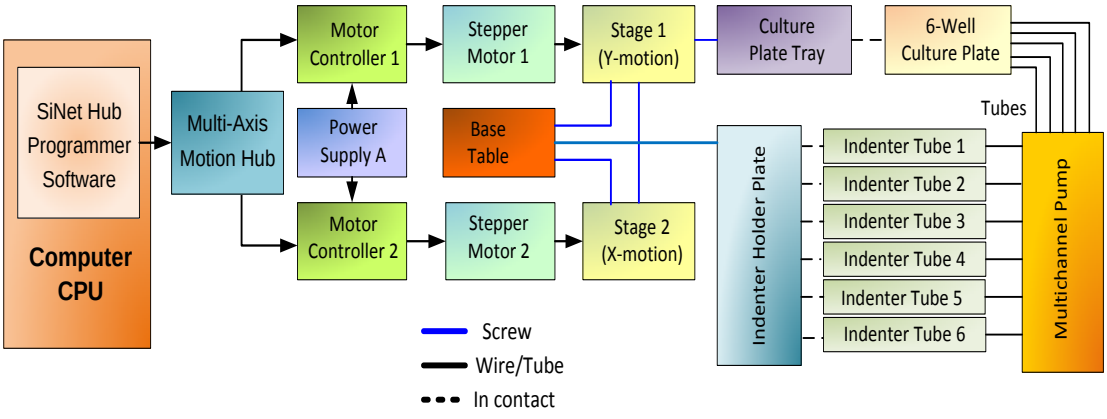

Figure.3.5 Interaction of system components and their connection.

In the multichannel hydromechanical stimulator, multiple cell-seeded constructs were individually placed in each well of a six-well standard culture plate. Each of the wells acted as a chamber for a construct and at the same time a fluid reservoir for pump to recirculate the culture media. Each construct was individually loaded. The culture plate was then mounted on a custom made tray that was attached to X-Y positioning stages. The stages were driven by mechatronic components that included two standalone stepper motors, two programmable motor drives and a single SiNet hub. The hub was networked with Si Programmer Windows software to achieve planar motion and allowed sliding contact for each of the six constructs against six cannulated indenters. The motion pattern was programmed as series of parallel lines in the X and Y directions so that the construct surface had a large centered region stimulated. Each of the indenters used for hydromechanical stimulation was connected to one channel of a multi-channel peristaltic pump. The culture media that filled the volume of each well of culture plate was pumped out, passed through suction tube, pump tubing, then the cannulated indenter and finally was pumped into the same well and injected on the surface of the construct.

3.4 Mechanical Components

3.4.1 Indenters and Tubes

The indenter was composed of a tip that was machined separately and then press-fitted at the end of a tube to meet the above-mentioned 1 to 3 requirements (Figure .3.6). The least amount of compression was applied by the weight of indenter itself; by attaching different weights to the indenter, the amount of applied compression on the construct could be increased. The weight had a hole in the center that let it to pass through the cannulated indenter and was held in position by a

stopper made of a cut plastic tubing that fitted around the indenter (Figure .3.7). The tip of indenter was rounded to reduce edge contact stress during sliding without flow, a small pocket and small pore for injecting the fluid into the pocket. The overall length of the indenter including the tip was about 110 mm.

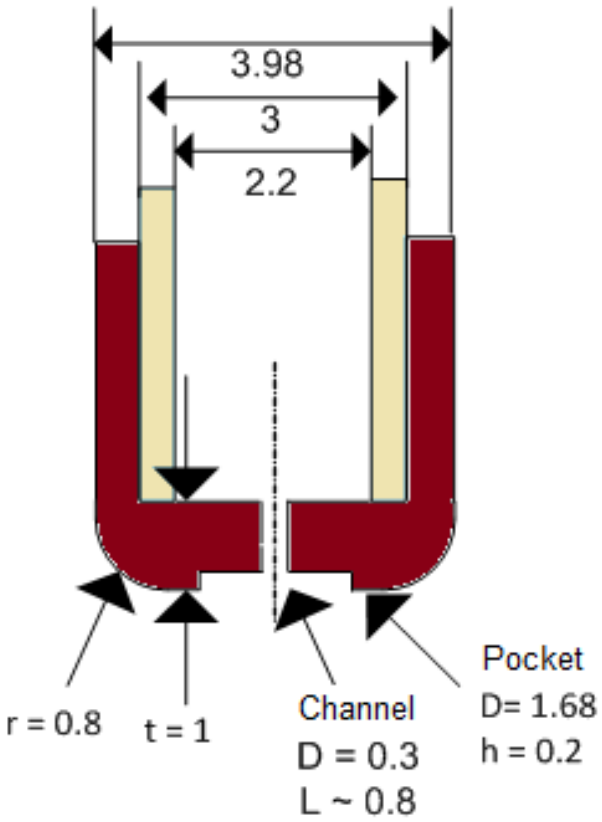

Figure .3.6 Schematic representation of the tip of the indenter (all dimensions in mm).

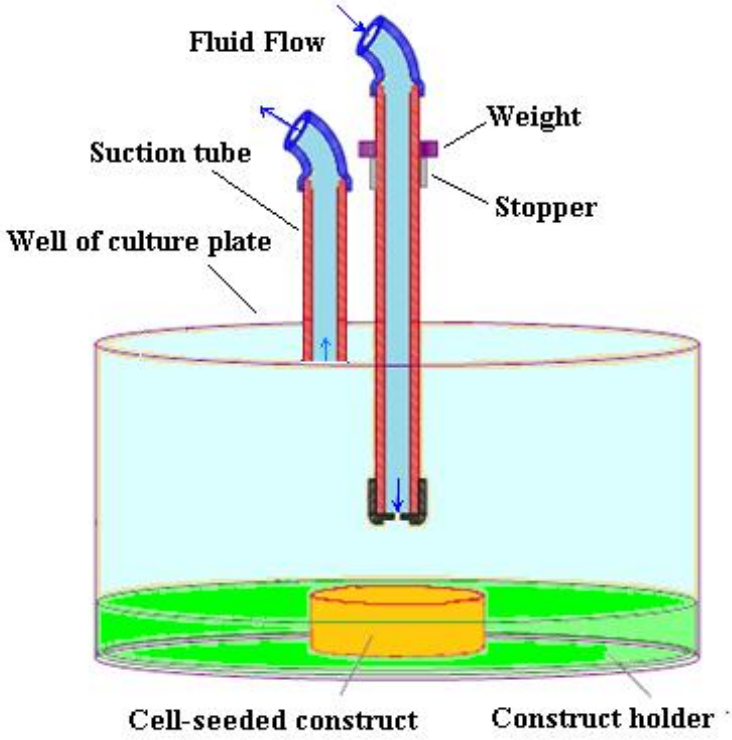

Figure .3.7 Simplified representation of an indenter and a construct held in a well of culture plate.

The fluid film between the surfaces allows the indenter to be classified as a hydrostatic bearing. Both the indenter and the tip were made from 316L stainless steel. This material was strong enough to resist bending due to shear loading at the tip, and did not corrode when it was directly exposed to the cell culture media inside the humid environment of the incubator.

A plastic tubing (long enough to connect to the pump) was attached at the end of each indenter to guide the fluid from the peristaltic pump to an individual indenter. It could be easily disconnected from the pump tubing, pulled out of its hole in indenter holder plate and sterilized in an autoclave.

A suction tube was located adjacent to the indenter to pump the culture media out of the well and let the fluid to be recirculated throughout the system (Figure .3.7).

3.4.2 Indenter Holder Plate

Six holes with diameter slightly larger than the external diameter of indenters were machined in a thick plate made from poly (methyl methacrylate) (PMMA) (Figure.3.8). In addition, six holes were machined for inserting the suction tubes and four holes were machined for screw to secure the plate to the mounting table and to position it on top of the culture plate with a small gap in between them (Figure.3.8). The thickness of indenter holder plate was calculated to allow a small gap between the top of culture plate and lower surface of indenter holder plate.

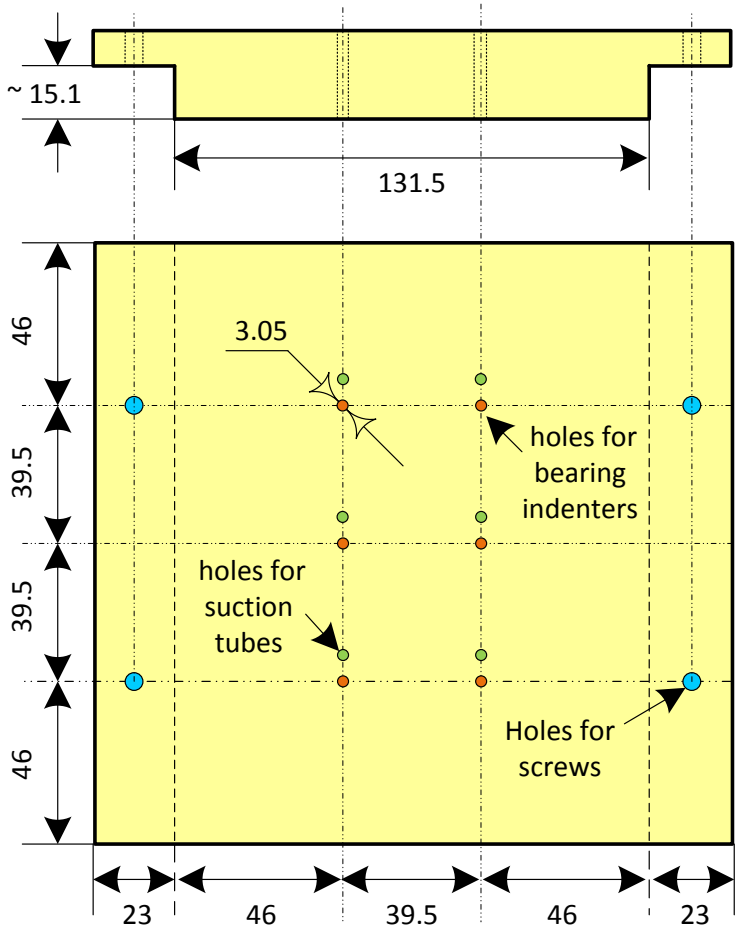

Figure.3.8 The top and side view of the indenter holder plate with dimensions (mm) and positions of holes. The size of the holes for the indenters and the suction tubes are the same.

3.4.3 Culture Plate and Holding Tray

The culture plate held the cell-seeded constructs and the cell culture media in its wells. Many aspects of the presented design were affected by the size of this culture plate, and specifically the inner size of its wells. The initial position of the indenter and maximum travel of construct under

indenter was carefully adjusted and programmed to avoid the contact of the indenter with the inner wall of culture plate well. The size of a standard six-well culture plate (Figure.3.9) influenced the dimensions of the indenter holder plate.

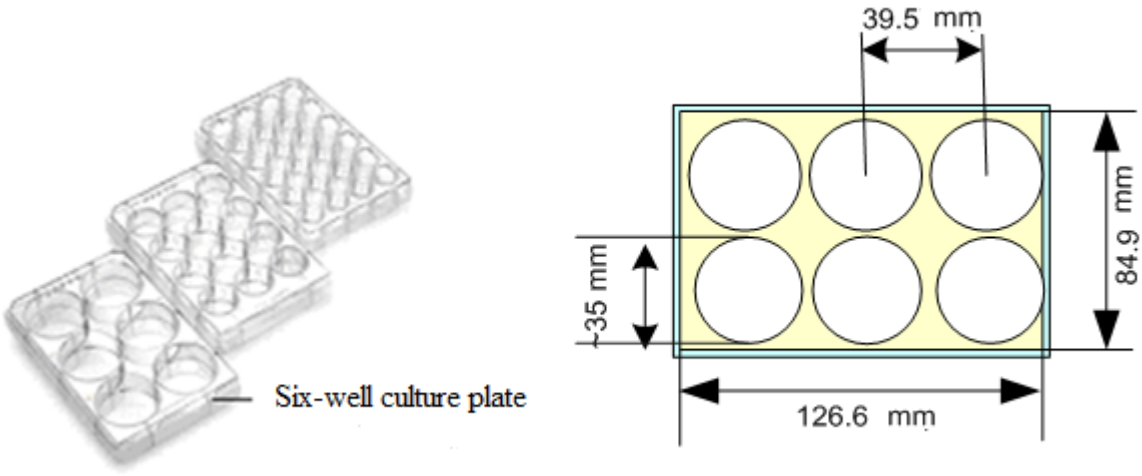

Figure.3.9 Standard six-well culture plate from Fisher Scientifics (well growth area = 950 mm^2, well volume = 17 ml).

The culture plate was held and placed in fixed position with respect to X-Y positioning stages via a holding tray (Figure.3.10). This tray connected the culture plate to the positioning stages. The tray was custom made from PVC in such a way that the inner dimensions of the tray were the same size as the external dimensions of the culture plate. The tray was attached to the positioning stage below it by four screws. The short projected wall on the side of the tray and a plastic adjustment screw held the culture plate in place and prevented from moving with respect to the stage (Figure.3.11). The tray could be easily sterilized by 70% ethanol.

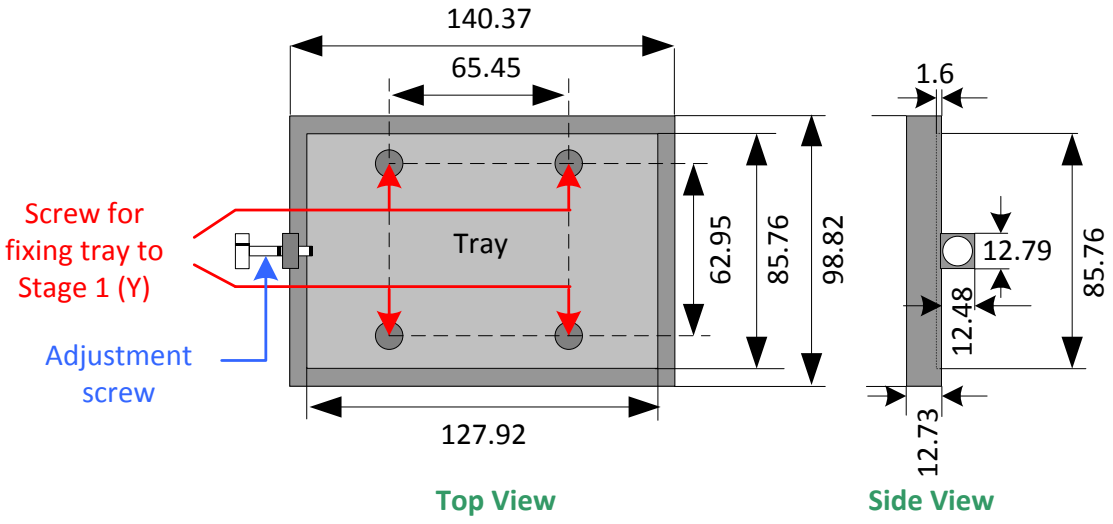

Figure.3.10 Drawing of the design of the holding tray (all dimensions in mm).

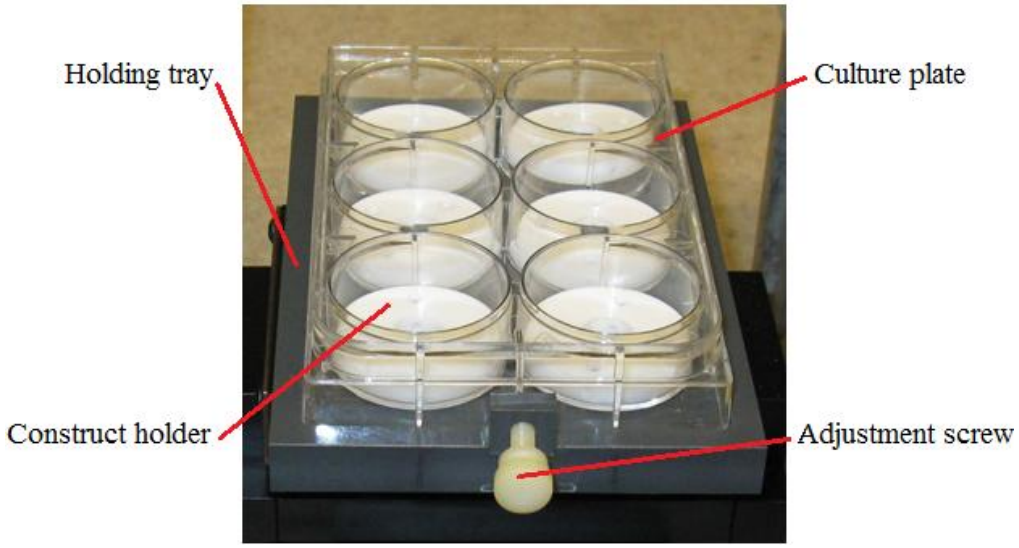

Figure.3.11 The culture plate in the holding tray.

3.4.4 Construct Holder

Cell-seeded constructs were placed in a custom built inserts (Figure.3.11) with the same height as the cell-seeded construct and the same external diameter of well of culture plate. The construct

holder was designed to have multiple interconnected channels in two axes. Almost all of the surfaces of the construct located in the center of the construct holder had access to the nutrient culture media through these channels. As shown in Figure.3.12 and Figure.3.13, four vertical channels let the culture media flow to the bottom of the well; and a large pocket made at the lower surface of the construct holder allowed the fluid of all channels to merge and stay at the lower surface. Four radial-horizontal channels passing through the vertical channels let some part of the fluid to be directed toward the middle of the construct and allowed the circumferential surface of the construct to receive the nutrient media. The cross section of construct holder, the construct, the indenter, the suction tube and indenter holder plate are shown in Figure.3.14. The construct holders were made from polytetrafluoroethylene (PTFE) to be biocompatible and can be easily machined and sterilized with 70% ethanol.

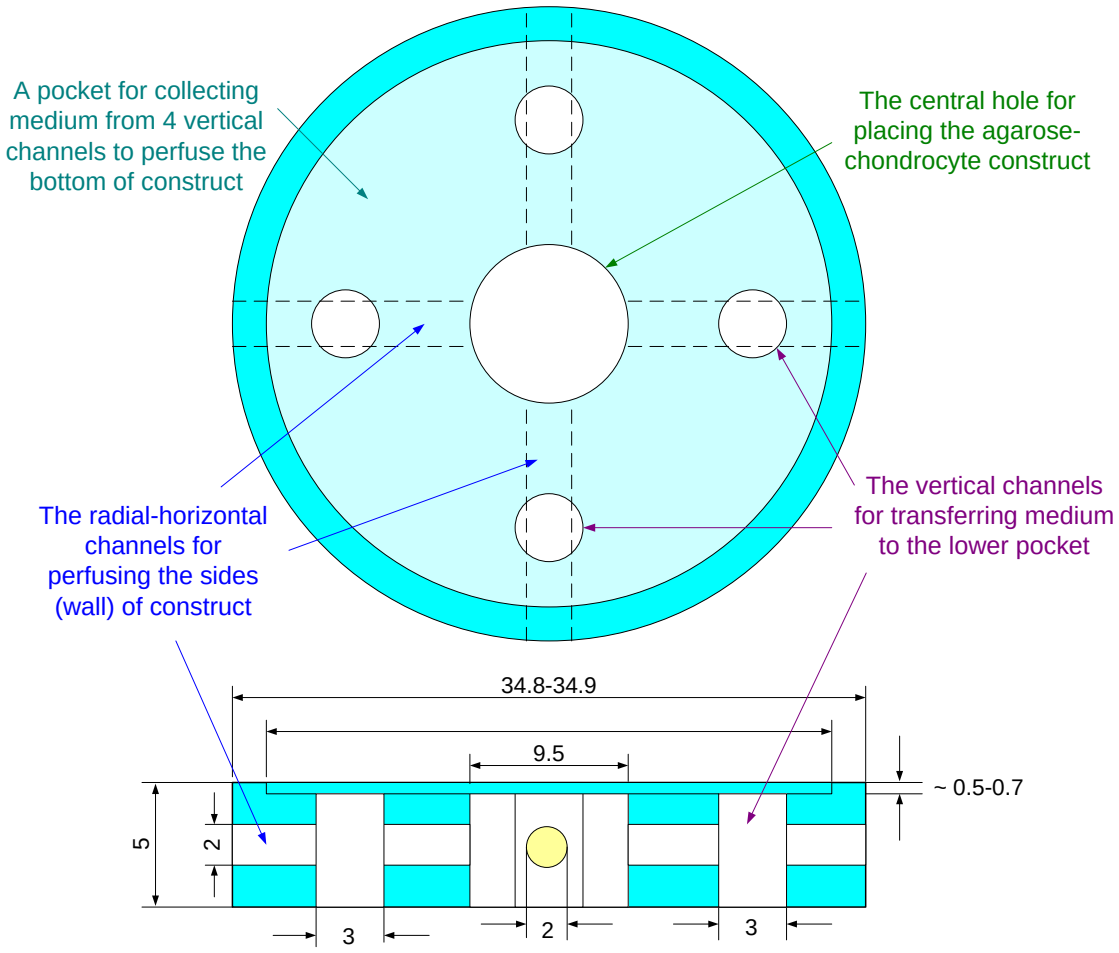

Figure.3.12 Drawing of bottom view of the designed construct holder with dimensions (mm).

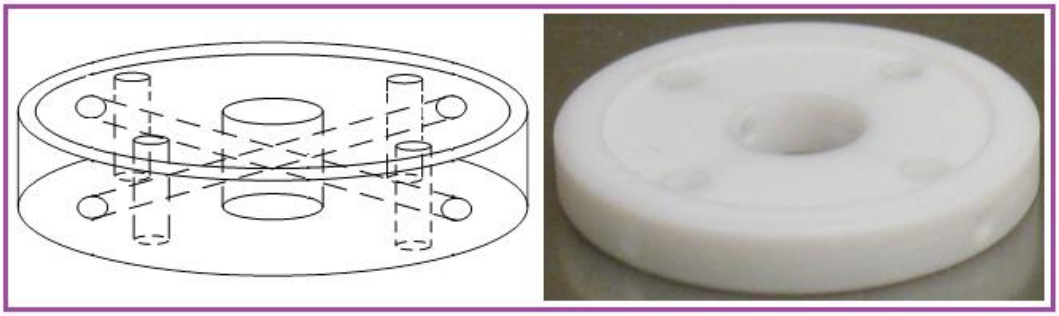

Figure.3.13 Schematic representation and fabricated construct holder with interconnected channels.

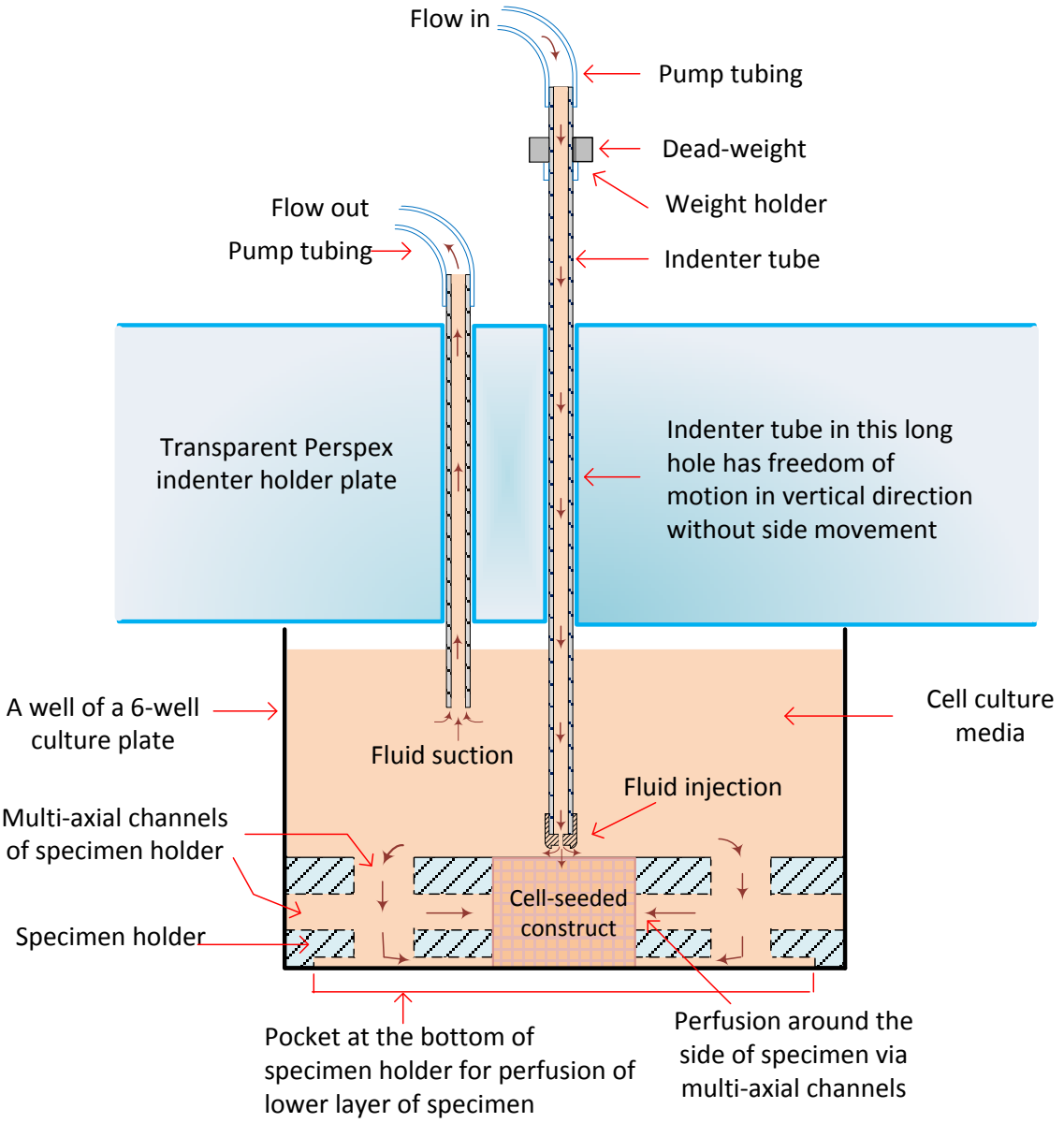

Figure.3.14 Schematic cross-sectional representation of the indenter, the suction tube, the specimen holder, and indenter holder plate.

3.4.5 Positioning Stages

Two positioning stages were needed in the system to move the construct horizontally in either the X or Y direction or combination of them. They were fixed to each other by four perpendicular screws. The positioning stages were connected to actuators to drive them in specific directions. Two identical stages, each had crossed roller positioning stages (PRC2-2X3710; PIC Design Inc., Middlebury, CT, USA) (Figure 3.15). Stepper motors were fixed to the stages by four screws on the NEMA 23 mount located at the end side of the stages. The crossed roller positioning stages transfer the rotation of the motor shaft to a screw with 3/8-10 Acme thread that had an advance of 0.8085 mm/rad (0.2 inch/ rev). This screw transmitted motion through the crossed roller slide located under the stage. Drawing and dimensions of the PRC2 crossed roller positioning stage are shown in Figure B.1 in Appendix B. The detailed specifications are explained in Table B.1 of Appendix B.

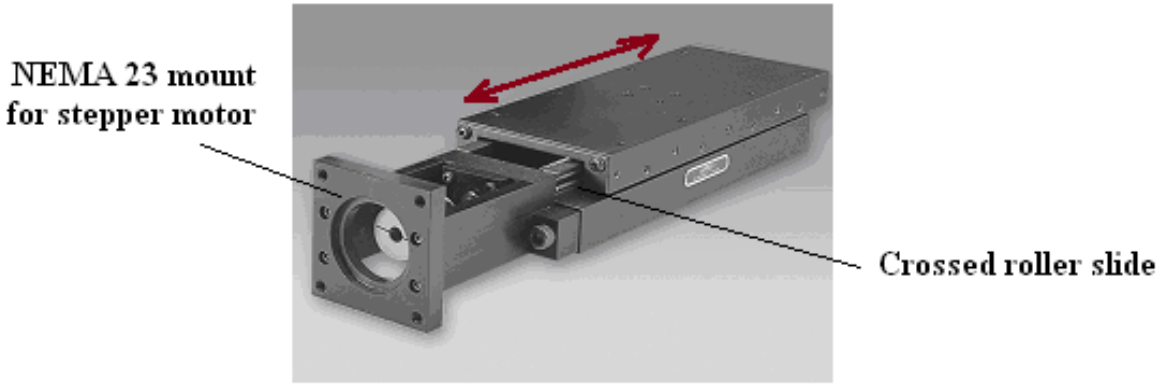

Figure 3.15 Crossed roller positioning stage [391].

3.4.6 Mounting Table

Mounting table provided a base to attach positioning stage and the indenter holder plate. The mounting table had a "U" shape and was made of seven plates (one lower plate, four side plates and two top plates) and four connecting bars that connected the top plates to the lower plate. The specific shape of the table allowed the movement of culture plate under the top plates of the table. It was made from aluminium and its parts were connected via screws. The table can be sterilized in the autoclave when the parts are disassembled. The mounting table before the complete assembly of the whole system is shown in Figure.3.16 and dimensions are in drawing of Figure.3.17.

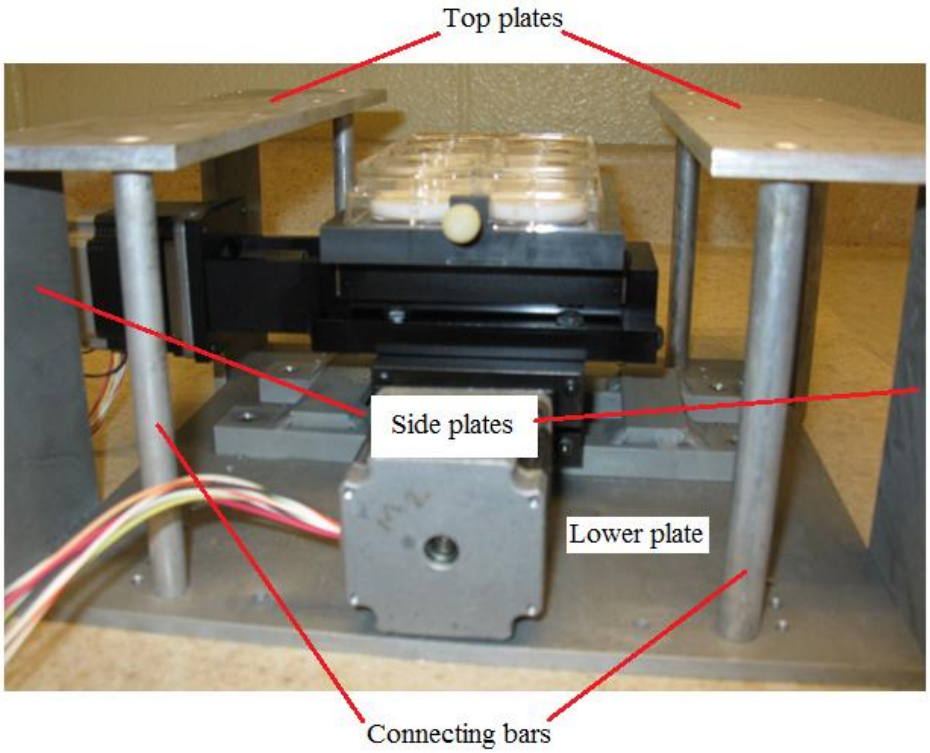

Figure.3.16 Front view of the fabricated mounting table.

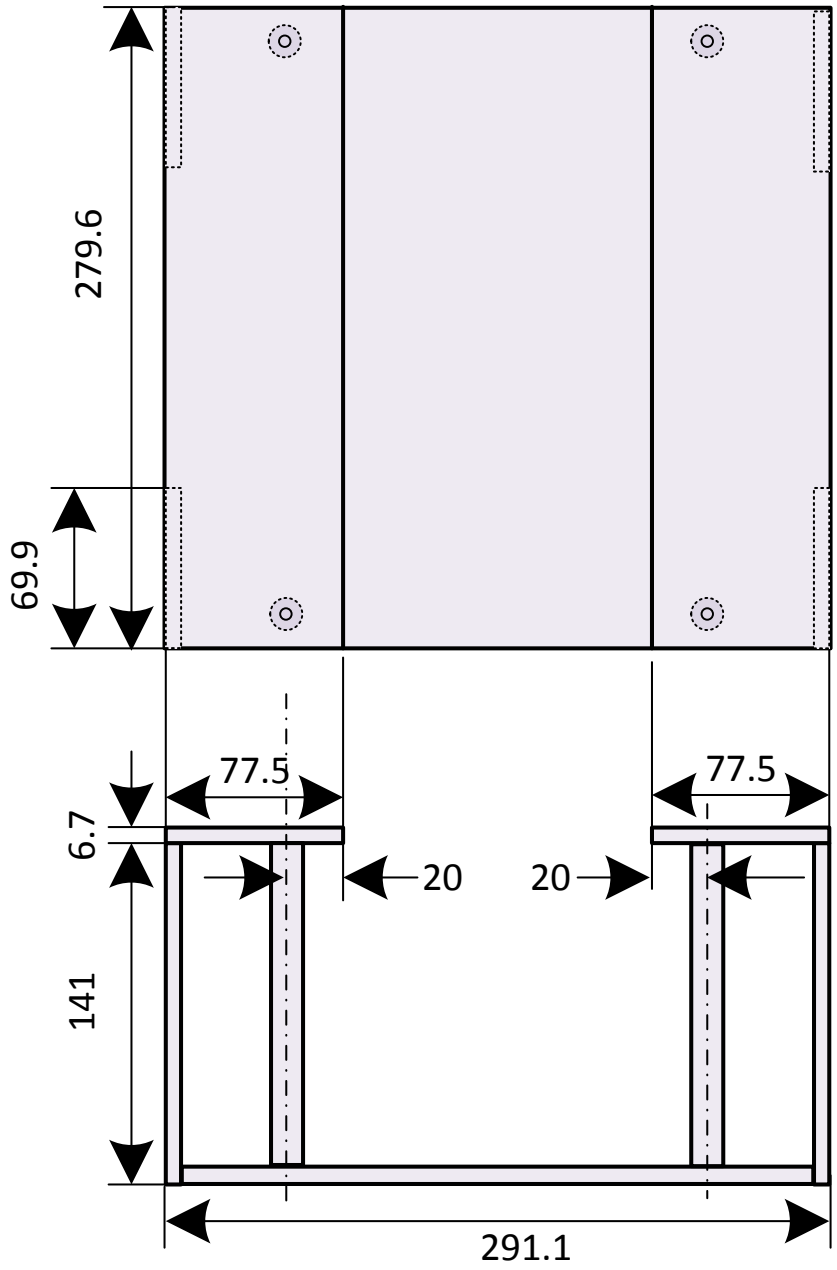

Figure.3.17 Dimensions of mounting table (mm).

3.5 Electrical Components

3.5.1 Stepper Motors

Two stepper motors were needed in the system, each to move one of the two positioning stages. Both of them were from Applied Motion Products (HT 23-396, NEMA 23 high torque step motor; Watsonville, CA, USA) with capability of 200 [steps/rev] (Figure.3.18).

Figure.3.18 HT 23-396 stepper motor [392].

3.5.2 Motor Controller and Power Supply

Both motor controllers were 1240i programmable step motor drives (Microstepping, 1.2 amps, 40 VDC) from Applied Motion Products for standalone operation with Si Programmer Windows software (Figure.3.19). They were operated in real time from the host PC. These controllers were networked via a single SiNet™ Hub to communicate with each other and to make specific patterns by defined X-Y motion. Both drives worked with a 24 VDC motor supply (with selectable step resolutions for software in the range of 2000 -50800 steps/ rev. The motor controllers required a 24VDC power supply (PSR-12-24, 12 A @ 24 VDC manufactured by Mean Well Direct) (Figure.3.20). The specifications of this motor drive are explained in Table B.4 of Appendix B.

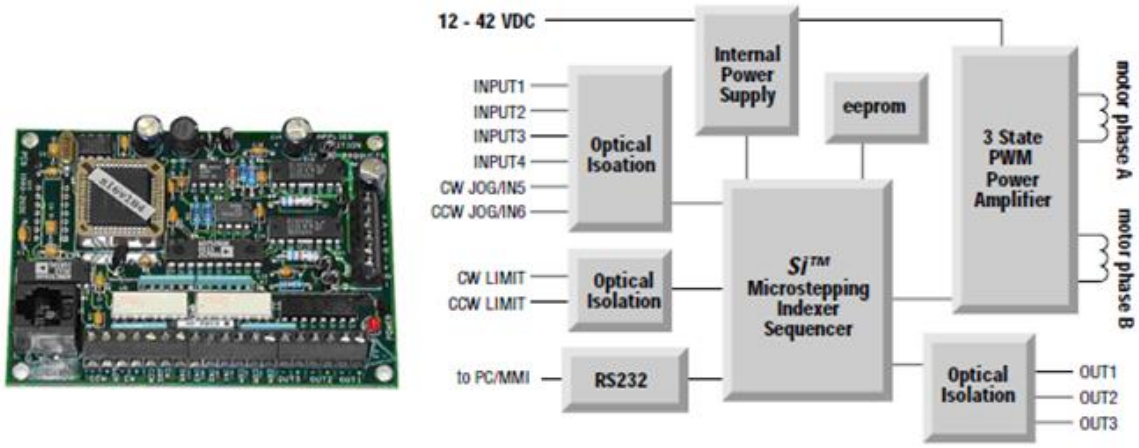

Figure.3.19 1240i programmable motor drive and its block diagram[392].

Figure.3.20 PSR-12-24, 12 A @ 24 VDC power supply [393].

3.5.3 SiNet Hub Programmer and Motion Programming

For creation of the combination of X and Y motion (in order for the indenter tip to trace a defined pattern) two motor drives were necessary. The two standalone motor controllers (1240i) required a hub to communicate with each other. In fact the hub allowed the two motors to be controlled in host mode from a single PC. The hub was connected to the host computer where the hub programmer software was installed for programming the desired motion. Multi-axis motion SiNet

Hub 444 with I/O was selected from Applied Motion (Figure.3.21). The allowable ranges that this hub could be programmed were ±16,000,000 [steps] for moving distance, 0.025-50 [rev/s] for moving speed, ±1-3000 [rev/s^2] for acceleration and 2000 - 50800 [steps/rev] for step resolution. An example of creating a reciprocating X-Y motion path in programming window of SiNet hub programmer is shown in Figure.3.22.

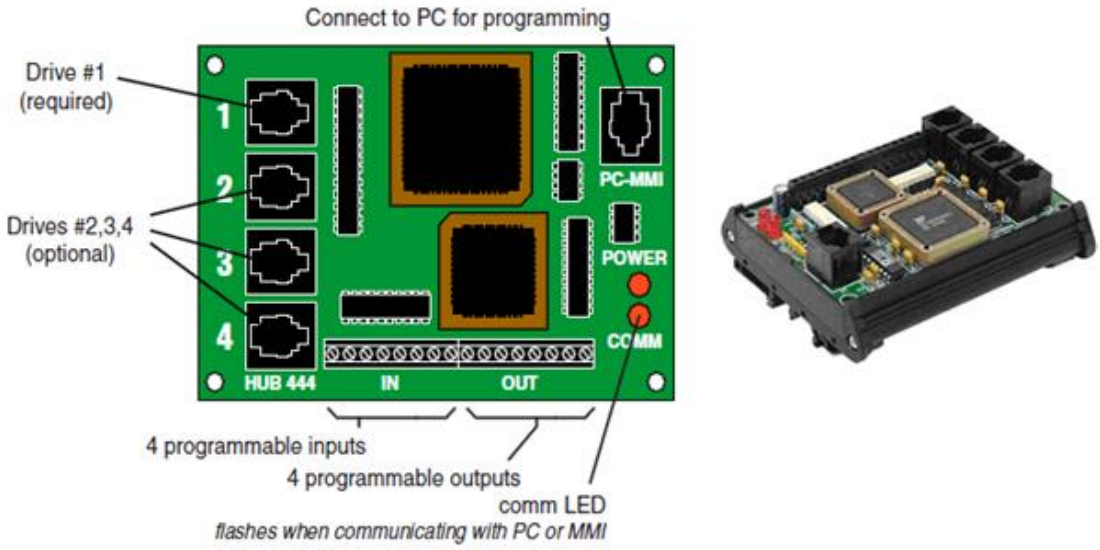

Figure.3.21 Multi-axis motion SiNet Hub [392].

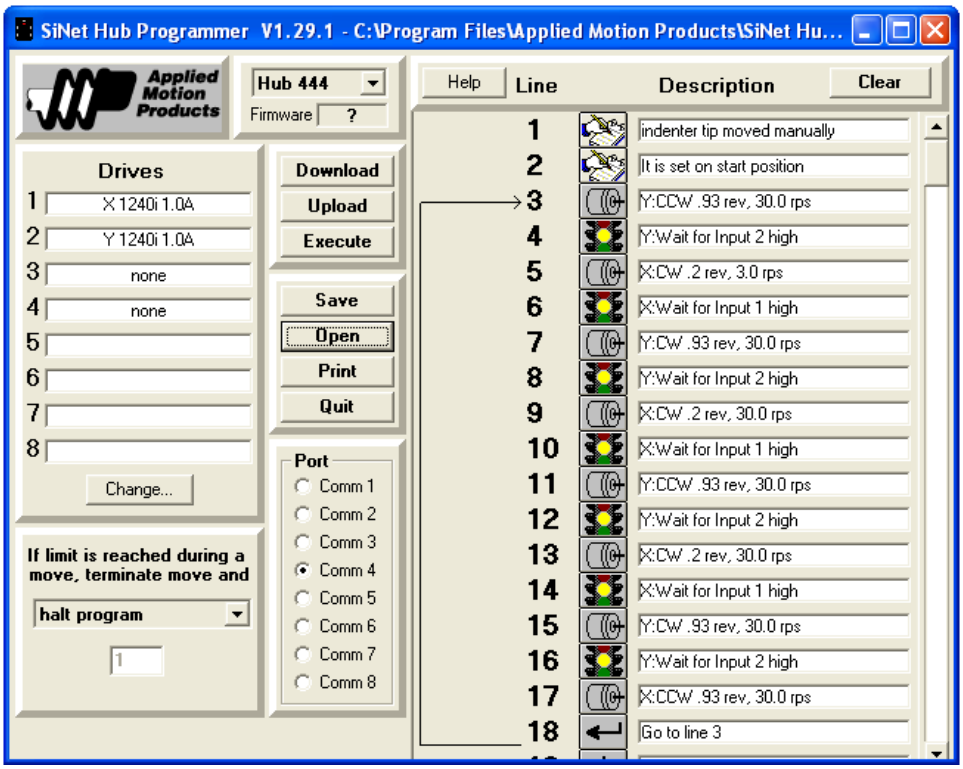

Figure.3.22 An example of creating X-Y motion in programming window of SiNet hub programmer.

To be able to program the motor drives for making a specific X-Y motion path, it was necessary to know the rotation of the motors with respect to the direction of the culture plate movements. The schematic representation of the position of the motors, indenter holder mechanism versus culture plate position is shown in Figure.3.23. This figure shows which motor is responsible for which movement (X or Y) and it assigns the clockwise or counter clockwise rotation of the motor with direction of the movement. The motion pattern could be programmed as series of parallel lines in the X and Y directions so that the construct surface could have a large centered region stimulated (Figure.3.24).

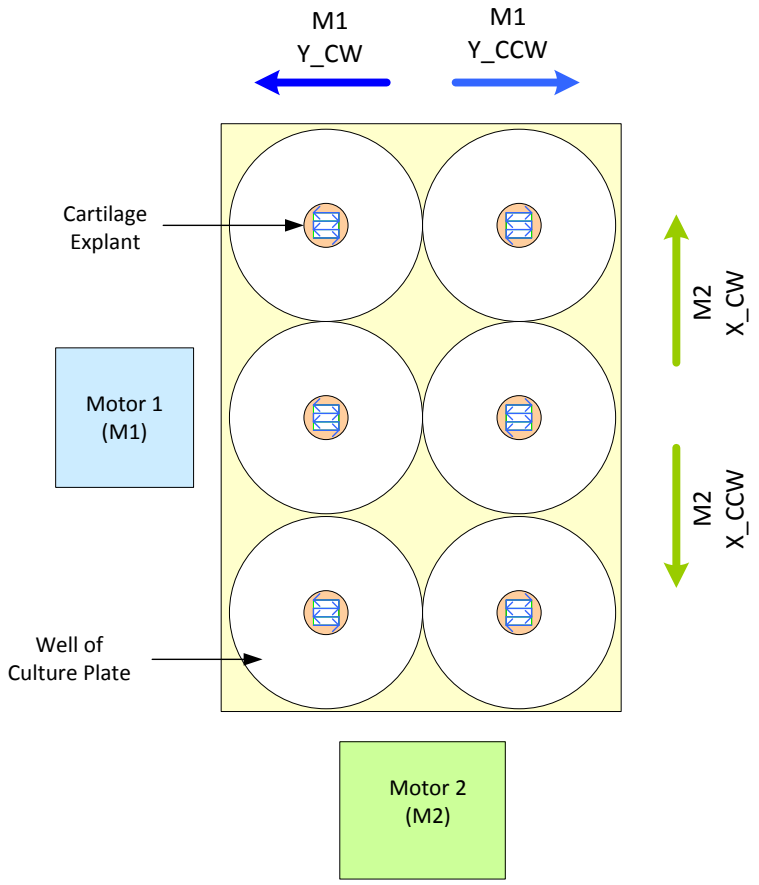

Figure.3.23 The rotations of motors in clockwise (CW) or counter clockwise (CCW) versus culture plate motions in X and Y directions (top view).

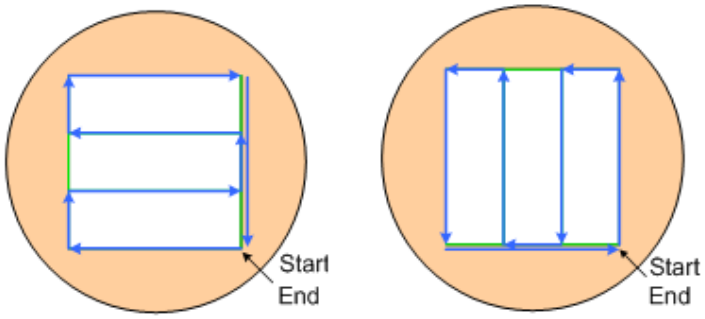

Figure.3.24 Two examples of the looped reciprocating motion path for construct under an indenter.

The diameters of cell-seeded constructs were ~10 mm. The central area on the top surface of the construct was selected for stimulation. Since the area was small there was not much difference between choosing this area as circle or square. The stimulation pattern was designed and programmed in such a way that the contact points between the indenter and top surface of the construct could cover most of the circular area, without going out of the circular border of the construct and moving over the construct holder. The designed pattern was a combination of lines in X and Y directions as shown in Figure.3.25. The construct travel was equal to the traveling distance of any of the positioning stages in every step. The full cycle of the stimulation pattern consisted of eight steps or eight lines, with 4 parallel long lines along Y axis, 3 short lines in between them along X axis and another long line in X axis to complete the cycle and to return to the starting point. Considering the diameter of the indenter tip, and the surface that it covers while moving, most of the surface was mechanically stimulated as shown in Figure 3.26. Two similar patterns could be used, but in different directions. The purpose of giving these two patterns was to have the option of stimulating the surface in both directions.

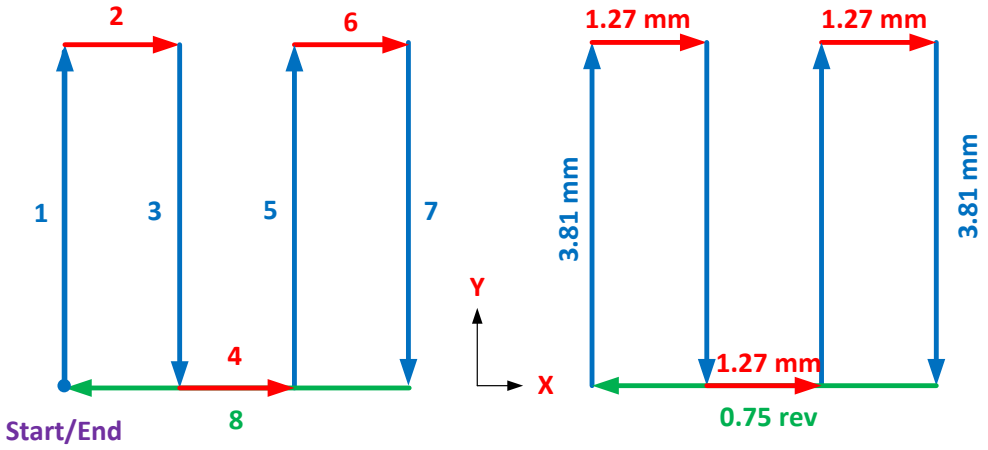

Figure.3.25 The designed stimulation pattern that combined X and Y motion. Each revolution of the motor moves the stage about 5.08 mm.

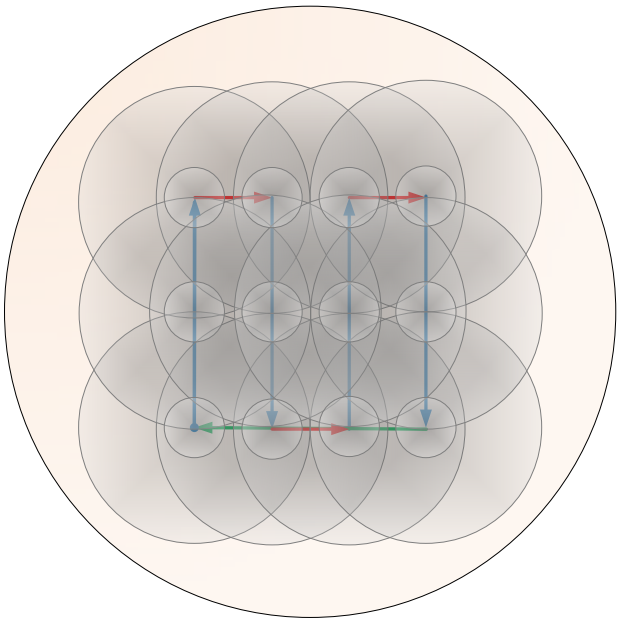

Figure 3.26 The surface area directly below the indenter as the construct moves. For better visualization, the entire circular contact surface is only shown for end of all lines and middle of long lines in Y direction. The smaller circles represent the pocket of the indenter.

3.6 Fluid Flow Components

3.6.1 Multichannel Peristaltic Pump

A peristaltic pump with variable flow rate was selected to recirculate the cell culture media from the well to the cannulated indenter and to eject onto the construct surface from the small channel at the tip. The pump had independent channels and thus could recirculate the culture media of the six wells separately. The associated materials of the pumps such as its housing, cassettes, rollers, 3-stop collared tubings and the wires needed to tolerate the 37ºC temperature and high humidity of inside the incubator for long time (~4-6 weeks). Due to importance of this capability, the

temperature and humidity tolerance of the pump and the method of safe sterilization of the parts were carefully checked before selection to avoid failure of the pump and its component during the defined periods of studies. Since the pump along with some other components of the system will be located inside the incubator, its dimensions were checked with respect to the available space inside the incubator (56 × 56 × 56 cm) and dimensions of assembled hydromechanical stimulator. The chosen pump was "ecoline" multichannel roller pump (Harvard Apparatus, Holliston, MA, USA) with up to 8 channels with the overall flow rate range of 0.005-150 ml/min, speed of 3.5- 350 rpm, voltage of either 115 or 230 VAC with 60 or 50 Hz respectively, and 100 W power consumption. The ranges of flow rates depended on the sizes of the tubing (Table.3.1). The dimensions of the pump were 138 × 169 × 313 mm (H×W ×D). The pump is shown in Figure.3.27.

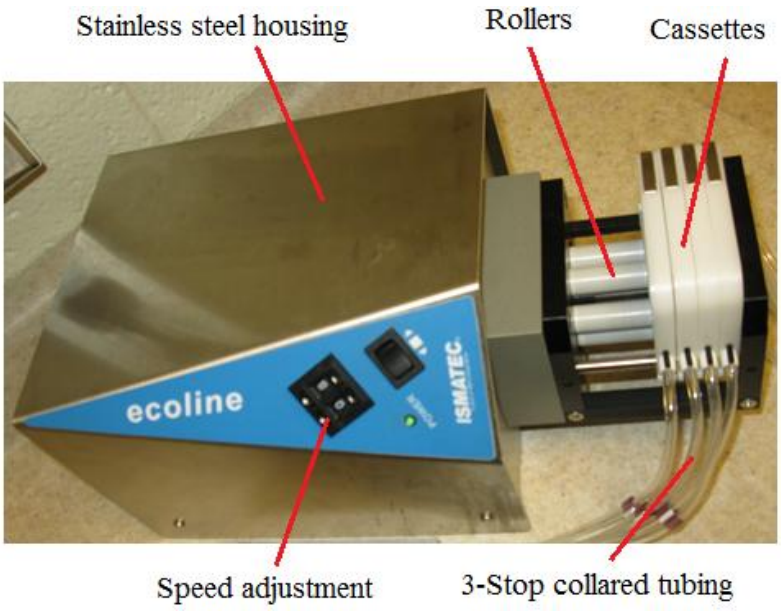

Figure.3.27 Multichannel variable flow rate peristaltic roller pump.

Each indenter was connected to one of the tubing of a multi-channel peristaltic pump (Figure.3.28). During the hydromechanical stimulation period, a continuous flow of culture media

was injected by the pump directly on top of the surface of construct (perpendicularly) while the constructs were being moved under the bearing indenter (either alone or weighted).The inner diameter of the tube was 2.79 mm. The range of achievable flow rate with this tube size is specified as 1.3- 130 ml/min (Table.3.1).

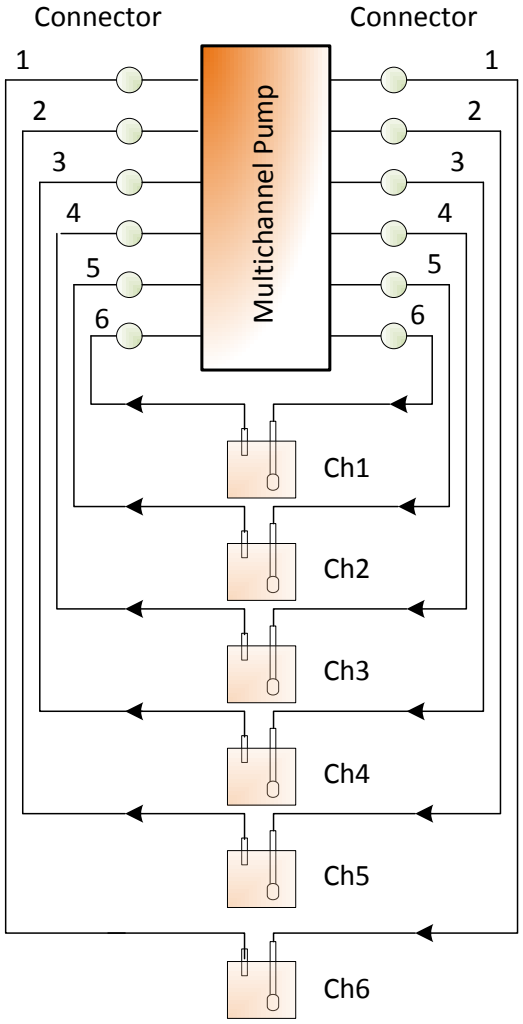

Figure.3.28 Multichannel pump and fluid flow circulation path.

Table.3.1 Minimum and maximum flow rates for different tubing sizes.

Fließraten pro Kanal / Flow rates per channel / Débits par canal			
Schlauch iØ	**Modell / Model / Modèle**	**VC-MS/CA8-6**	
Tube i.d	Kanäle / Channels / Canaux	8	
Ø int. mm	Rollen / Rollers / Galets	6	
	min⁻¹ / rpm / t/min (min./max.)	3.5	350
		ml/min	
0.13		0.005	0.49
0.19		0.010	0.98
0.25		0.017	1.7
0.38		0.038	3.8
0.44		0.050	5.0
0.51		0.067	6.7
0.57		0.084	8.4
0.64		0.10	10
0.76		0.15	15
0.89		0.20	20
0.95		0.22	22
1.02		0.26	26
1.09		0.29	29
1.14		0.32	32
1.22		0.36	36
1.30		0.40	40
1.42		0.47	47
1.52		0.53	53
1.65		0.61	61
1.75		0.67	67
1.85		0.73	73
2.06		0.87	87
2.29		1.0	100
2.54		1.2	120
2.79		1.3	130
3.17		1.5	150

3.6.2 Pump Tubings

The pump tubings were selected from material that could not degrade and release chemicals causing adverse effects and could be autoclaved or sterilized with ethanol. Tygon tubings (ID= 2.79 mm, t = 0.86 mm) came with the pump. One end of the tubing was extended to be connected to the short suction tube and the other end was connected to the indenter. Additional Tygon tubing for extending the length of collared tubing were from Fisher Scientific (Fisher Scientific Company, Toronto, ON, Canada) with 2.38 mm diameter and 5.56 mm outer diameter and approximate

lengths of 0.5-0.6 m. The standard straight connectors from Harvard Apparatus (for ID = 3 mm) were used to connect the 3-stop collared tubing and other tubing of almost similar size.

3.7 Assembly of System Components

After completing the fabrication of the custom designed components of the system, the parts that could be sterilized, were sterilized either in autoclave or with 70% ethanol. Then the sterilized mechanical parts were transferred to biological safety cabinet and then they were assembled when they were completely dry.

The electrical components including the power supply, the stand-alone motor drivers and hub were placed in a case (Figure.3.29) to be sealed later after testing their functionality (to protect them from damage). The motor drives were connected to the power supply (Figure.3.5). The SiNet hub was connected to the two 1240i drivers. The SiNet hub programmer software was installed on the host computer.

Figure.3.29 Electrical components enclosed in a case.

Each stepper motor was attached to the NEMA 23 mount at the end of positioning stage with screws. The positioning stages were located on top of each other and screwed to each other. The

holding tray was mounted on top of the stages. Then, the mounting table was assembled. The lower plate and four side plates were attached with screws. The assembled motors, positioning stages and holding tray were mounted on the lower surface of the table (almost in the middle) (Figure.3.30). Then the two top plates and four connecting bars were attached.

An empty culture plate on the tray, which contained unused sterile construct holders, was used to approximately adjust the position of culture plate with respect to the holes on the indenter holder plate. The final adjustment of the indenter positions with respect to constructs was done after placing the whole assembled system inside the incubator.

After passing the indenters through their holes in the indenter holder plate, the weights were attached to the indenters (Figure.3.31). The indenter holder plate was screwed onto the mounting table and the pump tubings were attached to the indenters and suction tubes. The top, front and side views of the assembled system are shown in Figure.3.32, Figure.3.33 and Figure.3.34 respectively. The assembled system components during a mechanical stimulation study are shown in Figure 3.35.

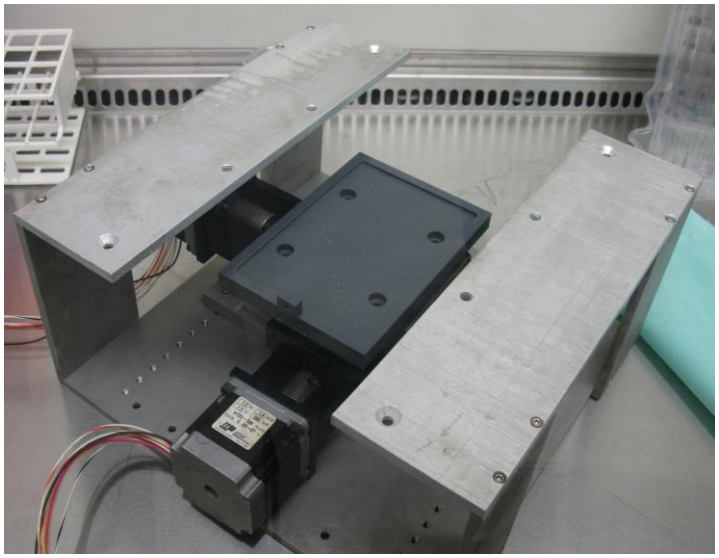

Figure.3.30 The procedure for assembly of motors, positioning stages and holding tray on the mounting table.

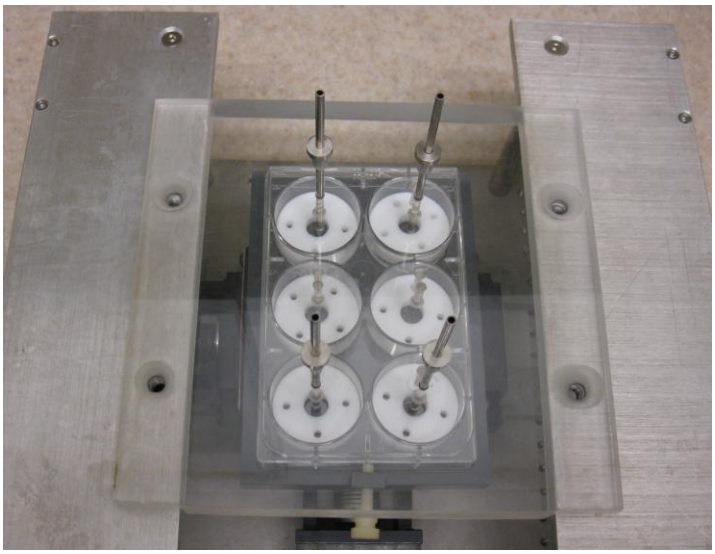

Figure.3.31 The indenter holder plate being attached to the top of the mounting table.

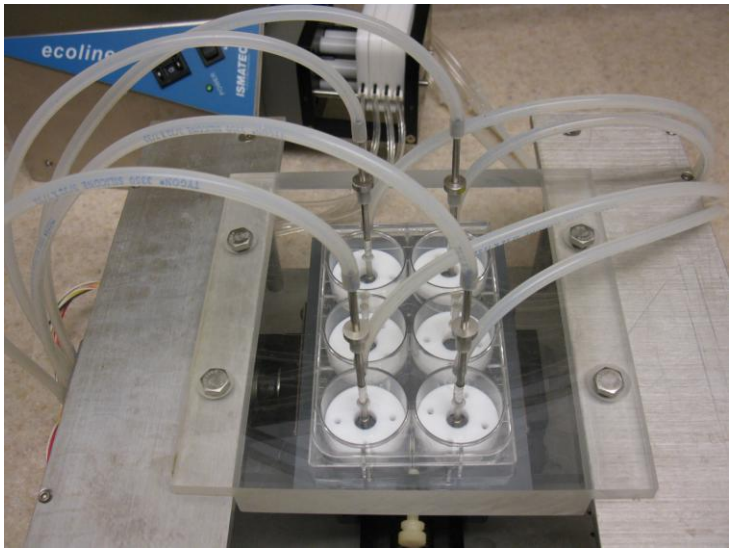

Figure.3.32 The indenter holder plate on the mounting table along with indenters and pump tubing (shown outside the incubator without constructs).

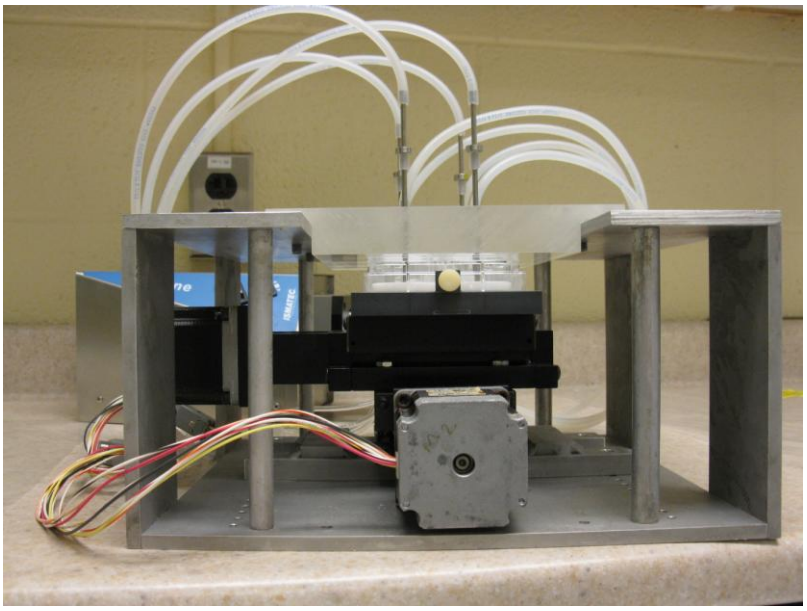

Figure.3.33 Front view of the mounting table (shown outside the incubator without constructs).

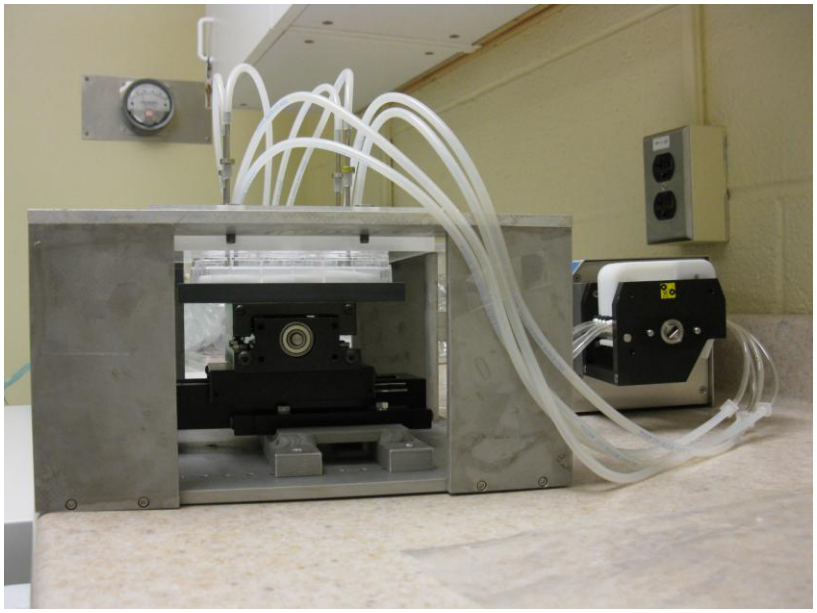

Figure.3.34 Side view of the mounting table (shown outside the incubator without constructs).

Figure 3.35 The assembled hydromechanical stimulation system shown inside incubator.

The multichannel pump was calibrated before being assembled, and many parameters of the system were configured and tuned before starting the long term studies.

3.8 Chapter Outlook

In this chapter, the mechanical and hydromechanical stimulation concepts were explained and the features of proposed technique and designed system were listed. The system's three main components were categorized (mechanical, electrical and fluid flow) and the components of each category were explained in details. The drawings of custom-designed parts were provided and the overall assembly of all components of the system were presented. The uses of this system in tests of its functionality, in configurations of its associated parameters, as well as details of experimental and analytical methods in preliminary and main experiments, will be explained in the next chapter.

Chapter 4

Experimental and Analytical Methods

Two major topics are considered in this chapter. First, the tests of system functionality are discussed. This includes tests of the programmed stimulation patterns, estimation of the maximum speed of each traveled path in every stimulation pattern, finding functional range of acceleration/deceleration, measurement of cycle times in each stimulation pattern, determination of an appropriate agarose concentration and finally a two-week preliminary experiment. The preliminary experiment explored the chosen parameters of the system over longer period of time when chondrocyte-seeded constructs were either mechanically or hydromechanically stimulated. This helped in finding the functional ranges of normal loads and flow rates out of 16 different combinations of these parameters.

Second, the main experiments and analyses for three different long-term studies are explained. In Study 1, four load-flow combinations were applied daily on agarose-chondrocyte constructs for 2 weeks and explored their effects on retained GAG in constructs and cell viability. In Study 2, three load-flow combinations were applied on cell-seeded constructs, 5 days/week for 3 weeks, using bidirectional stimulation pattern. The biochemical analyses were further expanded so the effects of the loading on both retained GAG and collagen in 3 separate layers of constructs and on released GAG and collagen into culture media were found. In Study 3, three load-flow combinations were applied on cell-seeded constructs, 3 days/week for 3 weeks using the unidirectional stimulation

pattern and the same biochemical analyses as for Study 2 were conducted for both central stimulated and side unstimulated area in 3 separate layers of constructs.

4.1 Tests of System Functionality

4.1.1 Motor Revolution versus Construct Traveling Distance

The movement of the construct against the indenter was driven by the motor. It was important for experimental consistency to have no relative motion between the elements of the mounting assembly so that all of the motor's angular motion (1 rev = 0.2 inch = 5.08 mm) was converted to the displacement of the constructs. The adjustment screw (for fixing the position of culture plate in the tray), and the fitted construct holder within the well of culture plate, and attachment of stages both to each other and to the mounting table by screws ensured that no spurious relative motion occurred.

4.1.2 Designed Stimulation Patterns

Two different stimulation patterns were used throughout the studies. One was a simple unidirectional reciprocating motion on a line in either direction X or Y with travelling distance of about 4.064 *mm*. The other one was bidirectional motion including combination of lines in X and Y directions as shown in Figure.3.25. The stimulation patterns were programmed with SiNet hub programmer software within the host computer. Details of the programmed paths are in Appendix C. Several pilot studies were conducted to select a functional range for the traveling distances as well as accelerations and decelerations.

4.1.3 Effect of Input Acceleration on Cycle Time

The inputs to the SiNet hub programmer are the driver (X or Y), the direction of rotation for motor (clockwise (CW) or counter clockwise (CCW)), the amount of revolution of motor (which was the same as traveling distance of construct), the speed, the acceleration and deceleration. The velocity of the motor versus time has a triangular shape (saw-tooth pattern). For the short (1.27 mm) and the long (3.81 mm) distances, the acceleration/deceleration (same value for both) was changed from 1, 2, 4 … and increased by multiples of 2 until 64 rev/s^2 (325.12 mm/s^2) was reached. The total time for traveling full cycle was calculated using elementary kinematic equations and eventually compared with the measurement of real cycle times. This gave some idea of the precision with which the motors could apply the displacement to the constructs.

The behavior of the motors over larger range of acceleration/deceleration, between 508-2540 mm/s^2 (100- 500 rev/s^2) with steps of 508 mm/s^2 (100 rev/s^2), was investigated on two lines with distances of 1.5748 mm and about 4.7244 mm. The graphs of total time and maximum speed versus acceleration were generated and the estimated values were compared with the measured ones. The same procedures were repeated for the simple unidirectional stimulation pattern, which traveled 4.064 mm in either the X or the Y direction. The estimated cycle times were calculated.

4.1.4 Real Cycle Time Measurement

The real time to finish one full cycle of the stimulation pattern was measured to be compared to the estimated time. Before selecting functional values for acceleration/deceleration and traveling distances, the first attempt was to minimize the full cycle time which was possible by increasing the acceleration/deceleration. The time for full cycle of bidirectional stimulation pattern was found

by measuring the time to complete 50, 100 and 200 loops with input acceleration/deceleration values of 100, 200, 300, 400 and 500 rev/s^2. The measured cycle times were compared with each other and with the estimated values from the software. After finalizing the parameters of bidirectional stimulation pattern (acceleration/deceleration of 50.8 mm/s^2 or 10 rev/s^2; with travelling distances of 1.27 mm or 0.25 rev and 3.81 mm or 0.75 rev), the cycle time was measured by running the SiNet hub program for 200 loops for 5 times, and the mean value was compared with the estimated time.

4.1.5 Maximum Speed for Each Path of Bidirectional Pattern

As it was mentioned before, each culture plate was driven in a "saw-tooth" velocity pattern, achieving a peak velocity at the midpoint of the traveled distance. For our selected value for acceleration/deceleration of 50.8 mm/s^2 and for each traveling distance of 1.27 mm and 3.81 mm, the maximum speed was read from the analyzed data of SiNet hub programmer software, as explained in Section 4.1.3. It could also be calculated using an elementary kinematic equation as the square root of the product of acceleration and distance. This gave peak velocity magnitudes of 8.03 mm/s for the 1.27 mm distance and 13.91 mm/s for the 3.81 mm distance.

4.1.6 Multichannel Pump Calibration

Minimum and maximum flow rate of multichannel pump using specific size of tubing was shown in Table.3.1. For the chosen tubing (inner diameter of 2.79 mm) the flow rate was supposed to range from 0.02167 to 2.167 ml/s. The velocity of the pump rollers could be adjusted by a digital

interface (0 to 99 for minimum to maximum speeds). The flow rate was directly proportional to the velocity of the pump rollers.

Two sets of experiments were run to calibrate all six channels of the pump. First the flow rates were measured when the digital input varied up to maximum of 99. This gave the overall behaviour of the pump over its full available range in each individual channel. Since in the present studies, the constructs were about to receive medium or low fluid flow rates, a second experiment considered the lower third of the available range. In this experiment, the flow rate was measured when the digital input varied in steps of 2, from 1 up to 31. The calibration procedure was done once with the 2.79 mm tubing, and was repeated with the indenter attached at the end of tubings to see if the small channel at the tip affected the flow rates significantly.

One digital timer and six graduated tubes (15 ml for collecting the fluid in low flow rates and 50 ml for larger flow rates), were used to measure the collected volume of each channel over specified time periods. The schematic representation of calibration is shown in Figure 4.1.

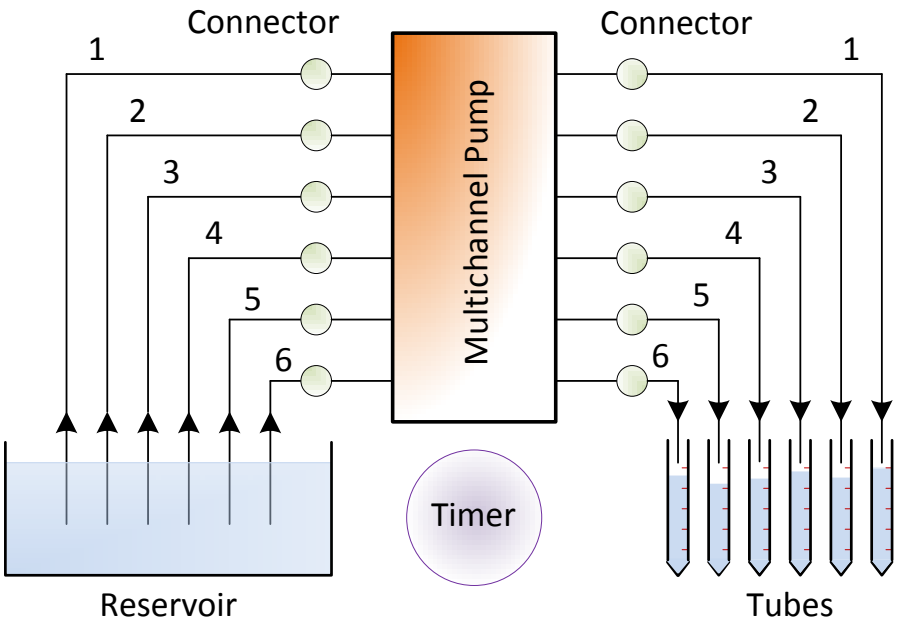

Figure 4.1. The setup of multichannel pump for calibration.

4.1.7 Pilot Study to Determine a Suitable Agarose Concentration

As it was shown in, Table A.1 in Appendix A, various concentrations of agarose between 1% to 4% had been used in previous studies involving the mechanical stimulation. Due to the different loading techniques used in the present thesis, a suitable agarose concentration needed to be determined. Thus, a short term pilot study was performed. However, it was recognized that in longer term studies, the constructs might perform a little differently.

The pilot study considered the visible changes in appearance of the constructs when subjected to static, dynamic and hydrodynamic loading (such as permanent deformation, crack or fracture). Different load/flow conditions were applied to the construct that had various agarose concentrations (Figure 4.2, Table 4.1). The total stimulation time was 30 minutes for every construct. For compression-no flow, the indenters were just in contact with the surface of stationary

construct and there was no fluid injected on top surface via indenter. For compression shear, the same loading condition as compression-no flow was applied to the moving construct under the indenter. The constructs were moved in such a way that created a bidirectional pattern and travelled distances of 1.27 mm and 3.81mm (Figure.3.25) with acceleration/deceleration of 50.8 mm/s^2. For compression shear-medium flow, the same conditions as compression shear were applied with the addition of fluid flow. The fluid was Dulbecco's Modified Eagles's Medium (DMEM) W/L-Glutamine (Fisher Scientific, HyClone, Cat# SH30249.02) containing 25 mM HEPES, 4.5 g/l Glucose, 4.00 mM L-Glutamine and Sodium Pyruvate. The fluid was pumped with medium flow rate (MF) of 11. 24 ml/min. A total of 36 constructs were tested in the pilot study (Table 4.1).

Table 4.1 Various combinations of load/flow conditions and agarose concentrations for 36 constructs in the pilot study (NF: no flow, MF: medium flow rate of 11.24 ml/min, C1, C2, C3= only compressions from 28.24 , 42.09 and 56.17 mN loads respectively, CS1, CS2, CS3 = C1, C2, C3 compressions respectively when there is sliding shear due to bidirectional motion of constructs).

Applied load	Description of conditions: load-flow-% agarose		
28.24 mN	C1-NF-1%	CS1-NF-1%	CS1-MF-1%
28.24 mN	C1-NF-2%	CS1-NF-2%	CS1-MF-2%
28.24 mN	C1-NF-3%	CS1-NF-3%	CS1-MF-3%
28.24 mN	C1-NF-4%	CS1-NF-4%	CS1-MF-4%
42.09 mN	C2-NF-1%	CS2-NF-1%	CS2-MF-1%
42.09 mN	C2-NF-2%	CS2-NF-2%	CS2-MF-2%
42.09 mN	C2-NF-3%	CS2-NF-3%	CS2-MF-3%
42.09 mN	C2-NF-4%	CS2-NF-4%	CS2-MF-4%
56.17 mN	C3-NF-1%	CS3-NF-1%	CS3-MF-1%
56.17 mN	C3-NF-2%	CS3-NF-2%	CS3-MF-2%
56.17 mN	C3-NF-3%	CS3-NF-3%	CS3-MF-3%
56.17 mN	C3-NF-4%	CS3-NF-4%	CS3-MF-4%

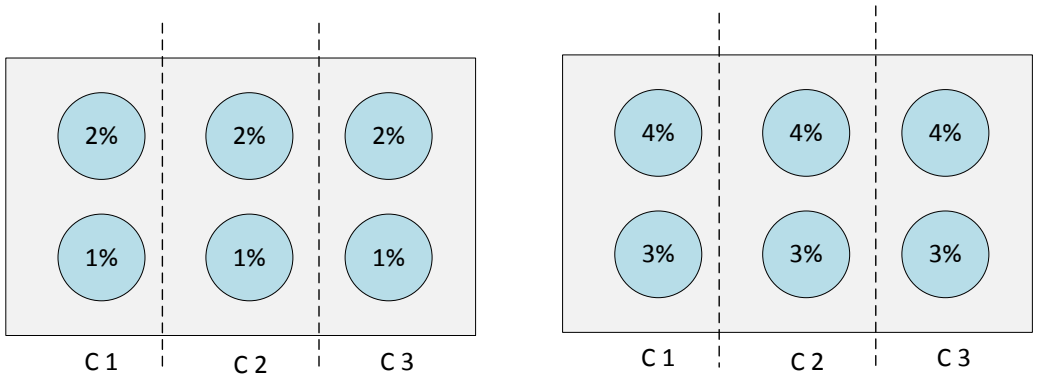

Figure 4.2 Settings of different compressions and agarose concentrations per channel for the pilot study.

Agarose hydrogels with 1%, 2%, 3% or 4% (w/v) concentrations were prepared by pouring the agarose powder (Type VII, low melting temperature, Sigma-Aldrich, www.sigmaaldrich.com, Cat# A0701) on phosphate buffered saline (PBS) (BioShop Canada Inc. Burlington, ON., Canada, Cat# PBS415.1) in four separate beakers and autoclaving it (without mixing) in 121ºC for 15 min to make it sterile (as would have been done for actual experiments with chondrocytes). Then, the hot liquid gels were placed in a room temperature environment until the thermometer probes inside the gel showed a temperature of about 40ºC. Next, the viscous liquid agarose was transferred into horizontally-oriented petri dishes (standard size: 60 x 15 mm; measured size: ID ~ 53 mm, depth ~12.5 mm) using a wide mouth pipet to make gels that were 5 mm in height. Finally, the solution was gelled in a refrigerator at 4ºC for about 15 min and cut with a custom designed core cutter that had a 10 mm inner diameter (Figure 4.3, Figure 4.4). The resulting constructs were placed in construct holders within the wells of culture plates.

There were two culture plates for compression-no flow, two for compression shear-no flow and two for compression shear-medium flow. Each culture plate had constructs of two agarose concentrations that were subjected to three compression pressures (Figure 4.2). After system set up

(Figure.3.31), the wells of the culture plates were filled with 7 ml DMEM. Each of the three compression pressures was applied to the constructs having each of the four concentrations of agarose (Figure 4.2) and after the 30 minutes of stimulation, the presence of any permanent deformation, cracks or fracture was recorded. This was done for compression-no flow, compression shear-no flow and compression shear-medium flow.

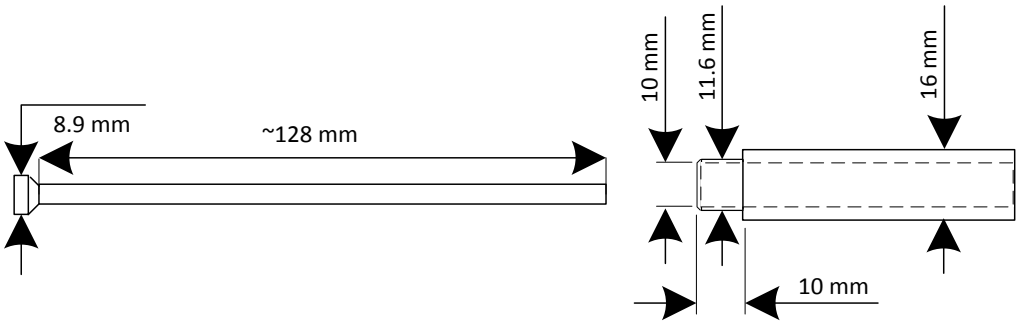

Figure 4.3. Right: core cutter used for the agarose gel; left: transfer bar for pushing the cut construct into the construct holder in an individual culture plate.

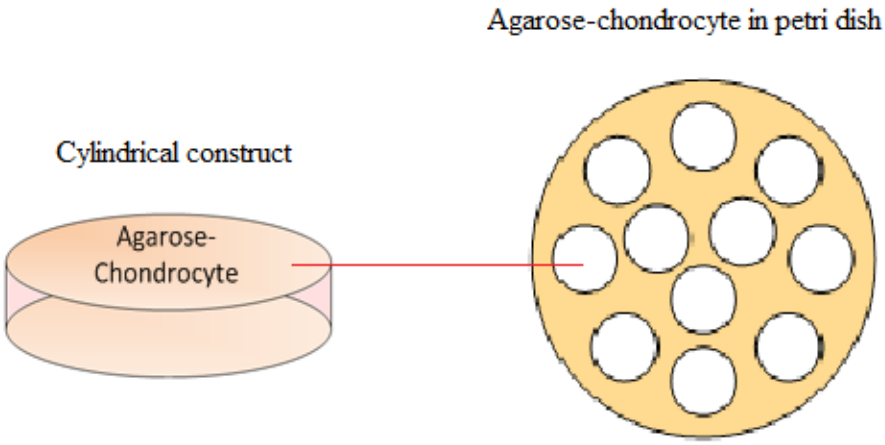

Figure 4.4 The cylindrical constructs cut from the gel in the petri dish (In the pilot study, there were no chondrocytes).

4.1.8 Normal Load Configuration

The indenters with added masses applied normal load to the agarose chondrocyte construct. The actual contact pressures and friction forces were estimated and discussed in the analyses sections. The approximate dead mass that generate certain amount of strains in constructs are estimated in Table G.1 of Appendix G.

4.1.9 Preliminary Experiments

The overall behaviour of the system and the physical gross effects of loading on agarose-chondrocytes were investigated in a two-week study. This allowed further commissioning of the stimulator system with refinement and optimization of the procedures. The general procedures for the experiments are shown in Figure 4.5. In the preliminary investigations, all of these procedures were followed except the last three steps which included the biochemical analyses (GAG or collagen analysis) and the statistical analysis.

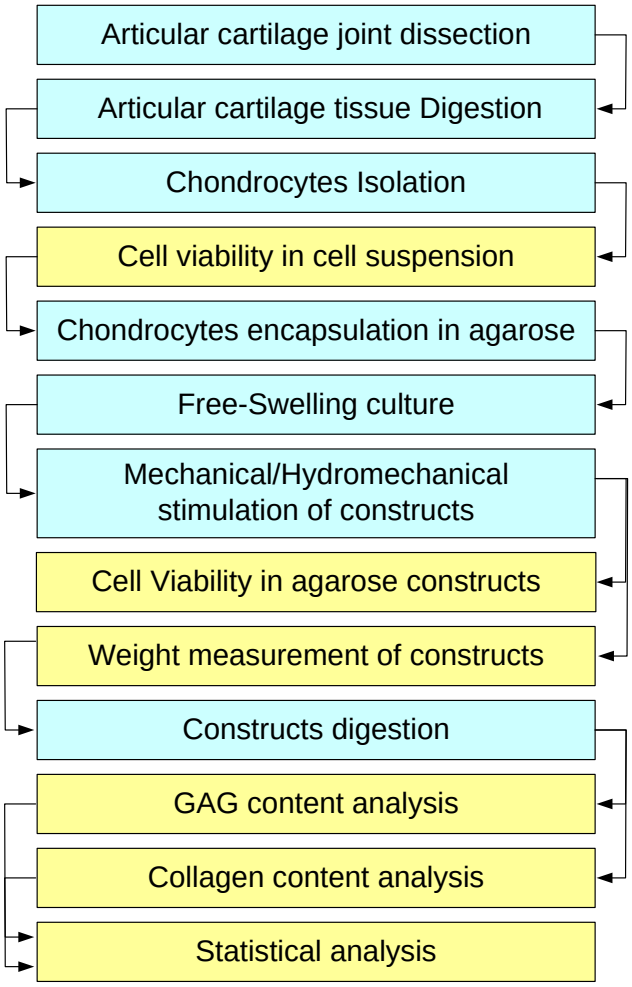

Figure 4.5 General procedures for the experiments of the present thesis (analysis are colored yellow).

4.1.9.1 Joint Dissection and Articular Cartilage Tissue Dissection

Multiple metacarpophalangeal joints of cows were obtained from a local abattoir within less than an hour of slaughter. The joint capsules with skin were thoroughly washed and sterilized once in 10% bleach in distilled water, and then in 70% ethanol in distilled water, for 1 h in each solution.

Then, they were dissected under sterile condition. The joint capsules were opened (Figure 4.6 a) to have full access to articular cartilage tissue covering the end of synovial joints (Figure 4.6 b).

The full depth of the articular cartilage tissue was shaved off from the surface of the joint using a fine-edged scalpel blade (no. 11). Then, these tissue flaps were washed three times in a solution of phosphate buffer saline (PBS) plus 2% antibiotics that consisted of 5,000 IU/ml penicillin, 5 mg/ml streptomycin (both from Fisher Scientific, MP, Cat# 1670049) to disinfect the tissue flaps (Figure 4.6 c). The articular cartilage tissue flaps were chopped with scalpel, pooled together and then placed in flasks (Figure 4.6 d). These flasks contained a solution of 1.5% collagenase II (Invitrogen, Cat # 17101-015) at 1.5 mg/ml, 1% sterile antibiotic solution (Fisher Scientific, Cat# 1670049) containing 5,000 IU/ml penicillin and 5 mg/ml streptomycin in Dulbecco's Modified Eagles's Medium (DMEM). The DMEM with high W/L- Glutamin (Fisher Scientific, HyClone, Cat# SH30249.02) containing 25 mM HEPES, 4.5 g/L Glucose, 4.00 mM L-Glutamine and Sodium Pyruvate. The flasks were placed in an incubator (Thermo Forma, model 310, direct heat CO_2 single steel interior incubator, Cat# 15-467-323GG) for digestion overnight (~16 h) at 37ºC interior temperature, 5% CO_2 gas and high humidity (~80%). Specifically, the flasks were placed on the reciprocating stage and it moved inside the incubator thus helping the digestion process by well mixing the solution and tissue slices.

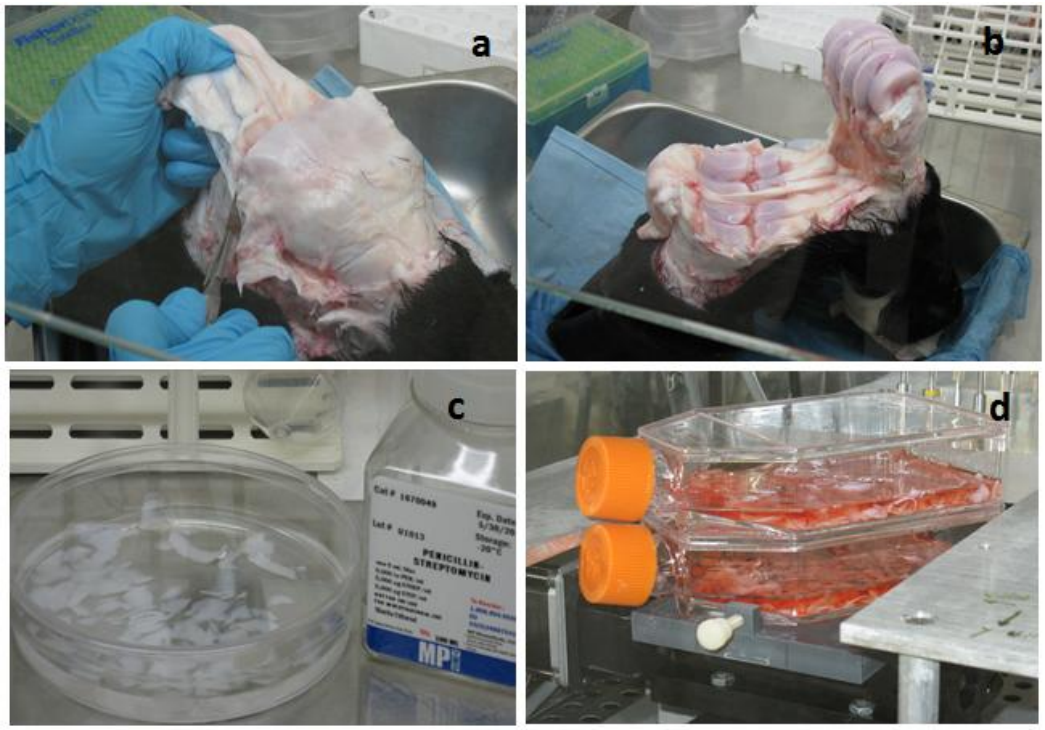

Figure 4.6. a) Removing skin and connecting tendons from a cleaned bovine synovial joint in the sterile environment of the biological safety cabinet; b) opening the joint and having access to articular cartilage surface; c) frequent washing of tissue slices in PBS and antibiotics; d) digesting tissue flaps in enzyme solution for several hours inside the incubator.

4.1.9.2 Chondrocyte Isolation

When the tissue flaps were completely digested, the solution was passed through sterile filters (stainless steel wire mesh with 250 meshes and pore size of about 60 micron). Then the filtered medium was transferred to sterile conical tubes and centrifuged at 600 g for 6 min to isolate the chondrocytes. The supernatant was removed; the pellet was washed two times in sterile DMEM and 10% (v/v) fetal bovine serum (FBS) (Fisher Scientific, HyClone, Cat # SH30396.03) and 1%

(v/v) penicillin-streptomycin antibiotic solution and mixed with solution by frequent pipetting. The cell suspension was centrifuged again; supernatant was removed and pellet was mixed with DMEM containing 20% FBS, 1% antibiotics, 1 µl/ml of ascorbic acid solution (100 µg/ml concentrations) (Sigma, Cat# A4403). Cells were uniformly distributed in the medium by pipetting them up and down many times. Cell suspension from all joints were then pooled together to further mix it with agarose solution.

4.1.9.3 Cell Viability in the Suspension

A small volume of about 100 µl of the cell suspension was transferred to a microcentrifuge tube and thoroughly mixed with the same volume of trypan blue (Thermo Scientific, HyClone, Cat# SV30084.01). It was mixed well to obtain a uniform cell suspension for accurate cell counting. The total number of viable cells was counted (as explained in Appendix D) with a hemocytometer (Hausser phase contrast hemocytometer (3 x1 in), Fisher Scientific, Cat # 02-671-54) under an inverted microscope (Fisher Scientific, micromaster inverted binocular microscope with infinity optics, Cat#12-575-250). The cell suspension was kept inside incubator to maintain its 37°C temperature to be ready for encapsulation in the agarose hydrogel.

4.1.9.4 Chondrocyte Encapsulation in Agarose Hydrogel

Agarose Gel Preparation

The agarose powder (Type VII, low melting temperature, Sigma, Cat# A0701) was poured on sterile phosphate buffered saline (PBS, 1X) (Sigma, Cat # P-549) in an autoclavable glass flask with 6% (w/v) concentration. Without mixing, the content was sterilized in an autoclave (Fisher Scientific, Barnstead SterileMax tabletop steam sterilizer, Cat# 14-4901) at 121ºC for 15 min.

Agarose and Cell Suspension Mixture

After removing the agarose solution from the autoclave, a sterile thermometer probe was placed inside it and then both thermometer and solution were placed in the safety cabinet. When temperature was close to 40ºC, a cell suspension of the same volume as agarose solution was added and quickly mixed by pipetting many times. This resulted in a 3% agarose-chondrocyte solution with estimated cell concentrations of about 6.89 million cells/ml. A number of Petri dishes and the container of agarose-chondrocyte solution were placed on top of a sterile pre-warmed hot plate inside the biological safety cabinet. The molten cell-agarose suspension was poured into each of the sterile Petri dishes in order to make constructs that were 5 mm in height. The solutions were then gelled at 4ºC in a refrigerator for about 20 minutes.

Cutting Agarose-Chondrocyte Constructs

The constructs that had formed in the Petri dishes were cut with a custom designed core cutter (Figure 4.3) to make cylindrical constructs (ID= 10 mm, h= 5 mm) with a volume of 0.393 mm^3 (Figure 4.4).

Culture of Agarose-Chondrocytes in Free Swelling Condition

When the gel was set, it was carefully cut into cylindrical shapes. Each cylindrical construct was then transferred to one well of a 24-well culture plate. About 2 ml of culture medium, containing 10% FBS, 1% antibiotics and 1 µl/ml of ascorbic acid (100 µg/ml concentrations) was added to each well and samples were incubated for 7 days in free swelling condition (Figure 4.7 b) inside the incubator at 37º C and 5% CO_2 with high humidity.

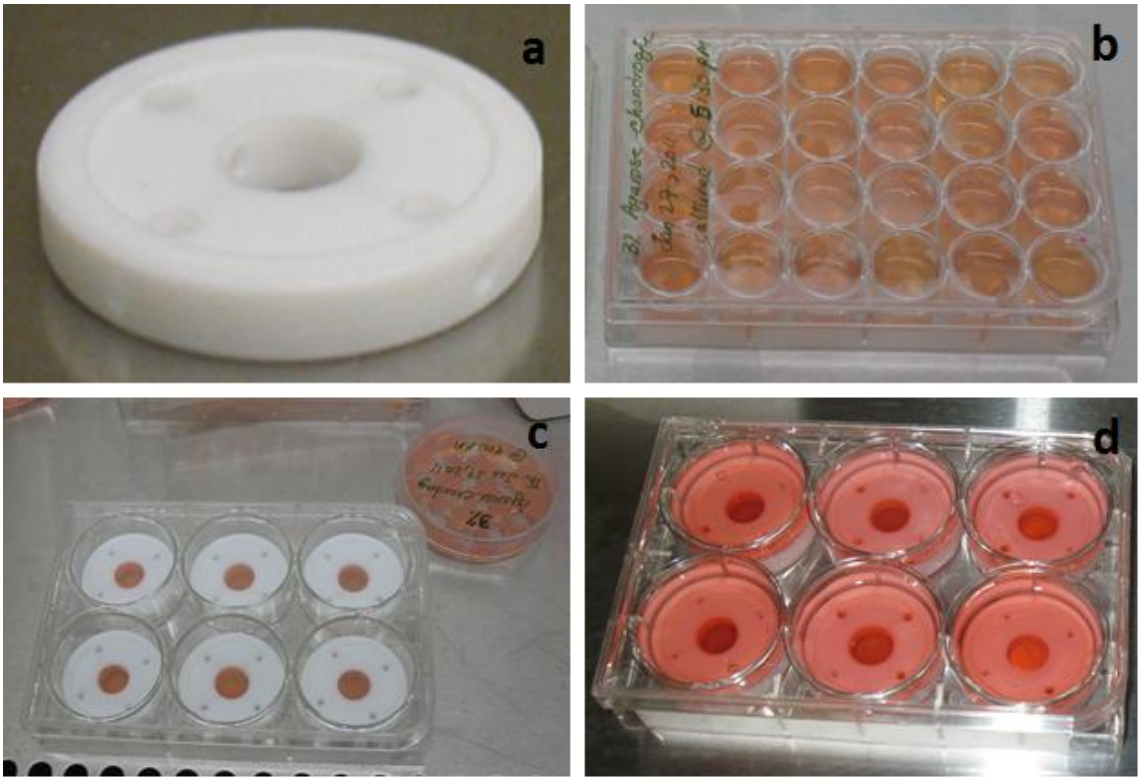

Figure 4.7**.** a) Construct holder; b) constructs culture in free swelling condition; c) transferring construct holders and constructs to six-well culture plate; d) culturing constructs.

4.1.9.5 Preparation for Stimulation

After free swelling period, the construct holders (Figure 4.7 a) and the constructs were transferred to 6-well culture plates (Figure 4.7 c). Then, about 7 ml of culture medium was added to each well, to almost fill the well (Figure 4.7 d). The culture plates were stored in the incubator while the simulator system was being prepared.

The whole stimulation system was disassembled to be able to thoroughly sterilize the parts either with steam sterilizer (Fisher Scientific, Barnstead Sterile Max tabletop steam sterilizer, Cat# 14-4901) or 70% ethanol. The components that could not be autoclaved were immersed in, or frequently sprayed with 70% ethanol. When all sterilized parts were completely dry, the entire

stimulator system was then assembled under sterile condition inside biological safety cabinet (BSC) before starting each study. Then, the hydromechanical stimulator and multichannel pump, and all groups of constructs were placed inside the incubator where all tests were carried out at 37ºC and 5% CO_2 (Figure 3.35). The indenter holder plate held the indenters in their vertical position and in their desired location above the constructs. The indenters were free to go up and down, if necessary, as they slide on the surface of agarose-chondrocyte constructs. According to the designed study, the custom-made weights (unique to each channel) were attached to each of the indenters and each indenter-weight assembly was weighed. Then the pump tubes were attached at the end of the indenter for those channels that were receiving fluid flow.

Before starting the experiment, the approximate positions of indenters within the well of culture plate were adjusted so that the stimulation started from the corner of the area that needed to be stimulated. For this purpose, a sterile culture plate containing only sterile construct holders (without the constructs) was placed under the indenter. Two separate programs (in the hub programmer software) containing simple bidirectional motion in either X or Y motion with very small distances of 0.254 mm and very slow acceleration of 25.4 mm/s^2 were used to finely adjust the position of the indenter tip. Each motion program was repeated until the indenter tip was in the desired location within the well.

4.1.9.6 Loads and Flow Rates

Three studies were conducted, each with two culture plates (group 1 and 2) that contained 6 constructs. Studies were differentiated by their flow rates and explored 16 different load/flow combinations (Figure 4.8). The values of loads and flow rates for individual channels of each study are presented in Table 4.2. The constructs in channels 1-5 of the culture plate were in contact with a loaded indenter and received the fluid flow for 25 min/day, 5 days/week for two weeks. The

constructs in channel 6 were not in contact with an indenter). The stimulation pattern was bidirectional as shown in Figure.3.25 except for somewhat longer line lengths (1.5748 and 4.724 mm) with the acceleration/deceleration set to 50.8 mm/s^2 for both types of lines.

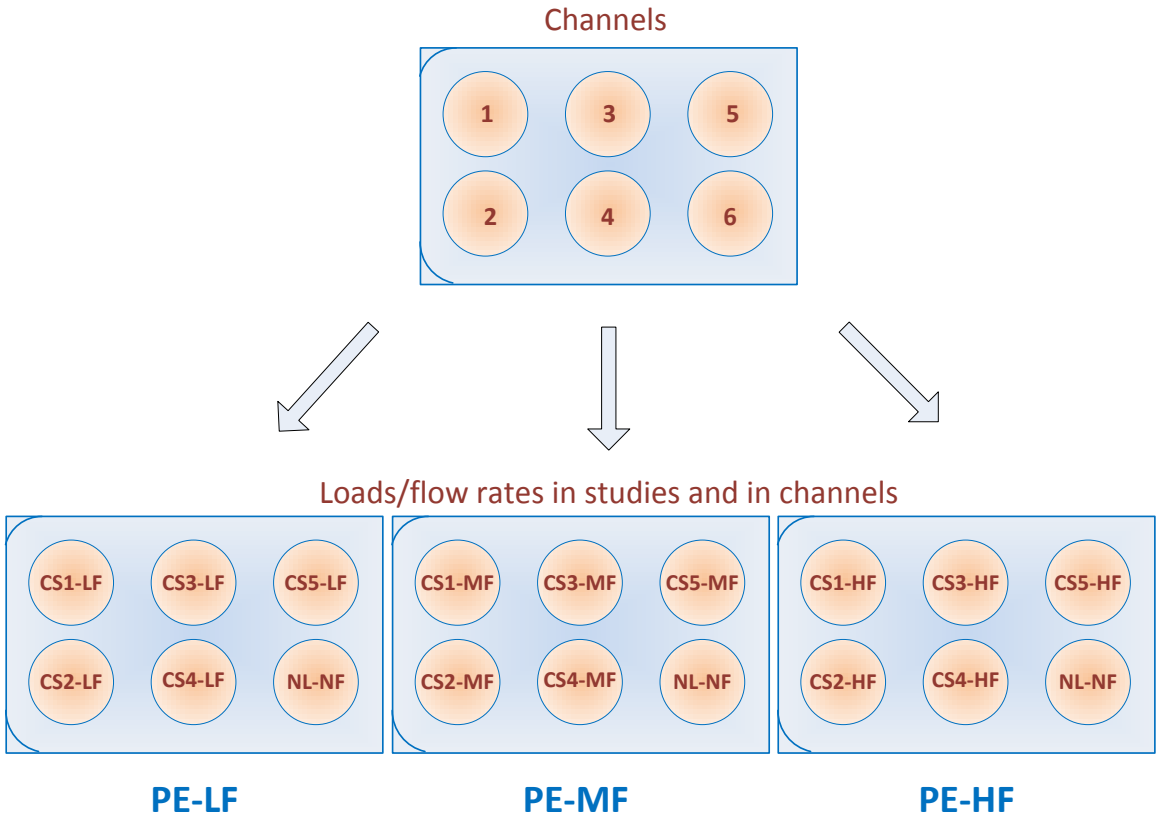

Figure 4.8 Arrangement of channels and assignment of loads/flow rates in each culture plate in 3 different preliminary experiments (PE); LF, MF and HF are low, medium and high flow rates respectively; CS1 to CS5 are mechanical loads (compression + shear) applied to constructs in Ch1 to Ch5; NL-NF is no load, no flow condition.

Table 4.2 Loads and flow rates in preliminary experiments (PE) performed (G: group, Ch: channel, LF: low flow rate, MF: medium flow rate, HF: high flow rate).

Study	Flow rate (ml/min)		Loads (mN)					
Both G1,G2	***Ch1-Ch5***	***Ch6***	***Ch1***	***Ch2***	***Ch3***	***Ch4***	***Ch5***	***Ch6***
PE-LF	5.5	0	28.24	37.37	42.09	56.17	65.92	0
PE-MF	11.24	0						
PE-HF	17.6	0						

The physical appearance of the construct, such as the presence of any crack or abnormal deformation due to load/flow conditions, was recorded for each study and each group every day after the hydromechanical stimulation. The constructs that did fail in this way were replaced with new free swelling construct and the stimulation procedures were continued on them in the next days. This was done to understand the frequency of such failures in order to find a safe and functional range for the future experiments.

4.1.9.7 Harvesting Method and Wet Weight Measurements

At the end of the culturing and mechanical stimulation period, the whole construct in each well of the culture plate was removed, and lightly patted dry and weighed (wet weight) with an analytical balance (Denver Pinnacle, model PI-314). Then, the construct was divided to three sections by two parallel cuts perpendicular to the stimulated surface (Figure 4.9) using a custom-made device with parallel razor blades. The thin slice in the middle (~ 0.8 mm) was used for cell viability analysis. One of the remaining sections of each construct had its mass measured and then was transferred to a 1.5 ml tube for enzymatic digestion in preparation for GAG analysis. The other section was reserved for attempting fixation methods or developing other histology assessments.

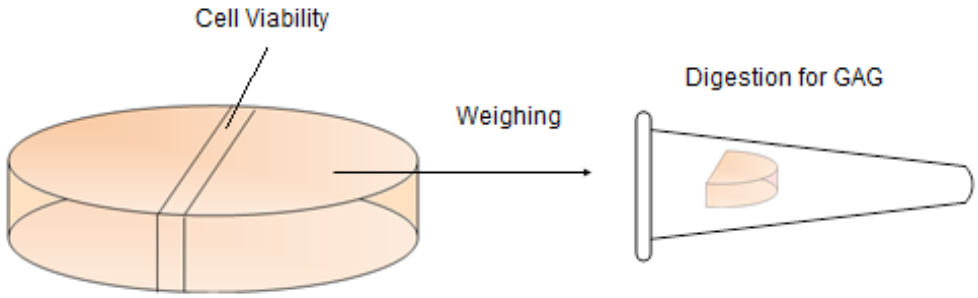

Figure 4.9 Harvesting method for cell viability and GAG analysis in the preliminary experiments.

4.1.9.8 Cell Viability within Agarose

The viability of chondrocytes in agarose hydrogel was investigated at the end of the preliminary experiments. The thin slices of the agarose-chondrocyte construct were placed in a staining solution containing 0.4% trypan blue (Thermo Scientific, HyClone, Cat# SV30084.01) in 0.85% saline for 5 min (method mentioned in [394]). Then, the trypan blue solution was removed and the slices were washed with PBS (1X) to get rid of the excessive stain. Next, the PBS was removed and the slices were immediately viewed using a microscope (Fisher Scientific micromaster inverted microscope Cat# 12575250). This method (Figure 4.10) was used only for the preliminary experiments. Another, more accurate performed procedure was used in subsequent studies which could detect both dead and live cells.

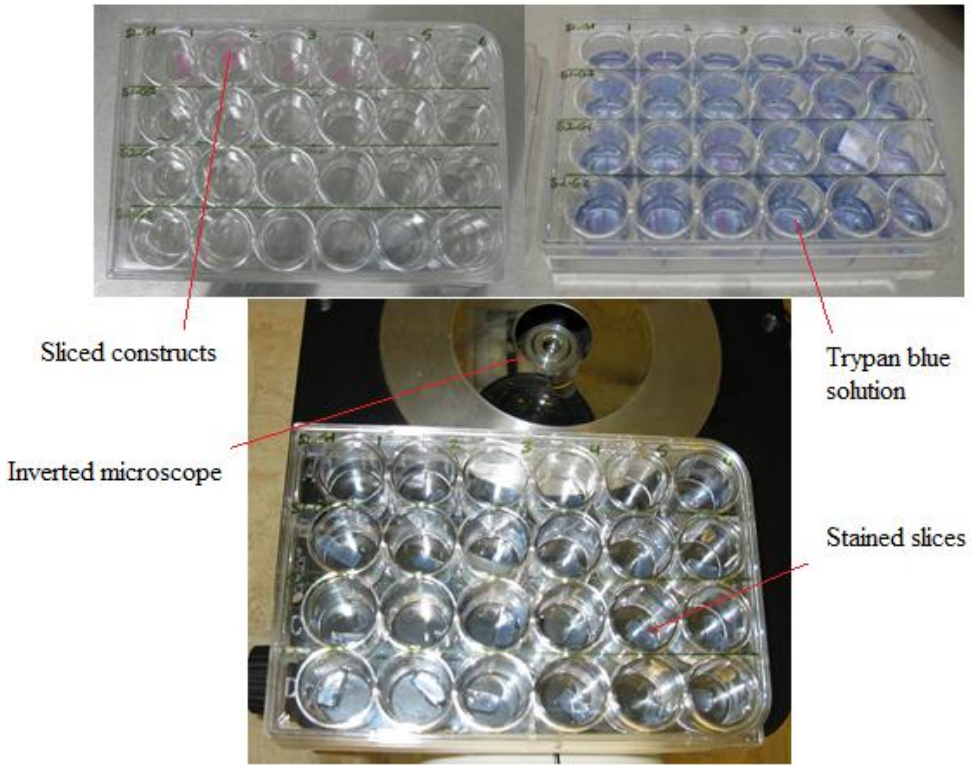

Figure 4.10 Trypan blue staining of the agarose-chondrocyte slices in preliminary studies.

4.1.9.9 Enzymatic Digestion of Constructs

After measuring the weight of the construct section, each construct was transferred to microcentrifuge tubes (~1.5 ml). The papain enzymatic digestion solution was prepared [395] for subsequent GAG or hydroxyproline assays. Briefly, each millilitre of the digestion buffer was prepared first by dissolving 2.72 mg of ammonium acetate (Sigma, Cat# A1542), 0.38 mg of Ethylenediamine-teraacetic acid (EDTA) (Sigma, Cat# E6758) and 0.31 mg of DL-dithiothreitol (DTT) (Sigma, Cat # D0632) in distilled water to make 1 ml volume. The desired volume of digestion buffer was made and then its pH was adjusted to 6.2, and stored at 4ºC until use. Papain

stock (Sigma, Cat# P-3125) was diluted with the digestion buffer to make 40 µg/mL concentration right before starting digestion of samples. About 600 µL of this working digestion solution (containing papain) was added to each microcentrifuge tube holding a sample. Then the cap was tightly closed to prevent evaporation of digestive solution, and all the samples were placed in an oven at 65ºC for 72 h (Figure 4.11). After the digestion process was completed, the digested constructs were centrifuged at 21000 × g for 30 min to separate the agarose from the digested solution. Then the supernatant of each centrifuged tube was transferred to another similar tube and were kept in -20ºC until later analysis. The digested samples could be used for analyzing GAG or collagen retained within the agarose-chondrocyte constructs.

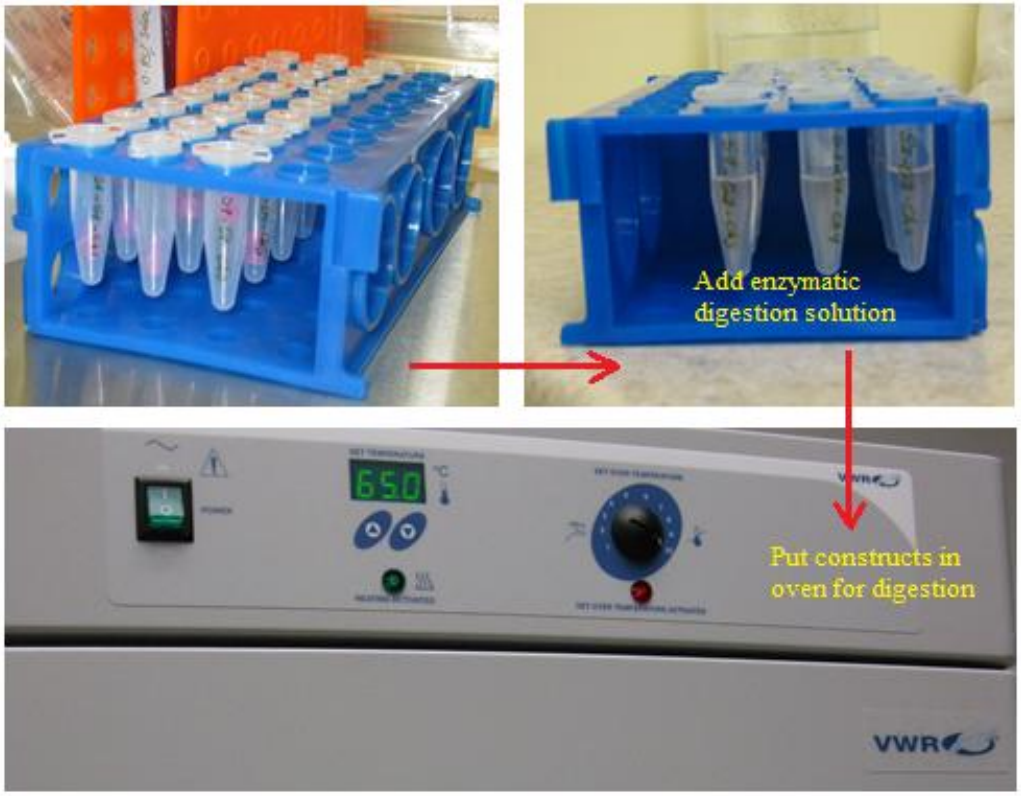

Figure 4.11 Preparing the constructs for enzymatic digestion.

4.2 Main Experimental Studies

4.2.1 Overview

After completing the two-week preliminary experiments and finding ranges of system parameters such as load and fluid flow that would not structurally damage the constructs, long-term studies were conducted to understand the effects of both mechanical and hydromechanical stimulation on the agarose-chondrocyte constructs and specifically on the amount of produced glycosaminoglycan (GAG) and collagen. The overview of conditions in various studies is presented in Table 4.3 and Table 4.4. The harvesting methods of the agarose-chondrocyte in each study were also different.

Table 4.3 Comparison of different experiments. NL: No load, CS: Compression and shear, NF: No flow, HF: High flow rate, LF: Low flow rate, T: Top layer, M: Middle layer, B: Bottom layer.

Study	Duration	Stimulation Period/interval	Stimulation pattern	Loading conditions	Analyses
1 A	3 weeks	30 min/day 5 days/week 2 weeks	Bidirection	NL-NF CS-NF CS-HF	Cell viability, Weight (sectioned) GAG content (retained in the construct)
1 B	3 weeks	30 min/day 5 days/week 2 weeks	Bidirection	NL-NF CS-NF CS-LF	
2	4 weeks	30 min/day 5 days/week 3 weeks	Bidirection	NL-NF (T,M,B) CS-NF (T,M,B) CS-F (T,M,B)	Cell viability, Weight (layered) GAG content (released+ retained) Collagen content (released+ retained)
3	4 weeks	15 min/day 3 days/week 3 weeks	Unidirection	NL-NF (T,M,B) CS-NF (T,M,B) CS-F (T,M,B)	

Table 4.4 Cell densities in different studies (same dimensions for constructs in all studies).

Study	Cell density	Cells per construct (~ 0.3925 ml)	Cell-gel concentration
1 A,B	6.320 million cells/ml	2.4806 million cells	3%
2	1.135 million cells/ml	0.4455 million cells	3%
3	2.660 million cells/ml	1.04405 million cells	3%

4.2.2 Study 1

4.2.2.1 Design of Study

In the first study, a total of 36 constructs were tested (Table 4.4) with various load/flow conditions (Table 4.5). For 3 weeks, both Study 1A and Study 1B were conducted with each culture plate of 6 constructs having conditions as shown in Figure 4.12. For the purposes of statistical analysis, the constructs subject to the same load/flow conditions were grouped together and the constructs that had no load and no fluid flow were grouped together and used as the controls.

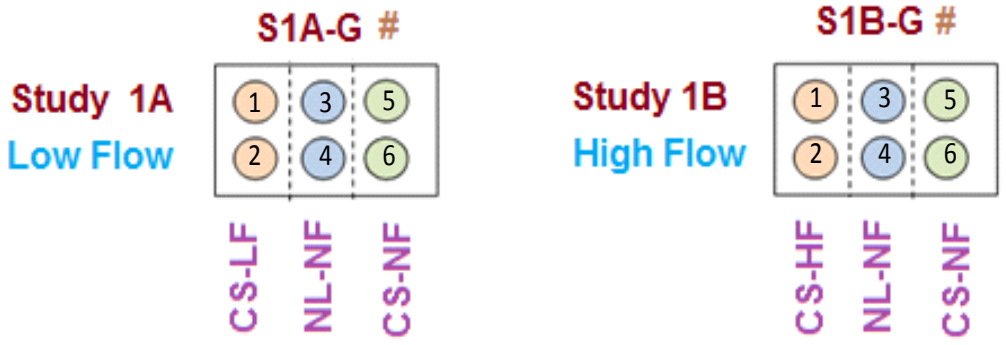

Figure 4.12 Load/flow conditions for Study 1A and 1B; CS-LF: compression, shear and low fluid flow; CS-HF: compression, shear and high fluid flow; NL-NF: no load, no fluid flow.

The constructs in channels 1 and 2 of each group of the studies were hydromechanically stimulated (exposed to compression, shear and fluid flow). In Study 1A these constructs received low fluid flow rate (LF: 7.72 ml/min) and in Study 1B, these constructs, received high fluid flow rate (HF: 14.82 ml/min). The constructs in channels 3 and 4 were exposed to no load and no fluid flow (NL-NF) and were used as controls. The constructs in channels 5 and 6 were only mechanically stimulated (exposed only to compression and shear without fluid flow). The values of normal loads and flow rates for each channel in each study are shown in

Table **4.5**.

Table 4.5 Compression on constructs and flow rate for each channel of Studies 1A and 1B.

Study	Flow rate (ml/min)	Compression (KPa)						
G1-G3	Ch1 & Ch2	Ch3-Ch6	Ch1	Ch2	Ch3	Ch4	Ch5	Ch6
S1-A	7.72	0	5.83	5.83	0	0	5.83	5.83
S1-B	14.82	0						

4.2.2.2 Materials and Methods

The joint dissection, chondrocyte isolation, cell viability in the suspension, chondrocyte encapsulation in agarose hydrogel and the preparation for stimulation were performed using the same methods as for the preliminary experiments (see Sections 4.1.9.1 - 4.1.9.5). The harvesting methods and measurements of constructs' wet weights were the same as described in Section 4.1.9.7. There was a difference in cell density, which for Study 1A and 1B was 6.32 x 10^6 cells/ml whereas in the preliminary experiments it was 6.89 x 10^6 cells/ml. The bidirectional (X-Y) stimulation pattern was similar to that shown in Figure.3.25. All six of the culture plates in studies 1A and 1B (each containing 6 constructs under various load/flow conditions) were stored in the

incubator along with the stimulator system. Each culture plate was stimulated sequentially for 30 min after which the medium inside each well containing the constructs was changed. The stimulation was done 5 days/week for 2 weeks. After one week of free swelling and two weeks of the stimulation, the constructs were removed from the culture condition and analyzed.

The harvesting method with mass measurement and the enzyme digestion of the constructs were done as previously described in Sections 4.1.9.7 and 4.1.9.9 respectively. However, the determination of the cell viability within the agarose was performed differently as explained in the next section.

4.2.2.3 Cell Viability by Fluorescence Microscope

The method of determining cell viability was changed from the preliminary experiments because the live and dead cells could be more accurately detected. The viability of chondrocytes within agarose was quantified after 21 days of construct culture after the last stimulation period. The central thin slices from agarose-chondrocyte constructs were placed inside each well of a 24-well culture plate and incubated (37°C and 5% CO_2 and high humidity) in a solution containing both fluorescent indicators of propidium iodide (PI, Sigma-Aldrich, Cat# P4170) and fluorescence diacetate (FDA, Sigma-Aldrich, Cat# F7378) for 15 min, to simultaneously detect both live and dead cells in a double-staining procedure with green and red colour respectively. Then, the slices were washed in PBS to remove excessive unabsorbed dye and were viewed using a digital inverted microscope fluorescent microscope (Life Technologies, Burlington, ON., Canada, www.lifetechnologies.com, EVOS XL) at wavelengths of 520±10 nm and 600±10 nm, for detecting each colour. At the same time, the pictures were captured using the built-in microscope camera at various magnifications.

4.2.2.4 Wet Weight Measurement and Enzymatic Digestion of Constructs

The wet weights of the sectioned constructs for GAG analysis were measured by analytical balance (Denver Pinnacle, model PI-314). The procedures of the enzymatic digestion were similar to Section 4.1.9.9.

4.2.2.5 Measurement of Retained GAG in Agarose-Chondrocyte

The amount of GAG content of the digested agarose-chondrocyte construct was quantified using a plate reader (96-well standard assay plates) and 1,9-Dimethylmethylene blue (DMMB) (PolySciences, Washington, PA) (Cat# 03610-1) dye-binding assay (originally by Farndale et al. 1986) [396] and modified by [397].

Before this measurement, the standard curve for analysis was generated using chondroitin sulfate sodium salt from shark cartilage (Sigma, Cat# C4384). The standard curve provided a relationship between the absorbency and certain concentrations of GAG. The procedures for generating standard curve were repeated until finding a linear relationship with good correlation.

The standard curve was generated by serial dilution of the GAG working solution to have variations of chondroitin sulphate concentrations, that ranged from 0 - 100 µg/ml. A part of each digested sample was directly mixed with DMMB dye solution, and a part of it was diluted in 1% BSA in PBS (dilution factor of 1/5) and then mixed with dye. The diluted combination was pipetted up and down many times (without creating bubbles) to make a homogenous solution. For every 10 µL of digested sample or GAG standard, 200 µL of DMMB dye solution was added in each well of the 96-well assay plate. Triplicate for each sample was taken. The plate content was measured immediately (due to instability of GAG and DMMB mixture) with the plate reader set at 525 nm wavelength. Finally the recorded values of optical density were converted to GAG

concentration according to the standard curve. The GAG content was normalized to wet weight of the corresponding section.

4.2.2.6 Statistical Analysis

Retained GAG values were presented as the average (mean) with standard deviation for the samples (total n=36) under each of the different load/flow conditions (NL-NF (n= 12), CS-NF (n=12), CS-LF (n= 6), CS-HF (n=6)). The results were analyzed using the Statistica Software (Academic version, StatSoft, www.statsoft.com). The results of retained GAG were compared for the different load/flow conditions using analysis of variance (ANOVA). Before the tests, normality was checked and a significance of $p < 0.05$ was assigned.

4.2.3 Study 2

4.2.3.1 Design of Study

In the second study, a total of 54 constructs were tested (Table 4.4) under various load/flow conditions. All of the 12 unstimulated constructs were cultured in separate 6-well culture plates (with the same construct holders as the stimulated constructs), received the same volume of cell media as the stimulated constructs and had the cell media changed on the same days as the cell media of the stimulated constructs. The 42 stimulated constructs were either mechanically (CS-NF) or hydromechanically (CS-F) stimulated (Figure 4.13). For the hydromechanical stimulation, the flow rate was 12.2 ml/min. The input conditions of Study 2 are shown in Table 4.6.

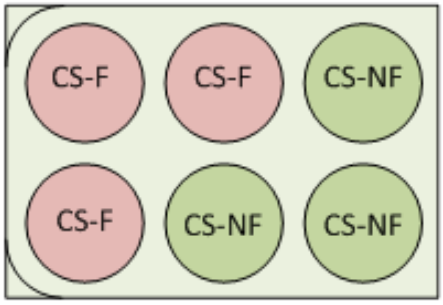

Figure 4.13 Load/flow conditions for the stimulated constructs in Study 2. CS-F: compression shear with flow (Ch1-3), CS-NF: compression and shear without flow (Ch4-6).

Table 4.6 Compression on constructs and flow rate for each channel of Study 2.

Study	**Flow rate (ml/min)**		**Load (mN)**	**Compression (KPa)**
G1-G6	***Ch1 –Ch3***	***Ch4-Ch6***	***Ch1-Ch6***	
S2	12.2	0	45.1	5.83

4.2.3.2 Materials and Methods

The joint dissection, chondrocyte isolation, viability assessment in cell suspension, chondrocyte encapsulation in agarose hydrogel and preparation for stimulation were performed with the same methods as for the preliminary studies (see Sections 4.1.9.1 - 4.1.9.5). The same bidirectional (XY) stimulation pattern and kinematic checks were used as in Study 1. Mass measurement was done in the same way as in Study 1 and the Preliminary Experiments. However, because of a new harvesting method more components were measured as discussed in the next section.

Once again, there was a difference in cell density, which for Study 2 was 1.135 x 10^6 cells/ml. Also, all of the constructs were in an "initial" free swelling condition (in 2 ml cell media in 24-well plates) for 9 days instead of 7 days and had an extra day of free swelling (in 7 ml cell media in 6-

well plates) before stimulation began as shown in Figure 4.14. In addition, the harvesting method changed as explained in the next section.

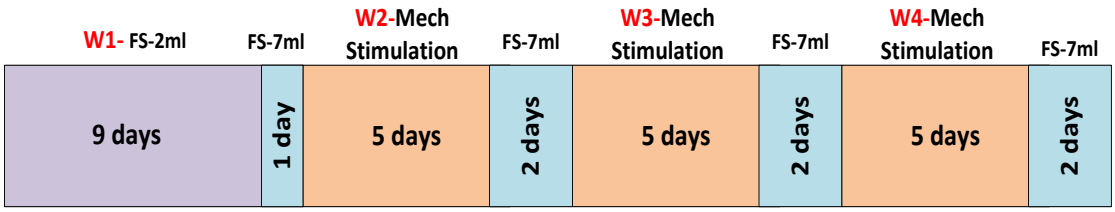

Figure 4.14 Time course of Study 2 (FS: free-swelling in 2 or 7 ml of culture media).

After 31 days of culture including 15 days of stimulation, the constructs were removed from the culture to be analyzed. Since for Study 2, the amounts of released GAG and released collagen were to be measured, samples of the cell media were collected every day while changing it (following the stimulation). All the cell media of the similarly loaded channels of each culture plate were collected in one tube. For instance, one tube was for collected cell media of CS-NF from culture plate 1, and one for all 3 CS-F from culture plate 1 and so on. In retrospect, this was a mistake because the ability to statistically analyse the construct-to-construct variation in chondrocyte stimulation that was reflected by both retained and released GAG and collagen was much impaired. Once collected, the culture media samples were immediately transferred to -20^{o}C and stored there to await biochemical analysis.

4.2.3.3 Harvesting Method

As mentioned above, the construct harvesting method was very different from the preliminary experiments and Study 1. The new harvesting method was developed to investigate layer-by-layer changes of GAG and collagen production. Thus, the agarose-chondrocyte constructs in Study 2

were sectioned parallel to the stimulated surface and each layer was analyzed separately for GAG or collagen as shown in Figure 4.15.

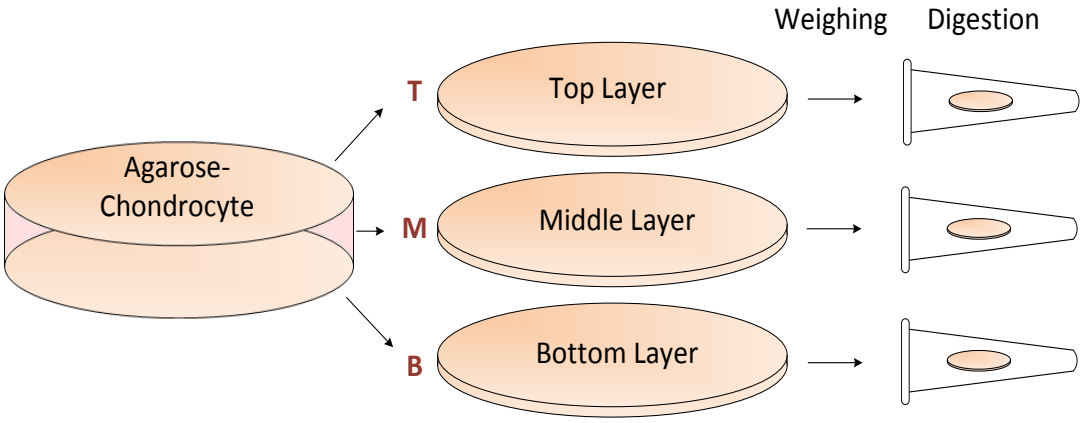

Figure 4.15 Harvesting method of constructs in Study 2.

To precisely cut the layers with thin thickness, a custom-made guide was used which was made with the same central hole size for holding construct and very thin slot in its side for passing the blade through it for cutting the construct. The sectioning procedure using this guide is shown in Figure 4.16. Using sterile tweezers, the construct along with the construct holder was removed from the culture plate and were place on top of the sterile cutting guide. Using the transferring bar, the construct was slid out of the construct holder and slowly and very lightly pushed to fit inside the hole of cutting guide. The top surface of the construct was leveled with the top surface of the cutting guide. While holding two sides of cutting guide, the thin blade was inserted through thin slot and moved along the slot to cut the construct and create a thin circular layer. The tip of the blade was pushed up, just a little, to separate the sectioned layer from the rest of the construct. The layers were weighted for biochemical analyses or, as explained in the next section, used for assessing the cell viability.

To be able to harvest the middle layer, the top of cutting guide was turned upside down and using the transfer bar, the construct was slightly pushed down with transferring bar so that the middle layer could be leveled with the top surface of the cutting guide, and the same procedures were followed as for cutting the top layer. The bottom layer was simply pushed out of the cutting guide by transferring bar.

The wet weight of whole construct was measured before sectioning. After each section was made, the wet weight of that layer was measured and immediately that layer was transferred to the corresponding labelled microcentrifuge tube in case that was about to be digested or was transferred to corresponding labelled well of culture plate to be stained with fluorescence probes for assessment of cell viability.

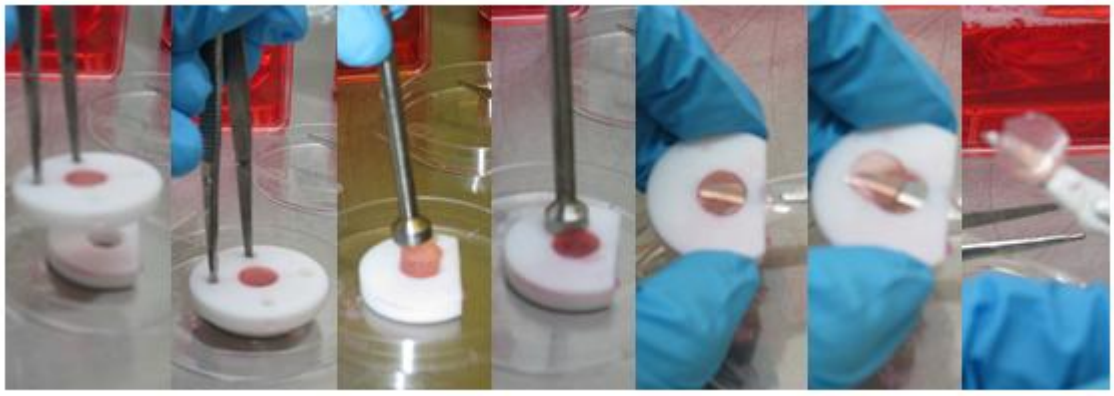

Figure 4.16 Layering method of agarose-chondrocyte in Study 2.

4.2.3.4 Cell Viability within Agarose Gel

Three construct from CS-NF loading conditions and three constructs from CS-F loading conditions and one from unstimulated samples (NL-NF) were used for cell viability analysis. Each layer of the

construct was separately placed in labeled 24-well plates. The rest of the procedures were similar to that explained in Section 4.2.2.3.

4.2.3.5 Enzymatic Digestion of Constructs and Measurement of Retained GAG

Each layer of the construct was transferred to a separate labelled microcentrifuge tube and the digestion process of the construct was conducted as it was explained in Section 4.2.2.4. The GAG content of each layer was normalized to the wet weight of the corresponding layer. Total volume of digestion buffer used for each layer was 600 µL.

4.2.3.6 Measurement of Released GAG into the Cell Media

The cell media samples that were collected each day after the mechanical or hydromechanical stimulation of each loading condition of each group (as explained in Section 4.2.2.2) were used for measuring the released GAG into the cell media. The amount of GAG was quantified by the amount of sulfated GAGs in Guanidine hydrochloride (Sigma-Aldrich, Cat# G4505) [398] and then its GAG content was measured using DMMB assay (as it was explained in Section 4.2.2.4).

The amount of released GAG into the media was also measured without precipitation, by simply removing 5 µL of the media and then transferring it to 96-plates (triple), and then mixing it with the same volume of 1% BSA in PBS (triple). Then 200 µl of DMMB dye was added and the rest of the procedures were the same as explained in Section 4.2.2.4.

4.2.3.7 Measurement of Retained Collagen in Agarose-Chondrocytes

The collagen content retained in the digested constructs was estimated by the amount of hydroxyproline content using the chloramine-T/ reagent assay [399]. First, trans-4-hydroxy-L-proline (Sigma, Cat# 56250) was dissolved in 0.001 N HCl to make hydroxyproline stock solution with final concentration of 100 µg/ml, and then it was stored at -20ºC until use. This stock was used for generating standard curve (to find relationship of hydroxyproline concentration with absorbency read from microplate reader). Then hydroxyproline assay buffer was made by mixing 5g citric acid (Sigma, Cat# 251275), 1.2 ml of glacial acetic acid , 7.23 g of sodium acetate (EMD, Cat # SX02255-1), 3.4 g sodium hydroxide (Sigma, Cat # 221465) in dH2O to make final volume of 100 ml solution and stored in 4ºC until use. This buffer would be used for making chloramine-T solution. The 0.05N chloramine-T solution was prepared by dissolving 0.282 g chloramine-T (Sigma, Cat# 857319) in 4 ml dH2O and then adding 6 ml of methyl-cellosolve (Sigma, Cat# 360503) and 10 ml of buffer (hydroxyproline assay buffer) to it. For color development two more solution was required rather than chloramine-T in this assay. They were perchloric acid and Ehrlich's reagent. The 3.15N perchloric acid was prepared by diluting 4.6 ml of 70% perchloric acid in 14.6 ml of dH2O (stored at room temperature). About 4 g of p-Dimethylaminobenzaldehyde (Ehrlich's reagent) (Sigma, Cat# 156477) was dissolved in 20 ml of methyl-cellosolve (Sigma) while heated up to 60ºC.

Aliquots of the digested sample were acid hydrolyzed first in 6N hydrochloric acid (HCl) (Sigma, Cat # 258148) in glass test tubes with screw cap (VWR, Cat# 89001-478), at 110°C for 18h using digital dry bath (Fisher Scientific, Cat#11715145DQ) (Figure 4.17) containing 4 module blocks (Fisher Scientific, 11715309Q) which each could hold 22 test tubes with 12-13 mm diameter. Then the hydrolyzate was neutralized by adding NaOH (100µL of 5.7 N NaOH for 100

µL of sample) and was diluted (1/10) by dH2O and then aliquots of 200 µL of hydrolate in 3 separate eppendorfs were made.

Figure 4.17 Digital dry bath (test tube heater) used for hydroxyproline assay.

To develop color, for either samples or standards, first 100 µL of the 0.05 N chloramine-T was mixed and waited for 20 min. Then 100 µL of the 3.15N perchloric acid was mixed and waited for 5 min. Finally 100 µL of Ehrlich's reagent was mixed and heated (using dry bath heater) at 60ºC for 20 min (the order of mixing is important). Then the tubes were cooled in cold tap water for 5 min. The samples were loaded in 96-well assay plates (Fisher Scientific, Cat#7200656) with either 200 µL of standard or sample in the wells (triple).

The standard curve was generated first using L-hydroxyproline (Sigma Aldrich). The developed color due to different concentrations of hydroxyproline content for standard curve generation is shown in Figure 4.18. Then the absorbency of either samples or standards was measured at 560 nm using microplate reader (SpectraMax Plus 384, www. moleculardevices.co). It was assumed that weight of hydroxyproline is 10% of the weight of collagen according to previous study [400]. The

collagen content of each layer was normalized to wet weight of the corresponding layer. The retained collagen contents of all three layers were summed to estimate total retained collagen content of construct.

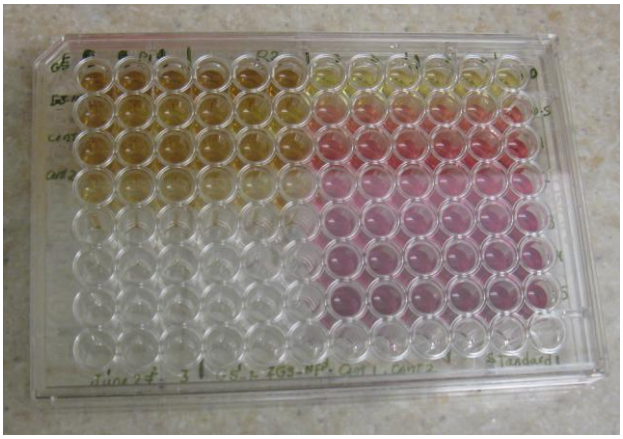

Figure 4.18 The developed color for different hydroxyproline concentrations for generating standard curve in 96-well assay plates. The darker shades contained more hydroxyproline concentration.

4.2.3.8 Measurement of Released Collagen into the Cell Media

For measuring the amount of released collagen into the media, the cell media was precipitated by ammonium sulfate (Sigma-Aldrich, Cat# A4915). Details of this protocol were learned from the Tissue Engineering Laboratory of Dr. Stephen Waldman (Queen's University, Kingston, ON). After defrosting the cell media, 70% ammonium sulfate in dH_2O was made. About 1.5 ml of 70% ammonium sulfate was slowly added to every 2 ml of medium and then they were mixed on shaker for an hour and then left at 4°C in the fridge overnight to precipitate. The tubes containing these mixtures were centrifuged at 14000 rpm for 30 minutes. The generated pellets were rinsed (without suspension) with 50 µL of cold 70% ethanol and were centrifuged again at 14000 rpm for 10 min

and the supernatant was discarded. The 10 min centrifugation and removal of supernatant was repeated three times and then the pellets were dried by leaving them uncovered in the freezer for an hour. Then these pellets were used for collagen content analysis using hydroxyproline assay as it was mentioned in Section 4.2.2.8.

4.2.3.9 Statistical Analysis

Data for retained, released and total (retained + released) GAG and collagen were presented as the average (mean) with standard deviation for three different load/flow conditions of NL-NF (n=11), CS-NF (n=18), and CS-F (n=18). The results were analyzed using the Statistica Software (Academic version, StatSoft, www.statsoft.com). The results of were statistically compared amongst different load/flow conditions and analyzed using analysis of variance (ANOVA) to determine the effect of load/flow conditions on both GAG and collagen production. Before the tests, normality was checked and significance of p-value less than 0.05 was assigned.

4.2.4 Study 3

4.2.4.1 Design of Study

The same flow rate as Study 2 was applied on the constructs with different compression as explained in Table 4.7. The extra weights on the indenters were removed and hence only the weights of indenters themselves were applied on the constructs. The study initially included 8 loaded groups (3 CS-F and 3 CS-NF per group) and 3 unloaded groups (6 NL-NF per group). The difference was that instead of analyzing all the samples at the end of study, some samples from each loading condition were analyzed in certain time points as shown in Figure 4.19. This figure shows the number of samples in every week of the study and specific time points that the

biochemical analyses were conducted. The stimulation pattern was set to be unidirectional reciprocating motion (4.064 mm distance in Y direction) in the center (Figure 4.20) with 50.8 mm/s^2 acceleration/deceleration. The constructs in loaded groups received the stimulation for 15 min/day, for 3 days/week for 3 weeks.

Table 4.7 Compression on constructs and flow rate for each channel of Study 3.

Study	**Flow rate (ml/min)**		**Load (mN)**	**Compression (KPa)**
G1-G6	***Ch1 –Ch3***	***Ch4-Ch6***	***Ch1-Ch6***	
S2	12.2	0	28.5	3.68

4.2.4.2 Materials and Methods

Most of the materials and methods were similar to Study 2 (Section 4.2.3.2), except for cell density and the initial free swelling time. The cell density was 2.66 million cells/ml in agarose and the initial free swelling period was 4 days (instead of 9 days).

4.2.4.3 Harvesting Method

Similar to Study 2, the constructs were sectioned into three thin layers. Then, the central stimulated area was cut away from the unstimulated area along two parallel lines which were 5 mm distance from each other as shown in Figure 4.21 and Figure 4.22. The central stimulated line was identified by slightly deformed path created on the top surface of loaded constructs. The procedures of harvesting layers, central and side sections are shown in Figure 4.22.

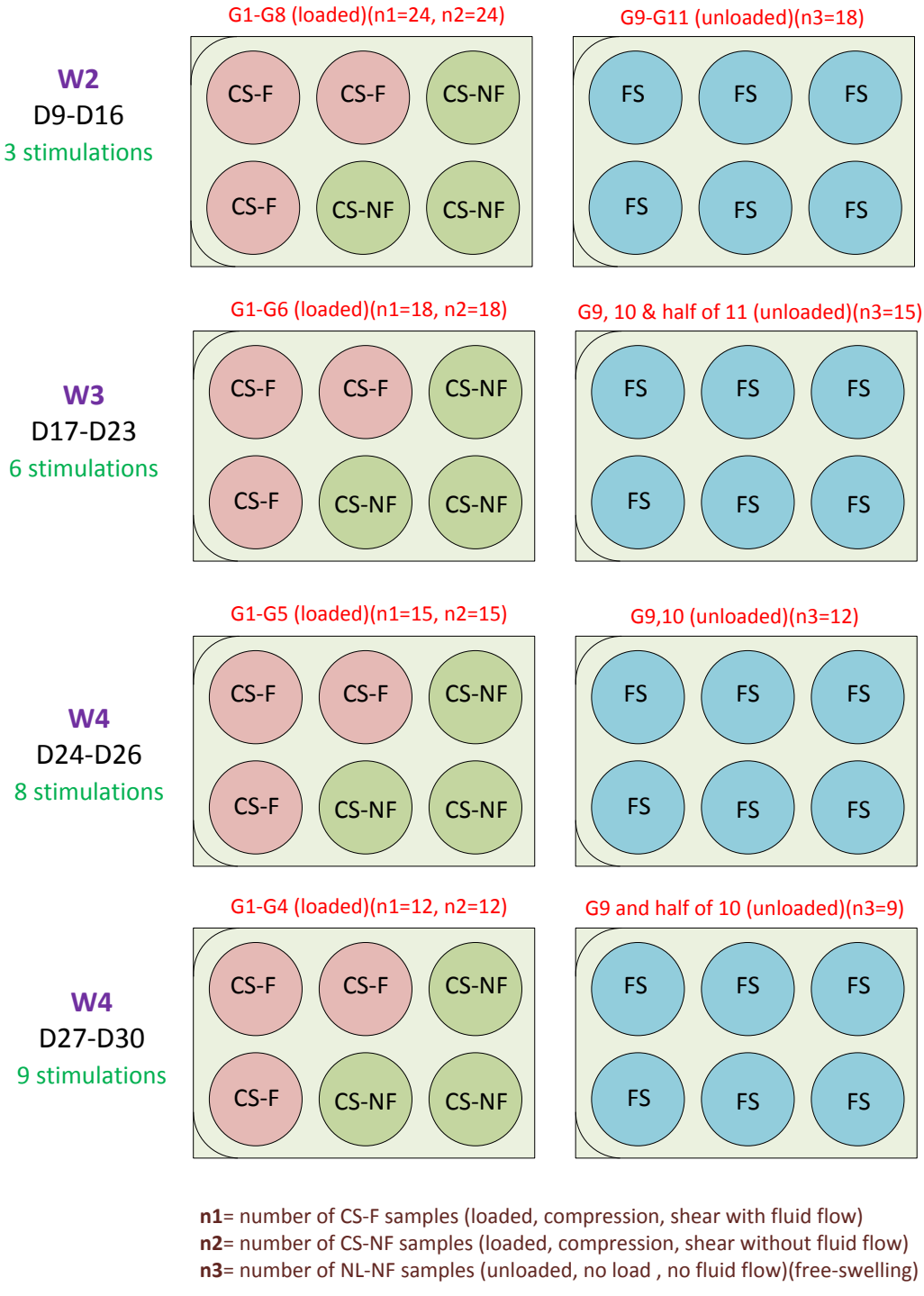

Figure 4.19 Design of Study 3.

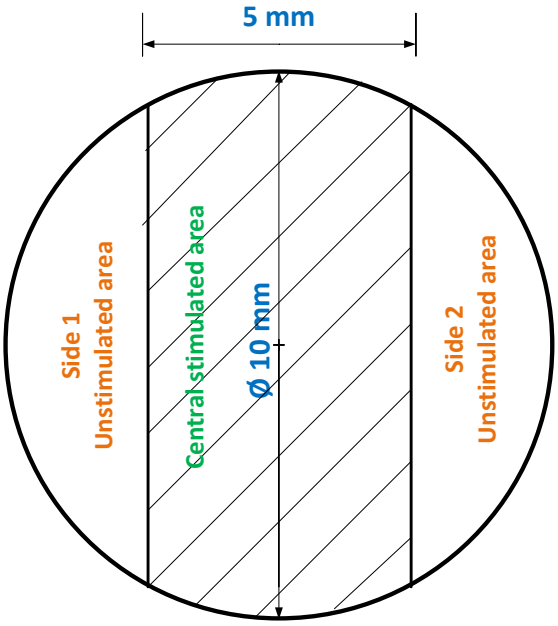

Figure 4.20 The stimulated area in unidirectional stimulation pattern.

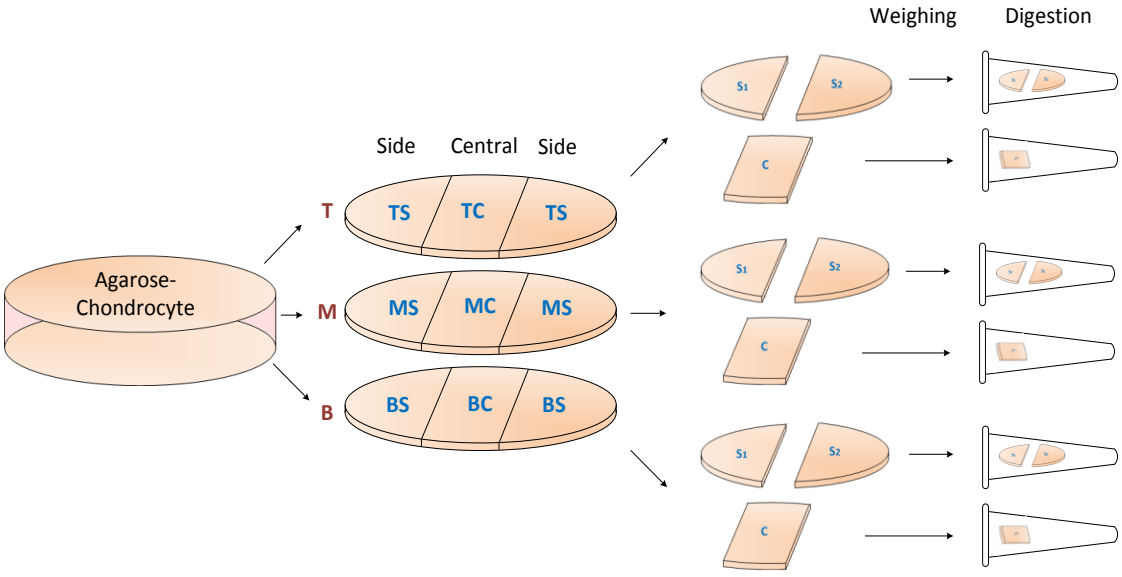

Figure 4.21 Harvesting method of constructs in Study 3.

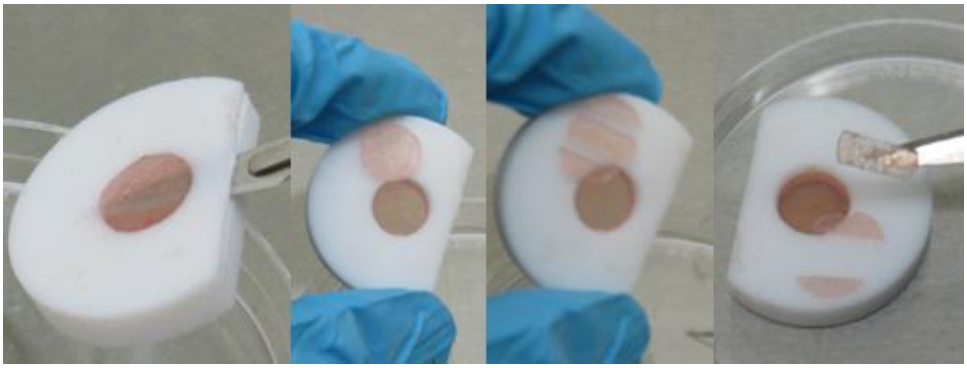

Figure 4.22 Layering and sectioning method of constructs in Study 3.

4.2.4.4 Weight Measurements of Construct and its Sections

The wet weight of whole construct was measured first before harvesting. After sectioning each layer of the construct, the wet weight of the central stimulated section was measured. Then the two side, unstimulated sections were weighed together (as they were also digested together in the same tube).

4.2.4.5 Cell Viability by Fluorescence Microscope

Three construct from three load/flow conditions of NL-NF, CS-F and CS-NF were used for cell viability analysis. Each section (either loaded or unloaded) of each layer of the construct was separately placed in labeled 24-well plates and incubated for about 15 min with propidium iodide (PI) and fluorescein diacetate (FDA). The rest of the procedures were similar to that explained in Section 4.2.1.4.

4.2.4.6 Enzymatic Digestion of Constructs

The side unstimulated sections and the central stimulated section of each layer were digested separately, as it was shown in Figure 4.21. The rest of procedures of the enzymatic digestion were similar to Section 4.1.9.9.

4.2.4.7 Measurement of Retained and Released GAG

The quantification procedures for retained and released GAG were the same as that explained in Section 4.2.1.6 and 4.2.1.7 respectively. The GAG content was normalized to the wet mass of the corresponding layer.

4.2.4.8 Measurement of Retained and Release Collagen

The quantification procedures for retained and released collagen were the same as that explained in Section 4.2.1.8 and 4.2.1.9 respectively. The collagen content was normalized to the wet weight of the corresponding layer.

4.2.4.9 Statistical Analysis

Data for retained, released and total (retained + released) GAG and collagen were presented as the average (mean) with standard deviation for three different load/flow conditions of NL-NF, CS-NF and CS-F at three different time points of D23, D26 and D31. The number of samples of each loading group at each time point is shown in Table 4.8.

Table 4.8. Number of samples of each loading group at each time point in Study 3.

Load-Flow	Day 23	Day 26	Day 31
NL-NF	3	3	7
CS-NF	3	3	10
CS-F	3	3	10

The results were analyzed using the Statistica Software (Academic version, StatSoft, www.statsoft.com). The results were statistically compared amongst different load/flow conditions and analyzed using analysis of variance (ANOVA) to determine the effect of load/flow conditions on both GAG and collagen production. Before the tests, normality was checked and significance of p-value less than 0.05 was assigned.

4.3 Chapter Outlook

This chapter presented the methods that were used to detect viability of chondrocytes in agarose constructs and also the methods that were employed to determine biochemical properties of cell-seeded constructs in all loading conditions. Both cell viability methods and biochemical analyses investigated depth-wise through the construct by measuring the properties of its three layers individually. Two measured biochemical properties were the amounts of proteoglycan and collagen. The amount of glycosaminoglycan (GAG) and hydroxyproline were quantified to estimate the contents of proteoglycan and collagen respectively. The quantification of released GAG and collagen into culture media was found important and then it was included then as part of analyses in the last two studies. The results will be presented in the next chapter.

Chapter 5

Experimental and Analytical Results

This chapter presents four main sections. The first section includes the results related to system functionality. It reports findings from short term pilot studies that helped to regulate fluid flow rates, to control or optimize motion of constructs, and to select proper concentration for agarose. Then the main findings from observations in 2-week preliminary experiments are reported and discussed. The second to fourth sections present the results and discussions of three main studies in this thesis. The last section provides conclusion on results of all the conducted experiments.

5.1 Functionality of Stimulator System

5.1.1 Motion of Constructs

Selected Acceleration/Deceleration and Travelling Distances of Constructs

The original settings for values of acceleration/deceleration and travelling distances in bidirectional stimulation pattern had to be lowered. It was found that at high accelerations /decelerations (> 254 mm/s^2), there was a problem of overshoot of motor while stopping at the end of its travel. In high accelerations/decelerations, the end point of cycle was not in the same location as the starting point (Figure.3.24) even after 5 minutes of stimulation period. The acceleration/deceleration of 101.6 mm/s^2 slightly shifted the contact points during a 15 min stimulation period. The accumulation of even tiny overshoots of the motor, caused displacement of the contact points of the indenter on the

surface in each cycle as shown in Figure 5.1. These small displacements over longer periods of time could greatly misplace the stimulation lines from their original positions. In this case, the indenter tip could make contact with the construct holder instead of travelling on the construct surface, which could damage either construct, construct holder or indenter.

To avoid these problems, and to have accurately positioned points, lines and area of stimulation, the acceleration/deceleration was lowered, at the expense of a little bit longer time for completing a cycle, and the size of the stimulation area was slightly decreased by defining shorter lines of travel. The acceleration/deceleration was set at lower value of 50.8 mm/s^2 and the stimulation area was considered to be smaller (3.81 × 3.81 mm) which included lines with 1.27 mm and 3.81 mm length (Figure 3.26) (instead of original settings of 101.6 mm/s^2 and longer lines of 1.57 mm and 4.72 mm). With these settings, over the 30 min stimulation period, there was no visible displacement of the starting and ending points of the cycles. Also, the indenter tip never reached the circular edge of the construct. The considered stimulation area was small enough not to exceed the construct edge but large enough to cover most of the surface of construct. The acceleration/deceleration was selected in such a way to avoid overshoot problem and misplacements of stimulation pattern, yet to provide a large number of repeating cycles over the 30 min stimulation period. These settings might need to be reconsidered in cases where constructs are to be stimulated for longer or shorter periods of time. The results for estimated cycle times and maximum speed by SiNet program and measured cycle times for uni/bidirectional patterns in specific accelerations are presented in Appendix E.

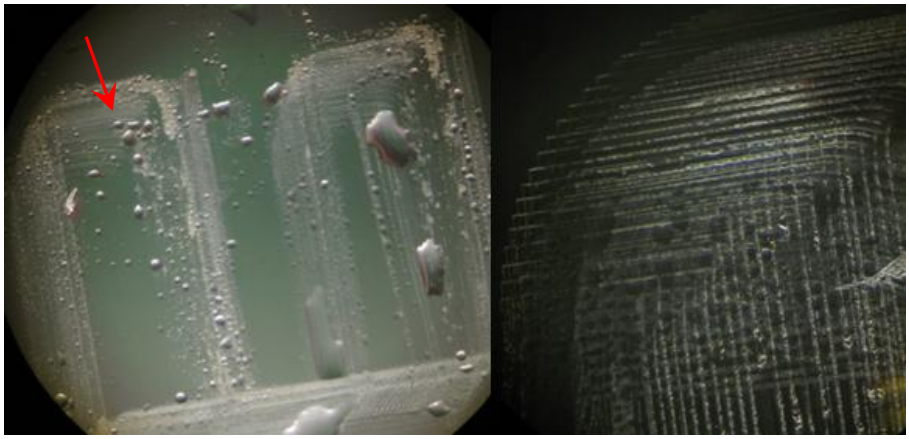

Figure 5.1 Shift of contact points in each cycle at a high acceleration/deceleration level (254 mm/s^2). The above patterns were created on the bottom of culture plate (not on construct) by a sharp point attached to the indenter tube tip instead of the usual hydrostatic bearing fixture.

Number of Cycles for Bi/Unidirectional Pattern in Specific Time Period

The numbers of cycles were measured as explained in Section 4.1.5. The numbers of cycles that can be completed in certain time periods are presented in Table 5.1.

Table 5.1 Number of cycles in specific time periods of stimulation.

Stimulation pattern	**Cycle time (s)**	**Freq. (Hz)**	**Time Period (min)**				
			10	15	20	25	30
			Number of cycles (rounded)				
Bidirectional	4.035	0.24783	148	223	297	371	446
Unidirectional	1.045	0.95693	574	861	1148	1435	1722

5.1.2 Flow Rates

The pump was calibrated as explained in Section 4.1.7. The speed of the pump roller could be changed using the speed setting analog interface which was connected to a built-in potentiometer,

graded from 1 to 99%, with 1% steps. The relationship of flow rate (ml/s) with respect to pump speed (%) for wide range between 0-99% is shown in Appendix F. There was a little bit of fluctuation in speeds of 50% and 70%, but there was consistency in response of all the six channels.

The measured flow rates, when the indenter was attached at the end of pump tubing are compared (Figure 5.2) with the measured flow rates without having indenter attached. As the speed increased the fluctuations from linear relationship with flow rate increased (specifically in speeds more than 19%). The mean difference between the flow rates with and without indenter attached in the speed range of 1-15 was 0.243 ml/min and in the range of 17-31 was higher by about 0.442 ml/min. This showed that use of the indenter and the small channel at its tip slightly affected the flow rate especially in higher speeds of the peristaltic pump.

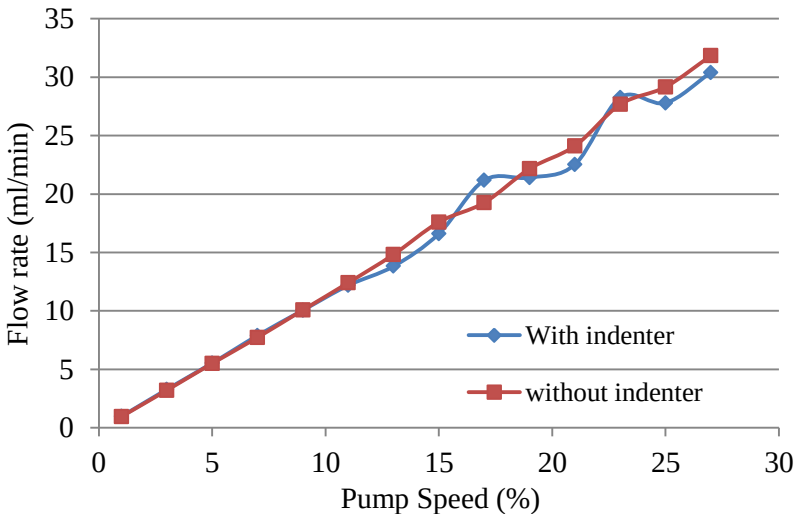

Figure 5.2 Measured flow rates in two different settings (average of 6 channels): 1) with indenter, 2) without indenter attachment at the end of the pump tubing.

5.1.3 Selection of Agarose Concentration

The agarose with different concentrations were made and loaded with variety of stimulation conditions as explained in Section 4.1.8 to be able to find a functional range to start the experiments. The appearance of deformation along the stimulated path, presence of any crack in agarose hydrogel or destruction of any part of the hydrogel specifically the surface due to extensive wear is reported in Table 5.2.

The record of observation showed that the increasing the amount of compressive load from 28.4 mN (C1) to 56.17 mN (C3) had no effect on the construct physical appearance in static condition when the indenters were in contact with the surface of the stationary constructs. But in dynamic conditions which involved the motion of constructs under the indenters, all compressions could deform the agarose gels except the one with 4% concentration. The construct with 1% concentration could not withstand CS2 load and cracked; as the load increased to CS3 both 1% and 2% agarose constructs cracked under the load and by the end of the stimulation period, there were signs of destruction of the hydrogel surface. When fluid flow was added, the record showed that this created different kind of loading to the surface as more constructs cracked under the same compressions.

In the tested ranges of concentrations, agarose with 3% and 4% concentration could withstand all kinds of the defined loads within the 30 min period of load/flow stimulation. Between these two concentrations, the use of 3% agarose has been more common than 4% (listed studies in A.7 in Appendix A.) to provide a 3D environment for chondrocytes to grow as they received the mechanical loads. The agarose with lower concentration is less stiff and can better transfer the loads to the chondrocytes that are to be seeded within it.

Table 5.2 Visible impact of various loading combinations on agarose hydrogels with different concentrations after 30 min of load/flow stimulation; N: No, Y: Yes, NF: no flow, MF: medium flow rate of 11.24 ml/min, C1, C2, C3= only compressions from 28.24, 42.09 and 56.17 mN loads respectively, CS1, CS2, CS3 = C1, C2, C3 compressions respectively when there is sliding shear due to bidirectional motion of constructs.

Load-Flow-Concentration	Deformation	Crack	Destruction
C1/ C2/ C3 / CS1- NF-1%	N	N	N
C1/ C2/ C3 / CS1- NF-2%	N	N	N
C1/ C2/ C3 / CS1- NF-3%	N	N	N
C1/ C2/ C3 / CS1- NF-4%	N	N	N
CS2- NF-1%	**Y**	**Y**	N
CS2- NF-2%	N	N	N
CS2- NF-3%	N	N	N
CS2- NF-4%	N	N	N
CS3- NF-1%	**Y**	**Y**	N
CS3- NF-2%	**Y**	**Y**	N
CS3- NF-3%	N	N	N
CS3- NF-4%	N	N	N
CS1- MF-1%	**Y**	**Y**	N
CS1- MF-2%	**Y**	**Y**	N
CS1- MF-3%	**Y**	N	N
CS1- MF-4%	N	N	N
CS2- MF-1%	**Y**	**Y**	**Y**
CS2- MF-2%	**Y**	**Y**	N
CS2- MF-3%	**Y**	N	N
CS2- MF-4%	N	N	N
CS3- MF-1%	**Y**	**Y**	**Y**
CS3- MF-2%	**Y**	**Y**	N
CS3- MF-3%	**Y**	N	N
CS3- MF-4%	N	N	N

As the concentration increases the applied mechanical loads may dissipate and be dampened before getting into the cells. While stimulation was operated for only 30 min and the long term

response of 3% agarose to the loading was unknown, but the use of agarose with this concentration of known to result in optimal matrix with chondrocytes [58], [401]. Therefore, this concentration was considered to be used for other experiments.

5.1.4 Preliminary Study

The loading conditions of the preliminary studies were explained in Section 4.1.10.6. The constructs were removed and replaced with new one from free swelling condition in case of having any crack or destruction of part of the hydrogel. This was done to track the frequency of such occurrence within the same loading condition within a specific period of time. The presence of any deformation, crack and destruction in the construct of each channel in days of cell medium change (5 days/week for 10 days observation) during the 2 week culture time is reported in Table 5.3. The number of times that construct of each channel was replaced after crack or destruction, is presented in Table 5.4.

Table 5.3 Frequency of observing any deformation, crack and destruction in 2 week culture period in preliminary experiments (PE) performed (G: group, Ch: channel, LF: low flow rate, MF: medium flow rate, HF: high flow rate).

Study	**Deformation / Crack / Destruction** (N or Y) **Frequency of Observing Deformation / Crack / Destruction** (Number 1-10)					
Both G1,G2	**Ch1**	**Ch2**	**Ch3**	**Ch4**	**Ch5**	**Ch6**
Comp. (kPa)	**3.65**	**4.83**	**5.44**	**7.26**	**8.52**	**0**
PE-LF	N / N / N 0 / 0 / 0	Y / N / N 2 / 0 / 0	Y / N / N 3 / 0 / 0	Y / Y / N 4 / 1 / 0	Y / Y / N 6 / 1 / 0	N / N / N 0 / 0 / 0
PE-MF	Y / N / N 1 / 0 / 0	Y / N / N 2 / 0 / 0	Y / N / N 4/ 0 / 0	Y / Y/ N 5 / 1 / 0	Y / Y / Y 7/ 1 / 1	N / N / N 0 / 0 / 0
PE-HF	Y / N / N 2/ 0 / 0	Y / N / N 4 / 0 / 0	Y / N / N 5 / 0 / 0	Y / Y / Y 8 / 1/ 1	Y / Y / Y 9 / 2 / 1	N / N / N 0 / 0 / 0

Table 5.4 Number of times that construct in channel was replaced after crack or destruction.

Ch/Study	PE-LF	PE-MF	PE-HF
Ch1	0	0	0
Ch2	0	0	0
Ch3	0	0	0
Ch4	1	1	2
Ch5	1	2	3
Ch6	0	0	0

The deformation in this observation was not deep and only a trace of the stimulation pattern was visible on the surface. When a trace of deformation was seen on the construct surface, it was recorded for the other days as well until the end of observation days or until any crack or destruction occurred for hydrogel. When hydrogel construct was replaced, these traces were recorded again.

The results showed that with the application of compressive loads, frictional shear and fluid flow rates in 2 weeks, the agarose-hydrogel constructs could withstand the combination of three compressive loads (28.24, 42.09 and 56.17 mN) with three flow rates (5.5, 11.24 and 17.6 ml/min) without any sign of crack or destruction. The constructs that were exposed to higher compression and higher fluid flow in channels 4 and 5 had trace of deformation earlier in their stimulation period and needed to be replaced more frequently.

These preliminary experiments helped in finding the safe functional range with the above combinations of load/flow. The safe range of fluid flow rates could not be decided for compressions between 28.24-56.17 mN, since the high flow rate caused no detrimental physical effects such as crack or hydrogel surface destruction. However, the higher flow rates probably produced more deformation or perhaps caused visible deformation earlier than the lower range of

flow rates. Because there were more incidences of damaged constructs for higher flow rates of 17.6 ml/min in higher compressions, the subsequent experiments had flow rates less than this amount.

Fluid Film Estimation

Inserting the following values in formula for fluid film presented in Section 3.1.1 for Preliminary Study:

R_o = 1.78 mm

R_i = 0.84 mm

η = 0.001 Pa s

$$h = \left[\frac{3\eta . {R_0}^2 Q}{F} \left(1 - \left(\frac{R_i}{R_0} \right)^2 \right) \right]^{\frac{1}{3}}$$

The fluid film thicknesses for various load and fluid flow conditions are presented in Table 5.5.

Table 5.5 Estimation of fluid film thickness (h) in various t combinations of normal compressive loads (F) and fluid flow rates (Q).

Study	**Ch1** F = 28.2 mN	**Ch2** F = 37.4 mN	**Ch3** F = 42.1 mN	**Ch4** F = 56.2 mN	**Ch5** F = 65.9 mN
PE-LF Q = 5.5 ml/min	h = 28.8 µm	h = 26.3 µm	h = 25.2 µm	h = 22.9 µm	h = 21.7 µm
PE-MF Q = 11.2 ml/min	h = 36.6 µm	h = 33.3 µm	h = 32.9 µm	h = 29.1 µm	h = 27.6 µm
PE-HF Q = 17.6 ml/min	h = 42.5 µm	h = 38.7 µm	h = 37.2 µm	h = 33.8 µm	h = 32.0 µm

5.2 Study 1

5.2.1 Wet Weights

The average wet weights for whole and half constructs are presented in Table 5.6. Considering the volume of each construct (~ 392.7 mm^3), the density based on wet weight of whole construct was 730.1 ± 91.9 mg/ml. Each individual wet weight was used for normalizing the corresponding amount of retained GAG in each construct (dividing the GAG content per corresponding wet weight).

Table 5.6 Measured wet weights (ww) of whole and half construct for different loading conditions and the number of samples (average ± standard deviation). CS: Compression and shear, NL: No load, NF, LF, HF are no, low and high flow.

	whole- ww (mg)- D 21	half- ww (mg)- D 21	
	Avg ± Std Dev	Avg ± Std Dev	n
CS-LF	260.6 ± 37.7	130.45 ± 28.0	6
CS-HF	254.6 ± 40.9	128.5 ± 46.9	6
CS-NF	295.6 ± 23.6	151.0 ± 22.5	12
NL-NF	306.9 ± 21.6	161.9 ± 20.9	12

The results of measured wet weights of the half construct that was used for GAG analysis showed that the control group (NL-NF) had the highest average wet weight and CS-HF had the lowest one. It was interesting that as the amount of compressive load or flow rate increased, the amount of wet weight was decreased. The reduction in average wet weight for the CS-LF and CS-HF might have been due to the fluid flow on top of the surface pushing fluid containing produced GAG and collagen out of the construct.

5.2.2 Cell Viability

The viability of chondrocytes was determined at the end of stimulation period as explained in Section 4.2.2.4. The images (10X magnification) from the fluorescence microscope for each construct of all three groups (G1-G3) of both studies (S1A and S1B) are presented in Figures 5.3 – 5.9. The chondrocyte viability of most of agarose-chondrocyte samples of all three groups of both studies after one week in free swelling and two weeks under mechanical or hydromechanical stimulation was very good. There were very few red dots (representing dead cells) and many bright green dots (representing live cells). The images showed no significant cell death in any of the samples or group-death of clustered cells. The difference in loading conditions imposed no change in pattern of cell viability. If there was cell death, there were with scattered (not clustered) and uniformly distributed pattern throughout the sectioned construct. Images captured with higher magnifications (20X or 60X) clearly showed signs of cell division (Figure 5.10). Similar cell divisions in other samples also showed that the number of cells was continuing to expand even after day 21 in culture.

The viability of twelve samples, which were cultured in free swelling (FS) condition (different from controls, cultured in 24-well culture plates, received 2 ml cell medium every other day), was also measured with the same technique. The images (10X magnification) showing cell viability for each of these constructs is shown in Figure 5.9. The images showed no significant cell death in any of the samples or group-death of clustered cells.

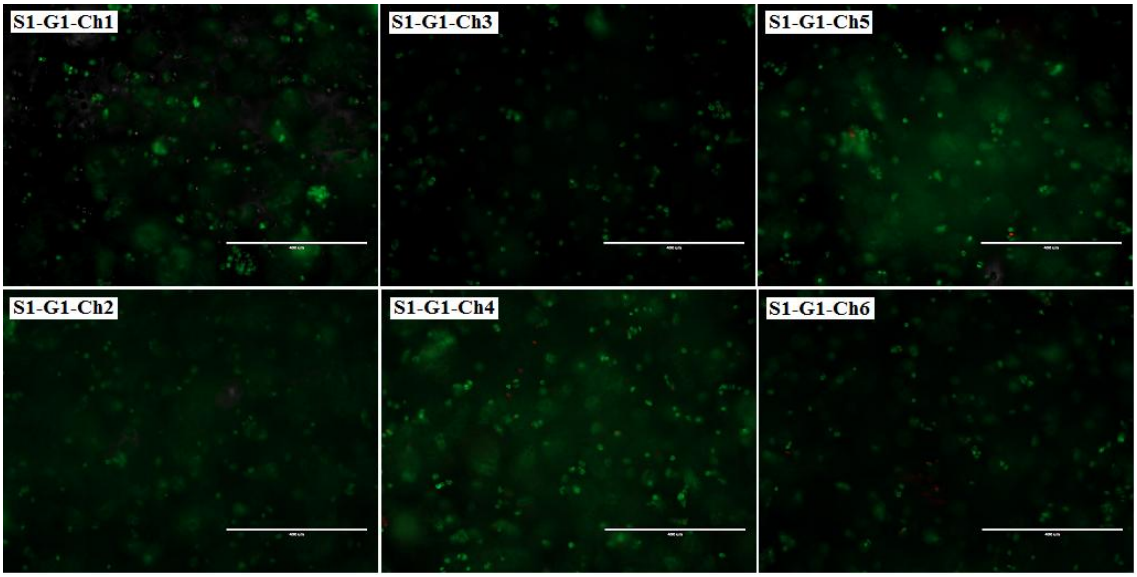

Figure 5.3 Cell viability in channels 1 to 6 of S1-G1 (10 X) from the fluorescence microscope at day 21.

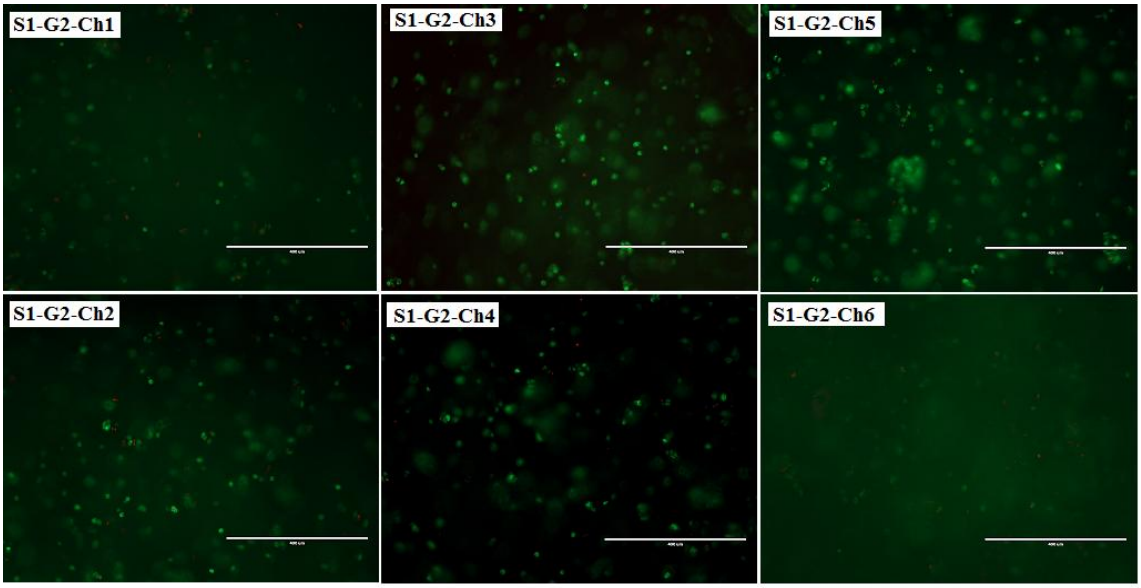

Figure 5.4 Cell viability in channels 1 to 6 of S1-G2 (10 X) at day 21.

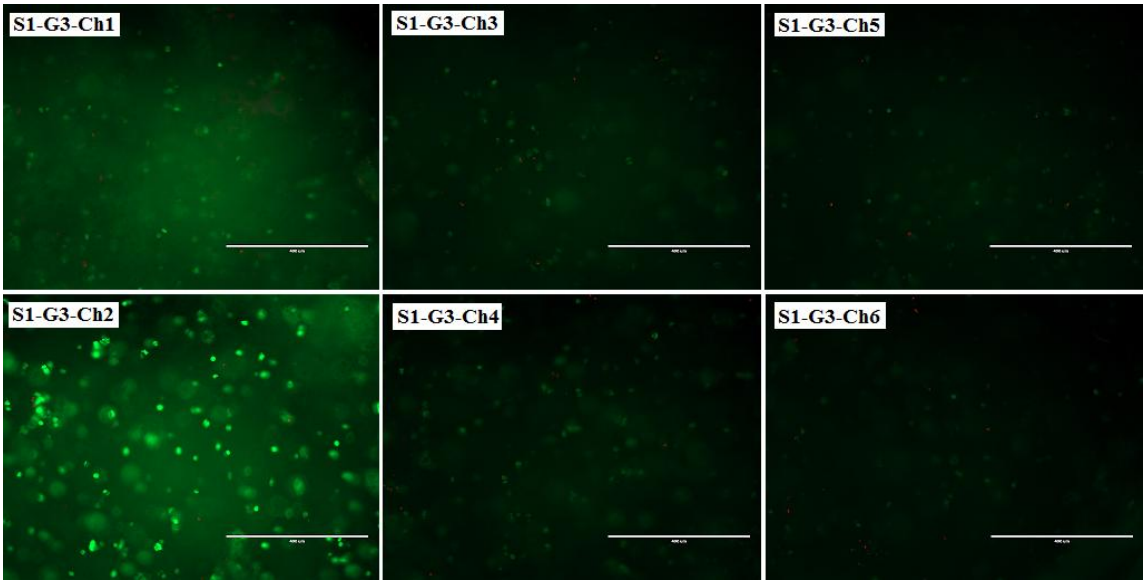

Figure 5.5 Cell viability in channels 1 to 6 of S1-G3 (10 X) at day 21.

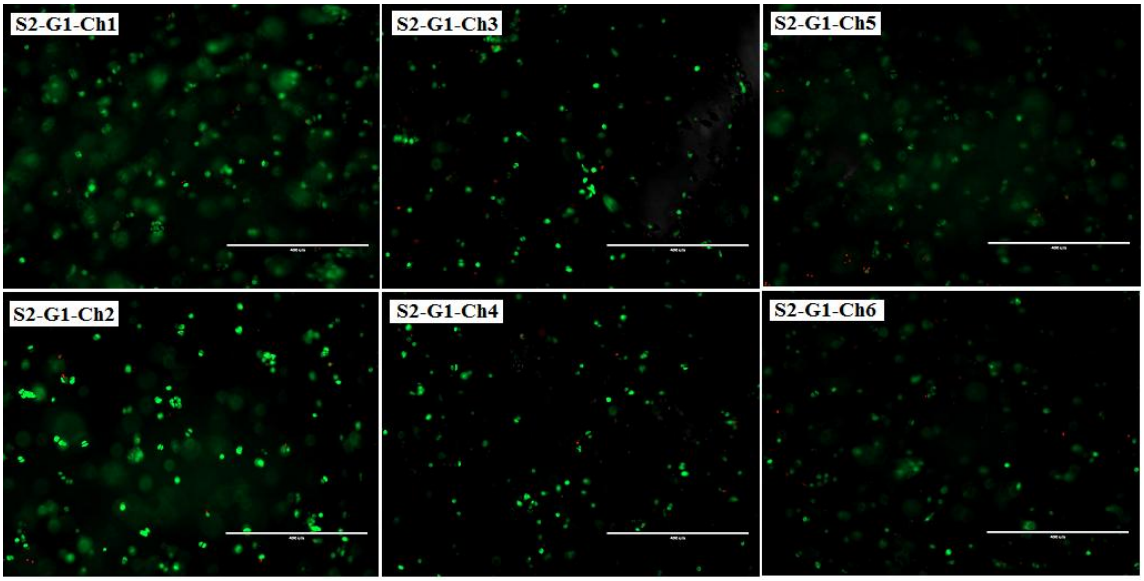

Figure 5.6 Cell viability in channels 1 to 6 of S2-G1 (10 X) at day 21.

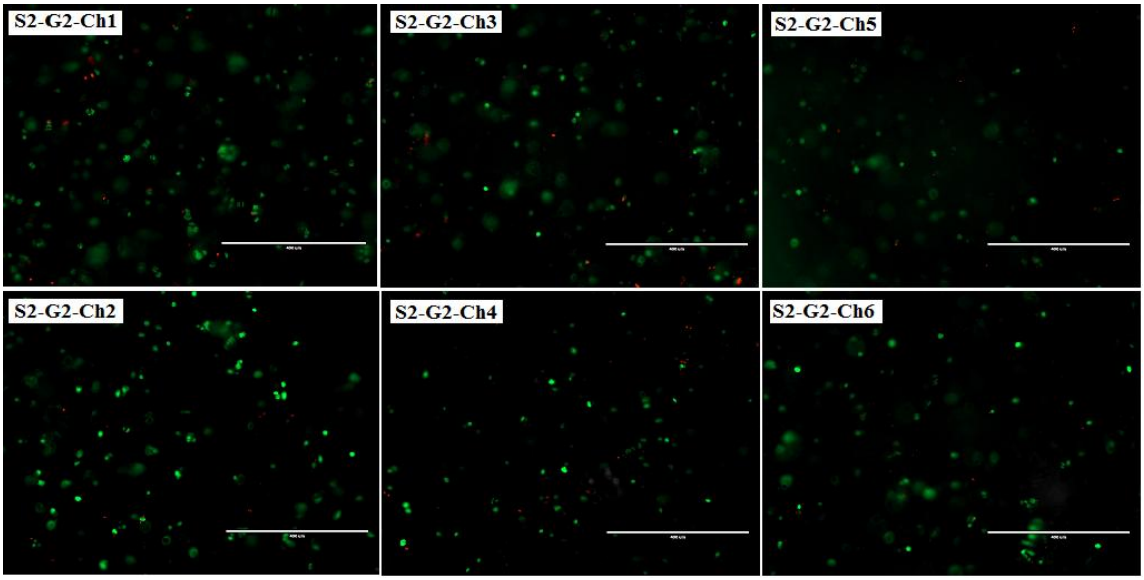

Figure 5.7 Cell viability in channels 1 to 6 of S2-G2 (10 X) at day 21.

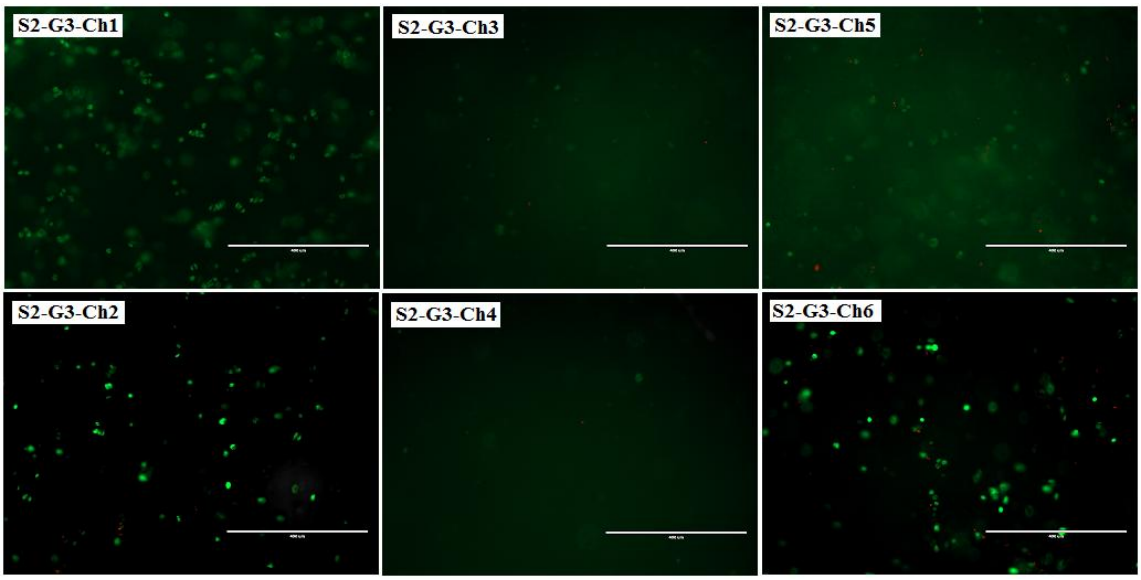

Figure 5.8 Cell viability in channels 1 to 6 of S2-G3 (10 X) at day 21.

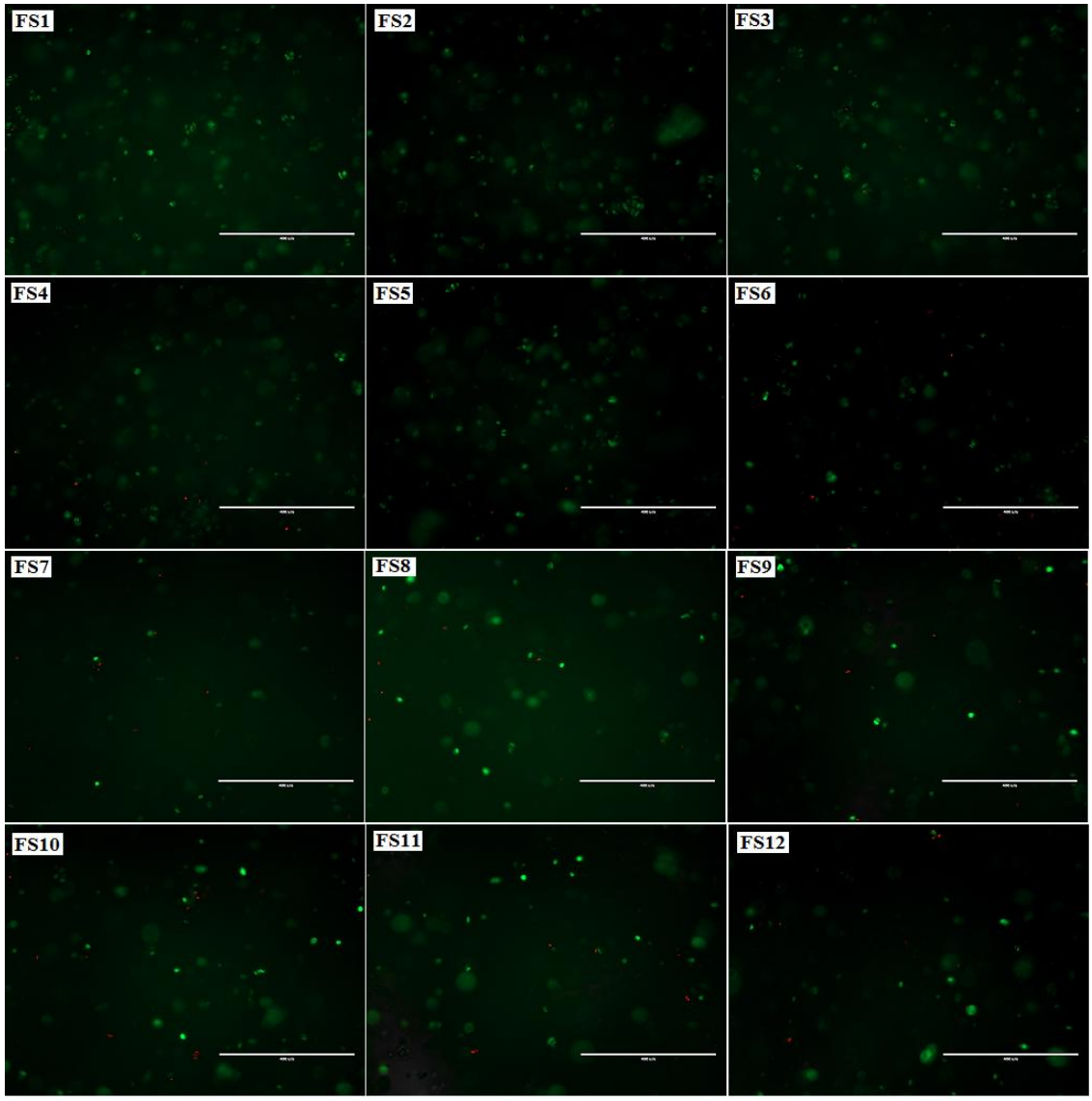

Figure 5.9 Cell viability of ten constructs in free swelling (FS) condition (10 X) at day 21.

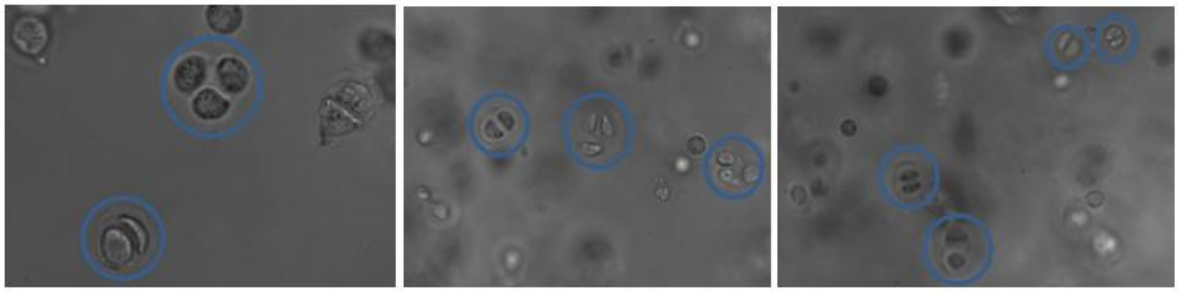

(a) (b) (c)

Figure 5.10 Cell division within agarose at day 21. a) S1B-G1-Ch3 (60X); b) S1A-G1-Ch6 (20X); c) S1B-G3-Ch1 (20X).

5.2.3 Retained GAG in Construct

The amount of retained glycosaminoglycan (GAG) in the agarose-chondrocyte constructs was calculated using the standard curve (relationship between absorbency and the GAG concentration) for each sample in all three groups of both studies (S1-A and S1-B). The generated standard curve was linear with a good correlation coefficient (~ 0.9736). The DMMB assay for measurement of retained GAG in constructs was performed as explained in Section 4.2.2.6. The results are presented in Table 5.7.

Table 5.7 Retained GAG (µg) at day 21 in Study 1.

Retained GAG (µg)- D21		
	Avg ± Std Dev	n
CS-LF	206.7 ± 81.7	6
CS-HF	200.0 ± 74.6	6
CS-NF	253.5 ± 141.3	12
NL-NF	298.5 ± 108.6	12

The retained GAG values were normalized to their corresponding wet weights and plotted (Figure 5.11).

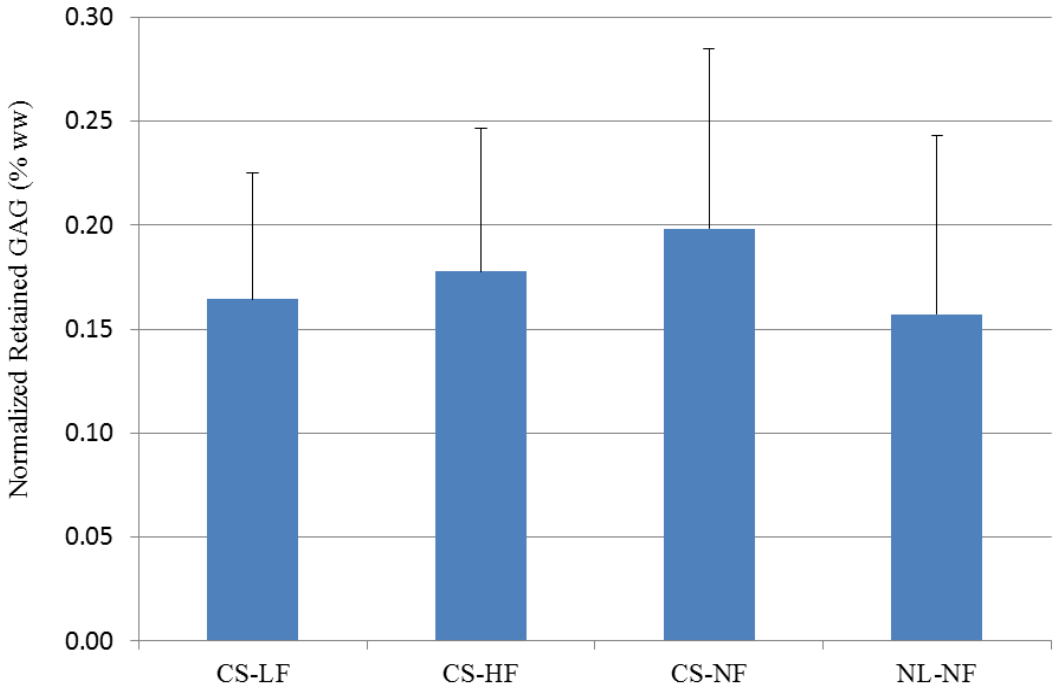

Figure 5.11 Retained GAG at day 21 (avg ± std dev). LF: low flow, HF: high flow, NF: no flow, NL: no load, CS: compression and shear.

5.2.4 Statistical Results of Study 1

In this study, the high flow (HF) was 14.82 ml/min and the low flow (LF) was 7.72 ml/min. Although there was a trend in the average values that suggested that the CS-NF condition had more retained GAG, no statistically significant differences were found between different groups. Statistical p-values, when means of GAG in different loading conditions are compared, are reported

in Table 5.8. The normalized GAG content of constructs in CS-NF, CS-HF and CS-LF groups were 26.1% ($p = 0.27$), 13.1% ($p = 0.63$) and 4.5% ($p = 0.86$) more than in NL-NF group. The GAG contents of samples under hydromechanical stimulation (CS-LF and CS-HF) were lower than the GAG content samples under only mechanical stimulation (CS-NF). But the statistical analysis could not reveal a significant difference between groups. Construct in CS-HF group could accumulate 8.3% ($p = 0.75$) more GAG than constructs in CS-LF group, and CS-HF and CS-LF groups had 10.3% ($p = 0.64$), and 17.1 % ($p = 0.43$) less GAG in their construct compared with the ones in CS-NF group.

Table 5.8 Statistical p-values when means of GAG in different loading conditions in Study1 are compared. LF: Low Flow, HF: High Flow (hydromechanical loading condition with Low and high fluid flow rates respectively), NF: No Flow (mechanical loading condition without fluid flow), NN: No load-No Flow (unloaded condition or free swelling). The p-value less than 0.05 shows a significant difference of means of the corresponding dependent between two specified loading conditions.

Dependent Variables	GAG compare	HF,LF	LF-NN	HF, NN	NF, NN	HF,NF	LF,NF
Retained GAG	NF>NN>LF>HF	0.8952	0.4894	0.4252	0.4659	0.1560	0.1891
Normalized retained GAG	NF>HF>LF>NN	0.7469	0.8661	0.63411	0.2759	0.6420	0.4293

5.2.5 Fluid Film Estimation

Inserting the following values in formula for fluid film presented in Section 3.1.1 for Study 1A and 1B.

$R_o = 1.78$ mm

$R_i = 0.84$ mm

Q_{1A} = 7.72 ml/min = 0.12867 × 10^{3} mm^3/s

Q_{1B}= 14.82 ml/min = 0.247× 10^{3} mm^3/s

$F_{1A} = F_{1B}$ = 45.1 mN

η = 0.001 Pa s

The fluid film thicknesses for two fluid flow conditions are:

h_{1A} = 21.08 µm (CS-LF loading condition)

h_{1B} = 40.46 µm (CS-HF loading condition)

The fluid film was calculated with assumption of having rigid surface in contact with the indenter. Due non-rigidity of agarose and its deformability, the fluid films in these studies are likely to be higher than the above-mentioned thicknesses.

5.3 Study 2

5.3.1 Wet Weights

The wet weights of three layers of the construct (top (T), middle (M) and bottom (B) layers) were measured at the end of the experiment (day 30) as explained in Section 4.2.3.4. The averages of wet weights of the construct layers, their standard deviations and the number of samples are given in Table 5.9. The total weight of construct was estimated by summing the wet weights of layers (top, middle and bottom layer). These wet weights were used in normalizing the GAG and collagen production.

Table 5.9 Wet weights of the construct layers and their sum at day 31. T, M and B are top, middle and bottom layers of constructs.

ww (mg) –D31

	T		M		B		T + M + B	
	Avg± Std.Dev	n	Avg± Std.Dev	n	Avg± Std.Dev	n	Avg± Std.Dev	n
CS-F	98.5 ± 13.6	6	72.2 ± 18.6	7	124.0 ± 49.0	18	294.8 ± 33.2	6
CS-NF	96.4 ± 22.4	18	81.3 ± 12.0	18	135.8 ± 34.5	18	313.5 ± 23.5	18
NL-NF	99.6 ± 25.1	12	98.9 ± 25.1	12	98.9 ± 22.1	12	297.4 ± 28.9	12

5.3.2 Cell Viability

Viability of chondrocytes was checked at the end of the 4-week culture (that included the 3-week stimulation period) as explained in Section 4.2.3.5. The images (10X magnification) from the fluorescence microscope for each layer of three CS-NF, three CS-F constructs and one NL-NF are presented in Figures 5.12 – 5.14. The chondrocyte viability of the samples under CS-NF and CS-F stimulation was quite good. There were few red dots (representing dead cells) scattered throughout the construct , but population of green dots (representing live cells) was much higher. The images showed no significant death of individual cells or as clusters in any of the samples. The images of different layers of sample in the control group (Figure 5.12) showed more live cells on the top surface comparing to the medium and bottom layer. In images of the CS-NF constructs, more uniform patterns of cell viability were visible, but in the CS-F constructs more clusters of viable cells were visible.

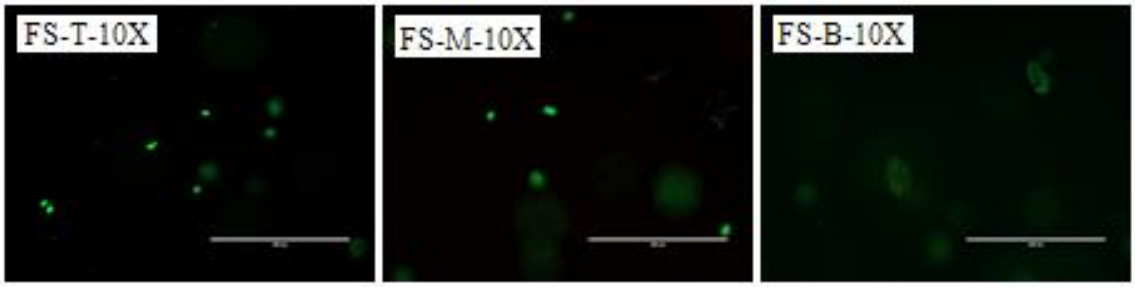

Figure 5.12 Cell viability in different layers (top (T), middle (M), bottom (B)) of free swelling (FS) constructs (2 ml media, changed every other day) at day 31.

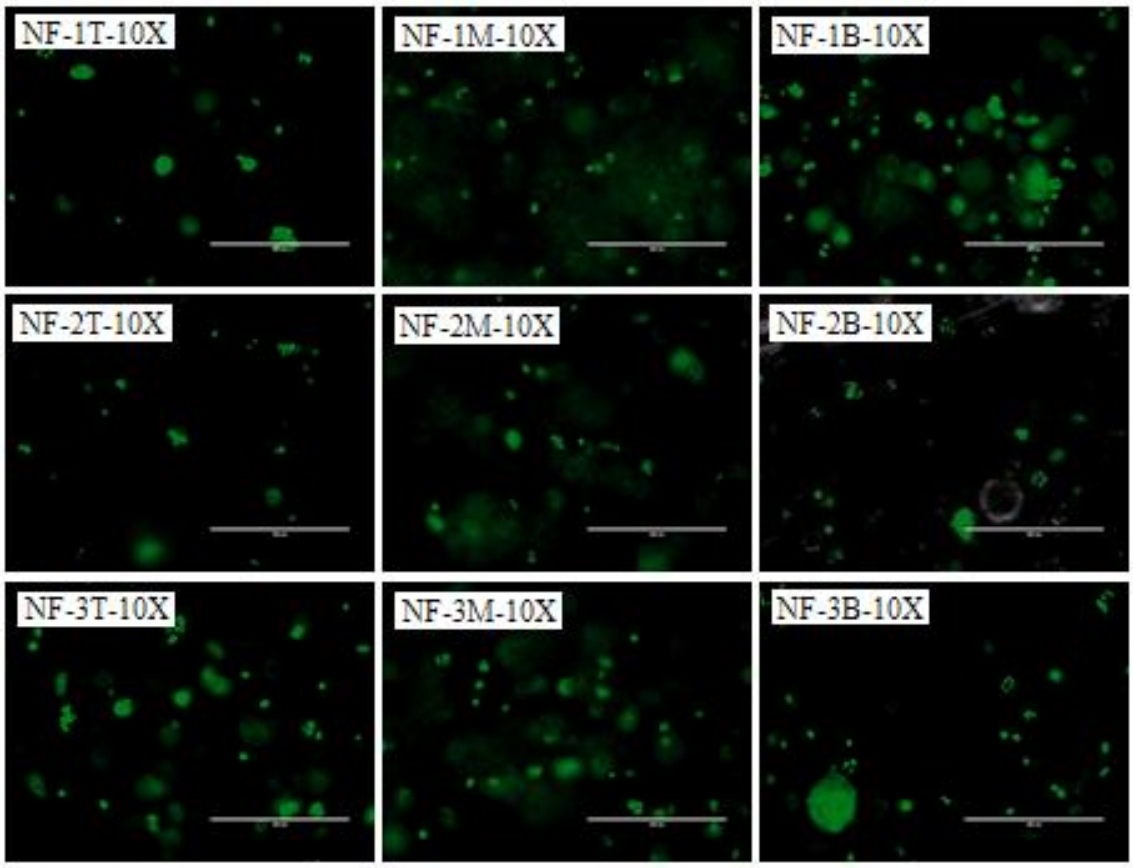

Figure 5.13 Cell viability in different layers in CS-NF constructs at day 31.

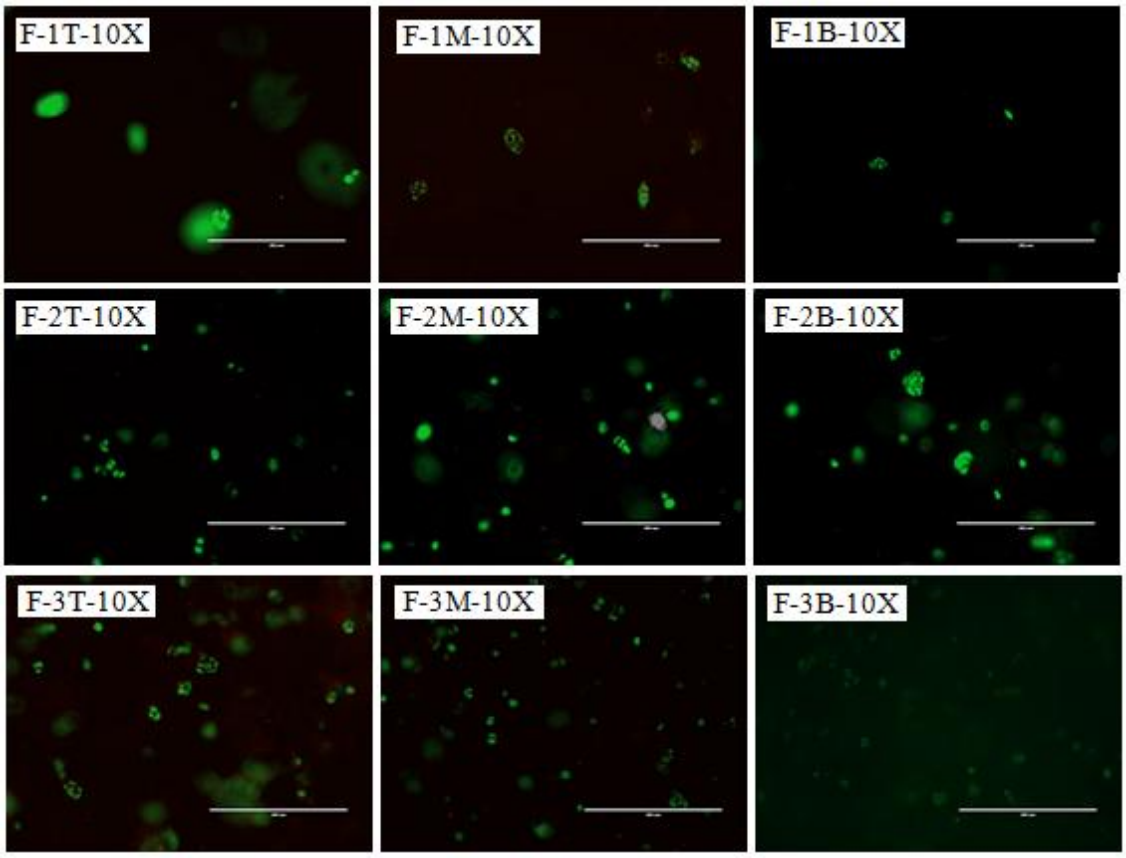

Figure 5.14 Cell viability in different layers in CS-F loading condition of Study 2 at day 31.

5.3.3 Retained GAG in Each Layer of Construct

The retained GAG was measured separately for each layer as explained in Section 4.2.3.6 as well as Sections 4.1.10.9 and 4.2.2.6 (for study 2, the dilution factor was 1/2 instead of 1/5). The results of retained GAGs in different layers of construct are presented in Figure 5.15 and the results of retained GAGs normalized to wet weight of corresponding layers are presented in **F**igure 5.16. Total retained GAG as summation of retained GAGs of all three layers for three different loading

conditions are presented in Figure 5.17. Total retained GAG normalized to total wet weight is shown in Figure 5.18.

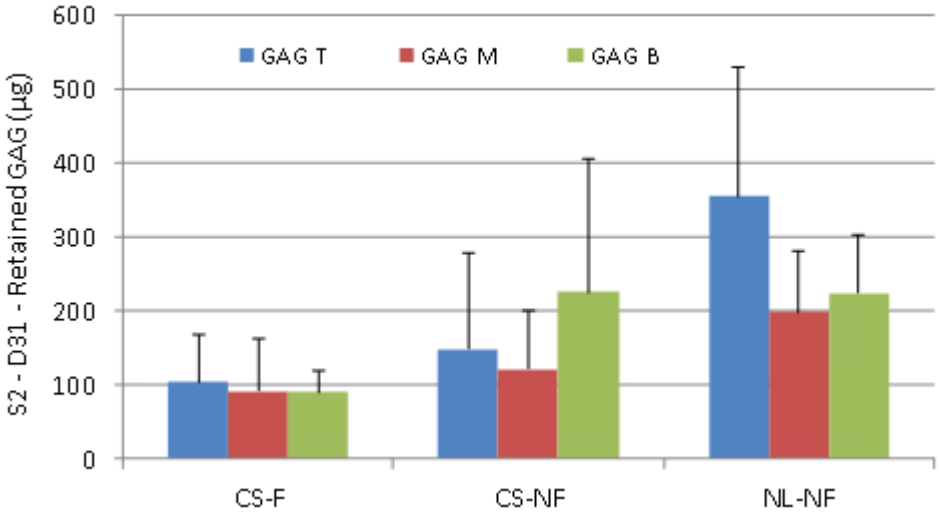

Figure 5.15 Retained GAG in the top (GAG T), middle (GAG M) and bottom (GAG B) layers of the constructs at day 31.

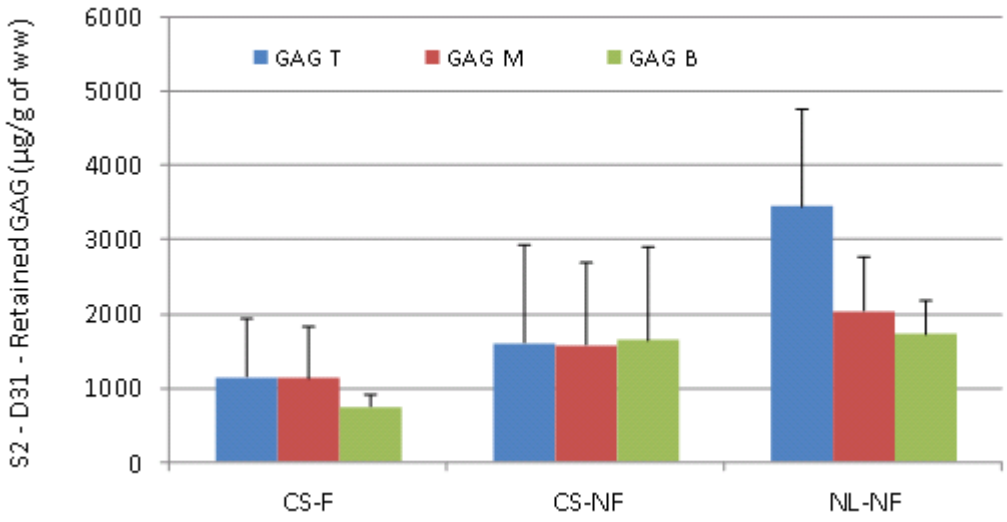

Figure 5.16 Normalized retained GAG (µg/g of wet weight) in the top (GAG T), middle (GAG M) and bottom (GAG B) layers at day 31.

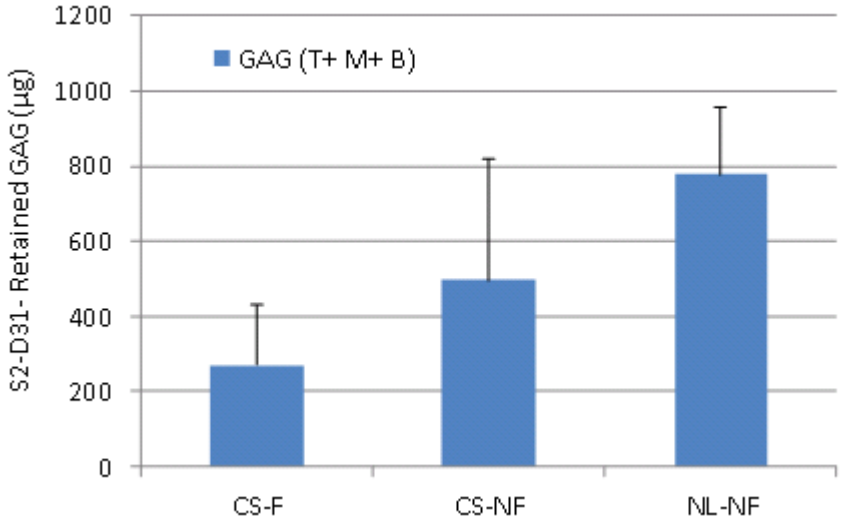

Figure 5.17 Retained GAG in the whole construct at day 31 (CS-F, n=6; CS-NF, n=18; NL-NF, n=12).

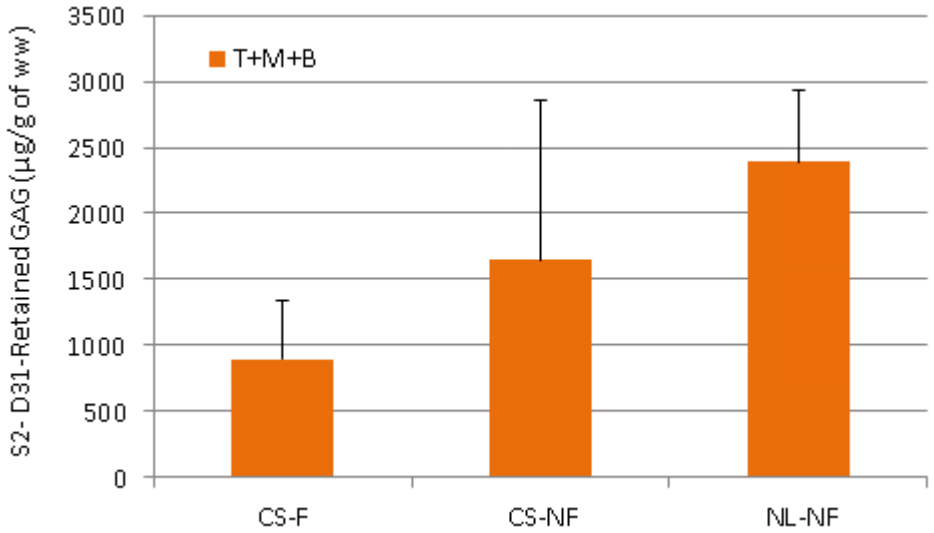

Figure 5.18 Normalized total retained GAG (µg/g of wet weight) at day 31 (CS-F, n=6; CS-NF, n=18; NL-NF, n=12).

5.3.4 Released GAG into Culture Media

Cumulative release of GAG into the culture media on days of stimulation (Figure 5.19) showed highest average released GAG for the CS-F constructs and lowest for the NL-NF constructs. The culture media for the NL-NF constructs was combined by mistake and thus they could not be included in statistical analysis.

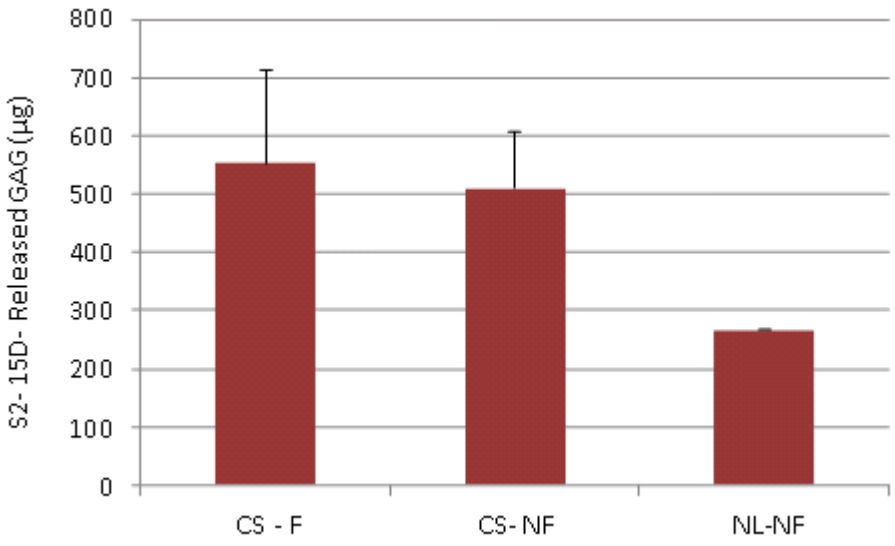

Figure 5.19 Released GAG into the media at 15 days (CS-F, n=6; CS-NF, n=6; NL-NF, n=1).

5.3.5 Total GAG Production

The total GAG production was found by summation of the total retained GAG (GAG_{T+M+B}) and total released GAG for every group of each loading condition.. Since only one value represented the amount of total released GAG for NL-NF constructs, the average of the retained GAG for all 12 NL-NF constructs was used to determine the total GAG. The result of total GAG (retained +

released) is presented in Figure 5.20 and its normalized amount to total wet weight is shown in Figure 5.21. When total GAG production was normalized and if it was assumed that the standard deviation of the NL-NF constructs was about the same as for the CS-F and CS-NF, it was clear that no statistically significant differences would have been detected between any of these groups.

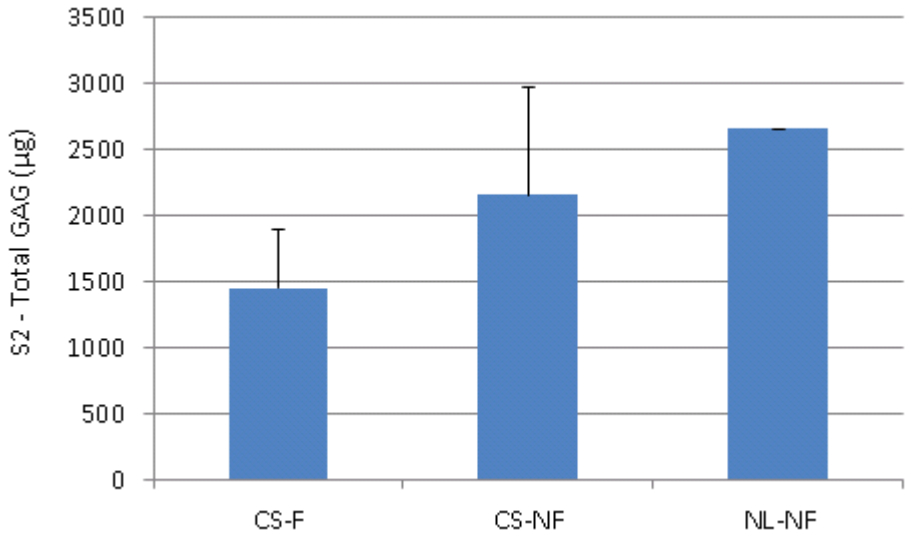

Figure 5.20 Total GAG (retained + released) at day 31 (CS-F, n=6; CS-NF, n=6; NL-NF, n=1).

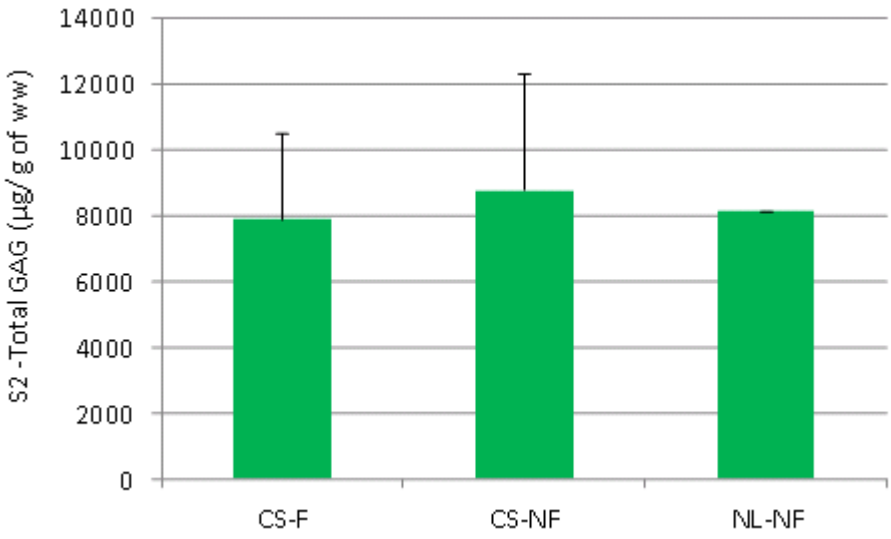

Figure 5.21 Normalized total GAG (µg/g of wet weight) at day 31 (CS-F, n=6; CS-NF, n=6; NL-NF, n=1).

5.3.6 Retained Collagen in Each Layer of Construct

The retained collagen content in each layer of the constructs was measured as explained in Section 4.2.3.8. The retained collagen (µg) and normalized retained collagen (as µg/g wet weight) of the three layers of construct under three different stimulation conditions are presented in Figure 5.22 and Figure 5.23 respectively.

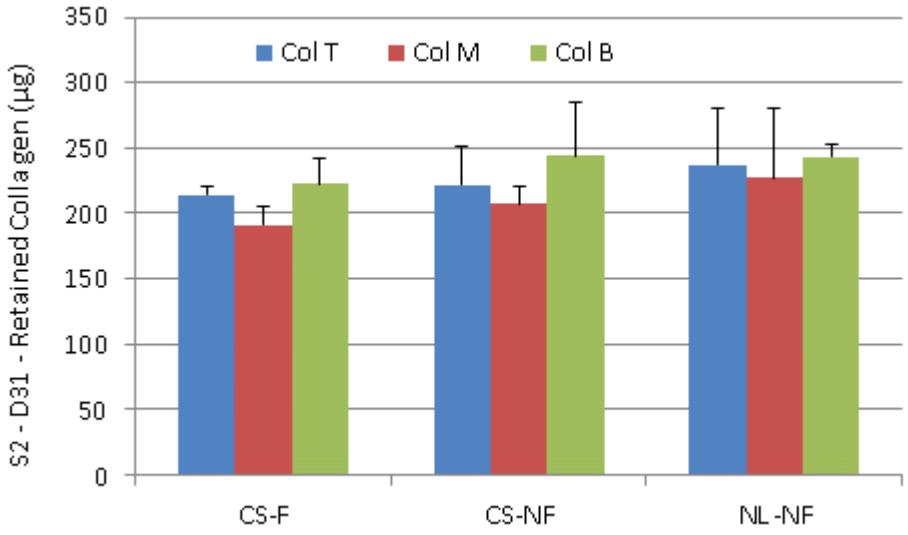

Figure 5.22 Retained collagen at day 31 in the top (Col T), middle (Col M) and bottom (Col B) layers. Number of samples (CS-F, CS-NF, NL-NF) for each layer are Col T (6, 18, 12), Col M (7, 18, 12), Col B (18, 18, 12).

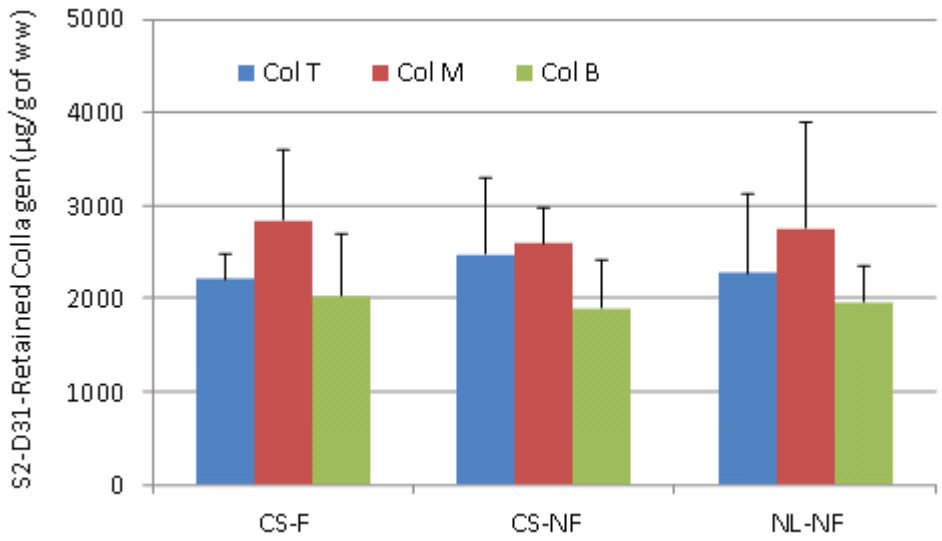

Figure 5.23 Normalized retained collagen (µg/g of wet weight) at day 31 in the top (Col T), middle (Col M) and bottom (Col B) layers. Number of samples (CS-F, CS-NF, NL-NF) for each layer are Col T (6, 18, 12), Col M (7, 18, 12), Col B (18, 18, 12).

Total retained collagen (which was the summation of retained collagen of all three layers) for the different stimulation conditions are shown in Figure 5.24. The normalized total retained collagen values are shown in and Figure 5.25.

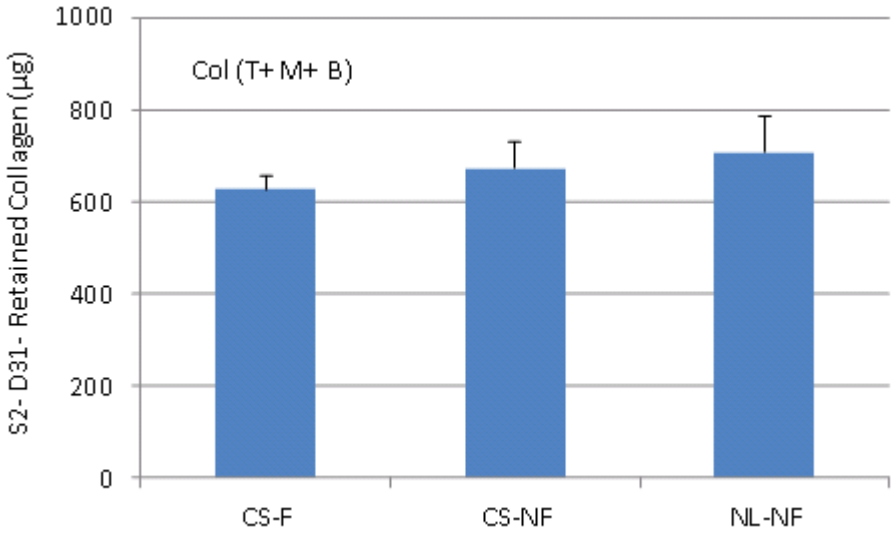

Figure 5.24 Total retained collagen at day 31 (CS-F, n = 6; CS-NF, n = 18; NL-NF, n = 12).

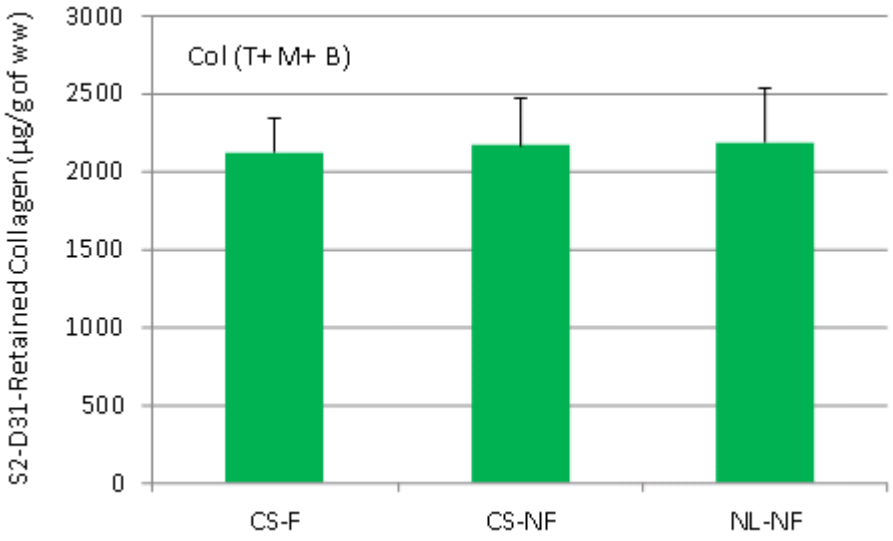

Figure 5.25 Normalized total retained collagen (µg/g of wet weight) at day 31. (CS-F, n = 6; CS-NF, n = 18; NL-NF, n = 12).

5.3.7 Released Collagen into Culture Media

The released collagen was measured as explained in Section 4.2.3.7. The released collagen was measured for every day of stimulation for all groups (group 1 to 6) and for all loading conditions. The average release of collagen into media per day is shown in Figure 5.26. The average accumulated released collagen during 15 days for different loading conditions is presented in Figure 5.27.

The released collagen during 15 days for the different stimulation conditions is presented in Figure 5.27. As mentioned previously, the culture media for the NL-NF constructs was combined by mistake and thus they could not be included in statistical analysis. Again it did appear that if the standard deviation was the same for the NL-NF constructs as for say the CS-F constructs, there would have been statistically significant differences between all of the stimulation groups. This issue was considered further in the next section.

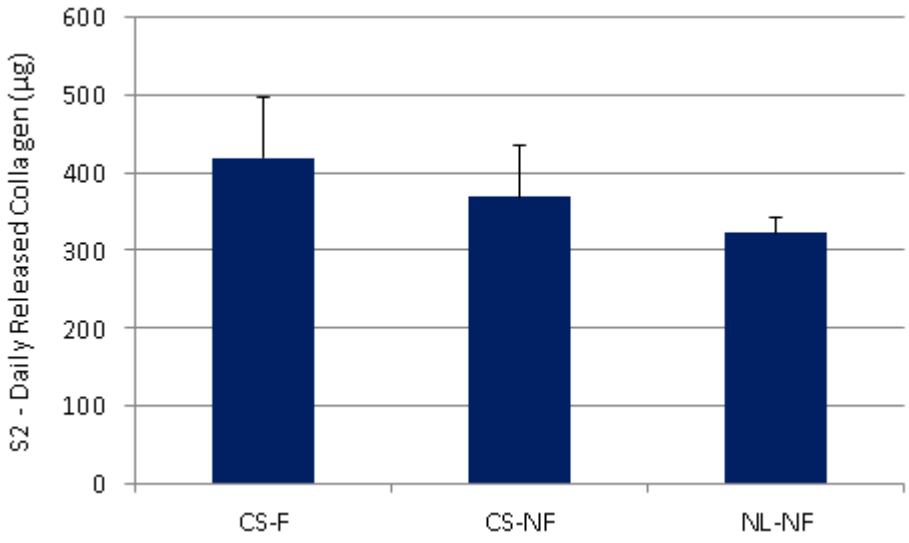

Figure 5.26 Released collagen per day (n=15) from samples under 3 different loading conditions.

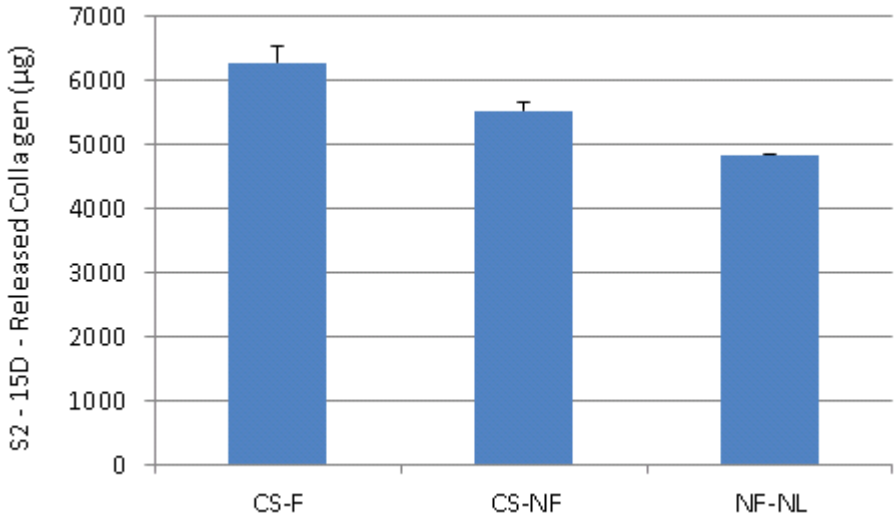

Figure 5.27 Accumulated released collagen during 15 days of stimulation (CS-F, n=6; CS-NF, n=6; NL-NF, n=1).

5.3.8 Total Collagen Production

The total collagen (total retained + cumulative released) and normalized total collagen for the different stimulation conditions are presented in Figure 5.28 and Figure 5.29 respectively. When the normalized total collagen was considered, statistical analysis revealed that the average total collagen for the CS-F was higher than for the CS-NF ($p = 0.0423$). Since the NL-NF data had n =1, it could not be considered. However, if it was assumed that it would have had a standard deviation equal to that of the CS-F, statistical analysis would have revealed that total collagen production was highest for the CS-F, intermediate for the CS-NF and lowest for the NL-NF, but this could not be considered as an evidence-based finding of Study 2.

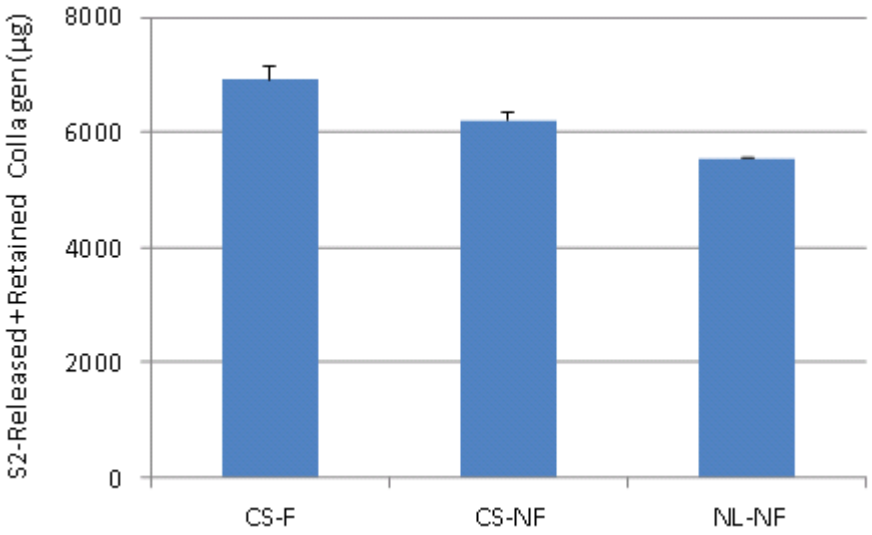

Figure 5.28 Total collagen (released + retained) at day 31 in Study 2.

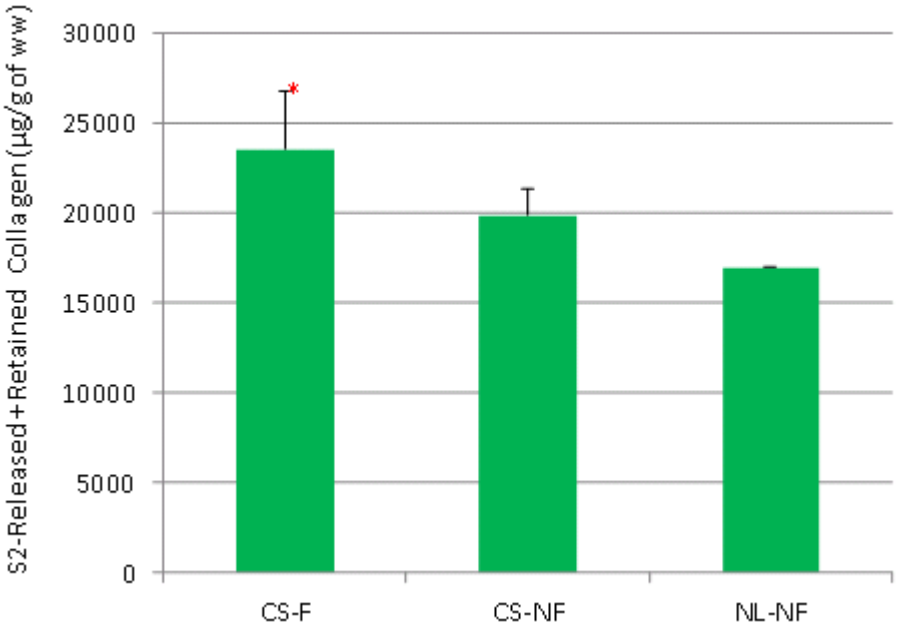

Figure 5.29 Normalized total collagen (µg/g of wet weight) at day 31 (CS-F, n=6; CS-NF, n=6; NL-NF, n=1).

5.3.9 Statistical Results of Study 2

The statistical results are reported in Table 5.10 and Table 5.11 when the means of dependent variables in different loading conditions are compared (load-wise comparison for the same layers). The statistical results are reported in Table 5.12 and Table 5.13 when means of variables in different layers or sections are compared (depth-wise comparison for same loading condition).

Table 5.10 Statistical p-values when means of collagen dependent variables were compared for different loading conditions in Study 2. F: Flow (hydromechanical loading condition with fluid flow), NF: No Flow (mechanical loading condition without fluid flow), NN: No load-No Flow (unloaded condition or free swelling). The p-value less than 0.05 shows a significant difference of means of the corresponding dependent between two specified loading conditions.

Collagen Dependent Variables- Study 2	Collagen comparison	F & NF	F & NN	NF & NN
Retained collagen-Top	F < NF < NN	0.343	0.210	0.453
Retained collagen- Middle	F < NF < NN	0.086	0.054	0.221
Retained collagen- Bottom	F < NN < NF	0.032	0.001	0.947
Total retained collagen	F < NF < NN	0.051	0.022	0.323
Normalized retained collagen- Top	F < NF < NN	0.516	0.316	0.610
Normalized retained collagen- Middle	F > NF > NN	0.669	0.391	0.356
Normalized retained collagen- Bottom	F < NF < NN	0.913	0.550	0.736
Normalized total retained collagen	F < NF < NN	0.857	0.837	0.977
Total released collagen	F > NF > NN	0.0001	0.004	0.005
Normalized total released collagen	F > NF > NN	0.029	0.119	0.120
Total collagen (retained+ released)	F > NF > NN	0.0002	0.005	0.012
Normalized total collagen (retained+ released)	F > NF > NN	0.042	0.143	0.161

Table 5.11 Statistical p-values when means of GAG dependent variables were compared for different loading conditions in Study 2.

GAG Variables- Study 2	GAG Comparison	F & NF	F & NN	NF & NN
Retained GAG- Top	NN > NF > F	0.262	0.005	0.027
Retained GAG- Middle	NN > NF > F	0.478	0.058	0.117
Retained GAG- Bottom	NF > NN > F	0.016	0.003	0.982
Total retained GAG	NN > NF > F	0.089	0.001	0.065
Normalized retained GAG- Top	NN > NF > F	0.272	0.005	0.022
Normalized retained GAG- Middle	NN > NF > F	0.363	0.079	0.378
Normalized retained GAG- Bottom	NN > NF > F	0.033	0.0006	0.865
Normalized total retained GAG	NN > NF > F	0.103	0.0008	0.158
Total released GAG	F > NF > NN	0.626	0.190	0.088
Normalized total released GAG	F > NF > NN	0.062	0.136	0.007
Total GAG (retained + released)	NN > NF > F	0.329	0.332	0.798
Normalized Total GAG (retained + released)	F > NF > NN	0.750	0.598	0.738

Table 5.12 Statistical p-values when means of GAG dependent variables were compared for different layers in Study 2.

GAG Variables-Study 2	GAG Comparison	T & M	T & B	M & B
Retained GAG - Flow (F)	M > B > T	0.927	0.912	0.993
Retained GAG – No Flow (NF)	B > M > T	0.597	0.229	0.073
Retained GAG – No load No flow (NN)	T > B > M	0.100	0.151	0.628
Normalized Retained GAG - F	M > T > B	0.737	0.587	0.265
Normalized Retained GAG - NF	B > T > M	0.964	0.950	0.907
Normalized Retained GAG - NN	T > M > B	0.050	0.020	0.386

Table 5.13 Statistical p-values when means of collagen dependent variables were compared for different layers in Study 2.

Collagen Variables-Study 2	Collagen Comparison	T & M	T & B	M & B
Retained Collagen- F	B > T > M	0.010	0.099	0.001
Retained Collagen-NF	B > T > M	0.131	0.073	0.003
Retained Collagen–NN	B > T > M	0.742	0.757	0.402
Normalized Retained Collagen- F	M > T > B	0.126	0.032	0.008
Normalized Retained Collagen- NF	M > T > B	0.075	0.021	0.001
Normalized Retained Collagen- NN	T > M > B	0.858	0.004	0.175

5.3.10 Fluid Film Estimation

Inserting the following values in formula for fluid film presented in Section 3.1.1 for Study 2 (CS-F):

R_o = 1.78 mm

R_i = 0.84 mm

$Q_2 = 0.203 \times 10^{3}$ mm^3/s

F_2 = 45.1 mN

η = 0.001 Pa s

$$h = \left[\frac{3\eta . R_0^{\,2} Q}{F} \left(1 - \left(\frac{R_i}{R_0} \right)^2 \right) \right]^{\frac{1}{3}}$$

The fluid film thickness is approximately:

h_2 = 32.25 µm

5.4 Study 3

5.4.1 Cell Viability

The cell viability of samples in this study was checked as explained in 4.2.4.5. The pictures (10X magnification) from the fluorescence microscope for three CS-NF, three CS-F and one NL-NF constructs are presented in Figures 5.17 – 5.19. The chondrocyte viability of three samples under CS-NF and CS-F stimulation was quite good after four weeks in culture including three weeks stimulation. The captured images showed no significant cell death in any of the samples. Similar to Study 2, there were more uniform pattern of cell viability in the CS-NF constructs, but in the CS-F constructs more clusters of viable cells formed.

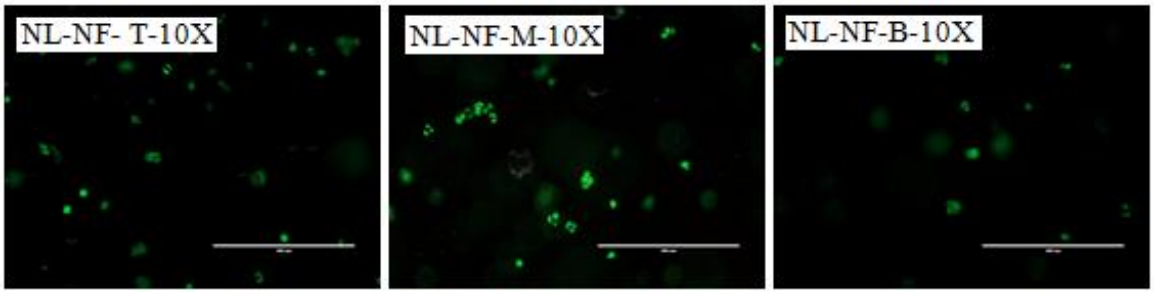

Figure 5.30 Cell viability in different layers (top (T), middle (M), bottom (B)) of a NL-NF construct at day 31.

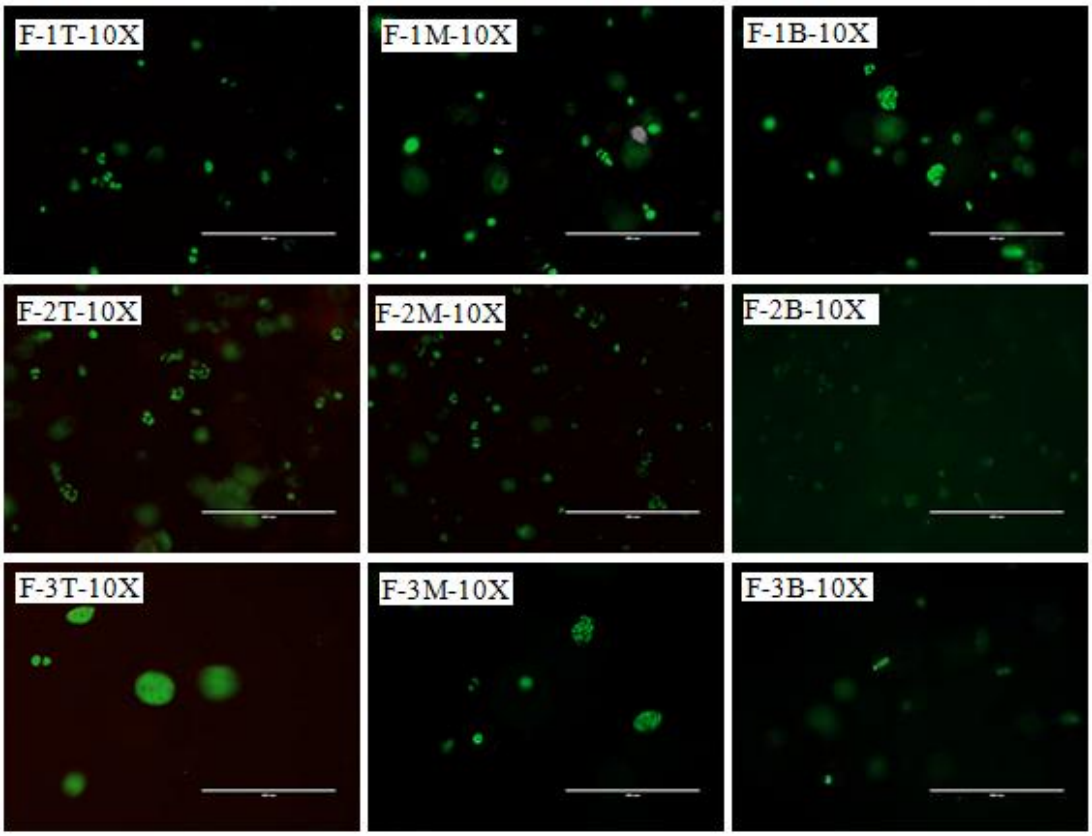

Figure 5.31 Cell viability in different layers of CS-F constructs of S2 at day 31.

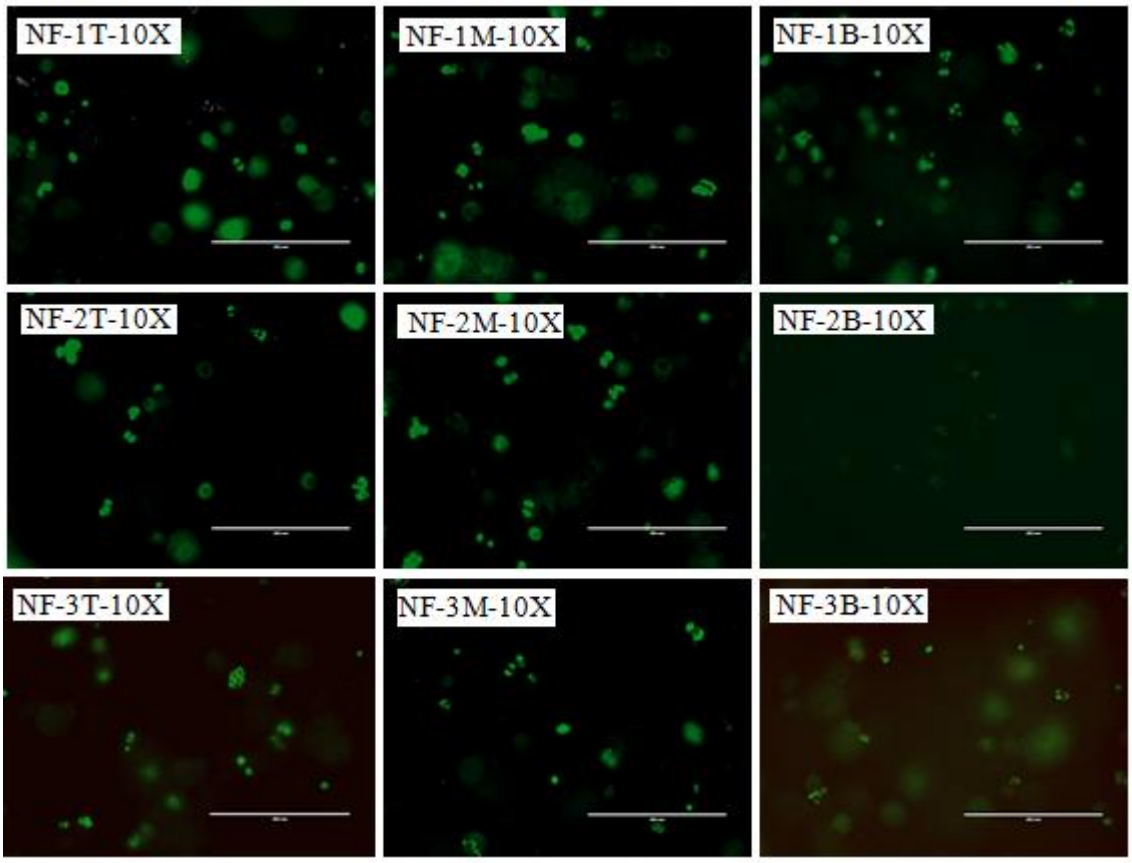

Figure 5.32 Cell viability in different layers of CS-NF constructs of S2 at day 31.

5.4.2 Wet Weights

The constructs were harvested and the weight of the central stimulated area and sum of unstimulated sides were measured separately for all three layers under all 3 types of load/flow conditions at different time points, as explained in Section 4.2.4.3 and Section 4.2.4.3. The wet weights of the separate sections of the constructs at day 23, day 26 and day 30 (since the first day in culture) are presented in Table 5.14 along with the average measured weight of the whole construct before cutting and the sum of wet weights of sections after cutting it to six sections. No

statically significant difference was detected for the various stimulation groups. On average 9.6% - 11.5 % of the construct's weight was lost in different days and loading conditions due to cutting. The wet weights of constructs and sections were used to normalize the GAG and collagen contents.

Table 5.14 Wet weights (ww) of the construct layers and sections in various loading conditions at days D23, 26 and 30 in study 3 (Layer/Section names: TC: top central, TS: top sides, MC: middle central, MS: middle sides, BC: bottom central, BS: bottom sides; n= number of samples per group, each sample is the mean of 3 repeats)

	ww (mg) - D23			ww (mg)- D26			ww (mg)- D30		
	CS-F	CS-NF	NL-NF	CS-F	CS-NF	NL-NF	CS-F	CS-NF	NL-NF
n	3	3	3	3	3	3	10	10	7
	Avg ± Std Dev			Avg ± Std Dev			Avg ± Std Dev		
Whole	303 ± 19	341 ± 0	332 ± 6	319 ± 9	322 ± 6	323 ± 22	316 ± 18	317 ± 15	338 ± 15
TC	58 ± 3	59 ± 1	49 ± 9	51 ± 13	58 ± 6	50 ± 6	50 ± 13	51 ± 8	58 ± 3
TS	44 ± 8	47 ± 4	49 ± 7	41 ± 10	44 ± 3	44 ± 6	41 ± 11	44 ± 6	52 ± 7
MC	51 ± 14	57 ± 8	53 ± 12	54 ± 5	48 ± 2	49 ± 5	54 ± 9	47 ± 11	56 ± 11
MS	41 ± 6	52 ± 11	39 ± 4	42 ± 2	42 ± 3	41 ± 5	47 ± 9	39 ± 11	47 ± 8
BC	51 ± 7	54 ± 13	61 ± 9	52 ± 12	60 ± 6	47 ± 2	52 ± 16	61 ± 18	53 ± 16
BS	38 ± 5	44 ± 13	57 ± 8	45 ± 14	44 ± 2	41 ± 7	44 ± 14	53 ± 18	47 ± 13
Sum	283 ± 16	312 ± 17	309 ± 22	284 ± 11	296 ± 1	271 ± 6	289 ± 20	293 ± 12	313 ± 14

5.4.3 Retained GAG

Retained GAG values for different sections of the constructs were measured as explained in section 4.2.4.7. They are reported as GAG in µg and normalized GAG as µg/g for both day 23 (Table 5.15) and day 26 (Table 5.16). The results for day 30 are presented in Figure 5.33 and Figure 5.34 and their normalized amount are shown in Figure 5.35 and Figure 5.36.

Table 5.15 Retained GAG (μg) of different layers and sections in various loading conditions at day 23, 26 in study 3.

	Retained GAG (μg)- D23		
	CS-F	CS-NF	NL-NF
	Avg ± Std Dev	Avg ± Std Dev	Avg ± Std Dev
TC	67.78 ± 3.09	74.67 ± 1.34	68.29 ± 1.42
TS	57.38 ± 4.13	75.26 ± 1.23	68.86 ± 2.50
MC	29.54 ± 24.93	64.78 ± 4.44	59.21 ± 14.92
MS	21.03 ± 20.92	68.39 ± 11.28	60.16 ± 4.43
BC	18.93 ± 26.58	72.89 ± 3.65	72.54 ± 1.46
BS	25.14 ± 21.71	69.22 ± 4.61	72.72 ± 1.35
Sum	219.81 ± 9.86	425.22 ± 14.35	401.78 ± 21.06
	Retained GAG (μg)- D26		
TC	68.38 ± 2.07	71.47 ± 1.63	72.30 ± 3.81
TS	71.23 ± 2.97	75.65 ± 2.72	68.71 ± 0.98
MC	68.82 ± 2.67	66.49 ± 2.07	69.46 ± 1.66
MS	61.64 ± 14.39	56.67 ± 11.86	56.53 ± 9.11
BC	72.66 ± 2.91	45.25 ± 17.67	57.15 ± 11.85
BS	66.94 ± 5.26	56.36 ± 8.04	69.73 ± 2.62
Sum	409.67 ± 10.32	371.90± 35.79	393.88 ± 20.92

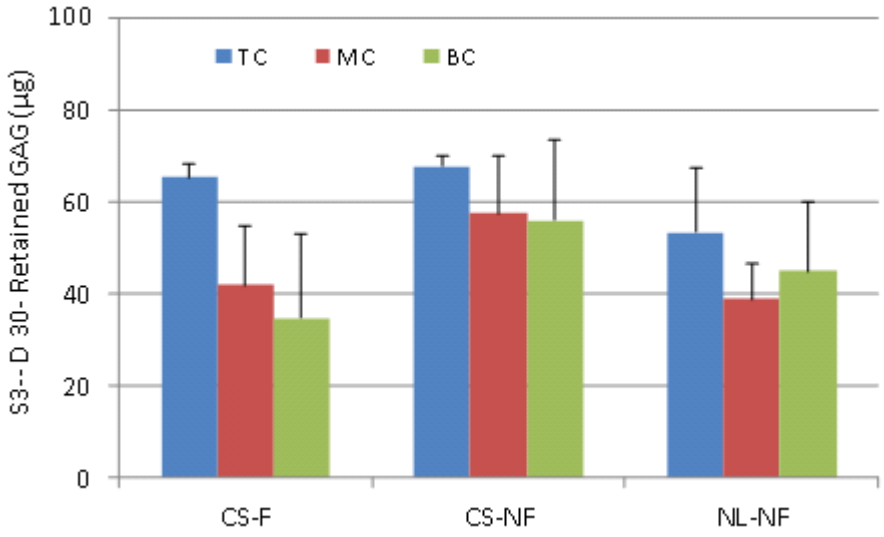

Figure 5.33 Retained GAG in central stimulated sections for 3 layers at day 30, (CS-F, n=10; CS-NF, n=10; NL-NF, n=7).

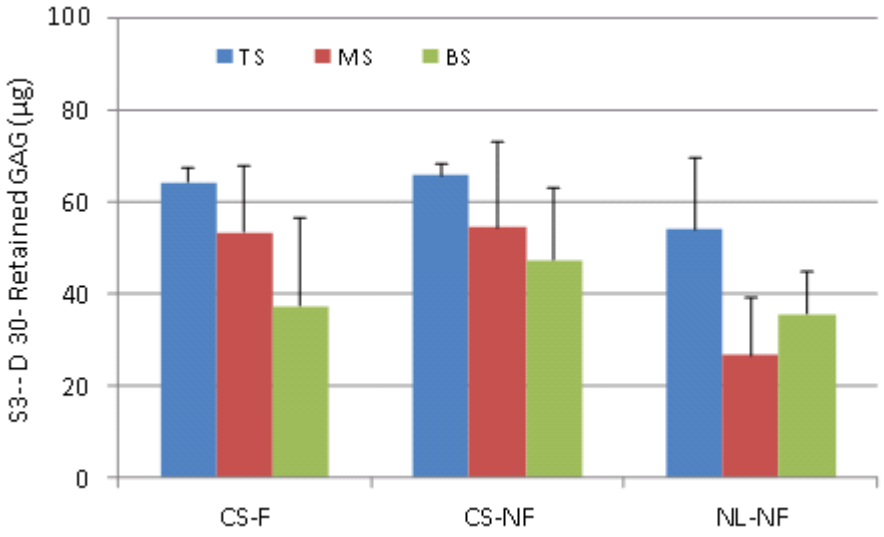

Figure 5.34 Retained GAG in side unstimulated sections for 3 layers at day 30, (CS-F, n=10; CS-NF, n=10; NL-NF, n=7).

Table 5.16 Normalized retained GAG (μg/g of wet weight) of different layers and sections in various loading conditions at day 23, 26 and 30 in study 3.

	Retained GAG (μg/g)- D23		
	CS-F	CS-NF	NL-NF
	Avg ± Std Dev	Avg ± Std Dev	Avg ± Std Dev
TC	1098.55 ± 29.69	1242.50 ± 22.25	1246.17 ± 25.88
TS	1782.0 ± 244.39	1813.56 ± 29.54	1294.41 ± 47.16
MC	644.91 ± 326.37	1330.27 ± 91.19	1622.13 ± 408.87
MS	527.20 ± 80.04	1026.91 ± 169.35	1361.01± 100.16
BC	401.98 ± 63.69	1320.54 ± 66.21	1489.55 ± 30.04
BS	674.13 ± 61.70	1256.18 ± 83.60	1608.88 ± 30.01
Sum	832.62 ± 37.35	1299.58 ± 43.86	1421.73 ± 74.54
	Retained GAG (μg/g)- D26		
TC	1243.351± 37.65	1129.4 ± 25.81	1628.33 ± 85.71
TS	1695.98 ± 70.82	1572.70 ± 56.60	1827.28 ± 26.12
MC	1344.06 ± 52.06	1396.93 ± 43.56	1244.78 ± 29.79
MS	1464.11 ± 341.90	1523.30 ± 318.70	1682.54 ± 271.03
BC	1225.27 ± 49.13	878.74 ± 343.06	1188.21 ± 246.44
BS	1490.89 ± 117.2	1186.54 ± 169.25	1549.63 ± 58.31
Sum	1391.07 ± 35.04	1259.82 ± 121.24	1489.16 ± 79.09

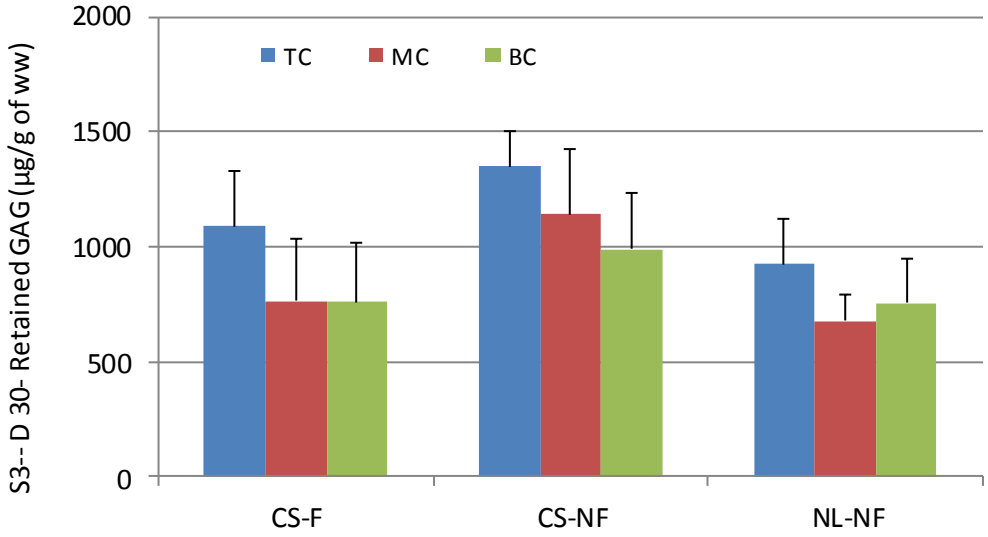

Figure 5.35 Retained GAG in central stimulated sections normalized to wet weight of the corresponding section for 3 layers at day 30, (CS-F, n=10; CS-NF, n=10; NL-NF, n=7).

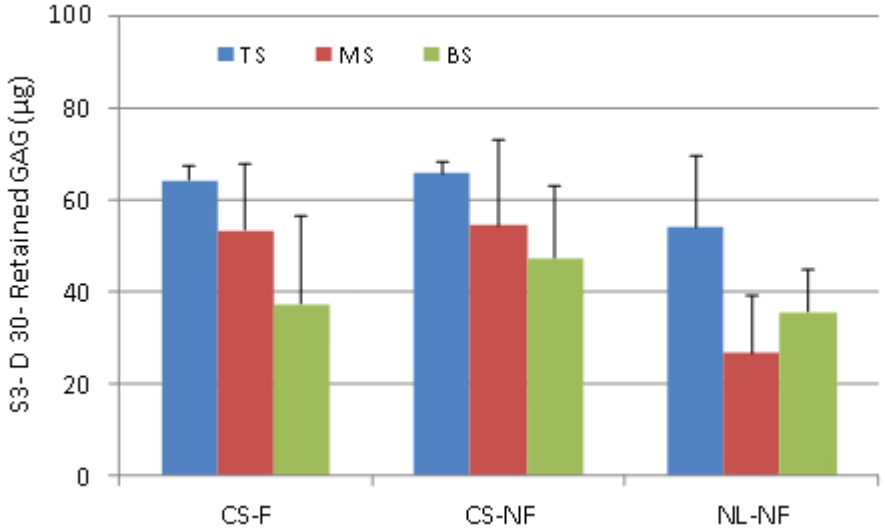

Figure 5.36 Retained GAG in side unstimulated sections normalized to wet weight of the corresponding section, for 3 layers at day 30, (CS-F, n=10; CS-NF, n=10; NL-NF, n=7).

5.4.4 Released GAG

The released GAG into the media was measured four times per week on days of changing the cell culture medium as explained in Section 4.2.4.7. The accumulated released GAG at day 23, 26 and 30 for different load/flow conditions are shown in Figure 5.37.

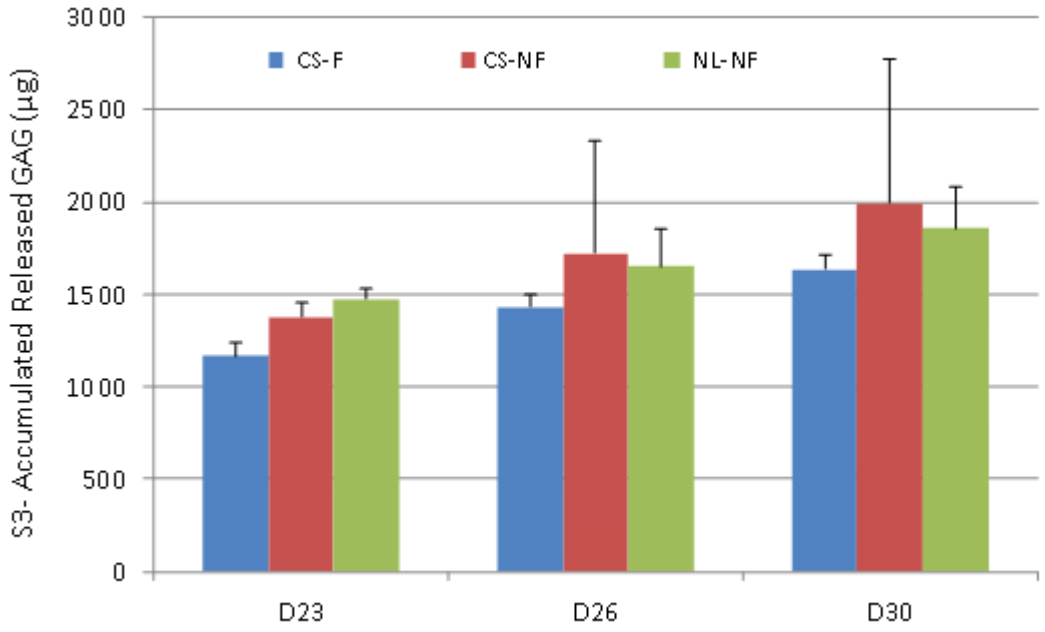

Figure 5.37 Total released GAG at day 23, 26 and 30 for the three stimulation conditions.

5.4.5 Total GAG Production

Total GAG was found by adding the amount of retained GAG (Ret GAG) in the whole construct (sum of retained GAG in three layers) to the total released GAG (Rel GAG). Total GAG production (released+ retained) at days 23, 26 and 30 for CS-F, CS-NF and NL-NF constructs are shown in Figure 5.38.

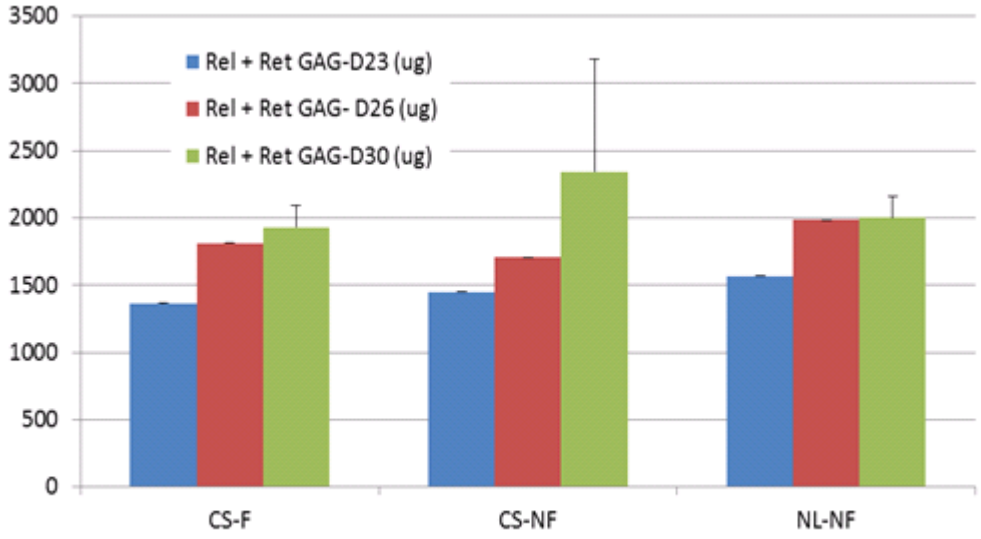

Figure 5.38 Total GAG production at days 23, 26 and 30.

5.4.6 Retained Collagen

Retained collagen in all central stimulation sections versus retained collagen in side unstimulated sections are presented in Figure 5.39. Retained GAG in each layer of the construct is shown in Figure 5.40. Total retained collagen is shown in Figure 5.41.

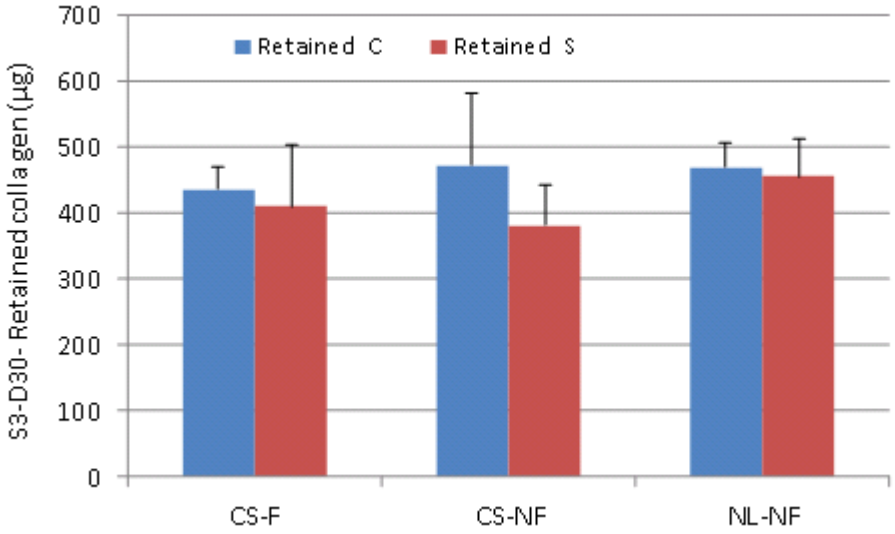

Figure 5.39 Retained collagen in central stimulated, and side unstimulated sections of all layers, day 30.

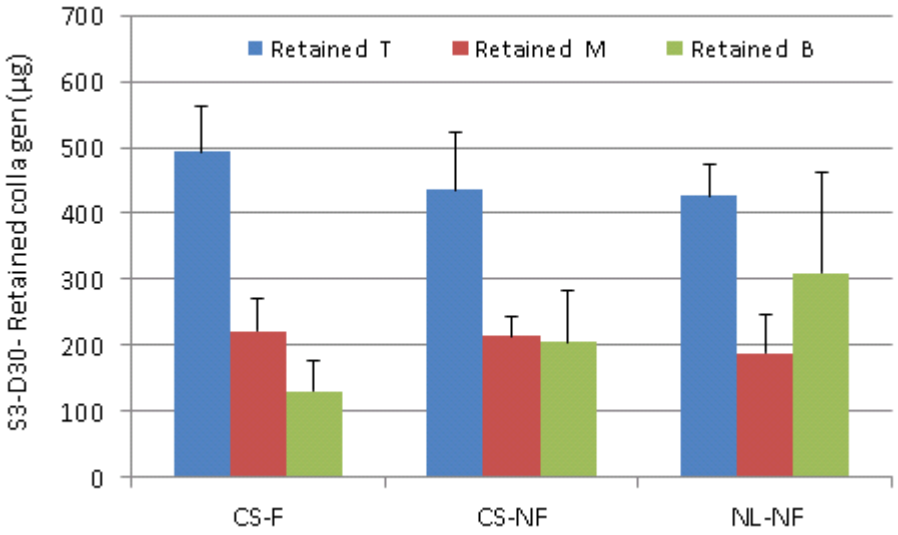

Figure 5.40 Retained collagen in layers of construct (sum of C (central) and S (sides) sections), day 30.

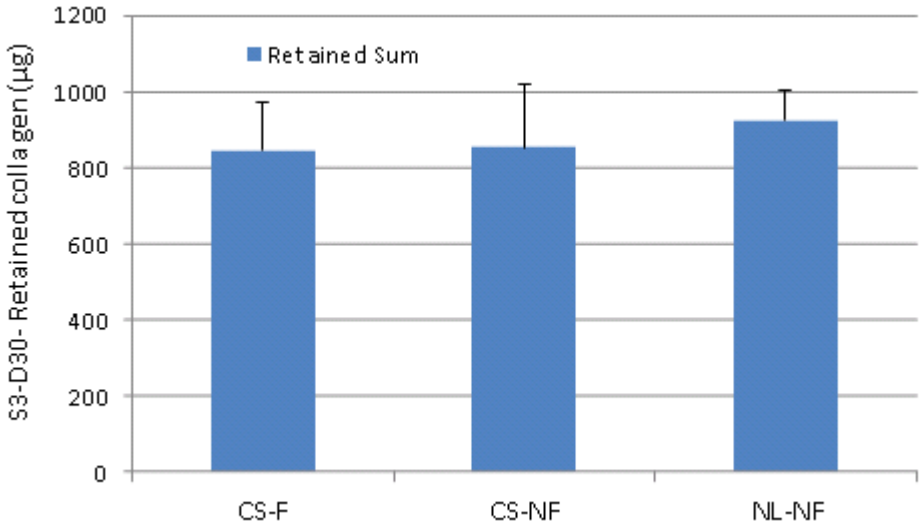

Figure 5.41 Total retained collagen in construct, day 30.

5.4.7 Released Collagen

The released collagen was measured as explained in Section 4.2.4.8. The result is presented in Figure 5.42.

5.4.8 Total Collagen Production

Total collagen (µg) was estimated by adding the accumulated released collagen up to day 30 (during stimulation period) and the amount of retained collagen at day 30. The results are presented in Figure 5.43.

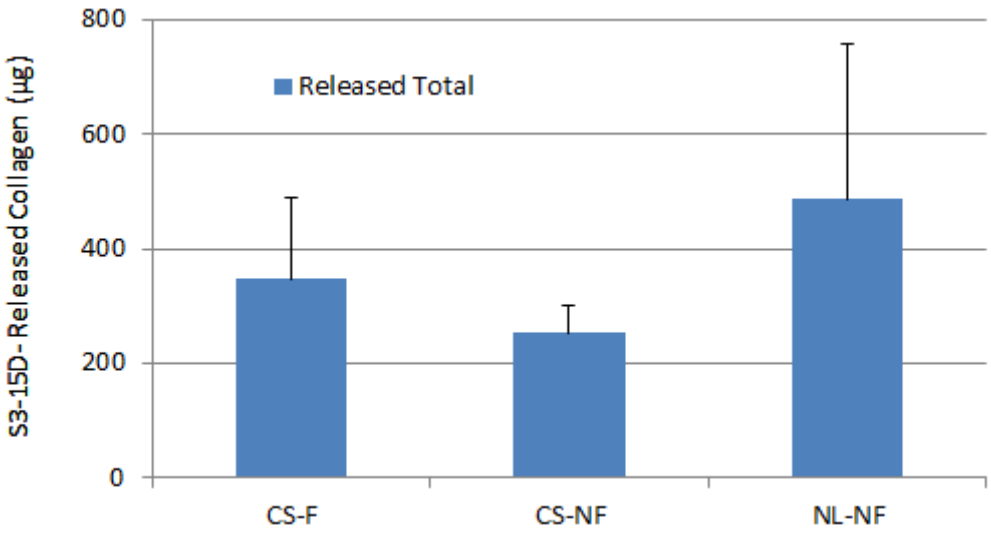

Figure 5.42 Total released collagen into culture media.

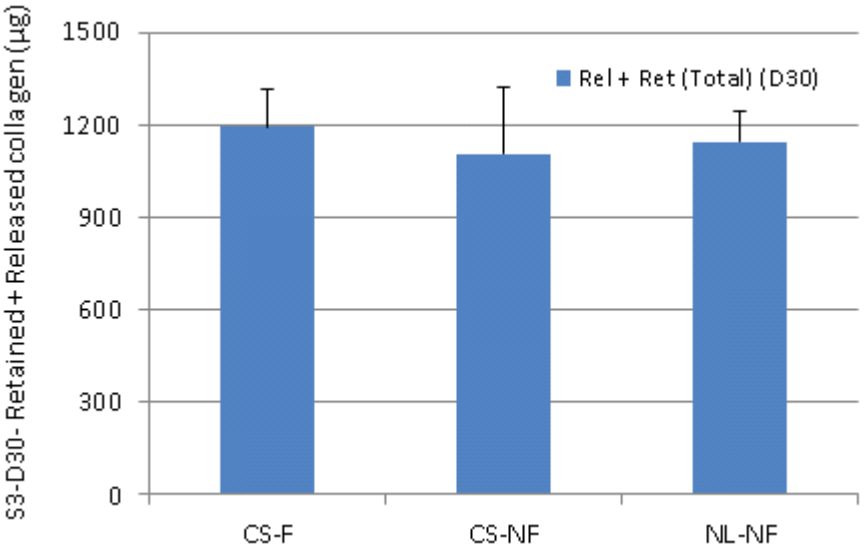

Figure 5.43 Total Collagen production (retained + released) in construct at day 30.

5.4.9 Statistical Results of Study 3

The statistical results are reported in Table 5.17 and Table 5.18 when the means of dependent variables in different loading conditions are compared (load-wise comparison for the same layers). The statistical results are reported in Table 5.19 and Table 5.20 when means of dependent variables in different layers or sections are compared (depth-wise comparison for same loading condition).

Table 5.17 Statistical p-values when means of collagen variables were compared for different loading conditions in Study 3. F: Flow (hydromechanical loading condition with fluid flow), NF: No Flow (mechanical loading condition without fluid flow), NN: No load-No Flow (unloaded condition or free swelling). The p-value less than 0.05 shows a significant difference of means of the corresponding dependent between two specified loading conditions.

Collagen Variables- Study 3	F & NF	F & NN	NF &NN
Retained collagen- Top layer- Day 30	0.403	0.607	0.718
Retained collagen- Middle layer - Day 30	0.835	0.740	0.814
Retained collagen- Bottom layer- Day 30	0.200	0.076	0.810
Retained collagen- Central section- Day 30	0.125	0.863	0.144
Retained collagen- Side sections- Day 30	0.683	0.986	0.662
Total retained collagen- Day 30	0.942	0.768	0.845
Total released collagen- Day 30	0.319	0.489	0.210
Total collagen (released + retained) - Day 30	0.708	0.362	0.355
Normalized retained collagen- Top layer - Day 30	0.856	0.671	0.510
Normalized retained collagen- Middle layer- Day 30	0.716	0.976	0.805
Normalized retained collagen- Bottom layer- Day 30	0.409	0.274	0.865
Normalized retained collagen- Central section - Day 30	0.414	0.792	0.684
Normalized retained collagen- Side section - Day 30	0.923	0.809	0.833
Normalized total retained collagen - Day 30	0.686	0.962	0.722
Normalized total released collagen - Day 30	0.340	0.539	0.257
Normalized total collagen (retained+ released)- Day 30	0.708	0.362	0.355

Table 5.18 Statistical p-values when means of GAG variables were compared for different loading conditions in Study 3.

GAG Variables - Study 3	F, NF	F, NN	NF, NN
Retained GAG- Top layer central section- Day 30	0.229	0.179	0.115
Retained GAG- Top layer side section - Day 30	0.410	0.261	0.206
Retained GAG- Top layer-Day 30	0.266	0.217	0.153
Retained GAG- Middle layer - Day 30	0.385	0.098	0.062
Retained GAG- Bottom layer - Day 30	0.278	0.771	0.384
Retained GAG- Central section - Day 30	0.125	0.863	0.144
Retained GAG- Side section - Day 30	0.600	0.195	0.128
Total retained GAG - Day 30	0.285	0.440	0.130
Total released GAG - Day 30	0.580	0.601	0.768
Total GAG (retained + released) - Day 30	0.476	0.562	0.665

Table 5.19 Statistical p-values when means of GAG variables were compared for different layers or sections in Study 3. F: Flow (loading with fluid flow), NF: No Flow (loading without fluid flow), NN: No load-No Flow (unloaded condition or free swelling). T, M and B are Top, Middle, Bottom layers. C and S are central and side sections of construct respectively. . The p-values with asterisk show a significant difference of means of the corresponding dependent variable between two specified loading conditions.

Study 3- GAG dependent variables	GAG Comparison	T & M	T & B	M & B	C & S
Retained GAG- F- Day 30	T > M > B; S > C	0.017	0.029	0.344	0.576
Retained GAG- NF- Day 30	T > M > B; C > S	0.202	0.127	0.713	0.581
Retained GAG- NN- Day 30	T > M > B; C > S	0.115	0.331	0.467	0.298
Normalized Retained GAG-F- Day 30	T > M > B; S > C	0.256	0.162	0.755	0.245
Normalized Retained GAG-NF-Day 30	T > M > B; S > C	0.352	0.031	0.477	0.583
Normalized Retained GAG-NN-Day 30	T > B > M; C > S	0.177	0.324	0.645	0.970

Table 5.20 Statistical p-values when means of collagen variables were compared for different layers or sections in Study 3. F: Flow (loading with fluid flow), NF: No Flow (loading without fluid flow), NN: No load-No Flow (unloaded condition or free swelling). T, M and B are Top, Middle, Bottom layers. C and S are central and side sections of construct respectively. The p-values with asterisk show a significant difference of means of the corresponding dependent variable between two specified loading conditions.

Collagen Variables- Study 3	Collagen comparison	T & M	T & B	M & B	C & S
Retained Collagen- F -Day 30	T > M > B ; C > S	0.001	0.0002	0.06	0.668
Retained Collagen - NF -Day 30	T > M ~B ; C > S	0.006	0.014	0.869	0.250
Retained Collagen – NN -Day 30	T > B > M; C ~ S	0.016	0.009	0.773	0.411
Normalized Retained Collagen- F -Day 30	T > M > B; S > C	0.004	0.002	0.151	0.591
Normalized Retained Collagen - NF -Day 30	T > M > B; S > C	0.004	0.001	0.502	0.712
Normalized Retained Collagen - NN -Day 30	T > M > B; C > S	0.039	0.011	0.936	0.969

5.4.10 Fluid Film Estimation

Inserting the following values in formula for fluid film presented in Section 3.1.1 for Study 2 and for Study 3 (CS-F):

R_o = 1.78 mm

R_i = 0.84 mm

Q_3 = 12.2 ml/min = 0.203 × 10^{3} mm^3/s

F_3 = 28.5 mN

η = 0.001 Pa s

$$h = \left[\frac{3\eta . R_0^{\,2} Q}{F} \left(1 - \left(\frac{R_i}{R_0} \right)^2 \right) \right]^{\frac{1}{3}}$$

h_3 = 52.69 µm

5.4.10.1 Comparing Fluid Film Thicknesses in all Studies

The estimated fluid film thickness based on load and flow rates in all studies are compared in Table 5.21. For the same loads (F_{1A}, F_{1B} or F_2), higher flow rates result in having thicker fluid film, whereas for the same flow rates (Q_2 and Q_3), higher load results in a fluid film with less thickness.

Table 5.21 The estimated film thickness based on different load and flow condition in various studies. These estimated film thicknesses are much higher than the likely surface roughness of the agarose.

Study	Load (mN)		Flow rate (ml/s)		Fluid Film Thickness (μm)	
S_{1A}	F_{1A}	45.1	Q_{1A}	0.129	h_{1A}	21.08
S_{1B}	F_{1B}	45.1	Q_{1B}	0.247	h_{1B}	40.46
S_2	F_2	45.1	Q_2	0.203	h_2	32.25
S_3	F_3	28.5	Q_3	0.203	h_3	52.69

5.5 Concluding Remarks

Comparing Study 1 with the other two studies, it was found that measuring released amount of GAG or collagen into culture media in addition to the amount of retained in the construct is very important. Especially for mechanically or hydromechanically stimulated samples, the released proteins may contain information that may represent the actions of loading and response of cells within the constructs. The high amount of accumulated released protein into culture media especially in long-term culture and stimulation is better not to be neglected.

Comparing some results of Study 2 and 3, it was found that stimulation parameters in Study 2 may be closer to the one that really show the effect of dynamic loading on both collagen and GAG. The number of stimulations per week and short stimulation time per day may have been mild in Study 3 so the cells within the construct could not differentiate the signals they receive from two types of loads to respond.to their surrounding environment. However, there might some aspects of results of Study 3 that needs to be revealed through more statistical analysis.

The efforts to understand the effect of loading at different depth of construct by layering the construct parallel to the stimulated surface was promising. Depth-dependent response was also revealed in some of the results. Overall, the developed hydromechanical stimulator presented its effectiveness in some parts of our studies and its potential can be revealed by including more biochemical or mechanical analysis so more understanding of effect of loading can be established. The results of all experiments will be further interpreted and more discussed in the next chapter.

Chapter 6

Discussion

This chapter, in general, relates and interprets the results of all presented experiments in this thesis and compares them with findings of other similar research studies. It explains the rational for choosing the parameters of the studies and their sequences and the reasons for some of the modifications throughout the experiments. More specifically, it compares the functions of the presented hydromechanical stimulator with similar designed/developed mechanical stimulators by other research groups. It presents the agarose hydrogel as a 3D model for bovine articular chondrocytes throughout culture and stimulation period and discusses its role in production of cartilage-like matrix. The variations of cell densities in the hydrogel constructs in the presented studies are explained and their possible effects that are related to protein production. The effects of both mechanical and hydromechanical stimulations on collagen and GAG released from samples or retained in layers/sections of constructs are discussed. These results are compared with accumulation of these two markers in similar mechanically stimulated constructs in other studies.

6.1 Mechanical Loading and Hydromechanical Stimulator

The functionality of the articular cartilage and its overall health can be modified by the physical activities while exercising the synovial joints. The necessity of moderate mechanical loading, in maintenance of cartilage health has been supported by previous in vitro studies [26]. *In vitro*

application of mechanical stimuli has also been suggested as a beneficial factor in directing the growth and maturation of in vitro engineered cartilage tissue. In order to address the cues that are essential in the functional growth of cartilage, a few studies have integrated the different mechanical loadings in their stimulation techniques [41-52], [72], [328], [373]. Incorporation of such stimuli could enhance some matrix syntheses or the mechanical properties of cell-seeded scaffolds.

Bioreactor-like environment for cells and providing appropriate chemical and mechanical environment for them are important in tissue engineering of cartilage and also other tissues [402]. Recent efforts on creating more advanced bioreactors have focused on addition of several different mechanical stimuli as well as providing good culturing environment in the same device. These bioreactors, with some capability of mechanical stimulations, have been designed in such a way to incorporate different loading components such as compression, shear, or fluid perfusion to better represent the complex in vivo loading condition of the articular cartilage tissue. Most of these efforts have been directed towards gaining more knowledge about the mechanisms that transform the macroscopic mechanical loads into cellular and intracellular actions. Continuing this general effort and addressing complex *in vivo* loading condition of synovial joints, the present thesis reports on the development of a new hydromechanical stimulator for articular chondrocytes for general applications in cartilage tissue engineering. A unique approach has been adopted in this stimulation. The stimulation technique incorporates sliding indentation along with direct fluid perfusion on the surface of the construct. The sliding path can be programmed as unidirectional or bidirectional manner with specified length and direction. Many stimulation patterns could be tailored using this feature based on the size of the construct and requirements of each experiment. Both indenter and direct fluid perfusion from the indenter can create shear force on the surface of

the constructs. None of the previous studies which adopted the sliding contact technique to apply stimulation [45], [52], [371-373], [403-405] had a dynamically moving fluid perfusion pattern on the surface of the constructs.

The stimulation technique developed in the present thesis has several potential advantages. It can localize the fluid perfusion to the same indentation contact points. Multiple constructs can be stimulated at the same time and different dead loads can be applied to each. Each indenter supplies cell culture media directly to the top surface of the construct from a central pressurized pocket. Thus, localized hydrostatic pressure and fluid-flow induced shear are applied to the construct surface. At the same time, the fluid film (which is formed in between the contact points) helps protect the construct from surface damage.

6.2 The Rationales of Sequence and Parameters of Studies

Some of the system inputs such as approximate range of strain, the culturing period, the stimulation time, the stimulation intervals and the sliding speed , were set as close as possible to earlier studies in the literature. This was done to allow some comparison of the outcomes. However, because the present stimulator is unique, not all of the system parameters could be matched exactly. The rationales for the experimental parameters of the experiments are explained in the following subsections.

6.2.1 Preliminary Studies

Preliminary experiments were necessary to find approximate functional and non-destructive ranges for the combination of applied load and fluid flow rates. The repetitive application of loads and

fluid perfusion over time could damage the constructs. Macroscopic physical changes in appearance were detected in these preliminary studies.

Various concentrations of agarose had been used in previous studies. They were 1% [406, 407], 2% [47], [50], [58], [71], [284], [371], [408-412], 3% [80], [353], [356], [357], [389], [394], [413-418], or 4% [348], [419]. However, most of these studies had simpler stimulation techniques than those of the present thesis. Therefore, it was necessary to explore the effect of various loading conditions of our stimulator to find optimal agarose concentration. The preliminary study revealed that 3% agarose did not show any sign of permanent deformation or surface destruction when exposed to fluid flow rates less than 17.6 ml/min combined with applied loads less than 56 mN. Thus, 3% agarose was chosen for the main experiments of the present thesis. However, 2% agarose might have been more conducive to cell metabolism and thus, in future, conditions might sought to permit its use.

Typical compressive strains in the order of 5-20% have been applied to cell-agarose constructs [420], which is similar to physiological strain levels [58]. Lee et al. [394] applied 15% compressive strain at various frequencies (0.3, 1, 3 Hz) to 3% agarose-chondrocyte constructs up to 48 h to investigate its influences on metabolic processes such as synthesis of glycosaminoglycans and DNA. Similarly, Chowdhury et al [345] explored the effects of compression (15% stain at 1 Hz) using various duty cycles of dynamic load over 48 h culture period for 3% agarose-chondrocytes. However, Mauck et al [58] applied 10% axial dynamic compressive strain on 2% agarose-chondrocyte at 1 Hz frequency for longer period of time (4 weeks). They used a load application schedule of 5 days per week with 3 times of 1h-on, 1h-off loading per day.

The studies which incorporated two to three loading types also used similar or slightly lower ranges of compressive strains. For instance, in a study by Waldman et al [44] various combinations of compression-shear (C-S) were investigated including 2%C-2%S, 2%C-5%S, 5%C-2%S and 5%C-5%S strains. These conditions were applied for 3 days per week on one-month-old *in vitro* grown cartilage for 400 cycles per day. In other studies [41], [43], spheres in oscillating rotation (± 60º at 0 or 0.6 Hz) and reciprocal vertical displacement (0.1 Hz) were loaded against polyurethane-chondrocyte construct pins with 5, 10 or 20% strain amplitudes in the vertical direction. The effects of this stimulation (vertical compression alone or compression with surface sliding) on mRNA expression of type I and type II collagen of constructs were investigated. In studies by Kock et al [373], 0.5% agarose-chondrocyte constructs, sandwiched in between two layers of 3% cell-free agarose, were stimulated by sliding motion of a cylindrical glass indenter (Ø4.5 mm) over the surface of construct. The sliding indentation was applied at 10% strain and 1 Hz for 4 h/day for 5 days/week for 28 days to investigate the changes in collagen content and to detect depth-variation of extracellular matrix distribution. Kaupp et al [371] used a spherical glass bead (3 mm diameter) to provide a moving point of contact stimulation (MPS). This technique applied dynamic compression, shear and friction across the surfaces of 2% agarose-chondrocyte constructs. A dead load of 10 mN was applied and the reciprocal motion was sinusoidal with 3 mm amplitude at a frequency of 0.5, 1 or 2 Hz for durations between 5 and 60 min over 3 consecutive days. Clearly, there has been considerable variation in stimulation conditions with no consensus regarding the most beneficial for stimulating chondrocyte metabolic activity. However, the experiments of the present thesis are perhaps closest to those of Kaupp et al [371] except for the present addition of direct perfusion.

The compressive load in the present thesis was chosen to provide approximately 20% strain (in Study 1 and 2), or less (in Study 3), on 3% agarose-chondrocyte constructs. In addition to selecting an appropriate agarose concentration for the applied load and flow combinations, the preliminary experiments examined the viability of cells (both loaded and unloaded) within the constructs during 2-week culture period.

6.2.2 Study 1

The parameters of this study such as sliding velocity, distance, stimulation pattern, and stimulation period were all similar to the preliminary study. Appropriate combinations of fluid flow rates and compressive loads were selected based on the ranges found in the preliminary study. As explained previously, a bidirectional motion pattern (in both X and Y axis) was applied over the construct surface, rather than a simple reciprocating motion in only one direction, in an attempt to more evenly stimulate the chondrocytes. The main purpose of Study 1 was to determine the effects of both mechanical (compression + sliding indentation) and hydromechanical (compression + sliding indentation + fluid perfusion+ fluid induced shear) stimulations on viability of chondrocytes and glycosaminoglycan (GAG) production within the constructs after 3 weeks culture period and 2 weeks stimulation. Another purpose was to determine how changes in the amount of fluid flow rate altered the abovementioned effects. It was also of interest to find out whether higher flow rates could result in having higher GAG production in the construct compared with the lower flow rates while they were combined with the same compressive load and sliding motion.

The GAG production had shown some dependency on the flow rate in studies by Degala et al [421], [422]. They exposed chondrocyte seeded alginate scaffolds with different concentrations to a

range of 5-50 µL/min fluid flow rates and found that Ca^{2+} signalling response to direct perfusion on constructs increased monotonically with flow rate. Their study was also based on previous finding [423] that oscillatory fluid-induced shear stress increased intracellular calcium levels and sulfated GAG production, which suggested the role of calcium in modulating the biochemical pathways that lead to sulfated GAG production.

The studies that investigated the effect of *in vitro* application of fluid flow on the chondrocytes have mostly used laminar flow parallel to the surface of the constructs [424], [89], [88], [69], [90], [87], whereas in the present thesis the fluid flow is initially directed perpendicular to the loaded surface of the construct and then it is forced parallel to the construct surface. Gemmiti et al [89], [88], [69] reported the exposure of the constructs to this type of flow using a parallel-plate bioreactor to apply mechanical stimulus in the form of shear stress. The fluid flow at rate of 3 ml/min was continuously applied on scaffold-free constructs for 72 h which resulted in the shear stress between 0.07 – 0.15 Pa (due to thickness variations between samples). Chen et al [90] exposed the surface of 2% agarose chondrocyte constructs to an oscillatory flow rate of 5 ml/min which based on the dimension and arrangements of their chamber, resulted in about 0.012 Pa shear stress across the surface of hydrogel. Davisson et al [87] seeded polyglycolic acid (PGA) scaffolds with ovine articular chondrocytes at a flow rate of 2.5 ml/min for 4 h first and then decreased the flow rate to 0.05 ml/min and fluid velocity of 10 µm/s through the constructs. They reported 40% increase in GAG synthesis and deposition after 9 days of continuous perfusion compared with static controls. In another study by Xu et al [425], the effect of perfusion was investigated on agarose (2% with 4 million cells/ml) at continuous yet very low flow rate of ~ 0.417 µl/min for 7 days (12 days of total culture time including 7 days of perfusion). They found that continuous fluid perfusion made no difference in GAG production of the agarose constructs. Khan et al [426]

cultivated engineered articular cartilage tissue constructs under a continuous, yet very low culture media flow rate of 5 - 10 µl/min for one week (after 2 weeks of pre-culture). They found 50-70% increase in proteoglycan and collagen content. These results were similar to those of through-thickness perfusion culture within the same period of time that used higher flow rates of 240-800 µl/min [87], [427], [428]. In Schulz et al [369], there was an intermittent medium perfusion at a steady flow rate of 0.5 ml/min for 10 min followed by 50 min rest period for 21 days on 3% agarose-chondrocyte constructs. Direct perfusion had positive effect on both cell proliferation and cell differentiation.

It was learned from these studies that fluid perfusion could apply shear stress on the surface of construct that might stimulate cell-seeded constructs or encourage the cells to produce more GAG. According to these studies, the continuous application of fluid perfusion was likely to establish an effect on matrix production. Considering the direction of fluid flow, the through-thickness perfusion applied higher flow rates compared with parallel-to- surface perfusion to reach to similar effect on GAG and collagen.

Study 1 was divided into two separate studies with two different hydromechanical loading regimes on the constructs (Study 1A and 1B, representing low and high fluid flow rates respectively) that were exposed to fluid flow in addition to the compression and sliding indentation. Both of the fluid flow rates were chosen to be within the range suggested by the preliminary studies suggested (less than 17.6 ml/min when combined with about 45.1 mN compressive load). This avoided macroscopic and physical damage on the surface of the constructs during the 2-week stimulation period. The minimum flow rate was about 7.7 ml/min since lower rates (less than 5.5 ml/min) created small bubbles when the cell medium was ejected from the microchannel (~ 0.3 mm diameter) of the indenter tip. These bubbles were probably a result of the chemical contents of the

cell medium (such as fetal bovine serum), because such bubbles were not present while testing with distilled water or phosphate buffered saline (PBS). Bubbles probably created an undesirable scenario, in that they caused an interruption in the continuous supply of fluid to the surface. The higher flow rate was chosen in the hopes of showing an influence of flow rate.

6.2.3 Study 2

The design of Study 2 was based on three main rationales. First, the response of chondrocyte within the agarose construct to load/flow stimulation needed to be explored over a longer period of time than in Study 1. Second, the depth-dependent effects of load/flow stimulation were to be investigated by developing a new method for harvesting the cell-seeded constructs. Due to the organized structure of articular cartilage, the importance of tissue engineering of this tissue with zonal organization has been addressed in a few studies [114], [373], [401], [404], [429-434]. However, none have experimentally investigated separate layers (depth wise) of mechanically stimulated samples to find differences of their protein accumulations. Therefore in Study 2 , instead of using full-thickness of half constructs (acquired by cutting perpendicular to the stimulated surface); as was done in Study 1, three layers of constructs, parallel to the stimulated surface were harvested. The biochemical analyses were performed for each individual layer. Third, more biochemical measurement procedures were conducted and more data were acquired compared with Study 1. It was realized that in addition to retained GAG, the GAG released into culture media should be measured along with both retained and released collagen. This was based on the recent study by Grad et al [405] which had a somewhat similar stimulation technique (sliding surface motion) probably with a pressurized fluid film providing some perfusion. They found that a

substantial amount of GAG was released into the medium. Therefore, in the subsequent studies (Study 2 and 3) of the present thesis, the GAG within the construct and GAG released into the cell medium were both measured. In this way, it was hoped that the true and complete effectiveness of the hydromechanical stimulation in GAG production could be determined. It should be noted that the released GAG and collagen results of Study 2 were measured after the completion of Study 3. Thus, the planning of Study 3 did not benefit from the knowledge of the complete findings of Study 2. This is further discussed in subsequent sections.

6.2.4 Study 3

The design and analyses of Study 3 had three main features. First, the responses of the chondrocyte-agarose constructs to load/flow stimulation were investigated for more localized stimulation area compared to Study 2. In Study 3, a linear reciprocating stimulation pattern was adopted with frequency of 0.96 Hz.

Second, the chondrocyte-agarose constructs were exposed to a reduction in load, number and duration of stimulation in the 3-week period compared with Study 2. Instead of 30 min/day for 5 days/week stimulation with ~ 45 mN of applied load in Study 2, the stimulation was performed for 15 min/day for 3 days/week with ~ 28 mN in Study 3. This was done because Kaupp et al [371] had suggested that such a stimulation time and interval were beneficial for chondrocytes within agarose constructs, while they were being stimulated on similar unidirectional stimulation pattern. Third, for the biochemical analysis, after harvesting the construct in layers (as in Study 2), central stimulated area was separately analyzed from the two unstimulated sides. This could help in understanding if the effects of stimulation on GAG and collagen stayed localized or they were propagated on the unstimulated sides as well.

It was important to note that it was thought that the stimulation in Study 2 had been too harsh. In Study 3, many of the conditions used by Kaupp et al [371] were adopted. The findings of the present thesis compared with those of Kaupp et al [371] are discussed in subsequent sections.

6.3 Using Agarose Constructs

The encapsulation of articular chondrocytes within an agarose hydrogel has been well-characterized as an experimental model system to investigate the mechanotransduction of chondrocytes. This model system preserved the phenotype of chondrocytes during their long-term culture [435], [436] without negative effect on the viability of cells. Load can be applied to agarose-chondrocyte constructs right after seeding due to its favorable biocompatibility and mechanical properties [394]. Consistent with these studies, the chondrocytes in all of our experiments were also successfully cultured for 2, 3 and 4 weeks period and maintained their round shape and viability. We were expecting to have more cell death in dynamically loaded (different combination of loads and fluid flows) samples compared with static condition (no load and no flow), but interestingly the chondrocytes in the constructs in all of the loading conditions had similar viability in all of the experiments.

Reaching a similar GAG content to that of natural articular cartilage had been a challenge in most of the studies using this hydrogel [58], [375] and only a fraction of it could be produced after 3 weeks of dynamic loading. Calf cartilage plugs had about 57 ± 11 mg/ml of GAG as shown by Sah et al [321], whereas Mauck et al [58] found that he agarose-chondrocyte constructs contained only about one-quarter of this value after 21 days of receiving dynamic loading. Similar levels of GAG were found by Buschmann et al [375] after about 27 days of stimulation.

Kock et al [437] explored the extent to which matrix distribution was modulated by changing the agarose concentration and investigated how this alteration affected the mechanical properties of cultured constructs after 21 and 42 days. They showed that matrix content (including GAG and collagen) per wet weight did not change significantly in lower agarose concentrations. However, distributions of GAG and collagen in lower agarose concentrations were more homogeneous. Therefore, with no correlation between the agarose concentration and quantity of matrix within constructs, and with no correlation between lowering agarose concentration and increased release of matrix components into culture media, matrix-matrix interaction was suggested as possible influencing factor in the assembly of matrix molecules [437]. They also thought that constructs with lower agarose concentrations might less hinder the proteoglycan aggregate formation and their conclusion was mostly based on comparing the approximate length of aggrecan molecule (± 0.4 μm) [438] and the pore size of 2% agarose (0.12 μm) [431]. Therefore, based on this finding, with the use of 3% agarose-chondrocyte in the present thesis, non-homogenous distribution of GAG or collagen might have been expected. However, the 3% agarose might provide less space for newly formed proteoglycan compared with 2% or lower concentrations, but it might better withstand higher loads with less need for preculture time.

The effects of variations of cell densities in enhancing the process of cartilage regeneration have not been explored in the present thesis. Previous studies which looked at the influence of cell density [281-284] of the chondrocytes found contradictory results. Considering both mechanical and biochemical properties, Mauck et al [283] found that higher seeding density (60 vs 10 million cell/ml) and higher serum concentration (20% vs 10% FBS) made no significant difference in both proteoglycan and collagen contents.

The cell densities in the present thesis were the maximum that could be obtained after isolating them from certain number of joints. As the number of samples was increased fewer cells were present per volume of the construct. The samples in Study 1 had the highest cell density of 6.32 million cells/ml compared to 1.14 and 2.66 million cells/ml in Study 2 and 3 respectively, with approximate cell numbers of 2.48, 0.45, 1.04 million cells per agarose construct (~ 0.392 ml). The cell density used in Study 1 was comparable to cell seeding density of Kock et al [356]. The GAG deposition in their study was approximately 75 µg/ µg DNA by day 14 and about 225 µg/ µg DNA by day 28 in 3% agarose-chondrocytes (OD = 10 mm, h = 3 mm) with no difference between control and loaded groups (compressed at 0.33 Hz and 1 Hz). In Study 1 of the present thesis, the GAG depositions in half of the constructs (OD = 10 mm, h = 5 mm) under various loading conditions were 207 ± 82 µg (CS-LF), 200 ± 75 µg (CS-HF), 299 ± 141 µg (CS-NF) and 253 ± 152 µg (NL-NF) by day 21. The cell seeding density of about 2 million cells/ml in agarose was reported by Toyoda et al [80] and Bougault et al [62], [410], which is close to the cell-seeding density in our third study. It is possible that the stimulations used in the present thesis might have been more effective with higher cell densities. This hypothesis will be considered in future studies.

6.4 GAG and Collagen Production

6.4.1 Released GAG and Collagen

In agreement with the findings of the present thesis, other studies found that their constructs also released some of the produced GAG or collagen into medium [58], [405], [425], [440-444]. Some of these studies found that the release of matrix molecules was enhanced by the application of dynamic loading.

Mauck et al [58] found that the released GAG into medium was 13 µg/day per disk on day 7 of the culture and below 10 µg/day by day 28. This did not support the daily increase of released GAG found by Buschmann [375]. In the studies of the present thesis, higher amounts of GAG were released daily into the medium compared with Mauck et al [58]. However, consistent with their finding and contrary to Buschmann study there was not a significant increase from one day to the next day throughout the 3-week stimulation period. In Study 2, the released GAG was 38.1 ± 11.8 µg/day (n = 90), 37.3 ± 11 µg/day (n = 90) and 17.7 ± 8.5 µg/day (n =15) for CS-F, CS-NF and NL-NF loading conditions respectively. This might better represent the changes in daily release of GAG into media considering daily detection of changes in the release rate and also considering the high number of quantified samples in our study. The higher values of released GAG in Study 2 compared with a study by Mauck et al [58] might be because of the higher volume of the culture medium per day considering the cell density in agarose. In Study 2 and 3, each construct with cell density of 1.14 and 2.66 million cells/ml contained about 0.45 and 1.04 million cells respectively. Each construct was fed with 7.5 ml of culture medium per day. Using higher medium volume per construct, there was 0.0594 and 0.139 million cells/ml feed medium per day in Study 2 and 3 respectively. However, Mauck et al [58] had agarose constructs with higher cell densities and had 1.7 million cells per ml culture medium per day.

Kisiday et al. [445] found increased proteoglycan loss to the medium due to dynamic compression (sinusoidal displacement with 2.5% strain amplitude superimposed on 5% static offset) during 39 days, but interestingly total proteoglycan accumulation in the dynamically loaded peptide hydrogel scaffold was significantly higher than controls (in free swelling condition) after 16 and 39 days of loadings. The compressed samples at day 16 accumulated about 5.8 µg/mg wet weight of GAG (~ 38% higher than controls at day 16), which increased to about 15.5 µg/mg wet

weight at day 39 (~ 22% higher than controls at day 39). On days 8, 16 and 39, control samples lost 32%, 36% and 22% of total GAG into medium, which increased to 47%, 39% and 37% for dynamically loaded samples. Roberts [442] found that by day 28 the cumulative GAG released into the media was about 800 μg for poly (ethylene glycol) (PEG) and about 1300 μg for oligo (lactic acid)-b-PEG-b-oligo (lactic acid) (PEG-LA) hydrogels. The constructs that were loaded for 4 weeks (without free swelling period beforehand) released 3-folds higher GAG compared with the constructs that were loaded for 2 weeks (without free swelling period beforehand). They also found that the constructs that were in free swelling condition for 2 weeks before the 2-week loading period were releasing less GAG into medium compared with the ones that were loaded for 4 weeks without free swelling period beforehand.

In agreement with their studies, in the present Study 2 the total amount of released GAG after 3 weeks of loading was about 2-fold higher for both hydromechanically and mechanically stimulated samples (CS-F and CS-NF respectively) compared with unloaded ones (NL-NF). The released collagen in Study 2 was also higher from samples under both dynamic loading conditions with less difference from the control (compared with GAG), as CS-F samples had 1.3-fold and CS-NF had 1.14-fold higher released collagen than controls. The higher release rate of GAG during 3-week stimulation period might suggest more pressurization or movement of fluid within/ out of the construct due to loading that has been transferred from the top layer to the layers underneath.

More and more published data have confirmed the high amount of released protein into the media which have substantially affected the results of total GAG and collagen production during the culture/stimulation period. Considering only GAG and collagen content that are retained within the cell-seeded scaffold or engineered tissue is likely to be a great shortcoming of any study. For instance, Grad et al [405] which adopted the ball and oscillation stimulator to apply load on

polyurethane scaffolds seeded with chondrocytes, found no statistically significant difference in the amount of GAG retained in the constructs between control and two loaded groups. The samples in one of their loading groups (LG1) were receiving dynamic compression only and the samples in the other loading group (LG2) were exposed to dynamic compression and sliding surface motion. They found 658 ± 218 µg of retained GAG in control samples, 821 ± 181µg in LG1 samples and 805 ± 163 µg in LG2 samples. However, when the released GAG was also measured to account for total GAG production of scaffolds, they found much higher values of 2.23 ± 0.37 mg for controls, 2.90 ± 0.29 mg for LG1 and 2.96 ± 0.32 mg for LG2 samples, confirming approximately 30% GAG retention within the scaffolds in their study. Their GAG retention was similar to results of Lee et al [446]. Consistent with findings of Grad et al [405] and Lee et al [446], the results of Study 2 and 3 also revealed the game-changing role of the released proteins into media and the amount of total protein production.

In agreement with results of Gard et al [405], more released GAG and collagen into media was found for samples under loading in Study 2. Also, similar to their findings, significant difference in total protein production (collagen in our Study 2) of samples under various loading conditions were found only by the inclusion of released proteins in the analyses (but protein accumulation within construct was unaffected by loading conditions).

The total released GAG in Study 2 was found to be highest for CS-F constructs compared with the CS-NF constructs and no significant differences were found between CS-F and CS-NF constructs. These two groups could not be compared statistically with the NL-NF constructs, as there was only one sample for measurement because of the inadvertent mixing of cell media for all unloaded samples. The result of released collagen in Study 2 for constructs under CS-F loading condition showed about a 29.8% increase and the ones under CS-NF loading condition showed

about 14.2% increase in total released collagen (μg) compared to constructs under NL-NF condition.

6.4.2 Retained GAG and Collagen

Despite the fact that the cell viability was high in Study 1 throughout the 3-week study, the measured GAG in the various stimulated constructs did not show any statistically significant differences at the end of this period. It was a shortcoming of Study 1 that the amount of GAG released into the medium was not measured. It had been hoped that the present stimulation method was powerful enough to show a GAG increase in the construct alone. Furthermore, some increase in GAG production might have occurred mostly on the superficial layer and the present analysis used a full-height segment of the construct for GAG assessment. Therefore, the specimen-to-specimen scatter might have masked the beneficial effects of our stimulation. In the subsequent studies (Study 2 and 3) of the present thesis, the GAG within the construct and released into the cell medium were both measured. In this way, it was hoped that the effectiveness of the hydromechanical stimulation in GAG production could be determined.

In Study 2 about, 9.1%, 10.8% and 13.2% of total collagen was retained within the construct in CS-F, CS-NF and NL-NF loading conditions, respectively. But, the effect of loading on total retained collagen could not be determined, because there was no significant difference in total collagen retention in constructs under various loading conditions. Similar to collagen, total GAG retention of samples in this study in NL-NF group was higher than CS-NF group, and both were higher than CS-F group. However, the difference between CS-F and NL-NF groups was statistically significant which showed the reduction of total GAG retention due to hydrodynamic

stimulation. But, this reduction could not necessarily be translated as an inhibitory effect of this stimulation on GAG production, because this downregulation was not reflected (statistically) in total GAG production (released + retained). Therefore, it seemed that the effect of hydrodynamic stimulation was to shift GAG from the constructs to the media.

In Study 3, a lower percentage of total GAG and higher percentage of total collagen were retained in the agarose hydrogel. About 15.3%, 16.2% and 12.7% of total produced GAG, whereas 71.2%, 77.2% and 65.9% of total collagen were retained in agarose hydrogel in CS-F, CS-NF and NL-NF conditions respectively. The lower GAG retention range compared to Lee et al [446] and Gard et al [405] might be due to differences in material properties of their polyurethane or fibrin-polyurethane construct versus that of the agarose hydrogel used in our study. Larger pore size of polyurethane (~ 90 - 300 μm) compared with agarose (~ 0.12 μm for 2%) might have provided more space for aggrecan to grow inside the pores and stay there, whereas this growth may become limited due to smaller size of pores in agarose compared with size of aggrecan [438], [431]. Pore-to-volume ratio might have been another influential factor in fluid flux within and out of the construct. The agarose used in the present thesis might have had higher pore-to-volume ratio than their 85% porous polyurethane and possibly have better facilitated the interstitial fluid to be transferred out of the construct. It is also possible that the fluid within the agarose had experienced higher pressure which led to flux of fluid from its outer surface into the culture media. Another difference might be attributed to the stimulation technique or to parameters associated with sliding motions.

6.4.2.1 Layered/Sectional Analyses of Retained GAG and Collagen

Analysis of retained GAG in layers of samples in Study 2 revealed that GAG retention in top layer was significantly affected by both of the loading conditions. The GAG accumulation in top layer of samples in NL-NF group was higher than in CS-NF and CS-F groups. Top layer of samples in NL-NF loading condition had the highest normalized retained GAG compared with middle and bottom layers. This was perhaps due to high exposure of the top surface to fresh culture media and the higher sub-surface strain. Analysis of accumulated GAG in layers of samples in CS-F and CS-NF groups showed that none of these stimulations could localize GAG in a certain layer.

However, analysis of retained collagen in layers of samples in Study 2 showed that collagen localized differently in layers under different loading conditions. The hydromechanical stimulation caused significantly higher collagen in the top layer compared with the middle layer (considering values that were not normalized). Comparing the normalized retained collagen of layers under different loading conditions, it was found that both mechanical and hydromechanical stimulation localized most of the collagen in middle layer. In both CS-F and CS-NF groups, the accumulation of collagen in top and middle layers was significantly higher than the bottom layer.

Comparing GAG and collagen response, it was apparent that the loading conditions of Study 2 affected the GAG accumulation and not collagen accumulation in top layer of the constructs; and both stimulation techniques affected the localization of collagen in certain layers (top and middle), but could not influence the GAG localization.

In Study 3, no significant difference in retained GAG could be established due to loading in any of the top, middle or bottom layers and in any of the central and side sections. However, hydromechanically stimulated samples could accumulate significantly higher GAG in their top layers compared with middle and bottom layers (comparing values before normalization to wet

weight), with no difference in accumulation between central stimulated and side unstimulated sections.

The analysis of retained collagen in layers and sections of the samples used in Study 3 (similarly to GAG) revealed no significant difference due to loading in any of the top, middle or bottom layers or in any of the central and side sections. However, the top layer could accumulate significantly more collagen compared with middle and bottom layers in both mechanically and hydromechanically stimulated samples.

Comparing GAG and collagen response, it was apparent that loading condition of Study 3 affected none of the GAG or collagen accumulation in any of the layers of the constructs. It was found that both stimulation techniques affected the localization of collagen in certain layers (top and middle), but only hydromechanical stimulation could localize considerably higher GAG in top layer. No significant difference in either GAG or collagen accumulation was established between central stimulated and side unstimulated sections of constructs. This suggested that localized stimulation and therefore localized stress and strain might not be able to localize the protein accumulations as well, and side sections could be affected by the loads. Therefore, the idea of using the side sections as controls was rejected.

Each loading condition in Study 3 made a difference on the protein accumulation of the layers and confirmed the depth-dependent response. However, the retained GAG and collagen in each of the layers were insensitive to loading conditions. This might be was due to reduction of load, stimulation period per day, or number of stimulation times per week compared with Study 2.

6.4.3 Total GAG and Collagen Production

Total GAG or collagen production was calculated by summing the retained GAG or collagen within the construct and the GAG or collagen into the culture media during the stimulation period. Total GAG productions in both studies did not show statistically significant differences due to loading condition. However, total collagen production was significantly affected by loading condition in Study 2. Total collagen production of samples in the CS-F group (hydromechanically stimulated) was significantly higher than samples in CS-NF group (mechanically stimulated). Under different loading conditions, the considerable difference in total collagen production of the samples was affected by the substantial difference of released collagen and not any difference in the retained collagen. There was a high percentage of collagen release into the media in this study. In Study 3, no statistically significance differences were found when total collagen productions of samples in different loading conditions were compared.

6.5 Concluding Remarks

Many parameters are involved in each of our studies. Some of these parameters are related to stimulator and its surrounding environment, some of them are related to construct properties and some can be linked to contents of culture media. Each of these parameters plays a role in the final results of our experiments. For the stimulator itself, these parameters include indenter shape and geometry, contact area, the applied normal load, the acceleration/deceleration and velocity of construct motion (under indenter), the stimulation pattern, the stimulated area, the cycle time or frequency of reciprocating movement, the pump flow rate, the fluid film thickness, the stimulation time per day, number of stimulations per week and the overall length of stimulation. For the

chondrocyte-agarose constructs, these parameters include the macro-geometry, surface roughness, stiffness, pore size, pore-to volume ration, pore connectivity, cell density, cell distribution, cell source, source age and culture time of construct before stimulation. The parameters related to culture media include composition, the concentration of their ingredients, the presence of any serum or growth factor, the feed media per construct per day, the frequency of their change and the fluid rheology. Parameters associated with the surrounding environment (incubator) may also influence the results. These include temperature, pH, percentage of CO_2 , humidity and the presence of bacteria. Efforts were made to control these parameters during the experiments. Yet, even minor changes in these parameters might have led to major change in the final result, because the effects of small variations in these parameters might have accumulated.

The differences in results of the present studies and those of other similar studies (adopting sliding contact techniques) may be related to difference in initial setting of some of the above parameters (Table 6.1). The comparison reveals a considerable difference in cell density of the present thesis samples versus those of other studies. Despite the survival of cells and maintenance of their round shape throughout the experiments, the low initial cell density might have influenced the insensitivity of GAG (and sometimes collagen) production to loading conditions.

The unresponsiveness of GAG production to hydromechanical stimulation might be attributed to the presence of the fluid film that separated the contact surfaces. It might be that the perfusion associated with the pressurized fluid film promoted GAG/collagen production, but the reduction in friction associated with the presence of the fluid film might have discouraged GAG/collagen production. As a result, these two effects might have canceled each other out. Thus, a thinner or even a partial fluid film might provide better overall benefit.

Table 6.1 Approximate ranges of some parameters and significant findings in studies which adopted the sliding stimulation techniques.

Ref.	Construct material/cell density	Compression /Deformation	Duration /Intervals	Significant findings
Wimmer et al [45] [a]	Polyurethane 10 million cells/scaffold V= 0.201 ml ~ 49.7 million cells/ml	Dynamic compression at 0.1Hz and 5, 10 or 20% strain plus equal static offset strain and ball oscillation at 0.6Hz with ±60º amplitude	1 h/ time, 2 times/day, 3 days with free swelling in between the loading intervals	Increase of mRNA expression and release of superficial zone protein with respect to controls
Shahin et al [49]	PGA & PGA-alginate 20 and 40 million cells/ml	2.2% cyclic + 6.5% static compression; 0.05 Hz	10 min/day 2.5 weeks (shear direction changed after each 5 min)	Enhanced (on per cell basis) the synthesis of both GAG & collagen type II by up to 5.3- and 10-fold respectively; collagen type II as percentage of total collagen also increased due to stimulation 3.4-fold
Kaupp et al [50]	2% agarose; 10 million cells/ml; construct volume= 530 µL	constant compressive load of 10 mN on (with 3 mm Ø glass indenter tip) ; sinusoidal reciprocation with 3 mm amplitude (from centre of construct); 0.5, 1 and 2 Hz	between 5- 60 minutes for 3 consecutive days	Frequency-dependent response of gene expression to stimulation; 1 Hz resulted in maximum expression of PRG4 and collagen type II.
Grad et al [405] [b]	Polyurethane 5 million cells/scaffold D=8, h=4 mm ~ 24.87 million cells/ml	15% of scaffold height compression with or without sinusoidal ball oscillation between 10-20% scaffold height at 1Hz and rotation of ± 25º at 1Hz	1 h/day for 3 weeks	Both compression and oscillation over the surface made lowest friction coefficient compared with compression only and control groups.
Huang et al [372]	2% agarose 20 million cells/ml	20% of axial strain and sliding velocity of ± 2.5 mm/s (0.1 Hz) over ±12.5 mm	21 days preculture; sliding contact for 3 h/day, 5 days/week for 3 weeks	DNA (~ 1.2 % ww) content decreased, GAG (~ 1.6% ww) and collagen (~ 0.4% ww) contents increased compared with controls (~ 1.5%, 1%, and 0.3% respectively.)

Ref.	Construct material/cell density	Compression /Deformation	Duration /Intervals	Significant findings
Kock et al [373]	0.5% agarose between two layers of 3% cell free agarose 20 million cells/ml Construct size: Cylindrical disk Ø6 mm	4 days preculture; 10% strain in depth ; indenter moved back and forth each second, 1Hz	for 4 h/day, 5 days/week for 28 days	Depth-dependent response at gene-expression levels, with the highest response in the highest strains regions. Increased the collagen content; no influence on retained or released GAG
Study 2 of the present thesis	3% agarose 1.135 million cells/ml Ø 10 mm t = 5 mm	10 days preculture; Hydromechanical stimulation (CS-F): 45.1 mN (5.83 KPa) load + 12.2 ml/min flow rate+ bidirectional sliding motion on construct surface (0.25 Hz) + ~ 32 µm fluid film Mechanical stimulation (CS-NF): 45.1 mN load + bidirectional sliding motion (446 cycles/30 min)	0.25 Hz, 30 min/day, 5 days/week, 3 weeks	CS-F and CS-NF samples had higher collagen (normalized to wet weight) accumulation in top vs bottom layer and middle vs bottom layer; accumulative released collagen and total collagen production (both normalized and not normalized) of CS-F samples were higher than CS-NF ones.
Study 3 of the present thesis	3% agarose 2.66 million cells/ml	1 week preculture; 28.5 mN (3.68 KPa) + 12.2 ml/min flow rate + unidirectional sliding motion on construct surface (0.96 Hz) + ~ 53 µm fluid film Mechanical stimulation (CS-NF): 28.5 mN load + unidirectional sliding motion (861 cycles/15 min)	0.96 Hz, 15 min/day, 3 days/week, 3 weeks	No statistically significant differences due to loading; higher collagen (both normalized and not normalized data) accumulation in top vs middle and top vs bottom layer in all loading conditions; higher GAG in top vs middle and middle vs bottom layer.

1. Similar reference: [41]
2. [72], [42], [43]

Chapter 7

Conclusions and Future Directions

In the present thesis, a preliminary set of experiments and three main studies were completed. The preliminary experiments determined loads, speeds and the percentage agarose to be used in the constructs such that experiments could be run without destroying the construct. Study 1 imposed a stimulation regime and reported measurements of retained GAG. Study 2 was similar but also reported measurements of GAG released into the culture media and collagen both retained and released into the culture media. Furthermore, Study 2 cut the constructs into top, middle and bottom layers to examine the distribution of retained GAG and collagen. Study 3 had a different stimulation motion and cut the construct into more sections than in Study 2.

1) The designed simulator system successfully applied the desired range of stimulations for long period within incubator environment.
2) In the short-term pilot studies and preliminary experiment, it was found that 3% agarose was optimal for the type of performed stimulation.
3) The results of preliminary study, with bidirectional hydromechanical stimulation (30 min/day, 5 days/week for 2 weeks) on 3% chondrocyte-agarose constructs, suggested the use of loads less than 56 mN and flow rates less 17.6 ml/min for long-term experiments to avoid the detrimental effect on the constructs.

4) Study 1, started to establish some effects of mechanical loading on the amount of retained GAG in 2-week stimulation and a total of 21 days of culture, but only retained GAG was measured. In subsequent studies retained collagen along with released GAG and released collagen were measured.
5) In Study 2, the hydromechanical stimulation could make a significant difference in total collagen production of the chondrocyte-agarose constructs compared with just mechanical stimulation. This indicated that application of compression and cyclic frictional shear along with fluid flow perfusion resulted in an increase in total collagen compared with the cases when there was no fluid flow perfusion. This was mostly the contribution of released collagen into media as the total retained collagen showed no dependency on specific loading conditions. This showed that chondrocytes within agarose could sustain stress and strain from their surrounding environment and respond by producing more matrix proteins. The analyses on separate layers showed that retained collagen was mostly localized in the middle layer, then top layer and then bottom layer in all loading conditions of this study. A limitation of this study was that the culture media for all constructs in the unloaded condition were mixed and there was only one data representing the accumulated released GAG or released collagen. Therefore, a conclusion regarding the statistically significant differences caused by the two stimulation conditions (CS-F and CS-NF) compared with the unstimulated controls (NL-NF) could not be made.
6) In Study 2, the effect of loading on released GAG and total GAG could not be established. The hydromechanical stimulation reduced the GAG accumulation in top layer and decreased total retained GAG.

7) In Study 3, localization of collagen in top layer of the construct was more pronounced under hydromechanical stimulation.
8) In Study 3, localized stimulation in the central region of construct could not localize the protein accumulations.
9) In Study 3, reduction in applied load, stimulation time per day and number of stimulations per week caused the failure of the mechanical or hydromechanical stimulation to strongly affect total GAG or collagen.

7.1 Future Directions

The present thesis shows that the hydromechanical stimulator can provide an appropriate environment for chondrocytes seeded inside agarose hydrogel to encourage them to produce collagen. The next steps will address the optimization of loading, culturing time and duration of hydromechanical stimulation on the chondrocytes growth activities inside the agarose gel. The conducted experiments generated new questions and inspiration for future work.

Considering the novelty of stimulation technique and also the fact that loading combinations as this, has not been attempted by other researchers, there remain many investigations to better understand both the system and the effects of its loading on cell-seeded constructs. Some of the future work could involve:

1) Further characterization of localized loads in contact points of indenter and construct surface in both fluid flow and no fluid flow conditions.
2) Further experimental/theoretical investigation into fluid film thickness during the fluid flow condition.

3) More depiction of the dynamics of load distribution throughout the surface and depth of construct with current indenter using theoretical models.

4) Further understanding of dynamics of fluid flow distribution on the surface and penetration into the construct using the current hydrostatic indenter and culture media as fluid.

5) Further exploration of the effect of changing cell density in constructs on the protein production

6) Further investigation of the effect of loading on mechanical properties of construct and in layers of construct

7) Additional analysis to characterize the amount of lubricin to track superficial zone properties in top surface exposed to frictional shear.

8) Further analysis using the construct layers with less thickness to better resemble the zones of cartilage

9) The use of other biomaterials such as decellularized collagen to reinforce the agarose and seed the chondrocytes .into a construct that is more like articular cartilage.

10) Attempt to stimulate chondrocytes in natural articular cartilage and measure the effects on the production of GAG, collagen, lubricin, etc.

Appendix A

Studies Involved Mechanical Stimulations of Agarose-Chondrocyte Constructs

Table A.1. Common agarose types and concentration used.

Agarose Type	Agarose %	References
Type VII	2	[58], [71], [411]
Type VII	3	[80], [356, 357], [394], [413], [416- 418]
Type VII	4	[348]
Type IX (ultra-low gelling point)	4	[419]
Low melting	2.5	[62]
Low melting	2	[410]
Low melting	1	[406]
Low melting	2	[412]
Not defined	3	[389], [414], [353], [415]
Not defined	2	[408, 409]
Not defined	3.3	[369]

Table A.2. Common cell sources and the age of sources used.

Source	**Joint Location**	**Age**	**Reference**
Steer	Metacarpophalangeal (MCP)	18 month	[295], [394], [414]
Steer	(MCP)	18-30 month	[389]
Cow (bovine)	Metatarsophalangeal (MTP)	12–18 month	[80]
Cow (bovine)	MCP	Adult	[419], [413]
Cow (bovine)	MCP	Mature	[348]
Calf (bovine)	Femoral condyles of knee	1-2 week	[409]
Calf (bovine)	Femoral condyles of knee	2-3 week	[412]
Calf (bovine)	Glenohumeral	4-6 month	[71]
Calf (bovine)	Carpometacarpal (CMC)	4-6 month	[408]
Cattle (bovine)	CMC	2-4 week	[447]
Cattle (bovine)	MCP	18 month	[353], [357], [416]
Porcine	MCP	Unknown	[369]
Pig	Knee	3 month	[356]
Pig	MCP	12 month	[418]
Dog (canine)	Femoral condyle	2-4 years	[411]
Mouse	Ventral parts of the rib cages	Embryonic	[62]
Wistar rat	Knee and hip	Unknown	[415]
Chick	Tibiotarsus	15 days	[417]
Human	Osteoarthritic knee	Adult, 50-70 years old	[406]

Table A.3. Common shapes and sizes of agarose-chondrocyte samples in different studies. Dimensions in millimeter, volume in cube millimeter. W: width (mm), D: diameter (mm), L: length (mm), H: height (mm), V: volume (mm^3).

Shape	W	D/ L	H	V	References
Cylindrical		4	--	-	[411]
		4	1.6	20.106	[412]
		4	2.34	29.405	[447]
		4	5	62.832	[348]
		5	2.3	45.160	[408]
		5	5	98.175	[295], [357], [394], [416]
		6.76	1.7	61.014	[58]
		8	1.5	75.398	[71]
		8	8	402.124	[415]
		10	1	78.540	[414]
		10	3	235.619	[369], [356]
		13	3	398.197	[62]
		13	--	--	[410]
Rectangular	4	4	1.6	25.6	[409]
	5	5	5	125	[389], [413], [419]
	12	9	6	648	[417]
Ring		OD= 6, ID= 3	--	--	[406]

Table A.4. Some of the cell densities (million cells/ml) used.

Cells Density	Reference
1.25	[439]
2	[62], [80], [410]
2.5	[439]
3	[369]
4	[295], [416], [418], [357]
5	[439]
6	[356]
10	[419], [413], [389], [414], [415], [439]
15	[71]
20	[439]
15-30	[409]
30	[408], [411], [447]
40	[439]

Table A.5. Different types of loadings used.

Loading Type on Agarose-chondrocytes	Reference
Dynamic compressive (DC) loading	[58], [296], [299], [351], [363], [394], [448-450], [440]
Hydrostatic pressure	[80], [451]
Compression + Hydrostatic pressure	[348]
Fluid Perfusion	[452]
Rotating wall bioreactor (dynamic culturing)	[282]

Table A. 6. Loading characteristics in previous studies; SC: static compression, DC: dynamic compression, IC: intermittent compression, HP: hydrostatic pressure, I: intermittent.

Load Type	**Load/Strain**	**Frequency**	**Loading intervals/times**	**Reference**
SC	20% per minute		30 min	[419]
SC	5 MPa			[348]
DC	15%	1 Hz	48 h	[345]
DC	15%	0.3, 1, 3 Hz	48 h	[394]
DC	15%	1 Hz	10 min, 1.5 h, 6 h, 15 h, 48 h comp	[418]
DC	0-10%	1 Hz, trapezoidal wave form	10 min	[413]
DC	0-15 %	1 Hz sinusoidal	60, 120, 360 min	[357]
DC	0.5 %	0.01 -5 Hz		[71]
DC	2.5% Dyn + 7% Stat.	1 Hz	24 h	[412]
DC	1% Dyn + 10 % Stat	0.1, 0.5, 1 Hz	--	[411]
DC	5%, 10%, 15 %	0.5, 1, 3 Hz	24 h	[415]
DC	10%	1 Hz	3 times, 1h on, 1 h off, 5 days/week	[58]
IC	0-5MPa	1 Hz	2 h	[348]
IC	20 kPa	0.33 Hz	2 sec on, 1 sec off, 30 min	[62]
IC	30 kPa	0.2 Hz	30 min	[62]
Static HP	5 MPa		4 h	[80], [451]
Pulsatile HP	5 MPa	1 Hz, sinusoidal	4h	[80],[451]
I Perfusion	0.5 ml/min		1 h/day , 10 min flow, 50 min rest, 21 days	[369]

Table A.7 Common analysis on the agarose-chondrocytes used.

Measurements/Analysis	Method	Reference
Cell viability	Stain 0.8 mm from sample center with trypan blue	[394]
	Using light microscopy after trypan blue staining	[80]
	Using a florescence dye kit (LIVE/DEAD Viability/Cytotoxicity Kit	[443]
	Using a Calcein AM (green) and ethidiumhomodimer (red) fluorometric staining kit	[369]
Cell content/number	Using DNA content: 8 pg DNA per chondrocyte	[443]
	By quantification of DNA content from aliquots of papain digests of the hydrogels using the ds-DNA Quantitations Kit	[369]
Total sulfated GAG	A colorimetric reaction using method of Farndale et al (1986)	[443], [417]
	Using DMMB assay	[58], [408], [414], [409], [369], [71], [356]
Total collagen content	Using a colorimetric procedure adapted for use with a microtiter plate reader	[58]
	Using OHP content (conversion of 1:10 ratio of OHP)	[408]
Type VI collagen distribution	Using confocal microscopy	[409]
Total DNA content	Hoescht 33258 method	[345], [414], [409], [416], [417]
	According to Hoemann et al. (2002); 5-125 ng of calf thymus DNA was used as standard	[443]
	Using the quantitative ds-DNA Quantitations Kit	[356]
PG	6 µm sections were stained for PG with 0.2% (w/v) Safranin-O and counterstained with 0.04 % (w/v) Fast Green FCF and Weigert iron hematoxylin.	[453]
	Using Alcian blue precipitation method	[345]
Hydroxyproline content of insoluable collagen	By a modified method of Stegemann by Urban and McMullin (1985)	[394]
Incorporation of $^{35}SO_4$	Using Alcian blue precipitation method	[416]
Cell deformation	Using bright field microscopy	[413]
Calcium (Ca^{2+} signaling behaviors)	Using UltraView software (Perkin Elmer) associated with the confocal system.	[413]
Intercellular displacement	Using digital image correlation	[348]
Histological analysis	Fixing samples and using hematoxylin stain	[414]
	Alcian blue stain to verify PG accumulation	[369]
	Fixing samples and using toluidine blue stain, sections photographed by phase-contrast microscope	[71]

Appendix B

Technical Specifications of Some Components of the System

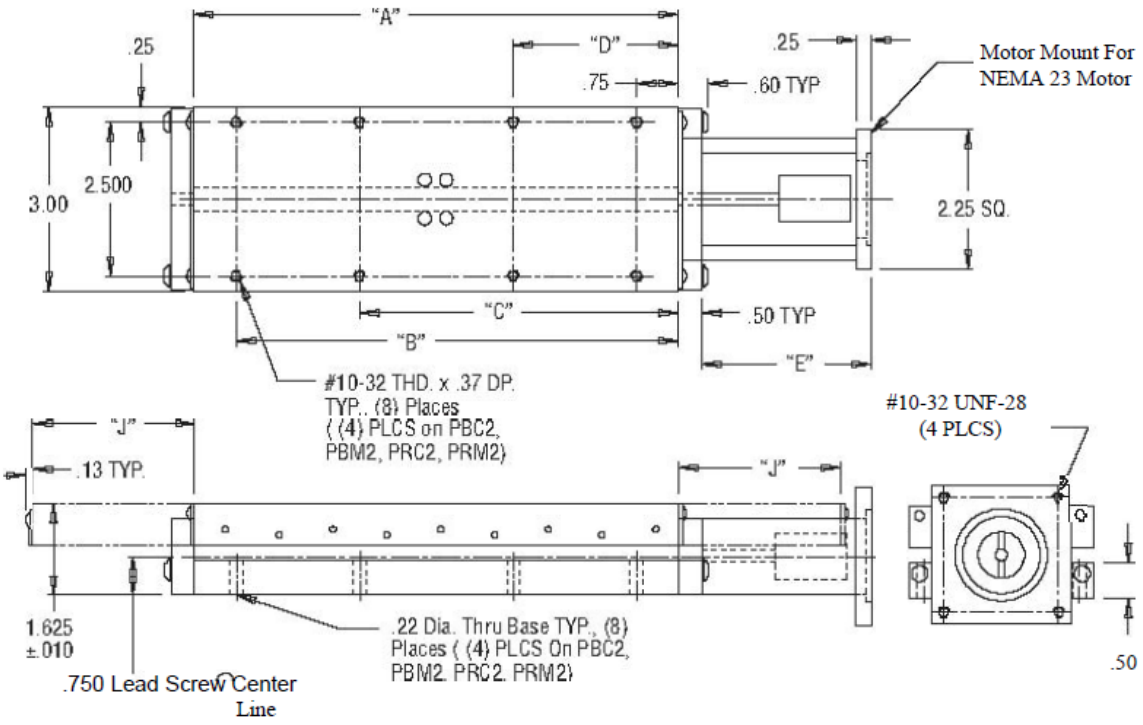

A	B	C	D	E	F	G	H	I	J	Part Number
4.00	N/A	3.25	0.75	2.00	2.75	0.75	3.25	N/A	1.00	**PB 2 / PR 2**

Figure B.1 Drawing of PCR2 crossed roller positioning stage (all dimensions in inch 1 in = 25.4 mm) [391].

Table B.1 Specifications of PCR2 crossed roller positioning stage [391].

Characteristics	**Measures**
Slide type	Crossed roller slide
Mount	NEMA 23 mount
Travel	50.8 mm (2 in)
Overall length	177.8 mm (7 in)
Screw thread	3/8-10 Acme
Advance	0.8085 mm/rad (0.200 in/rev)
Maximum load (carriage at full travel position)	680.6 N (153 lbs)
Maximum load (carriage centered on base)	1067.6 N (240 lbs)
Maximum moments (load centered on carriage top), roll axis, X	27.79 Nm (246 lbs-in)
Maximum moments (load centered on carriage top), pitch axis, Y	14.24 Nm (126 lbs-in)
Maximum moments (load centered on carriage top), yaw axis, Z	7.12 Nm (63 lbs-in)
Flatness (no load)	± 0.0002 m/m
Straightness	± 0.0002 m/m
Repeatability	within 0.010 mm (0.0004 in)
Positional accuracy	± 0.0006 m/m
Break-a way torque	0.071 – 0.106 Nm (10-15 oz-in)

Table B.2: Specifications of SiNet™ Hub [392].

Power	Power is provided by Si™ indexer-drive on Port 1 Provides up to 50 mA for MMI via PC/MMI port
Communication	Ports 1 - 4: RS232, 9600 bps, 8 data bits, one stop bit, no parity. MMI: same. PC when running SiNet Programmer software: 19200 bps. Max cable length, any port: 50 feet.
Physical	Constructed on .062″ fiberglass printed circuit board with 4 .156″ mounting holes (nylon spacers included). 4.2″ x 2.85″ x 0.72″. Two red LEDs. Operating temperature range: 0 - 70° C. Optional DIN rail mounting kit (fits ENS0022 35 mm rail).
Program	Move distances: +/- 16,000,000 steps Move speeds: .025 to 50 (rev / s) Accel/Decel range: 1 to 3000 (rev / s^2) Time delays: .01 to 300 seconds Loop counts: 1 to 65,535 Number of nested loops: unlimited Number of subroutines: unlimited Maximum size of messages displayed by an MMI Prompt: 60 characters (80 for an MMI Menu instruction) Maximum total size of all MMI Prompt messages: 1500 characters Steps/rev: 2,000 - 50,800 (200-50,800 with Si-100 indexer)
Connectors	RJ11 for drives and PC/MMI. Screw terminals for programmable inputs and outputs. Accept AWG 16-28 wire
Programmable Inputs	Optically isolated, 2200 ohms internal impedance, 5–24 VDC
Programmable Outputs	Optically isolated (photo darlington), 28 VDC max, 100 mA max.

Table B.3: Specifications of 1240i stepper motor drive [392].

Characteristics	**Measure**
DC bus voltage	12-42 VDC motor supply (including ripple)
Software selectable motor current	0.2 - 1.2 amps/phase
Software selectable Step resolutions	2,000 - 50,800 steps per revolution
Software selectable idle current reduction	0%, 25%, 50% or 100%
Communication	via RS232 or optional RS485
Usable power	48 watts

Table B.4: Specifications of single output 24V power supply [393].

	Characteristics	**Measure**
Output	DC voltage	24 V
	Rated current	13A
	Current range	0 ~ 13 A
	Rated power	312 W
	Ripple & noise (max)	150 m Vp-p
	Voltage Adj. range	20 ~ 26.4 V
	Voltage tolerance	± 1.0 %
	Line regulation	± 0.2 %
	Load regulation	± 0.5 %
	Set up, rise time	800ms, 50ms/230 VA, 2500 ms, 50 ms/115 VAC at full load
	Hold time	16 ms/230 VAC, 16 ms/115VAC at full load
Input	Voltage range	88 ~ 264 VAC and 124 ~ 370 VDC
	Frequency range	47 ~ 63 Hz
	Power factor	PF > 0.95/230VAC, PF>0.98/115VAC at full load
	Efficiency	87%
	AC current 115 VAC	5A
	AC current 230 VAC	2.5 A
	Inrush current	20A/115VAC 40A/230VAC
	Leakage current	< 1mA / 240VAC
Protection	Over load	105 ~ 135% rated output power. Protection type: Hiccup mode.
	Over voltage	27.6 ~ 32.4V
	Over temperature	80 ºC ± 5 ºC
Environment	Working temperature	-20 ~ +65 ºC
	Working humidity	20 ~ 90 % RH non-condensing
	Storage temp., humidity	-40 ~ +85 ºC, 10 ~ 95% RH
	Temp. coefficient	± 0.03% /ºC (0 ~ 50 ºC)
	Vibration	10 ~ 500 Hz, 2 G 10 min./ 1 cycle, 60 min

Table B.5 Specifications of 1240i motor drive [392].

Characteristics	**Measure**
DC bus voltage	12-42 VDC motor supply
Software selectable motor current	0.2 - 1.2 amps/phase
Software selectable Step resolutions	2,000-50,800 steps per revolution
Software selectable idle current reduction	0%, 25%, 50% or 100%
Communication	via RS232 or optional RS485
Usable power	48 watts

Appendix C

Programming Stepper Motor Drives with SiNet Hub Programmer Software

Select the drive models to use for each axis in "Configure Drive" window: both drives are 1240i

Named the axis: X and Y

Specified the amount of steps/rev: 20,000

Specified the motor current: entered the running current of motor

Specified the motor limits (employed limit sensor so that the loads do not travel beyond its intended limits to cause any damage), selected "all axes same" and limits switched are "Closed". Closed means that the limit switch or sensor is closed at the end of travel limit and is normally open.

Specified the units, selected "all axes same", and named the unit: "*rev*", 20000 rev/unit

In the main programming window, the following lines were entered:

1. Prompt MMI: wait for MMI to enter: Choose: "Display text and wait for Enter," enter "Please Enter to Move," in the phrase box.

   Note: MMI is Man Machine Interface or an operator panel

2. Feed to length: distance: 0.75 (*rev*) (= 0.15 *inch*), Speed: 10 (rev / s), Accel/ Decel = 10 (rev / s^2) sec, Axis : Y, CW

   Note: Feed to length is a function used for point to point movement; which receives inputs such as distance, motor speed, acceleration and deceleration and drive direction of rotation.

3. **Y:** Wait for input 1, falling edge

   Note: The program needs to wait for input to happen before it goes into motion. We need to tell the hub programmer which input the sensor is wired to and what input condition to look for. In "falling edge" mode, the hub waits for input voltage to go high, then low.

4. Feed to length: distance: 0.25 (*rev*) (= 0.05 *inch*), Speed: 10 (*rev* / *s*), , Accel/ Decel = 10 (*rev* / s^2), Axis : X, CW
5. **X:** Wait for input 2, falling edge
6. Feed to length: distance: 0.75 (*rev*) (= 0.15 *inch*), Speed: 10 (*rev* / *s*), Accel/ Decel = 10 (*rev* / s^2), Axis : Y, CCW
7. **Y:** Wait for input 1, falling edge
8. Feed to length: distance: 0.25 (*rev*) (= 0.05 *inch*), Speed: 10 (*rev* / *s*), Accel/ Decel = 10 (*rev* / s^2), Axis : X, CW
9. **X:** Wait for input 2, falling edge
10. Feed to length: distance: 0.75 (*rev*) (= 0.15 *inch*), Speed: 10 (*rev* / *s*), Accel/ Decel = 10 (*rev* / s^2), Axis : Y, CW
11. **Y:** Wait for input 1, falling edge
12. Feed to length: distance: 0.25 (*rev*) (= 0.05 *inch*), Speed: 10 (*rev* / *s*), , Accel/ Decel = 10 (*rev* / s^2), Axis : X, CW
13. **X:** Wait for input 2, falling edge
14. Feed to length: distance: 0.75 (*rev*) (= 0.15 *inch*), Speed: 10 (*rev* / *s*), Accel/ Decel = 10 (*rev* / s^2) , Axis : Y, CCW
15. **Y:** Wait for input 1, falling edge
16. Feed to length: distance: 0.75 (*rev*) (= 0.15 *inch*), Speed: 10 (*rev* / *s*), Accel/ Decel = 10 (*rev* / s^2), Axis : X, CCW

Appendix D

Cell Counting with Hemocytometer

A cover slip was placed over the counting chambers. Then, about 10 µl of the mixture of trypan blue and cell suspension was inserted into each chamber of the hemocytometer using a micropipette and tip. The cells inside the mixture in the chambers were viewed under the microscope. The number of cells overlaying four of the one millimetre squared areas was counted. The viable cell concentration in the suspension was determined according to the formula given by the hemocytometer supplier:

$$(\text{Viable cells counted in } 4 \text{ mm}^2 \times 10^4) / 8 = \text{Viable cells/ml}$$

Appendix E

Estimated Cycle Times and Maximum Speeds by SiNet Program

Over the wide range of accelerations /decelerations of 50.8 – 2540 mm/s^2, the traveling time and maximum speed on each line (short line: 1.57 mm and long line: 4.72 mm) are reported. The calculated cycle time for bidirectional stimulation pattern (3 short lines + 5 long lines) are also reported in Table E. 1. After selecting the experimental settings for travelling distances of construct in X or Y direction over the simulation pattern, the travelling time and maximum speed on each line (short line: ~ 1.27 mm and long line: ~ 3.81 mm) were measured. These results along with the calculated cycle times are reported in Table E.2.

Table E.1 Estimated traveling time, maximum speed and cycle time (50.8 - 2540 mm/s^2).

	Short line = 1.5748 (mm)		Long line = 4.7244 (mm)		Cycle time (s)
Accel/Decel (mm/s^2)	Time (s)	Max Speed (mm/s)	Time (s)	Max Speed (mm/s)	Time/cycle (s)
50.8	0.352	8.9444	0.608	15.4518	4.096
101.6	0.249	12.6492	0.43	21.8521	2.897
152.4	0.203	15.4920	0.351	26.7635	2.364
203.2	0.176	17.8887	0.304	30.9037	2.048
254	0.157	20.0000	0.272	34.5516	1.831
508	0.111	28.2844	0.192	48.8630	1.293
1016	0.079	39.9999	0.136	69.1027	0.917
1524	0.064	48.9900	0.111	84.6333	0.747
2032	0.056	56.5683	0.096	97.7265	0.648
2540	0.05	63.2455	0.086	109.2611	0.58

In bidirectional stimulation pattern, the travelled distance was (4.064 mm) in either X or Y direction. When the speed was set at 55.88 mm/s and acceleration/deceleration at 71.12 mm/s^2 within SiNet program, the estimated cycle time was 0.956 s and the peak speed was 17 mm/s at 2.032 mm. The measured cycle time was 1.045 s on average with about 0.089 s difference with the estimated time for each cycle of motion path with bidirectional pattern.

Table E.2 Estimated traveling time, maximum speed and cycle time (5.08- 325.12 mm/s^2).

Short line: ~ 1.27 (mm)			Long line: ~ 3.81 (mm)		
Accel/Decel (mm/s^2)	Time (s)	Max Speed (mm/s)	Time (s)	Max Speed (mm/s)	Time/ Cycle (s)
1	1	2.5400	1.732	4.3993	11.66
2	0.707	3.5921	1.225	6.2215	8.246
4	0.5	5.0800	0.866	8.7991	5.83
6	0.408	6.2215	0.707	10.7762	4.759
8	0.354	7.1841	0.612	12.4435	4.122
10	0.316	8.0320	0.548	13.9121	3.688
12	0.289	8.7991	0.5	15.2400	3.367
14	0.267	9.5037	0.463	16.4612	3.116
16	0.25	10.1600	0.433	17.5976	2.915
18	0.236	10.7762	0.408	18.6649	2.748
20	0.224	11.3594	0.387	19.6748	2.607
22	0.213	11.9136	0.369	20.6350	2.484
24	0.204	12.4435	0.354	21.5524	2.382
26	0.196	12.9515	0.34	22.4328	2.288
28	0.189	13.4407	0.327	23.2796	2.202
30	0.183	13.9121	0.316	24.0965	2.129
32	0.177	14.3683	0.306	24.8869	2.061
34	0.171	14.8107	0.297	25.6530	1.998
36	0.167	15.2400	0.289	26.3967	1.946
38	0.162	15.6576	0.281	27.1196	1.891
40	0.158	16.0645	0.274	27.8242	1.844
42	0.154	16.4612	0.267	28.5115	1.797
44	0.151	16.8483	0.261	29.1826	1.758
46	0.147	17.2273	0.255	29.8384	1.716
48	0.144	17.5976	0.25	30.4800	1.682
50	0.141	17.9603	0.245	31.1084	1.648
52	0.139	18.3164	0.24	31.7246	1.617
54	0.136	18.6649	0.236	32.3291	1.588
56	0.134	19.0078	0.231	32.9220	1.557
58	0.131	19.3441	0.227	33.5051	1.528
60	0.129	19.6748	0.224	34.0777	1.507
62	0.127	20.0000	0.22	34.6410	1.481
64	0.125	20.3200	0.217	35.1953	1.46

Measured Cycle Time for Bi/Unidirectional Pattern in Specific Accelerations

The cycle times were measured as explained in Section 4.1.4. The 200 cycles were completed in 807.00 ± 0.71 s (average ± standard deviation). Therefore, it took about 4.0350 ± 0.0035 s for bidirectional stimulation pattern (including five 3.81 mm and three 1.27 mm travelling lines when acceleration/deceleration was 50.8 mm/s^2 to complete a cycle and return to the starting point.

For the higher acceleration/deceleration and for different speeds of bidirectional pattern (1.57 mm and 4.72 mm lines), the cycle times were also measured. Both the estimated and the measured cycle times for acceleration/deceleration in the range of 508-2540 mm/s^2 were determined. In this range, there was difference of about 0.4210 ± 0.0092 s (average ± standard deviation) between the estimated and measured cycle times.

Table E.3 Cycle time in different speeds and accelerations/decelerations.

Speed (mm/s)	Accel/Decel (mm/s^2)	Average cycle time (s)	n
127	508	1.723 ± 0.0058	3
203.2	508	1.72 ± 0.00	3
254	508	1.72 ± 0.00	3
254	1016	1.325 ± 0.0071	2
254	1524	1.165 ± 0.0071	2
254	2032	1.08 ± 0.00	2
254	2540	1 ± 0.00	2

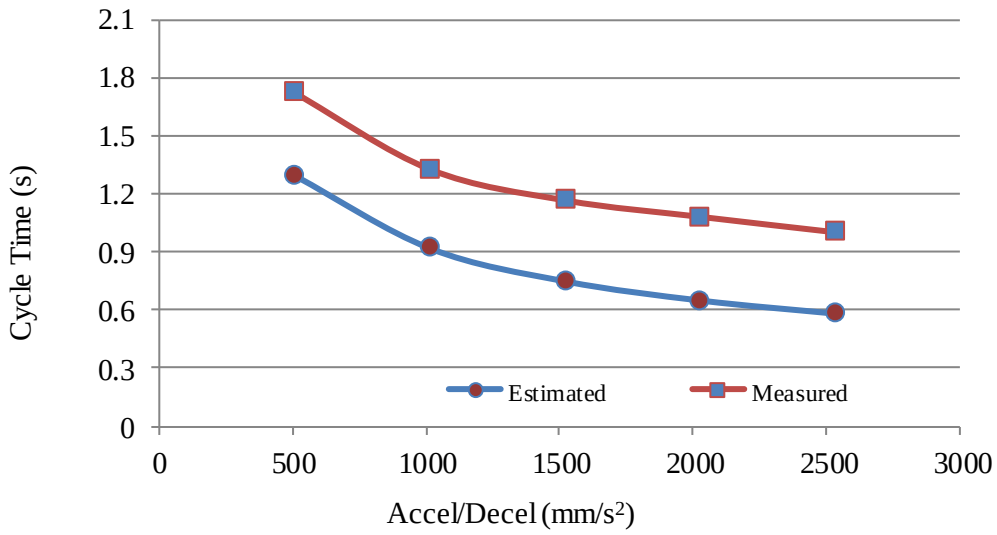

Figure E.1 Estimated vs measured cycle times at various acceleration/deceleration.

Appendix F

Multichannel Pump Calibration

The amount of flow rates of different channels are shown in Figure F.1 and Figure F.2.

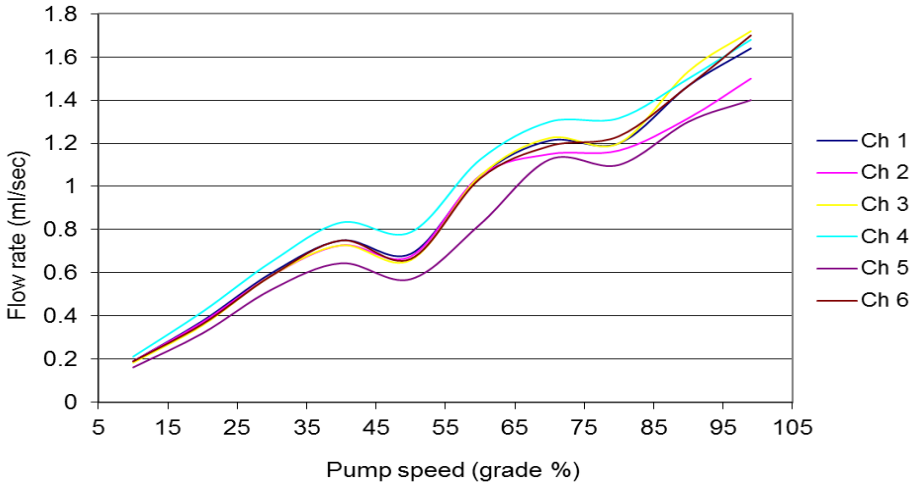

Figure F.1 Flow rate (ml/s) vs speed (%) of multichannel pump (1- 99% speed)**.**

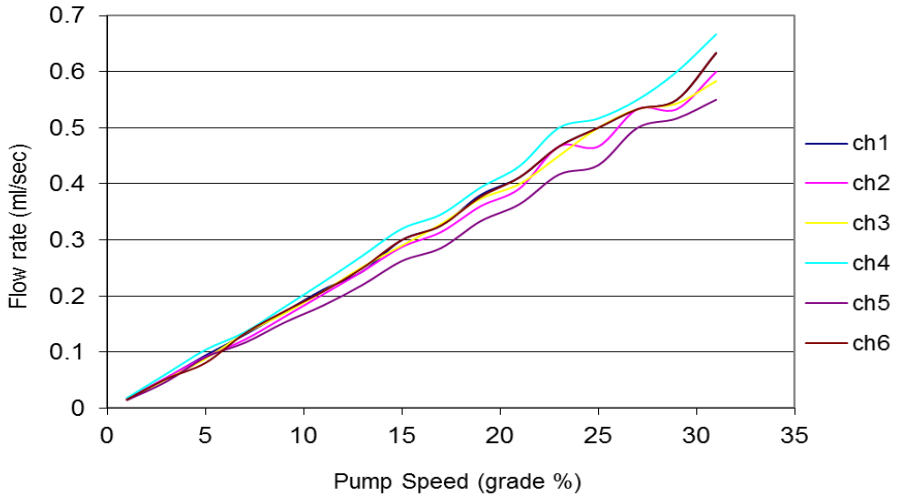

FigureF.2 Flow rate (ml/s) vs speed (%) of multichannel pump (1- 31% speed).

Appendix G

Strain Estimation

$\sigma = \varepsilon . E$

$P/A = \varepsilon . E$

$mg/A = \varepsilon . E$

$m = (A/g). \varepsilon . E$ The mass estimated from strain, E and A

Geometry of indenter tip

R (m)	***R. (m)***	***R² (m²)***	***R.² (m²)***	***A (m²)***
0.00178	*0.00084*	*3.1684E-06*	*7.056E-07*	*7.73711E-06*

Effective contact area of indenter tip (Figure .3.6).

$A = \pi (R^2 - R_0^2) \times 10^{-6}\ m^2$

$R = 1.78\ mm, R_0 = 0.84\ mm,\ g = 9.81\ m^2/s$

$A = 7.737114387 \times 10^{-6}\ m^2$

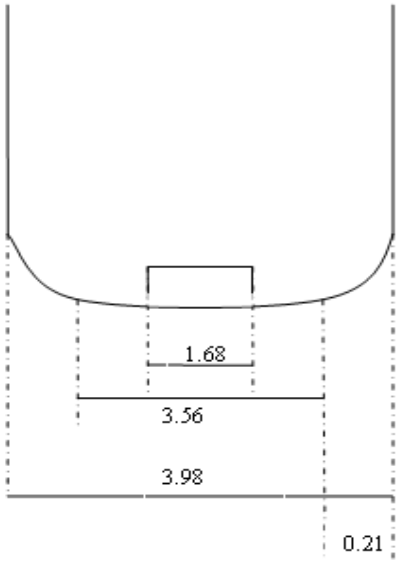

Table G.1 Dead mass estimation. Dynamic and equilibrium modulus data are adopted from study by Buckley et al [281] for three different concentrations of agarose.

	Pretest Temp. - Test Temp.	37ºC - 37ºC	37ºC- 37ºC	37ºC- 37ºC
	Agarose	2%	4%	6%
	Dynamic Modulus >	**28 kPa**	**90 kPa**	**160 kPa**
Strain		Mass [g] estimated from stress, strain & E		
5%	0.05	1.104	3.549	6.309
10%	0.1	2.208	7.098	12.619
15%	0.15	3.312	10.647	18.929
20%	0.2	4.417	14.196	25.238
25%	0.25	5.521	17.746	31.5479
30%	0.3	6.625	21.295	37.857
	Equilibrium Modulus >	**10 kPa**	**33 kPa**	**70 kPa**
Strain		Mass [g] estimated from stress, strain & E		
5%	0.05	0.3943	1.3013	2.7604
10%	0.1	0.7887	2.6027	5.5209
15%	0.15	1.1830	3.9040	8.2813
20%	0.2	1.5774	5.2054	11.0417
25%	0.25	1.9717	6.5067	13.8021
30%	0.3	2.3661	7.8081	16.5626

References

1. van Donkelaar CC, Schulz RM. Review on Patents for Mechanical Stimulation of Articular Cartilage Tissue Engineering. Recent Patents on Biomedical Engineering 2008; 1:1-12.

2. Cohen NP, Foster RJ, Mow VC. Composition and dynamics of articular cartilage: structure, function, and maintaining healthy state. J Orthop Sports Phys Ther 1998; 28: 203-215.

3. Williams GM, Klisch SM, Sah RL. Bioengineering cartilage growth, maturation, and form. Pediatr Res 2008; 63:527-534.

4. Eleswarapu SV. Multiscale Strategies for Cartilage Repair. ProQuest Dissertations and Theses 2011.

5. Coburn JM. Multi-targeted therapeutics for cartilage regeneration. ProQuest Dissertations and Theses 2012.

6. Johnstone B, Alini M, Cucchiarini M, Dodge GR, Eglin D, Guilak F, et al. Tissue engineering for articular cartilage repair--the state of the art. European cells & materials 2013;25:248-267.

7. Tuan RS, Chen AF, Klatt BA. Cartilage regeneration. J Am Acad Orthop Surg 2013; 21:303-311.

8. Kock L, Donkelaar CC, Ito K. Tissue engineering of functional articular cartilage: the current status. Cell Tissue Res 2012; 347:613-627.

9. Anderer U, Libera J. In vitro engineering of human autogenous cartilage. J Bone Miner Res 2002; 17:1420-1429.

10. Ingber D, Mow VC, Butler D, Niklason L, Huard J, Mao J, et al. Tissue Engineering and Developmental Biology: Going Biomimetic. Tissue Eng 2006; 12:3265-3284.

11. Lima EG, Mauck RL, Han SH, Park S, Ng KW, Ateshian GA, et al. Functional tissue engineering of chondral and osteochondral constructs. Biorheology 2004; 41:577-590.

12. Lu HH, Subramony SD, Boushell MK, Zhang X. Tissue Engineering Strategies for the Regeneration of Orthopedic Interfaces. Ann Biomed Eng 2010; 38:2142-2154.

13. Bock G, Goode J. Tissue engineering of cartilage and bone. Chichester, West Sussex ; Hoboken, NJ: J. Wiley, 2003.

14. Vinatier C, Guicheux J, Daculsi G, Layrolle P, Weiss P. Cartilage and bone tissue engineering using hydrogels. Biomed Mater Eng 2006; 16:S107-13.

15. Kim HW, Han CD. An overview of cartilage tissue engineering. Yonsei Med J 2000; 41:766-773.

16. Chung C, Burdick JA. Engineering cartilage tissue. Adv Drug Deliv Rev 2008; 60:243-262.

17. Freed LE, Guilak F, Guo XE, Gray ML, Tranquillo R, Holmes JW, et al. Advanced tools for tissue engineering: scaffolds, bioreactors, and signaling. Tissue Eng 2006; 12:3285-3305.

18. Mow VC, Wang CC. Some bioengineering considerations for tissue engineering of articular cartilage. Clin Orthop Relat Res 1999 ;(367 Suppl):S204-23.

19. Guilak F. Mechanobiology of Cartilage. 13th Institute of Biological Engineering Meeting (IBE 2008) 2008.

20. Guilak F, Jones WR, Ting-Beall HP, Lee GM. The deformation behavior and mechanical properties of chondrocytes in articular cartilage. Osteoarthritis Cartilage 1999; 7:59-70.

21. Guilak F. The deformation behavior and viscoelastic properties of chondrocytes in articular cartilage. Biorheology 2000; 37:27-44.
22. Griffin TM, Guilak F. The role of mechanical loading in the onset and progression of osteoarthritis. Exerc Sport Sci Rev 2005; 33:195-200.
23. Arokoski JP, Jurvelin JS, Vaatainen U, Helminen HJ. Normal and pathological adaptations of articular cartilage to joint loading. Scand J Med Sci Sports 2000; 10:186-198.
24. Nguyen QT. Mechanobiology and biomechanics of articular cartilage repair. ProQuest Dissertations and Theses 2012.
25. Rolfe R, Roddy K, Murphy P. Mechanical regulation of skeletal development. Current osteoporosis reports 2013;11:107-116.
26. Bader DL, Salter DM, Chowdhury TT. Biomechanical influence of cartilage homeostasis in health and disease. Arthritis 2011; 2011:979032.
27. Responte DJ, Lee JK, Hu JC, Athanasiou KA. Biomechanics-driven chondrogenesis: from embryo to adult. FASEB journal : official publication of the Federation of American Societies for Experimental Biology 2012;26:3614-3624.
28. Akimoto T, Kawanishi M, Ushida T. Mechanical stress and tissue engineering. Clin Calcium 2008; 18:1313-1320.
29. Estes BT, Gimble JM, Guilak F. Mechanical signals as regulators of stem cell fate. Curr Top Dev Biol 2004;60:91-126.
30. Choi JB, Youn I, Cao L, Leddy HA, Gilchrist CL, Setton LA, et al. Zonal changes in the three-dimensional morphology of the chondron under compression: the relationship among cellular, pericellular, and extracellular deformation in articular cartilage. J Biomech 2007; 40:2596-2603.
31. Guilak F, Fermor B, Keefe FJ, Kraus VB, Olson SA, Pisetsky DS, et al. The role of biomechanics and inflammation in cartilage injury and repair. Clin Orthop 2004:17-26.
32. Guilak F, Erickson GR, Ting-Beall HP. The effects of osmotic stress on the viscoelastic and physical properties of articular chondrocytes. Biophys J 2002; 82:720-727.
33. Butler DL, Goldstein SA, Guldberg RE, Guo XE, Kamm R, Laurencin CT, et al. The impact of biomechanics in tissue engineering and regenerative medicine. Tissue engineering.Part B, Reviews 2009; 15:477-484.
34. Mow VC, Ateshian GA, Spilker RL. Biomechanics of diarthrodial joints: a review of twenty years of progress. J Biomech Eng 1993; 115:460-467.
35. Mow VC, Holmes MH, Lai WM. Fluid transport and mechanical properties of articular cartilage: a review. J Biomech 1984; 17:377-394.
36. Myers ER, Mow VC. Biomechanics of cartilage and its response to biomechanical stimuli. : ACADEMIC PRESS, NEW YORK, NY (USA), 1983.
37. Han E. Tissue engineering of cartilaginous grafts with mechanically functional aggrecan. ProQuest Dissertations and Theses 2011.

38. Hung CT, Mauck RL, Wang C, Lima EG, Ateshian GA. A Paradigm for Functional Tissue Engineering of Articular Cartilage via Applied Physiologic Deformational Loading. Ann Biomed Eng 2004;32:35-49.
39. Guilak F. Functional tissue engineering. New York: Springer, 2003.
40. Guilak F. Functional tissue engineering: the role of biomechanics in reparative medicine. Ann N Y Acad Sci 2002; 961:193-195.
41. Wimmer MA, Grad S, Kaup T, Hanni M, Schneider E, Gogolewski S, et al. Tribology approach to the engineering and study of articular cartilage. Tissue Eng 2004; 10:1436-1445.
42. Grad S, Lee CR, Wimmer MA, Alini M. Chondrocyte gene expression under applied surface motion. Biorheology 2006; 43:259-269.
43. Grad S, Gogolewski S, Alini M, Wimmer MA. Effects of simple and complex motion patterns on gene expression of chondrocytes seeded in 3D scaffolds. Tissue Eng 2006;12:3171-3179.
44. Waldman SD, Couto DC, Grynpas MD, Pilliar RM, Kandel RA. Multi-axial mechanical stimulation of tissue engineered cartilage: review. Eur Cell Mater 2007;13:66-73; discussion 73-4.
45. Wimmer MA, Alini M, Grad S. The effect of sliding velocity on chondrocytes activity in 3D scaffolds. J Biomech 2009;42:424-429.
46. Schätti O, Grad S, Goldhahn J, Salzmann G, Li Z, Alini M, et al. A combination of shear and dynamic compression leads to mechanically induced chondrogenesis of human mesenchymal stem cells. European cells & materials 2011; 22:214-225.
47. Tran SC, Cooley AJ, Elder SH. Effect of a mechanical stimulation bioreactor on tissue engineered, scaffold-free cartilage. Biotechnol Bioeng 2011; 108:1421-1429.
48. Pingguan-Murphy B, Nawi I. Upregulation of matrix synthesis in chondrocyte-seeded agarose following sustained bi-axial cyclic loading. Clinics (São Paulo, Brazil) 2012; 67:939-944.
49. Shahin K, Doran PM. Tissue engineering of cartilage using a mechanobioreactor exerting simultaneous mechanical shear and compression to simulate the rolling action of articular joints. Biotechnol Bioeng 2012;109:1060-1073.
50. Kaupp JA, Weber JF, Waldman SD. Mechanical stimulation of chondrocyte-agarose hydrogels. Journal of visualized experiments: JoVE 2012:e4229.
51. Spitters TWGM, Leijten JCH, Deus FD, Costa IBF, van Apeldoorn AA, van Blitterswijk CA, et al. A dual flow bioreactor with controlled mechanical stimulation for cartilage tissue engineering. Tissue engineering.Part C, Methods 2013; 19:774-783.
52. Brady MA, Vaze R, Amin HD, Overby DR, Ethier C. The Design and Development of a High-Throughput Magneto-Mechanostimulation Device for Cartilage Tissue Engineering. Tissue Engineering, Part C: Methods 2014; 20:149-159.
53. Parkkinen JJ, Lammi MJ, Helminen HJ, Tammi M. Local stimulation of proteoglycan synthesis in articular cartilage explants by dynamic compression in vitro. J Orthop Res 1992; 10:610-620.

54. Buschmann MD. Chondrocytes in agarose culture: Development of a mechanically functional matrix, biosynthetic response to compression, and molecular model of the modulus. ProQuest Dissertations and Theses 1992.
55. Suh JK, Li Z, Woo SL. Dynamic behavior of a biphasic cartilage model under cyclic compressive loading. J Biomech 1995; 28:357-364.
56. Wong M, Siegrist M, Cao X. Cyclic compression of articular cartilage explants is associated with progressive consolidation and altered expression pattern of extracellular matrix proteins. Matrix Biol 1999; 18:391-399.
57. Buschmann MD, Kim YJ, Wong M, Frank E, Hunziker EB, Grodzinsky AJ. Stimulation of aggrecan synthesis in cartilage explants by cyclic loading is localized to regions of high interstitial fluid flow. Arch Biochem Biophys 1999; 366:1-7.
58. Mauck RL, Soltz MA, Wang CC, Wong DD, Chao PH, Valhmu WB, et al. Functional tissue engineering of articular cartilage through dynamic loading of chondrocyte-seeded agarose gels. J Biomech Eng 2000; 122:252-260.
59. Piscoya JL, Fermor B, Kraus VB, Stabler TV, Guilak F. The influence of mechanical compression on the induction of osteoarthritis-related biomarkers in articular cartilage explants. Osteoarthritis Cartilage 2005; 13:1092-1099.
60. Bian L, Zhai DY, Zhang EC, Mauck RL, Burdick JA. Dynamic compressive loading enhances cartilage matrix synthesis and distribution and suppresses hypertrophy in hMSC-laden hyaluronic acid hydrogels. Tissue engineering.Part A 2012; 18:715-724.
61. Fitzgerald JB, Jin M, Grodzinsky AJ. Shear and compression differentially regulate clusters of functionally related temporal transcription patterns in cartilage tissue. J Biol Chem 2006; 281:24095-24103.
62. Bougault C, Paumier A, Aubert-Foucher E, Mallein-Gerin F. Molecular analysis of chondrocytes cultured in agarose in response to dynamic compression. BMC Biotechnol 2008; 8:71.
63. Waldman SD, Spiteri CG, Grynpas MD, Pilliar RM, Hong J, Kandel RA. Effect of biomechanical conditioning on cartilaginous tissue formation in vitro. J Bone Joint Surg Am 2003;85-A Suppl 2:101-105.
64. Waldman SD, Spiteri CG, Grynpas MD, Pilliar RM, Kandel RA. Long-term intermittent compressive stimulation improves the composition and mechanical properties of tissue-engineered cartilage. Tissue Eng 2004; 10:1323-1331.
65. Lane Smith R, Trindade MC, Ikenoue T, Mohtai M, Das P, Carter DR, et al. Effects of shear stress on articular chondrocyte metabolism. Biorheology 2000; 37:95-107.
66. Buckley MR. Mapping the functional properties of soft biological tissues under shear loading. ProQuest Dissertations and Theses 2010.
67. Nugent GE, Aneloski NM, Schmidt TA, Schumacher BL, Voegtline MS, Sah RL. Dynamic shear stimulation of bovine cartilage biosynthesis of proteoglycan 4. Arthritis Rheum 2006; 54:1888-1896.

68. Chen S, Grodzinsky AJ. Dynamic Tissue Shear Deformation Can Enhance Chonrocyte Biosynthesis in 3-D Agarose Gel Culture: Effects of Medium Supplement and Developing Matrix. 52nd Annual Meeting of the Orthopaedic Research Society 2006.

69. Gemmiti CV, Guldberg RE. Shear stress magnitude and duration modulates matrix composition and tensile mechanical properties in engineered cartilaginous tissue. Biotechnol Bioeng 2009; 104:809-820.

70. Jin M, Emkey GR, Siparsky P, Trippel SB, Grodzinsky AJ. Combined effects of dynamic tissue shear deformation and insulin-like growth factor I on chondrocyte biosynthesis in cartilage explants. Arch Biochem Biophys 2003; 414:223-231.

71. Miyata S, Tateishi T, Ushida T. Influence of cartilaginous matrix accumulation on viscoelastic response of chondrocyte/agarose constructs under dynamic compressive and shear loading. J Biomech Eng 2008; 130:051016.

72. Grad S, Lee CR, Gorna K, Gogolewski S, Wimmer MA, Alini M. Surface motion upregulates superficial zone protein and hyaluronan production in chondrocyte-seeded three-dimensional scaffolds. Tissue Eng 2005; 11:249-256.

73. Journot BJ. The effects of cyclic hydrostatic pressure on chondrocytes in an alginate substrate. ProQuest Dissertations and Theses 2012.

74. Elder BD. Optimizing a scaffoldless approach for cartilage tissue engineering. ProQuest Dissertations and Theses 2009.

75. Parkkinen JJ, Ikonen J, Lammi MJ, Laakkonen J, Tammi M, Helminen HJ. Effects of cyclic hydrostatic pressure on proteoglycan synthesis in cultured chondrocytes and articular cartilage explants. Arch Biochem Biophys 1993; 300:458-465.

76. Lammi MJ, Inkinen R, Parkkinen JJ, Hakkinen T, Jortikka M, Nelimarkka LO, et al. Expression of reduced amounts of structurally altered aggrecan in articular cartilage chondrocytes exposed to high hydrostatic pressure. Biochem J 1994; 304 (Pt 3):723-730.

77. Parkkinen JJ, Lammi MJ, Inkinen R, Jortikka M, Tammi M, Virtanen I, et al. Influence of short-term hydrostatic pressure on organization of stress fibers in cultured chondrocytes. J Orthop Res 1995; 13:495-502.

78. Suh JK, Baek GH, Aroen A, Malin CM, Niyibizi C, Evans CH, et al. Intermittent sub-ambient interstitial hydrostatic pressure as a potential mechanical stimulator for chondrocyte metabolism. Osteoarthritis Cartilage 1999; 7:71-80.

79. Wong M, Siegrist M, Goodwin K. Cyclic tensile strain and cyclic hydrostatic pressure differentially regulate expression of hypertrophic markers in primary chondrocytes. Bone 2003; 33:685-693.

80. Toyoda T, Seedhom BB, Yao JQ, Kirkham J, Brookes S, Bonass WA. Hydrostatic pressure modulates proteoglycan metabolism in chondrocytes seeded in agarose. Arthritis Rheum 2003; 48:2865-2872.

81. Gavenis K, Kremer A, Von Walter M, Hollander DA, Schneider U, Schmidt-Rohlfing B. Effects of cyclic hydrostatic pressure on the metabolism of human osteoarthritic chondrocytes cultivated in a collagen gel. Artif Organs 2007; 31:91-98.

82. Elder BD, Athanasiou KA. Hydrostatic Pressure in Articular Cartilage Tissue Engineering: From Chondrocytes to Tissue Regeneration. Tissue Eng Part B Rev 2009.
83. Hall AC. Differential effects of hydrostatic pressure on cation transport pathways of isolated articular chondrocytes. J Cell Physiol 1999; 178:197-204.
84. Finger AR, Sargent CY, Dulaney KO, Bernacki SH, Loboa EG. Differential effects on messenger ribonucleic acid expression by bone marrow-derived human mesenchymal stem cells seeded in agarose constructs due to ramped and steady applications of cyclic hydrostatic pressure. Tissue Eng 2007; 13:1151-1158.
85. Hu JC, Athanasiou KA. The effects of intermittent hydrostatic pressure on self-assembled articular cartilage constructs. Tissue Eng 2006; 12:1337-1344.
86. Concaro S, Gustavson F, Gatenholm P. Bioreactors for Tissue Engineering of Cartilage. Adv Biochem Eng Biotechnol 2008.
87. Davisson T, Sah RL, Ratcliffe A. Perfusion increases cell content and matrix synthesis in chondrocyte three-dimensional cultures. Tissue Eng 2002; 8:807-816.
88. Gemmiti CV. Effect of fluid flow on tissue-engineered cartilage in a novel bioreactor. 2006.
89. Gemmiti CV, Guldberg RE. Fluid flow increases type II collagen deposition and tensile mechanical properties in bioreactor-grown tissue-engineered cartilage. Tissue Eng 2006; 12:469-479.
90. Chen T, Buckley M, Cohen I, Bonassar L, Awad HA. Insights into interstitial flow, shear stress, and mass transport effects on ECM heterogeneity in bioreactor-cultivated engineered cartilage hydrogels. Biomechanics and Modeling in Mechanobiology 2012; 11:689-702.
91. Malaviya P, Nerem RM. Fluid-induced shear stress stimulates chondrocyte proliferation partially mediated via TGF-beta1. Tissue Eng 2002; 8:581-590.
92. Hung CT, Valhmu WB, Ratcliffe A, Mow VC, Allen FD. Articular chondrocyte calcium response to transient fluid-induced shear stress. : ASME, NEW YORK, NY, (USA), 1997.
93. Mow VC, Ratcliffe A, Poole AR. Cartilage and diarthrodial joints as paradigms for hierarchical materials and structures. Biomaterials 1992; 13:67-97.
94. Steinert AF, Ghivizzani SC, Rethwilm A, Tuan RS, Evans CH, Noeth U. Major biological obstacles for persistent cell-based regeneration of articular cartilage. Arthritis Research & Therapy 2007; 9:213.
95. Serafini-Fracassini A, Smith JW, M.D. Structure and biochemistry of cartilage. Edinburgh: Churchill Livingstone, 1974.
96. Schmidt TA, Gastelum NS, Nguyen QT, Schumacher BL, Sah RL. Boundary lubrication of articular cartilage: Role of synovial fluid constituents. Arthritis & Rheumatism 2007; 56:882-891.
97. Mow VCH, Rik. Basic orthopaedic biomechanics & mechano-biology. 3rd ed. ed. : Philadelphia : Lippincott Williams & Wilkins, c2005, 2005.
98. Buckwalter JA, Mankin HJ, Grodzinsky AJ. Articular cartilage and osteoarthritis. Instr Course Lect 2005; 54:465-480.
99. Mow VC, Hayes WC. Basic orthopaedic biomechanics. New York: Raven Press, 1991.

100. Eyre DR, Weis MA, Wu J. Articular cartilage collagen: an irreplaceable framework? European cells & materials 2006;12:57-63.

101. Eyre DR, Wu JJ. Collagen structure and cartilage matrix integrity. The Journal of rheumatology.Supplement 1995; 43:82-85.

102. Responte DJ, Natoli RM, Athanasiou K. Collagens of Articular Cartilage: Structure, Function, and Importance in Tissue Engineering. Crit Rev Biomed Eng 2007; 35:363-411.

103. Kuettner KE. Articular cartilage and osteoarthritis. New York: Raven Press, 1992.

104. Cartilage ECM and chondrocyte,[http://www.bidmc.org/Research/Departments/Radiology/Laboratories/~/media/Images/CentersandDepartments/Radiology/Research/cartilage/cartilage_with_labels.ashx].

105. Roughley PJ. The structure and function of cartilage proteoglycans. European cells & materials 2006;12:92-101.

106. Schulz RM, Bader A. Cartilage tissue engineering and bioreactor systems for the cultivation and stimulation of chondrocytes. Eur Biophys J 2007; 36:539-568.

107. Stockwell RA. Chondrocytes. Journal of clinical pathology.Supplement (Royal College of Pathologists) 1978; 12:7-13.

108. Oldershaw RA. Cell sources for the regeneration of articular cartilage: the past, the horizon and the future. Int J Exp Pathol 2012; 93:389-400.

109. Muir H. The chondrocyte, architect of cartilage. Biomechanics, structure, function and molecular biology of cartilage matrix macromolecules. Bioessays 1995;17:1039-1048.

110. Buckwalter JA. Articular cartilage: injuries and potential for healing. J Orthop Sports Phys Ther 1998; 28:192-202.

111. Murakami T, Nakashima K, Yarimitsu S, Sawae Y, Sakai N. Effectiveness of adsorbed film and gel layer in hydration lubrication as adaptive multimode lubrication mechanism for articular cartilage. Proc Inst Mech Eng Part J 2011; 225:1174.

112. Graindorge S, Ferrandez W, Jin Z, Ingham E, Grant C, Twigg P, et al. Biphasic surface amorphous layer lubrication of articular cartilage. Med Eng Phys 2005; 27:836-844.

113. Pearle AD, Warren RF, Rodeo SA. Basic science of articular cartilage and osteoarthritis. Clin Sports Med 2005; 24:1-12.

114. Coates EE. Engineering zonal cartilage through utilization of a mesenchymal stem cell population. ProQuest Dissertations and Theses 2012.

115. DuRaine GD, Chan SMT, Reddi AH. Effects of TGF-β1 on alternative splicing of Superficial Zone Protein in articular cartilage cultures. Osteoarthr Cartil 2011; 19:103-110.

116. Articular cartilage zones, UK Centre for Tissue Engineering (UKCTE), http://www.ukcte.org/images/cartilage.jpg.

117. Mow VC, Kuei SC, Lai WM, Armstrong CG. Biphasic creep and stress relaxation of articular cartilage in compression? Theory and experiments. J Biomech Eng 1980; 102:73-84.

118. Armstrong CG, Lai WM, Mow VC. An analysis of the unconfined compression of articular cartilage. J Biomech Eng 1984; 106:165-173.
119. Ateshian GA, Warden WH, Kim JJ, Grelsamer RP, Mow VC. Finite deformation biphasic material properties of bovine articular cartilage from confined compression experiments. J Biomech 1997;30:1157-1164.
120. Wang C, Hung CT, Mow VC. An analysis of the effects of depth-dependent aggregate modulus on articular cartilage stress-relaxation behavior in compression. J Biomech 2001; 34:75-84.
121. Park S, Krishnan R, Nicoll SB, Ateshian GA. Cartilage interstitial fluid load support in unconfined compression. J Biomech 2003; 36:1785-1796.
122. Basalo IM, Mauck RL, Kelly TN, Nicoll SB, Chen FH, Hung CT, et al. Cartilage interstitial fluid load support in unconfined compression following enzymatic digestion. J Biomech Eng 2004; 126:779-786.
123. Mow VC, Gibbs MC, Lai WM, Zhu WB, Athanasiou KA. Biphasic indentation of articular cartilage--II. A numerical algorithm and an experimental study. J Biomech 1989; 22:853-861.
124. Lu XL, Miller C, Guo XE, Mow VC. Triphasic indentation of articular cartilage: the simultaneous determination of both mechanical properties and fixed charge density. J Biomech 2006;39:S25-S26.
125. Park S, Costa KD, Ateshian GA, Hong K. Mechanical properties of bovine articular cartilage under microscale indentation loading from atomic force microscopy. Institution of Mechanical Engineers.Proceedings.Part H: Journal of Engineering in Medicine 2009; 223:339-347.
126. Bae WC, Schumacher BL, Sah RL. Indentation probing of human articular cartilage: Effect on chondrocyte viability. Osteoarthritis Cartilage 2007; 15:9-18.
127. Lu XL, Sun D, Guo XE, Chen FH, Lai W, Mow VC. Indentation Determined Mechanoelectrochemical Properties and Fixed Charge Density of Articular Cartilage. Ann Biomed Eng 2004; 32:370-379.
128. Spilker RL, Suh JK, Mow VC. A finite element analysis of the indentation stress-relaxation response of linear biphasic articular cartilage. J Biomech Eng 1992;114:191-201.
129. Jurvelin J, Kiviranta I, Arokoski J, Tammi M, Helminen HJ. Indentation study of the biochemical properties of articular cartilage in the canine knee. Eng Med 1987; 16:15-22.
130. Kwan MK, Lai WM, Mow VC. A finite deformation theory for cartilage and other soft hydrated connective tissues--I. Equilibrium results. J Biomech 1990; 23:145-155.
131. Armstrong CG, Mow VC. Variations in the intrinsic mechanical properties of human articular cartilage with age, degeneration, and water content. The Journal of bone and joint surgery.American volume 1982; 64:88-94.
132. Zhu W, Lai WM, Mow VC. The density and strength of proteoglycan-proteoglycan interaction sites in concentrated solutions. J Biomech 1991; 24:1007-1018.
133. Mow VC, Zhu W, Lai W, Hardingham T, Hughes C, Muir H. The influence of link protein stabilization on the viscometric properties of proteoglycan aggregate solutions. Biochimica et Biophysica Acta: Protein Structure and Molecular Enzymology 1989;992:201-208.
134. Grodzinsky AJ, Levenston ME, Jin M, Frank EH. Cartilage tissue remodeling in response to mechanical forces. Annu Rev Biomed Eng 2000; 2:691-713.

135. Woo SL, Akeson WH, Jemmott GF. Measurements of nonhomogeneous, directional mechanical properties of articular cartilage in tension. J Biomech 1976; 9:785-791.
136. Williamson AK, Chen AC, Masuda K, Thonar E, Sah RL. Tensile mechanical properties of bovine articular cartilage: variations with growth and relationships to collagen network components. Journal of Orthopaedic Research 2003; 21:872-880.
137. Roth V, Mow VC. The intrinsic tensile behavior of the matrix of bovine articular cartilage and its variation with age. The Journal of bone and joint surgery.American volume 1980; 62:1102-1117.
138. Schmidt MB, Mow VC, Chun LE, Eyre DR. Effects of proteoglycan extraction on the tensile behavior of articular cartilage. Journal of orthopaedic research : official publication of the Orthopaedic Research Society 1990;8:353-363.
139. Setton L, Lai W, Mow VC. Swelling-induced residual stress and the mechanism of curling in articular cartilage in vitro. : ASME, NEW YORK, NY, (USA), 1993.
140. Setton LA, Zhu W, Mow VC. The biphasic poroviscoelastic behavior of articular cartilage: role of the surface zone in governing the compressive behavior. J Biomech 1993; 26:581-592.
141. Setton LA, Tohyama H, Mow VC. Swelling and curling behaviors of articular cartilage. J Biomech Eng 1998; 120:355-361.
142. Wilson W, van Donkelaar CC, van Rietbergen B, Huiskes R. A fibril-reinforced poroviscoelastic swelling model for articular cartilage. J Biomech 2005; 38:1195-1204.
143. Han E, Chen SS, Klisch SM, Sah RL. Contribution of proteoglycan osmotic swelling pressure to the compressive properties of articular cartilage. Biophys J 2011; 101:916-924.
144. Setton L, Mow VC. Generalized biphasic poroviscoelastic model for articular cartilage: Theory and experiments. : ASME, NEW YORK, NY (USA), 1992.
145. Huang CY, Mow VC, Ateshian GA. The role of flow-independent viscoelasticity in the biphasic tensile and compressive responses of articular cartilage. J Biomech Eng 2001; 123:410-417.
146. Kwan MK, Lai WM, Mow VC. Fundamentals of fluid transport through cartilage in compression. Ann Biomed Eng 1984; 12:537-558.
147. Neu CP, Komvopoulos K, Reddi A. The Interface of Functional Biotribology and Regenerative Medicine in Synovial Joints. Tissue Engineering, Part B: Reviews 2008; 14:235-248.
148. Katta J, Jin Z, Ingham E, Fisher J. Biotribology of articular cartilage - A review of the recent advances. Med Eng Phys 2008; 30:1349-1363.
149. Bhushan B. Modern tribology handbook. Boca Raton, Fla.: CRC Press, 2001.
150. Murakami T, Sawae Y, Nakashima K, Yarimitsu S, Sato T. Micro- and nanoscopic biotribological behaviours in natural synovial joints and artificial joints. Proc Inst Mech Eng Part J 2007; 221:237-245.
151. Komistek RD, Kane TR, Mahfouz M, Ochoa JA, Dennis DA. Knee mechanics: a review of past and present techniques to determine in vivo loads. J Biomech 2005; 38:215-228.
152. Hodge WA, Fijan RS, Carlson KL, Burgess RG, Harris WH, Mann RW. Contact pressures in the human hip joint measured in vivo. Proc Natl Acad Sci U S A 1986; 83:2879-2883.

153. Hodge WA, Carlson KL, Fijan RS, Burgess RG, Riley PO, Harris WH, et al. Contact pressures from an instrumented hip endoprosthesis. The Journal of bone and joint surgery.American volume 1989;71:1378-1386.
154. Unsworth A. Tribology of human and artificial joints. Proceedings of the Institution of Mechanical Engineers.Part H, Journal of engineering in medicine 1991; 205:163-172.
155. Dowson D. Bio-tribology. Faraday Discuss 2012; 156:9-30; discussion 87-103.
156. Nosonovsky M, Bhushan B. Multiscale friction mechanisms and hierarchical surfaces in nano- and bio-tribology. Materials Science & Engineering R: Reports 2007; 58:162-193.
157. Lizhang J, Fisher J, Jin Z, Burton A, Williams S. The effect of contact stress on cartilage friction, deformation and wear. Proceedings of the Institution of Mechanical Engineers.Part H, Journal of engineering in medicine 2011; 225:461-475.
158. Krishnan R, Kopacz M, Ateshian GA. Experimental verification of the role of interstitial fluid pressurization in cartilage lubrication. J Orthop Res 2004; 22:565-570.
159. Forster H, Fisher J. The influence of loading time and lubricant on the friction of articular cartilage. Proceedings of the Institution of Mechanical Engineers.Part H, Journal of engineering in medicine 1996; 210:109-119.
160. McNary SM, Athanasiou KA, Reddi AH. Engineering Lubrication in Articular Cartilage. Tissue Engineering Part B-Reviews 2012; 18:88-100.
161. Chan SMT, Neu CP, Komvopoulos K, Reddi AH. Dependence of nanoscale friction and adhesion properties of articular cartilage on contact load. J Biomech 2011; 44:1340-1345.
162. Katta J, Pawaskar SS, Jin ZM, Ingham E, Fisher J. Effect of load variation on the friction properties of articular cartilage. Proc Inst Mech Eng Part J 2007; 221:175-181.
163. Carter MJ, Basalo IM, Ateshian GA. The temporal response of the friction coefficient of articular cartilage depends on the contact area. J Biomech 2007; 40:3257-3260.
164. Caligaris M, Ateshian GA. Effects of sustained interstitial fluid pressurization under migrating contact area, and boundary lubrication by synovial fluid, on cartilage friction. Osteoarthritis Cartilage 2008; 16:1220-1227.
165. Forster H, Fisher J. The influence of continuous sliding and subsequent surface wear on the friction of articular cartilage. Proceedings of the Institution of Mechanical Engineers.Part H, Journal of engineering in medicine 1999; 213:329-345.
166. Jin ZM, Pickard JE, Forster H, Ingham E, Fisher J. Frictional behaviour of bovine articular cartilage. Biorheology 2000; 37:57-63.
167. Szeri AZ. Fluid film lubrication. 2nd ed ed. Cambridge ; New York: Cambridge University Press, 2011.
168. Chan SMT. Articular cartilage boundary lubrication, friction, and wear. ProQuest Dissertations and Theses 2010.
169. Wang H. Boundary lubrication of articular cartilage: The role of interstitial fluid pressure, surface porosities and equilibrium friction coefficient. ProQuest Dissertations and Theses 1997.

170. Szeri AZ. Fluid film lubrication : Theory and design. Cambridge, U.K. ; New York: Cambridge University Press, 1998.
171. Bansil R, Stanley E, LaMont JT. Mucin biophysics. Annu Rev Physiol 1995; 57:635-657.
172. Ikegawa S, Sano M, Koshizuka Y, Nakamura Y. Isolation, characterization and mapping of the mouse and human PRG4 (proteoglycan 4) genes. Cytogenet Cell Genet 2000; 90:291-297.
173. Schumacher BL, Block J, Schmid TM, Aydelotte MB, Kuettner K. A novel proteoglycan synthesized and secreted by chondrocytes of the superficial zone of articular cartilage. Arch Biochem Biophys 1994;311:144-152.
174. Swann DA, Slayter HS, Silver FH. The molecular structure of lubricating glycoprotein-I, the boundary lubricant for articular cartilage. The Journal of biological chemistry 1981; 256:5921-5925.
175. Chan SMT, Neu CP, Duraine G, Komvopoulos K, Reddi AH. Atomic force microscope investigation of the boundary-lubricant layer in articular cartilage. Osteoarthr Cartil 2010; 18:956-963.
176. Chan SMT, Neu CP, DuRaine G, Komvopoulos K, Reddi AH. Tribological altruism: A sacrificial layer mechanism of synovial joint lubrication in articular cartilage. J Biomech 2012; 45:2426-2431.
177. Graindorge S, Ferrandez W, Ingham E, Jin Z, Twigg P, Fisher J. The Role of the Surface Amorphous Layer of Articular Cartilage in Joint Lubrication. Institution of Mechanical Engineers.Proceedings.Part H: Journal of Engineering in Medicine 2006; 220:597-607.
178. Graindorge S, Ferrandez W, Jin Z, Ingham E, Fisher J. The natural synovial joint: a finite element investigation of biphasic surface amorphous layer lubrication under dynamic loading conditions. Proc Inst Mech Eng Part J 2006; 220:671-682.
179. Hills BA, Monds MK. Enzymatic identification of the load-bearing boundary lubricant in the joint. Br J Rheumatol 1998; 37:137-142.
180. Wilkins J. Proteolytic destruction of synovial boundary lubrication. Nature 1968; 219:1050-1051.
181. Walker PS, Dowson D, Longfield MD, Wright V. "Boosted lubrication" in synovial joints by fluid entrapment and enrichment. Ann Rheum Dis 1968; 27:512-520.
182. Ateshian GA. The role of interstitial fluid pressurization in articular cartilage lubrication. J Biomech 2009;42:1163-1176.
183. Kumar P, Oka M, Toguchida J, Kobayashi M, Uchida E, Nakamura T, et al. Role of uppermost superficial surface layer of articular cartilage in the lubrication mechanism of joints. J Anat 2001; 199:241-250.
184. Bell CJ, Ingham E, Fisher J. Influence of hyaluronic acid on the time-dependent friction response of articular cartilage under different conditions. Institution of Mechanical Engineers.Proceedings.Part H: Journal of Engineering in Medicine 2006; 220:23-31.
185. Bell CJ, Carrick LM, Katta J, Jin Z, Ingham E, Aggeli A, et al. Self-assembling peptides as injectable lubricants for osteoarthritis. Journal of Biomedical Materials Research, Part A 2006; 78A:236-246.
186. Pickard JE, Fisher J, Ingham E, Egan J. Investigation into the effects of proteins and lipids on the frictional properties of articular cartilage. Biomaterials 1998; 19:1807-1812.

187. Basalo IM, Raj D, Krishnan R, Chen FH, Hung CT, Ateshian GA. Effects of enzymatic degradation on the frictional response of articular cartilage in stress relaxation. J Biomech 2005; 38:1343-1349.
188. Basalo IM, Chen FH, Hung CT, Ateshian GA. Frictional response of bovine articular cartilage under creep loading following proteoglycan digestion with chondroitinase ABC. J Biomech Eng 2006; 128:131-134.
189. Naka MH, Morita Y, Ikeuchi K. Influence of proteoglycan contents and of tissue hydration on the frictional characteristics of articular cartilage. Proc Inst Mech Eng [H] 2005; 219:175-182.
190. Forsey RW, Fisher J, Thompson J, Stone MH, Bell C, Ingham E. The effect of hyaluronic acid and phospholipid based lubricants on friction within a human cartilage damage model. Biomaterials 2006;27:4581-4590.
191. Schumacher BL, Hughes CE, Kuettner KE, Caterson B, Aydelotte MB. Immunodetection and partial cDNA sequence of the proteoglycan, superficial zone protein, synthesized by cells lining synovial joints. Journal of orthopaedic research: official publication of the Orthopaedic Research Society 1999;17:110-120.
192. Jay GD, Torres JR, Rhee DK, Helminen HJ, Hytinnen MM, Cha C, et al. Association between friction and wear in diarthrodial joints lacking lubricin. Arthritis & Rheumatism 2007; 56:3662-3669.
193. Hills BA. Boundary lubrication in vivo. Proceedings of the Institution of Mechanical Engineers.Part H, Journal of engineering in medicine 2000; 214:83-94.
194. Hills BA, Crawford RW. Normal and prosthetic synovial joints are lubricated by surface-active phospholipid: a hypothesis. J Arthroplasty 2003;18:499-505.
195. Martin JA, Buckwalter JA. Roles of articular cartilage aging and chondrocyte senescence in the pathogenesis of osteoarthritis. Iowa Orthop J 2001; 21:1-7.
196. Vo N, Niedernhofer LJ, Nasto LA, Jacobs L, Robbins PD, Kang J, et al. An overview of underlying causes and animal models for the study of age-related degenerative disorders of the spine and synovial joints. Journal of orthopaedic research : official publication of the Orthopaedic Research Society 2013;31:831-837.
197. Buckwalter JA, Roughley PJ, Rosenberg LC. Age-related changes in cartilage proteoglycans: quantitative electron microscopic studies. Microsc Res Tech 1994; 28:398-408.
198. Quinn TM, Allen RG, Schalet BJ, Perumbuli P, Hunziker EB. Matrix and cell injury due to sub-impact loading of adult bovine articular cartilage explants: effects of strain rate and peak stress. Journal of orthopaedic research : official publication of the Orthopaedic Research Society 2001;19:242-249.
199. Levin A, Burton-Wurster N, Chen CT, Lust G. Intercellular signaling as a cause of cell death in cyclically impacted cartilage explants. Osteoarthritis Cartilage 2001; 9:702-711.
200. Pickvance EA, Oegema TR, Thompson RC. Immunolocalization of selected cytokines and proteases in canine articular cartilage after transarticular loading. Journal of orthopaedic research : official publication of the Orthopaedic Research Society 1993;11:313-323.
201. Meyer U, Wiesmann HP. Bone and cartilage engineering. Berlin ; New York: Springer, 2006.
202. Hunziker EB. Articular cartilage repair: basic science and clinical progress. A review of the current status and prospects. Osteoarthr Cartil 2002;10:432-463.

203. Hunziker EB, Rosenberg LC. Repair of partial-thickness defects in articular cartilage: cell recruitment from the synovial membrane. J Bone Joint Surg Am 1996; 78:721-733.
204. Hunziker EB. Growth-factor-induced healing of partial-thickness defects in adult articular cartilage. Osteoarthritis Cartilage 2001; 9:22-32.
205. Caplan A, Elyaderani M, Mochizuki Y, Wakitani S, Goldberg VM. Principles of cartilage repair and regeneration. Clin Orthop 1997:254-269.
206. Klussmann A, Gebhardt H, Liebers F, von Engelhardt LV, David A, Bouillon B, et al. Individual and occupational risk factors for knee osteoarthritis - study protocol of a case control study. BMC Musculoskelet Disord 2008; 9:26.
207. Arden N, Nevitt MC. Osteoarthritis: epidemiology. Best practice & research.Clinical rheumatology 2006;20:3-25.
208. Knecht S, Vanwanseele B, Stuessi E. A review on the mechanical quality of articular cartilage - Implications for the diagnosis of osteoarthritis. Clin Biomech 2006;21:999-1012.
209. Nelson DL. Stages of osteoarthritis, MedcoHealth, [http://www.davidlnelson.md/Osteoarthritis.htm].
210. Cole BJ, Pascual-Garrido C, Grumet RC. Surgical management of articular cartilage defects in the knee. The Journal of bone and joint surgery.American volume 2009; 91:1778-1790.
211. McCoy B, Miniaci A. Osteochondral autograft transplantation/mosaicplasty. The journal of knee surgery 2012; 25:99-108.
212. Miniaci A, Martineau PA. Technical aspects of osteochondral autograft transplantation. Instr Course Lect 2007; 56:447-455.
213. Harman BD, Weeden SH, Lichota DK, Brindley GW. Osteochondral Autograft Transplantation in the Porcine Knee. Am J Sports Med 2006; 34:913-918.
214. Kane P, Frederick R, Tucker B, Dodson CC, Anderson JA, Ciccotti MG, et al. Surgical restoration/repair of articular cartilage injuries in athletes. The Physician and sportsmedicine 2013;41:75-86.
215. Chahal J, Gross AE, Gross C, Mall N, Dwyer T, Chahal A, et al. Outcomes of osteochondral allograft transplantation in the knee. Arthroscopy 2013; 29:575-588.
216. Bugbee W, Cavallo M, Giannini S. Osteochondral allograft transplantation in the knee. The journal of knee surgery 2012; 25:109-116.
217. Bugbee WD, Convery FR. Osteochondral allograft transplantation. Clin Sports Med 1999; 18:67-75.
218. Hangody LR, Gál T, Szűcs A, Vásárhelyi G, Tóth F, Módis L, et al. Osteochondral allograft transplantation from a living donor. Arthroscopy 2012;28:1180-1183.
219. Scully WF, Parada SA, Arrington ED. Allograft osteochondral transplantation in the knee in the active duty population. Mil Med 2011; 176:1196-1201.
220. Hangody L, Vásárhelyi G, Hangody LR, Sükösd Z, Tibay G, Bartha L, et al. Autologous osteochondral grafting--technique and long-term results. Injury 2008; 39 Suppl 1:S32-S39.
221. Memon AR, Quinlan JF. Surgical treatment of articular cartilage defects in the knee: are we winning? Advances in orthopedics 2012; 2012:528423.

222. LaPrade RF, Botker JC. Donor-site morbidity after osteochondral autograft transfer procedures. Arthroscopy 2004; 20: e69-e73.
223. Chow JCY, Hantes ME, Houle JB, Zalavras CG. Arthroscopic autogenous osteochondral transplantation for treating knee cartilage defects: a 2- to 5-year follow-up study. Arthroscopy 2004; 20: 681-690.
224. Chiang H, Kuo T, Tsai C, Lin M, She B, Huang Y, et al. Repair of porcine articular cartilage defect with autologous chondrocyte transplantation. Journal of orthopaedic research: official publication of the Orthopaedic Research Society 2005; 23: 584-593.
225. Brittberg M, Lindahl A, Nilsson A, Ohlsson C, Isaksson O, Peterson L. Treatment of deep cartilage defects in the knee with autologous chondrocyte transplantation. N Engl J Med 1994; 331: 889-895.
226. Brittberg M. Autologous chondrocyte transplantation. Clin Orthop 1999:S147-S155.
227. Brittberg M, Tallheden T, Sjögren-Jansson B, Lindahl A, Peterson L. Autologous chondrocytes used for articular cartilage repair: an update. Clin Orthop 2001:S337-S348.
228. Tetteh ES, Bajaj S, Ghodadra NS. Basic science and surgical treatment options for articular cartilage injuries of the knee. J Orthop Sports Phys Ther 2012; 42: 243-253.
229. Batty L, Dance S, Bajaj S, Cole BJ. Autologous chondrocyte implantation: an overview of technique and outcomes. ANZ J Surg 2011; 81:18-25.
230. McNickle AG, L'Heureux DR, Yanke AB, Cole BJ. Outcomes of autologous chondrocyte implantation in a diverse patient population. Am J Sports Med 2009;37:1344-1350.
231. Cole BJ. A Randomized Trial Comparing Autologous Chondrocyte Implantation with Microfracture. J Bone Jt Surg (Am) 2008;90:1165.
232. Buechel F, Pappas MJ. Principles of human joint replacement design and clinical application /. : Berlin : Springer, c2011, 2011.
233. Pfeil JS, W. Minimally invasive surgery in total hip arthroplasty. : Heidelberg: Springer, c2010, 2010.
234. Bono JV, Scott RD(D. Revision total knee arthroplasty. New York: Springer, 2005.
235. Ducheyne P, Mauck RL, Smith DH. Biomaterials in the repair of sports injuries. Nature materials 2012; 11: 652-654.
236. Teuschl AH, Nuernberger S, Redl H, Nau T. Articular cartilage tissue regeneration-current research strategies and outlook for the future. European Surgery-Acta Chirurgica Austriaca 2013; 45: 142-153.
237. Melero-Martin JM, Santhalingam S, Al-Rubeai M. Methodology for optimal in vitro cell expansion in tissue engineering. Adv Biochem Eng Biotechnol 2009; 112:209-229.
238. Melero Martin JM. Expansion methods for chondroprogenitor cells in articular cartilage tissue engineering applications. PQDT - UK & Ireland 2005.
239. Mano JF, Reis RL. Osteochondral defects: present situation and tissue engineering approaches. Journal of tissue engineering and regenerative medicine 2007; 1: 261-273.
240. Langer R, Vacanti JP. Tissue engineering. Science (New York, N.Y.) 1993; 260: 920-926.
241. Langer R. Tissue engineering. Molecular therapy: the journal of the American Society of Gene Therapy 2000;1:12-15.

242. Langer R. Tissue engineering: perspectives, challenges, and future directions. Tissue engineering 2007; 13: 1-2.
243. Khademhosseini A, Vacanti JP, Langer R. Progress in tissue engineering. Sci Am 2009; 300: 64-71.
244. van der Kraan PM, Buma P, van Kuppevelt T, van den Berg WB. Interaction of chondrocytes, extracellular matrix and growth factors: relevance for articular cartilage tissue engineering. Osteoarthr Cartil 2002; 10: 631-637.
245. Capito RM, Spector M. Scaffold-based articular cartilage repair. IEEE Eng Med Biol Mag 2003;22:42-50.
246. Hutmacher DW, Sittinger M, Risbud MV. Scaffold-based tissue engineering: rationale for computer-aided design and solid free-form fabrication systems. Trends Biotechnol 2004; 22: 354-362.
247. Steward AJ, Liu Y, Wagner DR. Engineering Cell Attachments to Scaffolds in Cartilage Tissue Engineering. JOM 2011; 63: 74-82.
248. El-Ayoubi R, Degrandpre C, Diraddo R, Yousefi AM, Lavigne P. Design and Dynamic Culture of 3D-Scaffolds for Cartilage Tissue Engineering. J Biomater Appl 2011; 25: 429-444.
249. Haugh JM. Mathematical Modeling of Cartilage Regeneration in Cell-Seeded Scaffolds. ProQuest Dissertations and Theses 2010.
250. Freed LE, Engelmayr GC, Borenstein JT, Moutos FT, Guilak F. Advanced material strategies for tissue engineering scaffolds. Advanced materials (Deerfield Beach, Fla.) 2009; 21: 3410-3418.
251. Jeong GC. The effects of designed scaffold architecture and biodegradable material on chondrogenesis in vitro and in vivo. ProQuest Dissertations and Theses 2010.
252. Chan BP, Leong KW. Scaffolding in tissue engineering: general approaches and tissue-specific considerations. Eur Spine J 2008; 17 Suppl 4:467-479.
253. Furukawa KS, Imura K, Tateishi T, Ushida T. Scaffold-free cartilage by rotational culture for tissue engineering. J Biotechnol 2008; 133: 134-145.
254. Furukawa KS. Scaffold free-cartilage tissue engineering by mold technique. Materials Science and Technology (Japan) 2007; 44: 13-15.
255. Han E, Bae WC, Hsieh-Bonassera ND, Wong VW, Schumacher BL, Görtz S, et al. Shaped, stratified, scaffold-free grafts for articular cartilage defects. Clin Orthop 2008; 466: 1912-1920.
256. Kitahara S, Nakagawa K, Sah RL, Wada Y, Ogawa T, Moriya H, et al. In vivo maturation of scaffold-free engineered articular cartilage on hydroxyapatite. Tissue Eng Part A 2008; 14: 1905-1913.
257. Nagai T, Furukawa KS, Sato M, Ushida T, Mochida J. Characteristics of a scaffold-free articular chondrocyte plate grown in rotational culture. Tissue Eng Part A 2008; 14: 1183-1193.
258. Nagai T, Sato M, Furukawa KS, Kutsuna T, Ohta N, Ushida T, et al. Optimization of allograft implantation using scaffold-free chondrocyte plates. Tissue Eng Part A 2008; 14: 1225-1235.
259. Natoli RM, Revell CM, Athanasiou KA. Chondroitinase-ABC Treatment Results in Increased Tensile Properties in a Scaffold-less, Serum-free Model of Articular Cartilage Tissue Engineering. 54th Annual Meeting of the Orthopaedic Research Society 2008.

260. Tani G, Usui N, Kamiyama M, Oue T, Fukuzawa M. In vitro construction of scaffold-free cylindrical cartilage using cell sheet-based tissue engineering. Pediatr Surg Int 2010; 26: 179-185.
261. Masuda K, Sah RL, Hejna MJ, Thonar EJ. A novel two-step method for the formation of tissue-engineered cartilage by mature bovine chondrocytes: the alginate-recovered-chondrocyte (ARC) method. J Orthop Res 2003; 21: 139-148.
262. Park K, Huang J, Azar F, Jin RL, Min B, Han DK, et al. Scaffold-Free, Engineered Porcine Cartilage Construct for Cartilage Defect Repair-In Vitro and In Vivo Study. Artif Organs 2006; 30: 586-596.
263. Cohen S, Bano MC, Cima LG, Allcock HR, Vacanti JP, Vacanti CA, et al. Design of synthetic polymeric structures for cell transplantation and tissue engineering. Clin Mater 1993; 13:3-10.
264. Chang C, Kuo T, Lin F, Wang J, Hsu Y, Huang H, et al. Tissue engineering-based cartilage repair with mesenchymal stem cells in a porcine model. Journal of orthopaedic research: official publication of the Orthopaedic Research Society 2011; 29: 1874-1880.
265. Ishaug-Riley SL, Crane-Kruger GM, Yaszemski MJ, Mikos AG. Three-dimensional culture of rat calvarial osteoblasts in porous biodegradable polymers. Biomaterials 1998;19:1405-1412.
266. Furukawa KS, Imura K, Tateishi T, Ushida T. Scaffold-free cartilage by rotational culture for tissue engineering. J Biotechnol 2008; 133: 134-145.
267. Waldman SD, Grynpas MD, Pilliar RM, Kandel RA. Characterization of cartilagenous tissue formed on calcium polyphosphate substrates in vitro. J Biomed Mater Res 2002; 62: 323-330.
268. Waldman SD, Grynpas M, Pilliar RM, Kandel RA. The use of specific chondrocyte populations to modulate the properties of tissue-engineered cartilage. Journal of Orthopaedic Research 2003; 21:132-138.
269. Waldman SD, Couto DC, Omelon SJ, Kandel RA. Effect of Sodium Bicarbonate on Extracellular pH, Matrix Accumulation, and Morphology of Cultured Articular Chondrocytes. Tissue Eng 2004; 10: 1633.
270. Stewart MC, Saunders KM, Burton-Wurster N, Macleod JN. Phenotypic stability of articular chondrocytes in vitro: the effects of culture models, bone morphogenetic protein 2, and serum supplementation. J Bone Miner Res 2000; 15: 166-174.
271. Zhang Z, McCaffery JM, Spencer RG, Francomano CA. Hyaline cartilage engineered by chondrocytes in pellet culture: histological, immunohistochemical and ultrastructural analysis in comparison with cartilage explants. J Anat 2004; 205: 229-237.
272. Gigout A, Jolicoeur M, Buschmann MD. Low calcium levels in serum-free media maintain chondrocyte phenotype in monolayer culture and reduce chondrocyte aggregation in suspension culture. Osteoarthr Cartil 2005; 13: 1012-1024.
273. Gordana Vunjak-Novakovic RIF. Culture of cells for tissue engineering. Scitech Book News 2006;30:n/a.
274. Hench LL, Jones JR. Biomaterials, artificial organs and tissue engineering. Boca Raton: Cambridge: CRC Press; Woodhead, 2005.
275. Secretan CC. The role of cultured chondrocytes and mesenchymal stem cells in the repair of acute articular cartilage injuries. ProQuest Dissertations and Theses 2010.

276. Huang AH, Farrell MJ, Mauck RL. Mechanics and mechanobiology of mesenchymal stem cell-based engineered cartilage. J Biomech 2010; 43: 128-136.
277. Li WJ, Jiang YJ, Tuan RS. Cell-nanofiber-based cartilage tissue engineering using improved cell seeding, growth factor, and bioreactor technologies. Tissue Eng Part A 2008; 14: 639-648.
278. Vinatier C, Mrugala D, Jorgensen C, Guicheux J, Noel D. Cartilage engineering: a crucial combination of cells, biomaterials and biofactors. Trends Biotechnol 2009; 27: 307-314.
279. Lee DA, Noguchi T, Knight MM, O'Donnell L, Bentley G, Bader DL. Response of chondrocyte subpopulations cultured within unloaded and loaded agarose. J Orthop Res 1998; 16: 726-733.
280. Aydelotte MB, Kuettner KE. Differences between sub-populations of cultured bovine articular chondrocytes. I. Morphology and cartilage matrix production. Connect Tissue Res 1988; 18: 205-222.
281. Buckley CT, Thorpe SD, O'Brien FJ, Robinson AJ, Kelly DJ. The effect of concentration, thermal history and cell seeding density on the initial mechanical properties of agarose hydrogels. J Mech Behav Biomed Mater 2009; 2: 512-521.
282. Hu JC, Athanasiou KA. Low-density cultures of bovine chondrocytes: effects of scaffold material and culture system. Biomaterials 2005; 26: 2001-2012.
283. Mauck RL, Wang CC, Oswald ES, Ateshian GA, Hung CT. The role of cell seeding density and nutrient supply for articular cartilage tissue engineering with deformational loading. Osteoarthritis Cartilage 2003;11:879-890.
284. Mauck RL, Seyhan SL, Ateshian GA, Hung CT. Influence of seeding density and dynamic deformational loading on the developing structure/function relationships of chondrocyte-seeded agarose hydrogels. Ann Biomed Eng 2002; 30: 1046-1056.
285. Unsworth JM, Rose FR, Wright E, Scotchford CA, Shakesheff KM. Seeding cells into needled felt scaffolds for tissue engineering applications. J Biomed Mater Res A 2003; 66: 425-431.
286. Vunjak-Novakovic G, Obradovic B, Martin I, Bursac PM, Langer R, Freed LE. Dynamic cell seeding of polymer scaffolds for cartilage tissue engineering. Biotechnol Prog 1998; 14: 193-202.
287. Haycock JW. 3D cell culture methods and protocols. New York: Humana Press, 2011.
288. Timmins NE, Scherberich A, Fruh JA, Heberer M, Martin I, Jakob M. Three-dimensional cell culture and tissue engineering in a T-CUP (tissue culture under perfusion). Tissue Eng 2007; 13: 2021-2028.
289. Kitagawa T, Yamaoka T, Iwase R, Murakami A. Three-dimensional cell seeding and growth in radial-flow perfusion bioreactor for in vitro tissue reconstruction. Biotechnol Bioeng 2006; 93: 947-954.
290. Anton F, Suck K, Diederichs S, Behr L, Hitzmann B, van Griensven M, et al. Design and characterization of a rotating bed system bioreactor for tissue engineering applications. Biotechnol Prog 2008; 24: 140-147.
291. Ramage L, Nuki G, Salter DM. Signalling cascades in mechanotransduction: cell-matrix interactions and mechanical loading. Scand J Med Sci Sports 2009;19:457-469.
292. Mow VC, Huiskes R. Basic orthopaedic biomechanics & mechano-biology. 3rd ed ed. Philadelphia, PA: Lippincott Williams & Wilkins, 2005.

293. Risbud MV, Sittinger M. Tissue engineering: advances in in vitro cartilage generation. Trends Biotechnol 2002; 20: 351-356.
294. Kuo CK, Li W, Mauck RL, Tuan RS. Cartilage tissue engineering: its potential and uses. Curr Opin Rheumatol 2006; 18:64-73.
295. Chowdhury TT, Bader DL, Shelton JC, Lee DA. Temporal regulation of chondrocyte metabolism in agarose constructs subjected to dynamic compression. Arch Biochem Biophys 2003; 417: 105-111.
296. Mauck RL, Nicoll SB, Seyhan SL, Ateshian GA, Hung CT. Synergistic action of growth factors and dynamic loading for articular cartilage tissue engineering. Tissue Eng 2003; 9: 597-611.
297. Davisson T, Kunig S, Chen A, Sah R, Ratcliffe A. Static and dynamic compression modulate matrix metabolism in tissue engineered cartilage. Journal of orthopaedic research: official publication of the Orthopaedic Research Society 2002;20:842-848.
298. Lima EG, Bian L, Ng KW, Mauck RL, Byers BA, Tuan RS, et al. The beneficial effect of delayed compressive loading on tissue-engineered cartilage constructs cultured with TGF-beta3. Osteoarthr Cartil 2007; 15:1025-1033.
299. Kelly TA, Ng KW, Wang CC, Ateshian GA, Hung CT. Spatial and temporal development of chondrocyte-seeded agarose constructs in free-swelling and dynamically loaded cultures. J Biomech 2006; 39:1489-1497.
300. Mauck RL, Byers BA, Yuan X, Tuan RS. Regulation of cartilaginous ECM gene transcription by chondrocytes and MSCs in 3D culture in response to dynamic loading. Biomech Model Mechanobiol 2007; 6: 113-125.
301. Mauck RL, Yuan X, Tuan RS. Chondrogenic differentiation and functional maturation of bovine mesenchymal stem cells in long-term agarose culture. Osteoarthritis Cartilage 2006; 14:179-189.
302. Huang C, Reuben PM, Cheung HS. Temporal Expression Patterns and Corresponding Protein Inductions of Early Responsive Genes in Rabbit Bone Marrow-Derived Mesenchymal Stem Cells Under Cyclic Compressive Loading. Stem Cells 2005; 23:1113-1121.
303. Subramony SD, Dargis BR, Castillo M, Azeloglu EU, Tracey MS, Su A, et al. The guidance of stem cell differentiation by substrate alignment and mechanical stimulation. Biomaterials 2013; 34:1942-1953.
304. Babalola OM. Effects of physical stimuli on extracellular matrix assembly by chondrocytes and mesenchymal stem cells: Experimental and finite element analyses. ProQuest Dissertations and Theses 2010.
305. Huang AH, Farrell MJ, Kim M, Mauck RL. Long-term dynamic loading improves the mechanical properties of chondrogenic mesenchymal stem cell-laden hydrogel. European cells & materials 2010; 19:72-85.
306. Neiman VJ. Oscillating hydrogel based bioreactors for chondrogenic differentiation of mesenchymal stem cells. ProQuest Dissertations and Theses 2010.
307. Wartella KA. Effect of mechanical stimulation on mesenchymal stem cell seeded cartilage constructs. ProQuest Dissertations and Theses 2010.
308. Thorpe SD, Buckley CT, Vinardell T, O'Brien FJ, Campbell VA, Kelly DJ. Dynamic compression can inhibit chondrogenesis of mesenchymal stem cells. Biochem Biophys Res Commun 2008; 377:458-462.

309. Mauck RL, Yuan X, Tuan RS. On the Ability of Mesenchymal Stem Cells to form Functional Cartilaginous Tissues in Three Dimensional Agarose Culture. 2005 Summer Bioengineering Conference 2005.
310. Huang CY, Hagar KL, Frost LE, Sun Y, Cheung HS. Effects of cyclic compressive loading on chondrogenesis of rabbit bone-marrow derived mesenchymal stem cells. Stem Cells 2004; 22:313-323.
311. Elder SH, Kimura JH, Soslowsky LJ, Lavagnino M, Goldstein SA. Effect of compressive loading on chondrocyte differentiation in agarose cultures of chick limb-bud cells. J Orthop Res 2000; 18:78-86.
312. Cassino TR, Drowley L, Okada M, Beckman S, Keller B, Tobita K, et al. Mechanical Loading of Stem Cells for Improvement of Transplantation Outcome in a Model of Acute Myocardial Infarction: The Role of Loading History. Tissue Engineering, Part A: Tissue Engineering 2012; 18:1101-1108.
313. Williams JM,II. Chondrogenic differentiation of human adipose derived stem cells: The roles of mechanical loading, elevated calcium, and the extracellular calcium sensing receptor. ProQuest Dissertations and Theses 2012.
314. Liu H, Lin J, Roy K. Effect of 3D scaffold and dynamic culture condition on the global gene expression profile of mouse embryonic stem cells. Biomaterials 2006; 27:5978-5989.
315. Williams GM, Chan EF, Temple-Wong MM, Bae WC, Masuda K, Bugbee WD, et al. Shape, loading, and motion in the bioengineering design, fabrication, and testing of personalized synovial joints. J Biomech 2010; 43:156-165.
316. Mauck RL, Hung CT, Ateshian GA. Modeling of neutral solute transport in a dynamically loaded porous permeable gel: implications for articular cartilage biosynthesis and tissue engineering. J Biomech Eng 2003;125:602-614.
317. Waldman SD, Usmani Y, Tse MY, Pang SC. Differential effects of natriuretic peptide stimulation on tissue-engineered cartilage. Tissue Eng Part A 2008; 14:441-448.
318. Guilak F. Compression-induced changes in the shape and volume of the chondrocyte nucleus. J Biomech 1995; 28: 1529-1541.
319. O'Hara BP, Urban JP, Maroudas A. Influence of cyclic loading on the nutrition of articular cartilage. Ann Rheum Dis 1990; 49: 536-539.
320. Loening AM, James IE, Levenston ME, Badger AM, Frank EH, Kurz B, et al. Injurious mechanical compression of bovine articular cartilage induces chondrocyte apoptosis. Arch Biochem Biophys 2000;381:205-212.
321. Sah RL, Kim YJ, Doong JY, Grodzinsky AJ, Plaas AH, Sandy JD. Biosynthetic response of cartilage explants to dynamic compression. J Orthop Res 1989; 7: 619-636.
322. Sah RL, Doong JY, Grodzinsky AJ, Plaas AH, Sandy JD. Effects of compression on the loss of newly synthesized proteoglycans and proteins from cartilage explants. Arch Biochem Biophys 1991; 286: 20-29.
323. Guilak F, Meyer BC, Ratcliffe A, Mow VC. The effects of matrix compression on proteoglycan metabolism in articular cartilage explants. Osteoarthr Cartil 1994; 2: 91-101.

324. Steinmeyer J, Knue S. The proteoglycan metabolism of mature bovine articular cartilage explants superimposed to continuously applied cyclic mechanical loading. Biochem Biophys Res Commun 1997; 240: 216-221.
325. Quinn TM, Grodzinsky AJ, Buschmann MD, Kim YJ, Hunziker EB. Mechanical compression alters proteoglycan deposition and matrix deformation around individual cells in cartilage explants. J Cell Sci 1998; 111 (Pt 5):573-583.
326. Valhmu WB, Stazzone EJ, Bachrach NM, Saed-Nejad F, Fischer SG, Mow VC, et al. Load-controlled compression of articular cartilage induces a transient stimulation of aggrecan gene expression. Arch Biochem Biophys 1998; 353:29-36.
327. Steinmeyer J, Knue S, Raiss RX, Pelzer I. Effects of intermittently applied cyclic loading on proteoglycan metabolism and swelling behaviour of articular cartilage explants. Osteoarthritis Cartilage 1999; 7:155-164.
328. Frank EH, Jin M, Loening AM, Levenston ME, Grodzinsky AJ. A versatile shear and compression apparatus for mechanical stimulation of tissue culture explants. J Biomech 2000; 33:1523-1527.
329. Thibault M, Poole AR, Buschmann MD. Cyclic compression of cartilage/bone explants in vitro leads to physical weakening, mechanical breakdown of collagen and release of matrix fragments. J Orthop Res 2002; 20:1265-1273.
330. Sauerland K, Raiss RX, Steinmeyer J. Proteoglycan metabolism and viability of articular cartilage explants as modulated by the frequency of intermittent loading. Osteoarthritis Cartilage 2003; 11:343-350.
331. Wolf A, Raiss RX, Steinmeyer J. Fibronectin metabolism of cartilage explants in response to the frequency of intermittent loading. J Orthop Res 2003; 21:1081-1089.
332. Fitzgerald JB, Jin M, Dean D, Wood DJ, Zheng MH, Grodzinsky AJ. Mechanical compression of cartilage explants induces multiple time-dependent gene expression patterns and involves intracellular calcium and cyclic AMP. The Journal of biological chemistry 2004; 279:19502-19511.
333. Park S, Hung CT, Ateshian GA. Mechanical response of bovine articular cartilage under dynamic unconfined compression loading at physiological stress levels. Osteoarthritis Cartilage 2004;12:65-73.
334. Ackermann B, Steinmeyer J. Collagen biosynthesis of mechanically loaded articular cartilage explants. Osteoarthritis Cartilage 2005; 13:906-914.
335. Aufderheide AC, Athanasiou KA. A direct compression stimulator for articular cartilage and meniscal explants. Ann Biomed Eng 2006; 34:1463-1474.
336. Wolf A, Ackermann B, Steinmeyer J. Collagen synthesis of articular cartilage explants in response to frequency of cyclic mechanical loading. Cell Tissue Res 2007; 327:155-166.
337. Sauerland K, Steinmeyer J. Intermittent mechanical loading of articular cartilage explants modulates chondroitin sulfate fine structure. Osteoarthritis Cartilage 2007; 15:1403-1409.
338. Wei F, Golenberg N, Kepich ET, Haut RC. Effect of intermittent cyclic preloads on the response of articular cartilage explants to an excessive level of unconfined compression. J Orthop Res 2008; 26:1636-1642.

339. Nakagawa K, Teramura T, Takehara T, Onodera Y, Hamanishi C, Akagi M, et al. Cyclic compression-induced p38 activation and subsequent MMP13 expression requires Rho/ROCK activity in bovine cartilage explants. Inflammation Res 2012; 61: 1093-1100.

340. Waldman SD, Couto DC, Grynpas MD, Pilliar RM, Kandel RA. A single application of cyclic loading can accelerate matrix deposition and enhance the properties of tissue-engineered cartilage. Osteoarthr Cartil 2006; 14: 323-330.

341. Raizman I, De Croos JNA, St-Pierre J, Pilliar RM, Kandel RA. Articular cartilage subpopulations respond differently to cyclic compression in vitro. Tissue engineering.Part A 2009; 15: 3789-3798.

342. Lee DA, Frean SP, Lees P, Bader DL. Dynamic mechanical compression influences nitric oxide production by articular chondrocytes seeded in agarose. Biochem Biophys Res Commun 1998;251:580-585.

343. Chowdhury TT, Bader DL, Lee D. Dynamic Compression Inhibits the Synthesis of Nitric Oxide and PGE sub(2) by IL-1 beta -Stimulated Chondrocytes Cultured in Agarose Constructs. Biochem Biophys Res Commun 2001; 285: 1168-1174.

344. Roberts SR, Knight MM, Lee DA, Bader DL. Mechanical compression influences intracellular Ca2+ signaling in chondrocytes seeded in agarose constructs. J Appl Physiol 2001; 90: 1385-1391.

345. Chowdhury TT, Bader DL, Lee DA. Dynamic compression counteracts IL-1 beta-induced release of nitric oxide and PGE2 by superficial zone chondrocytes cultured in agarose constructs. Osteoarthr Cartil 2003; 11: 688-696.

346. Gu WY, Yao H, Huang CY, Cheung HS. New insight into deformation-dependent hydraulic permeability of gels and cartilage, and dynamic behavior of agarose gels in confined compression. J Biomech 2003; 36: 593-598.

347. Langelier E, Buschmann MD. Increasing strain and strain rate strengthen transient stiffness but weaken the response to subsequent compression for articular cartilage in unconfined compression. J Biomech 2003; 36: 853-859.

348. Knight MM, Toyoda T, Lee DA, Bader DL. Mechanical compression and hydrostatic pressure induce reversible changes in actin cytoskeletal organisation in chondrocytes in agarose. J Biomech 2006; 39: 1547-1551.

349. Sawae Y, Hanaki A, Suzuki E, Murakami T. Effects of cyclic compression on ECM synthesis and mechanical property in cultured chondrocyte-agarose construct. J Biomech 2006; 39: S220.

350. Chai DH, Grodzinsky AJ, arner EC, Griggs DW. Blocking Integrins Alters Chondrocyte Response to Dynamic Compression in Agarose Gel Culture. 52nd Annual Meeting of the Orthopaedic Research Society 2006.

351. Ng KW, Mauck RL, Statman LY, Lin EY, Ateshian GA, Hung CT. Dynamic deformational loading results in selective application of mechanical stimulation in a layered, tissue-engineered cartilage construct. Biorheology 2006; 43: 497-507.

352. Cassino TR, Anderson R, Love BJ, Huckle WR, Seamans DK, Forsten-Williams K. Design and application of an oscillatory compression device for cell constructs. Biotechnol Bioeng 2007; 98: 211-220.

353. Chowdhury TT, Arghandawi S, Brand J, Akanji OO, Bader DL, Salter DM, et al. Dynamic compression counteracts IL-1beta induced inducible nitric oxide synthase and cyclo-oxygenase-2 expression in chondrocyte/agarose constructs. Arthritis Res Ther 2008;10:R35.
354. Chowdhury TT, Arghandawi S, Akanji OO, Bader DL, Salter DM, Lee DA. Dynamic Compression Counteracts IL-1b-Induced iNOS and COX-2 Expression, via a p38 MAPK Pathway in Chondrocyte/Agarose Constructs. 54th Annual Meeting of the Orthopaedic Research Society 2008.
355. Raveenthiran SP, Chowdhury TT. Dynamic compression inhibits fibronectin fragment induced iNOS and COX-2 expression in chondrocyte/agarose constructs. Biomechanics and Modeling in Mechanobiology 2009; 8: 273-283.
356. Kock LM, Schulz RM, van Donkelaar CC, Thummler CB, Bader A, Ito K. RGD-dependent integrins are mechanotransducers in dynamically compressed tissue-engineered cartilage constructs. J Biomech 2009;42:2177-2182.
357. Akanji OO, Sakthithasan P, Salter DM, Chowdhury TT. Dynamic compression alters NF Kappa B activation and I Kappa B- alpha expression in IL-1 beta -stimulated chondrocyte/agarose constructs. Inflammation Res 2010;59:41-52.
358. Nebelung S, Gavenis K, Lüring C, Zhou B, Mueller-Rath R, Stoffel M, et al. Simultaneous anabolic and catabolic responses of human chondrocytes seeded in collagen hydrogels to long-term continuous dynamic compression. Ann Anat 2012; 194: 351-358.
359. Suh J. Dynamic unconfined compression of articular cartilage under a cyclic compressive load. Biorheology 1996; 33: 289-304.
360. Kim YJ, Bonassar LJ, Grodzinsky AJ. The role of cartilage streaming potential, fluid flow and pressure in the stimulation of chondrocyte biosynthesis during dynamic compression. J Biomech 1995; 28: 1055-1066.
361. Wong M, Wuethrich P, Buschmann MD, Eggli P, Hunziker E. Chondrocyte biosynthesis correlates with local tissue strain in statically compressed adult articular cartilage. J Orthop Res 1997; 15: 189-196.
362. Chahine NO, Ateshian GA, Hung CT. The effect of finite compressive strain on chondrocyte viability in statically loaded bovine articular cartilage. Biomech Model Mechanobiol 2007; 6: 103-111.
363. Buschmann MD, Gluzband YA, Grodzinsky AJ, Hunziker EB. Mechanical compression modulates matrix biosynthesis in chondrocyte/agarose culture. J Cell Sci 1995; 108 (Pt 4):1497-1508.
364. Waldman SD, Spiteri CG, Grynpas MD, Pilliar RM, Kandel RA. Long-term intermittent shear deformation improves the quality of cartilaginous tissue formed in vitro. J Orthop Res 2003; 21: 590-596.
365. Jin M, Frank EH, Quinn TM, Hunziker EB, Grodzinsky AJ. Tissue shear deformation stimulates proteoglycan and protein biosynthesis in bovine cartilage explants. Arch Biochem Biophys 2001; 395: 41-48.
366. Kawanishi M, Oura A, Furukawa K, Fukubayashi T, Nakamura K, Tateishi T, et al. Redifferentiation of dedifferentiated bovine articular chondrocytes enhanced by cyclic hydrostatic pressure under a gas-controlled system. Tissue Eng 2007; 13: 957-964.
367. Smith RL, Rusk SF, Ellison BE, Wessells P, Tsuchiya K, Carter DR, et al. In vitro stimulation of articular chondrocyte mRNA and extracellular matrix synthesis by hydrostatic pressure. J Orthop Res 1996; 14: 53-60.

368. Ikenoue T, Trindade M, Lee M, Lin E, Schurman D, Goodman S, et al. Meehanoregulation of human articular chondrocyte aggrecan and type II collagen expression by intermittent hydrostatic pressure in vitro. Journal of Orthopaedic Research 2003; 21: 110-116.
369. Schulz RM, Wustneck N, van Donkelaar CC, Shelton JC, Bader A. Development and validation of a novel bioreactor system for load- and perfusion-controlled tissue engineering of chondrocyte-constructs. Biotechnol Bioeng 2008; 101: 714-728.
370. Di Federico E, Bader DL, Shelton JC. Design and validation of an in vitro loading system for the combined application of cyclic compression and shear to 3D chondrocytes-seeded agarose constructs. Med Eng Phys 2014; 36: 534-540.
371. Kaupp JA, Tse MY, Pang SC, Kenworthy G, Hetzler M, Waldman SD. The effect of moving point of contact stimulation on chondrocyte gene expression and localization in tissue engineered constructs. Ann Biomed Eng 2013; 41: 1106-1119.
372. Huang AH, Baker BM, Ateshian GA, Mauck RL. Sliding contact loading enhances the tensile properties of mesenchymal stem cell-seeded hydrogels. European cells & materials 2012; 24: 29-45.
373. Kock LM, Ito K, van Donkelaar CC. Sliding indentation enhances collagen content and depth-dependent matrix distribution in tissue-engineered cartilage constructs. Tissue engineering.Part A 2013; 19: 1949-1959.
374. Hunt NC, Grover LM. Cell encapsulation using biopolymer gels for regenerative medicine. Biotechnol Lett 2010; 32: 733-742.
375. Buschmann MD, Gluzband YA, Grodzinsky AJ, Kimura JH, Hunziker EB. Chondrocytes in agarose culture synthesize a mechanically functional extracellular matrix. J Orthop Res 1992; 10: 745-758.
376. Christensen LH. Host tissue interaction, fate, and risks of degradable and nondegradable gel fillers. Dermatol Surg 2009; 35 Suppl 2:1612-1619.
377. Kessler MW, Grande DA. Tissue engineering and cartilage. Organogenesis 2008;4:28-32.
378. Benya PD, Shaffer JD. Dedifferentiated chondrocytes reexpress the differentiated collagen phenotype when cultured in agarose gels. Cell 1982; 30: 215-224.
379. Bounelis P, Daniel JC. The effect of ascorbate on embryonic chick sternal chondrocytes cultured in agarose. Tissue Cell 1983; 15: 683-693.
380. Aulthouse AL, Beck M, Griffey E, Sanford J, Arden K, Machado MA, et al. Expression of the human chondrocyte phenotype in vitro. In Vitro Cell Dev Biol 1989; 25: 659-668.
381. Albro MB, Li R, Banerjee RE, Hung CT, Ateshian GA. Validation of theoretical framework explaining active solute uptake in dynamically loaded porous media. J Biomech 2010; 43: 2267-2273.
382. Quinn TM, Schmid P, Hunziker EB, Grodzinsky AJ. Proteoglycan deposition around chondrocytes in agarose culture: construction of a physical and biological interface for mechanotransduction in cartilage. Biorheology 2002; 39: 27-37.
383. Mouw JK, Case ND, Guldberg RE, Plaas AH, Levenston ME. Variations in matrix composition and GAG fine structure among scaffolds for cartilage tissue engineering. Osteoarthritis Cartilage 2005; 13: 828-836.

384. Ng KW, Saliman JD, Lin EY, Statman LY, Kugler LE, Lo SB, et al. Culture duration modulates collagen hydrolysate-induced tissue remodeling in chondrocyte-seeded agarose hydrogels. Ann Biomed Eng 2007; 35: 1914-1923.
385. Ng KW, Kugler LE, Ateshian GA, Hung CT. Mechanical and Biochemical Properties of Engineered Chondrocyte-Seeded Hydrogel Constructs Recover over Time in Culture after Enzymatic Scaffold Removal. 53rd Annual Meeting of the Orthopaedic Research Society 2007.
386. Coleman RM, Case ND, Guldberg RE. Hydrogel effects on bone marrow stromal cell response to chondrogenic growth factors. Biomaterials 2007; 28: 2077-2086.
387. Rahfoth B, Weisser J, Sternkopf F, Aigner T, von der Mark K, Brauer R. Transplantation of allograft chondrocytes embedded in agarose gel into cartilage defects of rabbits. Osteoarthritis Cartilage 1998; 6: 50-65.
388. Weisser J, Rahfoth B, Timmermann A, Aigner T, Brauer R, von der Mark K. Role of growth factors in rabbit articular cartilage repair by chondrocytes in agarose. Osteoarthritis Cartilage 2001; 9 Suppl A: S48-54.
389. Knight MM, Bomzon Z, Kimmel E, Sharma AM, Lee DA, Bader DL. Chondrocyte deformation induces mitochondrial distortion and heterogeneous intracellular strain fields. Biomech Model Mechanobiol 2006; 5: 180-191.
390. Hamrock BJ, Hamrock BJ. Fundamentals of fluid film lubrication. New York: New York : Marcel Dekker, 2004.
391. PIC Design, [http://www.pic-design.com].
392. Applied Motion Products, [http://www.appliedmotionproducts.com].
393. Mean Well Direc, [http://www.meanwelldirect.co.uk].
394. Lee DA, Bader DL. Compressive strains at physiological frequencies influence the metabolism of chondrocytes seeded in agarose. J Orthop Res 1997; 15: 181-188.
395. Hollander AP, Heathfield TF, Webber C, Iwata Y, Bourne R, Rorabeck C, et al. Increased damage to type II collagen in osteoarthritic articular cartilage detected by a new immunoassay. J Clin Invest 1994;93:1722-1732.
396. Farndale RW, Buttle DJ, Barrett AJ. Improved quantitation and discrimination of sulphated glycosaminoglycans by use of dimethylmethylene blue. Biochim Biophys Acta 1986; 883: 173-177.
397. Goldberg RL, Kolibas LM. An improved method for determining proteoglycans synthesized by chondrocytes in culture. Connect Tissue Res 1990; 24: 265-275.
398. Hoemann CD. Molecular and biochemical assays of cartilage components. Methods Mol Med 2004; 101: 127-156.
399. Hall DA. Methodology of connective tissue research. 1St Ed ed. Oxford (Eng.): Joynson-Bruvvers, 1976.
400. Wu JP, Kirk TB, Zheng MH. Study of the collagen structure in the superficial zone and physiological state of articular cartilage using a 3D confocal imaging technique. Journal of orthopaedic surgery and research 2008; 3: 29.

401. Ng KW, Ateshian GA, Hung CT. Zonal Chondrocytes Seeded in a Layered Agarose Hydrogel Create Engineered Cartilage with Depth-Dependent Cellular and Mechanical Inhomogeneity. Tissue Engineering, Part A: Tissue Engineering 2009; 15: 2315-2324.
402. Darling EM, Athanasiou K. Articular Cartilage Bioreactors and Bioprocesses. Tissue Eng 2003; 9: 9-26.
403. Nguyen QT, Wong BL, Chun J, Sah RL. Controlling Cartilage Shear and Sliding In Vitro for Mechanobiology: Effects of Synovial Fluid and Platen Surface Roughness. 54th Annual Meeting of the Orthopaedic Research Society 2008.
404. Kock L, Van Donkelaar C, Ito K. Depth-Dependent Stimulation of Chondrocytes in Agarose by Sliding Indentation. 56th Annual Meeting of the Orthopaedic Research Society 2010.
405. Grad S, Loparic M, Peter R, Stolz M, Aebi U, Alini M. Sliding motion modulates stiffness and friction coefficient at the surface of tissue engineered cartilage. Osteoarthr Cartil 2012; 20: 288-295.
406. Enders JT, Otto TJ, Peters HC, Wu J, Hardouin S, Moed BR, et al. A model for studying human articular cartilage integration in vitro. J Biomed Mater Res A 2010;94:509-514.
407. Omata S, Sonokawa S, Sawae Y, Murakami T. Effects of both vitamin C and mechanical stimulation on improving the mechanical characteristics of regenerated cartilage. Biochem Biophys Res Commun 2012;424:724-729.
408. Lima EG, Bian L, Mauck RL, Byers BA, Tuan RS, Ateshian GA, et al. The effect of applied compressive loading on tissue-engineered cartilage constructs cultured with TGF-beta3. Conf Proc IEEE Eng Med Biol Soc 2006; 1: 779-782.
409. Dimicco MA, Kisiday JD, Gong H, Grodzinsky AJ. Structure of pericellular matrix around agarose-embedded chondrocytes. Osteoarthritis Cartilage 2007; 15: 1207-1216.
410. Bougault C, Paumier A, Aubert-Foucher E, Mallein-Gerin F. Investigating conversion of mechanical force into biochemical signaling in three-dimensional chondrocyte cultures. Nat Protoc 2009; 4: 928-938.
411. Bian L, Fong JV, Lima EG, Stoker AM, Ateshian GA, Cook JL, et al. Dynamic Mechanical Loading Enhances Functional Properties of Tissue-Engineered Cartilage Using Mature Canine Chondrocytes. Tissue Engineering, Part A: Tissue Engineering 2010; 16: 1781-1790.
412. Chai DH, Arner EC, Griggs DW, Grodzinsky AJ. Alphav and beta1 integrins regulate dynamic compression-induced proteoglycan synthesis in 3D gel culture by distinct complementary pathways. Osteoarthritis Cartilage 2010; 18: 249-256.
413. Pingguan-Murphy B, Lee DA, Bader DL, Knight MM. Activation of chondrocytes calcium signalling by dynamic compression is independent of number of cycles. Arch Biochem Biophys 2005; 444: 45-51.
414. De Rosa E, Urciuolo F, Borselli C, Gerbasio D, Imparato G, Netti PA. Time and space evolution of transport properties in agarose-chondrocyte constructs. Tissue Eng 2006; 12: 2193-2201.
415. Tasci A, Ferguson SJ, Buchler P. Numerical assessment on the effective mechanical stimuli for matrix-associated metabolism in chondrocyte-seeded constructs. J Tissue Eng Regen Med 2010.

416. Chowdhury TT, Salter DM, Bader DL, Lee DA. Signal transduction pathways involving p38 MAPK, JNK, NFkappaB and AP-1 influences the response of chondrocytes cultured in agarose constructs to IL-1beta and dynamic compression. Inflamm Res 2008; 57: 306-313.

417. Kock LM, Ravetto A, van Donkelaar CC, Foolen J, Emans PJ, Ito K. Tuning the differentiation of periosteum-derived cartilage using biochemical and mechanical stimulations. Osteoarthr Cartil 2010; 18: 1528-1535.

418. Chowdhury TT, Schulz RM, Rai SS, Thuemmler CB, Wuestneck N, Bader A, et al. Biomechanical modulation of collagen fragment-induced anabolic and catabolic activities in chondrocyte/agarose constructs. Arthritis Research & Therapy 2010; 12: R82.

419. Sawae Y, Shelton JC, Bader DL, Knight MM. Confocal analysis of local and cellular strains in chondrocyte-agarose constructs subjected to mechanical shear. Ann Biomed Eng 2004;32:860-870.

420. Guilak F, Ratcliffe A, Mow VC. Chondrocyte deformation and local tissue strain in articular cartilage: a confocal microscopy study. Journal of orthopaedic research: official publication of the Orthopaedic Research Society 1995; 13: 410-421.

421. Degala S. Fluid flow regulates articular chondrocyte mechanotransduction pathways in three-dimensional culture. ProQuest Dissertations and Theses 2010.

422. Degala S, Williams R, Zipfel W, Bonassar LJ. Calcium signaling in response to fluid flow by chondrocytes in 3D alginate culture. Journal of orthopaedic research: official publication of the Orthopaedic Research Society 2012; 30: 793-799.

423. Eifler RL, Blough ER, Dehlin JM, Haut Donahue TL. Oscillatory fluid flow regulates glycosaminoglycan production via an intracellular calcium pathway in meniscal cells. Journal of orthopaedic research: official publication of the Orthopaedic Research Society 2006; 24: 375-384.

424. Edlich M, Yellowley C, Jacobs CR, Donahue H. Oscillating fluid flow regulates cytosolic calcium concentration in bovine articular chondrocytes. J Biomech 2001; 34: 59-65.

425. Xu X, Urban JPG, Tirlapur U, Wu M, Cui Z, Cui Z. Influence of perfusion on metabolism and matrix production by bovine articular chondrocytes in hydrogel scaffolds. Biotechnol Bioeng 2006; 93: 1103-1111.

426. Khan AA, Suits JMT, Kandel RA, Waldman SD. The effect of continuous culture on the growth and structure of tissue-engineered cartilage. Biotechnol Prog 2009; 25: 508-515.

427. Mizuno S, Allemann F, Glowacki J. Effects of medium perfusion on matrix production by bovine chondrocytes in three-dimensional collagen sponges. J Biomed Mater Res 2001; 56: 368-375.

428. Pazzano D, Mercier K, Moran JM, Fong SS, DiBiasio DD, Rulfs JX, et al. Comparison of Chondrogenesis in Static and Perfused Bioreactor Culture. Biotechnol Prog 2000; 16: 893-896.

429. Klein TJ, Malda J, Sah RL, Hutmacher DW. Tissue Engineering of Articular Cartilage with Biomimetic Zones. Tissue Eng Part B Rev 2009.

430. Klein TJ, Rizzi SC, Reichert JC, Georgi N, Malda J, Schuurman W, et al. Strategies for zonal cartilage repair using hydrogels. Macromol Biosci 2009; 9: 1049-1058.

431. Ng KW, Wang CC, Mauck RL, Kelly TA, Chahine NO, Costa KD, et al. A layered agarose approach to fabricate depth-dependent inhomogeneity in chondrocyte-seeded constructs. J Orthop Res 2005; 23: 134-141.
432. Ito S, Sato M, Yamato M, Mitani G, Kutsuna T, Nagai T, et al. Repair of articular cartilage defect with layered chondrocyte sheets and cultured synovial cells. Biomaterials 2012; 33: 5278-5286.
433. Oswald ES, Chao PG, Cheng SL, Shin RH, Bulinski JC, Ateshian GA, et al. Zonal-Dependent Response of Chondrocytes to Osmotic Loading. 53rd Annual Meeting of the Orthopaedic Research Society 2007.
434. Guilak F, Alexopoulos LG, Haider MA, Ting-Beall HP, Setton LA. Zonal uniformity in mechanical properties of the chondrocyte pericellular matrix: micropipette aspiration of canine chondrons isolated by cartilage homogenization. Ann Biomed Eng 2005;33:1312-1318.
435. Benya PD, Shaffer JD. Dedifferentiated chondrocytes reexpress the differentiated collagen phenotype when cultured in agarose gels. Cell 1982; 30: 215-224.
436. Aulthouse AL, Beck M, Griffey E, Sanford J, Arden K, Machado MA, et al. Expression of the human chondrocyte phenotype in vitro. In vitro cellular & developmental biology: journal of the Tissue Culture Association 1989; 25: 659-668.
437. Kock LM, Geraedts J, Ito K, van Donkelaar CC. Low agarose concentration and TGF-β3 distribute extracellular matrix in tissue-engineered cartilage. Tissue engineering.Part A 2013; 19: 1621-1631.
438. Asanbaeva A, Masuda K, Thonar EJA, Klisch SM, Sah RL. Mechanisms of cartilage growth: modulation of balance between proteoglycan and collagen in vitro using chondroitinase ABC. Arthritis Rheum 2007; 56: 188-198.
439. Sengers BG, Heywood HK, Lee DA, Oomens CW, Bader DL. Nutrient utilization by bovine articular chondrocytes: a combined experimental and theoretical approach. J Biomech Eng 2005; 127: 758-766.
440. Mauck RL. Functional tissue engineering of articular cartilage: the effect of physical forces on the in vitro growth of engineered constructs. 2003.
441. Mesallati T, Buckley CT, Nagel T, Kelly DJ. Scaffold architecture determines chondrocyte response to externally applied dynamic compression. Biomechanics and modeling in mechanobiology 2013; 12: 889-899.
442. Roberts JJ. Hydrogels for cartilage tissue engineering in mechanically relevant environments. ProQuest Dissertations and Theses 2013.
443. Wu MH, Urban JP, Cui ZF, Cui Z, Xu X. Effect of extracellular ph on matrix synthesis by chondrocytes in 3D agarose gel. Biotechnol Prog 2007; 23: 430-434.
444. Heywood HK, Bader DL, Lee DA. Glucose concentration and medium volume influence cell viability and glycosaminoglycan synthesis in chondrocyte-seeded alginate constructs. Tissue Eng 2006; 12: 3487-3496.
445. Kisiday JD, Jin M, DiMicco MA, Kurz B, Grodzinsky AJ. Effects of dynamic compressive loading on chondrocyte biosynthesis in self-assembling peptide scaffolds. J Biomech 2004; 37: 595-604.
446. Lee CR, Grad S, Gorna K, Gogolewski S, Goessl A, Alini M. Fibrin-Polyurethane Composites for Articular Cartilage Tissue Engineering: A Preliminary Analysis. Tissue Eng 2005; 11: 1562-1573.
447. Tan AR, Dong EY, Ateshian GA, Hung CT. Response of engineered cartilage to mechanical insult depends on construct maturity. Osteoarthr Cartil 2010; 18: 1577-1585.

448. Lee DA, Knight MM, Bolton JF, Idowu BD, Kayser MV, Bader DL. Chondrocyte deformation within compressed agarose constructs at the cellular and sub-cellular levels. J Biomech 2000; 33: 81-95.
449. Lee DA, Noguchi T, Frean SP, Lees P, Bader DL. The influence of mechanical loading on isolated chondrocytes seeded in agarose constructs. Biorheology 2000; 37: 149-161.
450. Kelly TA, Wang CC, Mauck RL, Ateshian GA, Hung CT. Role of cell-associated matrix in the development of free-swelling and dynamically loaded chondrocyte-seeded agarose gels. Biorheology 2004; 41: 223-237.
451. Toyoda T, Seedhom BB, Kirkham J, Bonass WA. Upregulation of aggrecan and type II collagen mRNA expression in bovine chondrocytes by the application of hydrostatic pressure. Biorheology 2003; 40: 79-85.
452. Xu X, Urban JP, Tirlapur U, Wu MH, Cui Z, Cui Z. Influence of perfusion on metabolism and matrix production by bovine articular chondrocytes in hydrogel scaffolds. Biotechnol Bioeng 2006; 93: 1103-1111.
453. Tran-Khanh N, Chevrier A, Lascau-Coman V, Hoemann CD, Buschmann MD. Young adult chondrocytes proliferate rapidly and produce a cartilaginous tissue at the gel-media interface in agarose cultures. Connect Tissue Res 2010; 51: 216-223.